THE RELATIONSHIP BETWEEN INTRACELLULAR NUCLEOTIDES AND HYBRIDOMA CELL CULTURE PRODUCTIVITY AND VIABILITY

BY

NORMAN C. J. BARNABÉ

A Thesis
Submitted to the Faculty of Graduate Studies
in Partial in Fulfillment of the Requirements for the Degree of

DOCTOR OF PHILOSOPHY

Department of Microbiology
University of Manitoba
Winnipeg, Manitoba
Canada

THE UNIVERSITY OF MANITOBA

FACULTY OF GRADUATE STUDIES

*****

COPYRIGHT PERMISSION PAGE

THE RELATIONSHIP BETWEEN INTRACELLULAR NUCLEOTIDES AND HYBRIDOMA CELL CULTURE PRODUCTIVITY AND VIABILITY

BY

NORMAN C.J. BARNABÉ

A Thesis/Practicum submitted to the Faculty of Graduate Studies of The University of Manitoba in partial fulfillment of the requirements of the degree

of

DOCTOR OF PHILOSOPHY

ACKNOWLEDGMENTS

I would like to thank my advisor Dr. Michael Butler for his guidance during this project and members of my Ph.D. committee for their helpful advice. I would also like to express my gratitude to the following:

Dr. David Jan for help in developing the serum-free medium formulation and for providing a Mab purification protocol.

Dr. VanCaeseele for providing access to a fluorescent microscope.

Andrew Christie, Norm Huzel, Mike Berry and David Petch for their technical support.

J'aimerais aussi remercier mes parents, mes frères et mes soeurs pour leurs encouragements et pour avoir rendu la vie plus facile.

This work was supported by a Natural Science and Engineering Research Council industrial research grant in conjunction with Apotex Fermentation Inc. An NSERC graduate fellowship is also gratefully acknowledged.

ABSTRACT

Monoclonal antibody (Mab) production is dependent upon the metabolic state of hybridomas. The objective of this research project was to determine if the intracellular nucleotide pool could be used as an indicator of specific antibody productivity (qMab) or of cell viability. Serum-free cultures of the murine hybridoma (CC9C10) which secretes Mab against bovine insulin were used as a model in these studies.

Changes in qMab were monitored in relation to the measured intracellular nucleotide pool. Under certain culture conditions the qMab increased significantly (65 - 97 %) and was shown to be concomitant with an increase (13 - 65 %) in UDP-N-acetylgalactosamine and UDP-N-acetylglucosamine (UDP-GNac) and concomitant with a decrease in growth rate (22 -59 %). Hybridomas were then grown in conditions favorable for sugar-nucleotide accumulation. Supplementation of cultures with tunicamycin or NH_4Cl caused a x5 increase in intracellular UDP-GNac but without significantly affecting the qMab. Tunicamycin, but not NH_4Cl, inhibited Mab glycosylation. However, non-glycosylated Mab was secreted at the same rate as the glycosylated form. Therefore, neither the availability of UDP-GNac nor glycosylation appear to limit productivity in these cells. The data suggests that a reduction in growth rate rather than UDP-GNac accumulation may cause an increased qMab.

From a study of the relationship between cell viability and intracellular nucleotides, it was found that programmed cell death (apoptosis) was preceded by an intracellular decrease in CTP and UTP. These nucleotides may act as mediators of apoptosis and may be used as predictors of imminent cell death. The level of intracellular nucleotides depends on the availability of nutrients. Increasing medium glucose (0 - 25 mM) resulted in the proportional increase in NTP levels (> 45 %), although further enhancement was not observed at glutamine > 0.5 mM.

The relationships between intracellular nucleotides levels and cell viability are potentially useful for monitoring bioreactor cultures for large scale production processes.

Manipulating nucleotide levels by culture supplementation may prove to be an important tool for the control of cell growth and the prevention cell death.

LIST OF ABBREVIATIONS

Abbreviations

ADP	adenosine diphosphate
AMP	adenosine monophosphate
ANOVA	analysis of variance
AO	acridine orange
Apm^+	apoptotic cells with intact membranes
Apm^-	apoptotic cells with damaged membranes
ATP	adenosine triphosphate
BSA	bovine serum albumin
CDP	cytidine diphosphate
CHO	Chinese hamster ovary
CTP	cytidine triphosphate
DMEM	Dulbecco's Modification of Eagle's Medium
EB	ethidium bromide
EC	energy charge (ATP + 0.5ADP)/(SA)
EDTA	(ethylene dinitrilo)-tetraacetic acid
Fe-CS	iron-enriched calf serum
GDP	guanosine diphosphate
GTP	guanosine triphosphate
HGPRT	hypoxanthine guanosine phosphoribosyl transferase
HPLC	high performance liquid chromatography
H-SFM	Hybridoma Serum Free Medium
Ig	immunoglobulin
IMP	inosine monophosphate
J-SFM	Jan's serum-free formulation
Mab	monoclonal antibody
mJ-SFM	modified J-SFM

mT-SFM	modified T-SFM
NAD	nicotinamide adenine dinucleotide
NB-SFM	Norman Barnabé's serum-free formulation
N_{max}	maximum viable cell density
NTP	nucleotide triphosphate
NTP ratio	(ATP + GTP)/(CTP + UTP)
NTP/U ratio	NTP ratio/ U-ratio
OUR	oxygen uptake rate
PAGE	polyacrylamide gel electrophoresis
PBS	phosphate-buffered saline
Ppi	pyrophosphate
q_A	specific ammonium production rate
q_G	specific glucose consumption rate
q_L	specific lactate production rate
qMab	specific Mab production rate
q_Q	specific glutamine consumption rate
RPMI	Roswell Park Memorial Institute Medium
SA	sum of adenosine nucleotides (ATP + ADP + AMP)
SDS	sodium dodecyl sulfate
SU	sum of uridine nucleotides (UTP + UDP-GNac + UDP-Glc)
TCA	tricarboxylic acid cycle
T-SFM	Tharakan's serum-free formulation
UDP-Glc	uridine diphosphate-glucose
UDP-GalNac	uridine diphosphate-N-acetylgalactosamine
UDP-GlcNac	uridine diphosphate-N-acetylglucosamine
UDP-GNac	sum of UDP-GalNac and UDP-GlcNac
U-ratio	UTP/UDP-GNac
UTP	uridine triphosphate
V_I	viability index

$Y_{Lac/Glc}$	yield coefficient; moles of lactate produced per mole of glucose utilized
$Y_{NH4^+/Gln}$	yield coefficient; moles of ammonia produced per mole of glutamine utilized
μ_{max}	maximum growth rate

TABLE OF CONTENTS

LIST OF FIGURES

LIST OF TABLES

CHAPTER 1

1.0 Introduction

Hybridomas have been used extensively for the commercial production of monoclonal antibodies (Mabs), which have become important tools in biological research and medical applications. The increasing demand for large quantities of Mabs in these fields has led to studies aimed at maximizing the productivity of hybridoma cultures. Strategies for the enhancement of Mab yield have involved improving medium formulations (Glassy *et al.*, 1988; Long *et al.*, 1988) and designing high performance bioreactors (Altshuler *et al.*, 1986, Hagedorn and Kargi, 1990). In these cases, enhanced Mab production is the result of increased cell culture density, viability and longevity. Alternative methods of improving Mab yield have involved maximizing the specific Mab production rate on a per cell basis (Birch *et al.*, 1985; Velez *et al.*, 1986; Miller *et al.*, 1988a; Ramirez and Mutharasan, 1990; Bibila and Flickinger, 1991; Hayter *et al.*, 1992). These methods gave limited success as conditions that affect productivity also affected cell density and ultimately total Mab yield.

Traditionally, Mab production and culture viability has been monitored in relation to extracellular or environmental parameters such as temperature, pH, dissolved oxygen, nutrient consumption and metabolic waste accumulation. Since these parameters are insufficient to explain the behavior of cell cultures, it may be useful to analyze intracellular parameters such as the energetic or metabolic state of the cell (Costello, 1990; Ryll *et al.*, 1991). A good indicator of the metabolic state of the cell is the level of intracellular nucleotides and values of nucleotide ratios which will be the center of interest in this review. There are important relationships between nucleotide concentrations, protein synthesis and cell viability.

An understanding of how antibody synthesis and cell death are regulated may lead to the development of culture process control parameters that could maintain high qMab values over extended time periods. This would lead to improved overall antibody production during a large-scale process.

1.1 Immunoglobulin and monoclonal antibodies

Immunoglobulins or antibodies are members of a phylogenetically related family of proteins which make up the humoral component of the immune system. Their primary role is to recognize and bind antigens, foreign substances that elicit an immune response. This specific binding may neutralize the antigen by forming an immune complex or elicit effector functions such as complement-mediated cytolysis and antibody-dependent cell cytotoxicity to kill the foreign intruder (Roitt *et al.*, 1989). These properties make antibodies useful tools in diagnostics, therapy and purification.

The basic structure of immunoglobulins consists of two identical glycosylated heavy chains and two identical non-glycosylated light chains joined by disulphide bonds (Fig 1.1). The polypeptide chains fold into several globular domains. The N-terminal domain of each chain constitutes the variable region (V) which determines the specificity of the antibody whereas the constant regions are responsible for the effector functions (Roitt *et al.*, 1989). Immunoglobins (Ig) can be grouped into five major classes or types (IgG, IgM, IgA, IgD and IgE) which differ in constant regions and biological properties (Braun, 1992).

Immunoglobins are produced by B-lymphocyte cells each of which is committed to the production of one type of antibody molecule with a defined specificity (Yelton and Scharff, 1981). This homogeneous immunoglobulin is called a monoclonal antibody (Mab). Because the immune system of animals contains thousands of different lines of B-lymphocytes, the plasma of immunized animals contains a heterogeneous population of antibodies. This polyclonality of animal antisera is not reliable in many applications because of the variable specificity of each different batch, high cross-reactivity, low specificity (Bogard *et al.*, 1989). Monoclonal antibodies with a single specificity are therefore often desirable. The isolation of specific antibody secreting lymphocytes was proposed as a method of producing monoclonal antibodies *in vitro*. Lymphocytes in cell culture however have a finite life span and rarely survive beyond a couple of days. (Yelton and Scharff, 1981; Sikora and Smedley, 1984).

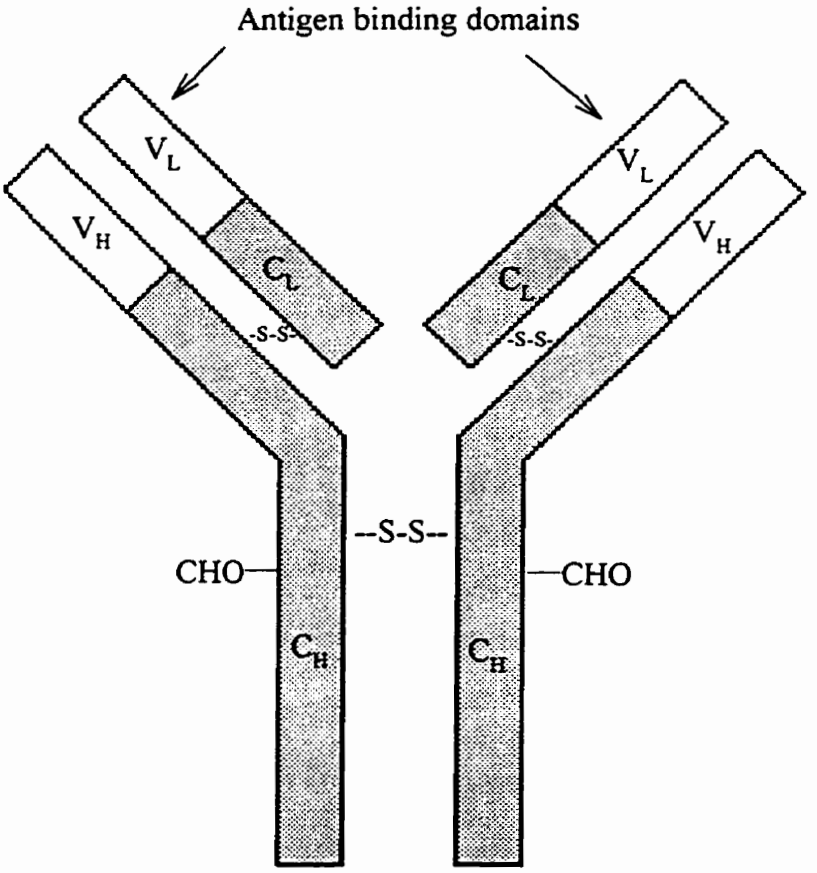

Figure 1.1 The basic structure of an immunoglobulin molecule (IgG). Interchain disulfide bonds (S-S) are indicated and CHO marks the approximate position in the heavy chain of the carbohydrate moiety. VL - variable region of the light chain, VH - variable region of the heavy chain, CL - constant region of the light chain, CH - constant region of the heavy chain (modified from Braun, 1992).

1.2 The generation of hybridoma cell lines

The limited life of B-lymphocytes poses problems when scaling up to produce large quantities of monoclonal antibodies. These problems are overcome by the use of cell hybridization, a procedure that combines the genetic characteristics of two cell populations. The advantage of this technique was shown by Kohler and Milstein (1975) who induced the fusion of a population of antibody secreting B-lymphocytes with myeloma cells which have the capacity of infinite growth. The resulting hybrids maintained characteristics of the parent lines such as antibody specificity of the lymphocyte and the immortal growth of the myeloma. These fused cells are known as hybridomas.

Monoclonal antibodies (Mabs) can be made to any substance that will be recognized as an antigen by the cells in the immune system of an animal. Immunization by scheduled injection of antigen in rats or mice increases the stimulation of B-lymphocyte clones which respond to the antigen (Sikora and Smedley, 1984). Lymphocytes which have been recovered from the spleen or lymph node can be fused to myeloma cells by the use of polyethylene glycol. Polyethylene glycol destroys the surface tension and allows cell membranes to fuse (Yelton and Scharff, 1981). Other techniques for inducing cell fusion include exposing cells to the Sendai virus or electric pulses (Kohler and Milstein, 1975; James, 1990).

To allow selection of hybrids, myelomas engineered with a genetic defect in the enzyme hypoxanthine-guanine phosphoribosyl transferase ($HGPRT^-$) have been used as fusion partners (Yelton and Scharff, 1981). HGPRT is a key enzyme in the salvage pathway of purine biosynthesis. Hybrid cells can be selectively grown in medium containing hypoxanthine, aminopterin and thymidine (HAT medium). Aminopterin blocks the *de novo* pathway for purine and pyrimidine synthesis forcing cells to use the salvage pathway which relies on the functionality of the HGPRT enzyme and the availability of thymidine and hypoxanthine. When a mixture containing unfused myelomas, unfused lymphocytes and hybridomas are plated out into HAT medium:

1. Myelomas (HGPRT $^{-}$) die because of a genetic defect in the purine biosynthesis salvage pathway.

2. Normal lymphocytes die after a few days due to limited life span.

3. Hybridomas which possess characteristics of the myeloma (infinite growth) and the lymphocyte (HGPRT $^{+}$) can grow.

Other genetic markers such as thymidine kinase (TK^{-}) have been used for selection of hybrids (Bogard *et al.*, 1989).

1.3 Applications of monoclonal antibodies

Hybridoma technology has led to the development of a wide range of Mabs which bind to proteins, carbohydrates, nucleic acids, haptens and other antigens. Monoclonal antibodies produced by hybridomas have been used in many areas of biological research. Their major applications are listed below (Mizrahi, 1986; Epstein *et al.*, 1989; Wang *et al.*, 1989; Benkovic, 1992)

1) prophylactic and therapeutic treatment of infections
2) improvement of the specificity and reproducibility of immunoassays
3) affinity chromatography
4) targeted drug therapy
5) study of antibody structure
6) in vivo imaging
7) catalysts

The increasing demand for large quantities of monoclonal antibodies has led to research aimed at improving the current methods for their production and understanding the kinetics involved.

1.4 Hybridoma cell culture

1.4.1 Growth media

Hybridomas are non-anchorage dependent cells which do not require a solid substratum for growth. *In vitro* suspension cultures of hybridomas can be grown in several different media, the compositions of which are based on early formulations developed by Eagle (1955). Eagle's basal medium consists of a chemically defined balanced salt solution containing amino acids, inorganic salts, vitamins and carbohydrates. The function of these components include the provision of energy substrates, biosynthesis precursors, enzyme co-factors and pH buffering. Glucose and glutamine are the two most heavily utilized media components and are the major carbon and energy sources in hybridoma cultures (Butler and Jenkins, 1989; Miller *et al.*, 1989a, 1989b).

Basal medium is generally insufficient in supporting cell growth on its own and must be supplemented with growth stimulating components. The most common source of these components is animal blood serum which is added to basal medium at 5 - 10 % v/v. Animal serum contains several growth factors and compounds essential for cell growth however its inclusion in growth medium has many disadvantages as listed below: (Butler, 1988; Glassy *et al.*, 1988)

1. primary cost factor in medium.
2. potential source of contamination (i.e. viral and mycoplasmal).
3. chemically undefined.
4. complicates product recovery.
5. variability of growth promoting properties from batch-to-batch.

In the last 20 years, efforts have been made to eliminate serum from media due to the undesirable properties of the supplement and over concerns about its safety in producing medical products for humans. Medium which excludes animal serum from its formulation is referred to as serum-free. Serum can be replaced by purified proteins such

as growth factors, hormones or carrier proteins (Barnes and Sato, 1980; Lambert and Birch, 1985; Murakami, 1989). Other supplements commonly added to serum-free media include lipids, fatty acids, trace elements and high molecular weight polymers (Kawamoto *et al.*, 1983; Bjare, 1992; Chattopadhyay *et al.*, 1995). The latter component protects cell membranes from shear forces.

Serum-free medium has several advantages and disadvantages associated with its use as shown in Table 1.1. Growing hybridomas in serum-free medium often requires an adaptation process which consists of weaning cells off of serum (Ozturk and Palsson, 1991a). A gradual reduction in serum concentration with time increases the probability of successful adaptation to serum-free medium. The number of generations required for adaptation is dependent on the cell line (Ozturk and Palsson, 1991a). Serum-free formulations appear to be cell line specific and individual optimization may be required for each cell type (Tharakan *et al.*, 1986). Growth rates in serum-free medium have been shown to sometimes differ remarkably among clones even if the origin of their parent cells were the same (Murakami, 1989). The uniqueness of growth requirements may be the result of the procedure used in the generation of hybridomas which involves chromosomal segregation and loss (Bogard *et al.*, 1989; James, 1990).

Advances in medium formulations have eliminated the need for protein supplements for certain hybridoma cultures (Schneider and Lavoix, 1990; Eto *et al.*, 1991). Protein-free medium is preferable to serum-free as a reduction in expensive protein supplements decreases the cost of medium and facilitates the purification of the monoclonal antibody.

Table 1.1 Advantages and disadvantages of serum-free media for hybridomas (adapted from Glassy *et al.*, 1988; Shacter, 1989).

Advantages
1. Consistent and chemically defined composition.
2. Improves reproducibility of cell culture and product yield.
3. Decreases potential of contamination.
4. Greatly simplifies purification of antibodies due to increased initial purity and absence of contaminating immunoglobulins.
5. Low or no dependence on animals.
6. Depending on the cell line, antibody secretion may be increased.
Disadvantages
1. Requires optimization for each hybridoma cell line.
2. May require serum hormones and growth factors which are difficult to isolate and purify.
3. Frequently results in longer lag periods.
4. Depending on the cell line, growth rate, maximum cell density and cell viability may be lower.
5. Protease inhibitors in serum may help protect cells from enzymes such as trypsin.

1.4.2 Batch and fed-batch cultures

In a batch culture system, cells are cultivated in flasks or larger vessels with no refreshment of medium. Under these conditions, the medium becomes limiting in nutrients or growth factors and waste components accumulate. The constantly changing environment causes cells to undergo metabolic and physiological changes. Hybridoma cells grown in batch culture generally follow the growth pattern shown in Fig.1.2. Growth curves usually consist of four distinct phases. 1. The lag phase is an initial period of slow or no growth following inoculation of the culture, the length of which often depends on the state of the cells at the time of inoculation (i.e. cells taken from an exponentially growing culture have a short lag phase whereas cells taken from a stationary culture tend to have an extended lag phase). 2. The exponential phase or log phase is a period of cell growth. Mammalian cells usually have a doubling time of between 15-25 hours depending on the cell type (Butler,1988). 3. The stationary phase is a period of no growth following the log phase. The cessation of growth may be due to the depletion of nutrients and/or the accumulation of inhibitory metabolites (Dalili *et al.*, 1990; Doyle and Butler, 1990; Duval *et al.*, 1992). 4. The death phase is a period of cell death.

Two modes of cell death have been identified in hybridoma cultures. Passive cell death also referred to as necrosis may be caused by the accumulation of metabolic by-products such as lactate and ammonium (Mercille and Massie, 1994a; Singh *et al.*, 1994). Active cell death or apoptosis involves the participation of the cell in its own demise through gene regulation (Hale *et al.*, 1996). Apoptosis is induced by glucose, glutamine or oxygen limitation (Mercille and Massie, 1994a, 1994b; Singh *et al.*, 1994). Both modes of cell death can be distinguished morphologically by the structure of the nuclear chromatin (Mercille and Massie, 1994a).

In a fed-batch culture system, medium or concentrated supplements are added to cultures in order to prevent nutrient limitation (Reuveny *et al.*, 1986; Bibila *et al.*, 1994). This culturing method however does not prevent the accumulation of waste products. Fed-batch protocols increase culture longevity by prolonging the stationary phase and reducing the death rate.

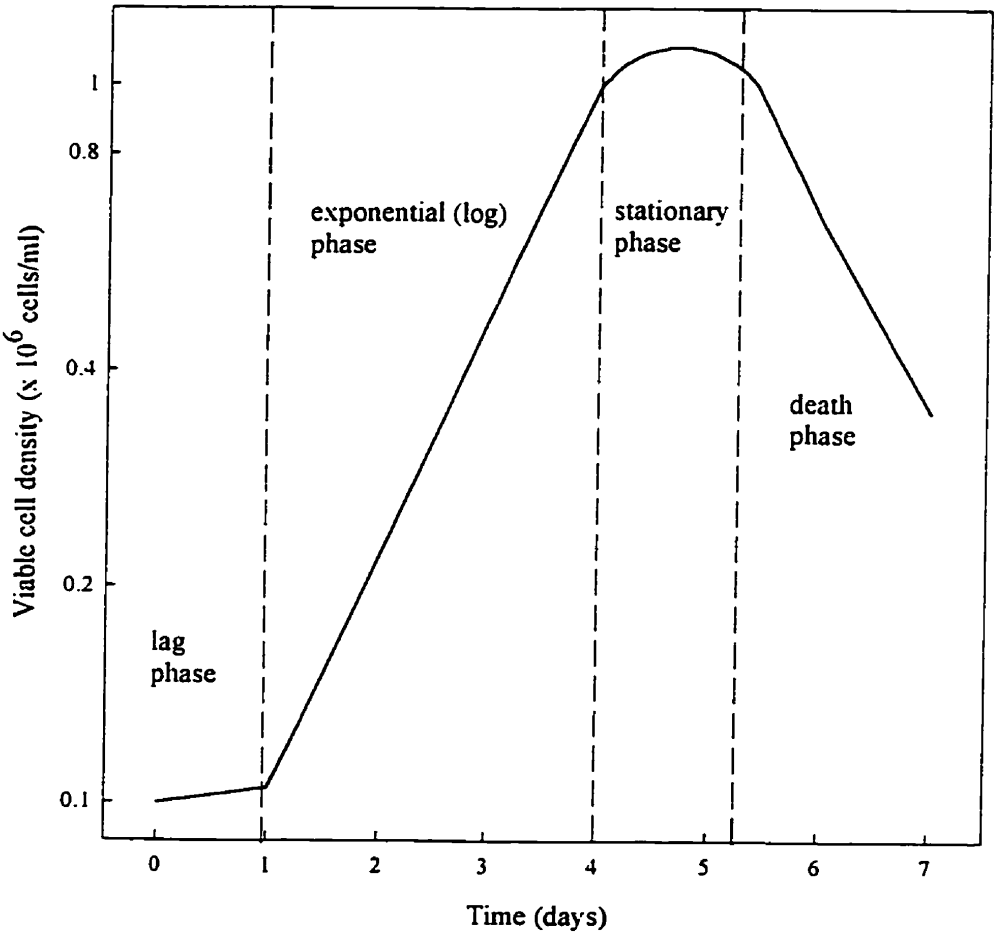

Figure 1.2 Typical hybridoma batch culture growth pattern (adapted from Butler, 1988) Growth phases are separated by dashed lines.

1.5 Glucose and glutamine metabolism

Glucose and glutamine are the two major energy and carbon sources of hybridoma metabolism (Butler and Jenkins, 1989; Miller *et al.*, 1989a, 1989b). The most heavily utilized of these components is glucose which is supplied at 5 - 25 mM in culture medium. A general scheme of glucose metabolism is shown in Fig.1.3. Glucose is primarily metabolized (> 90 %) via aerobic glycolysis, a pathway which converts the carbohydrate to lactate in the presence of oxygen and leads to the net formation of ATP (Fitzpatrick *et al.*, 1993; Petch and Butler, 1994). The almost complete conversion to lactate leads to a significant reduction of the medium pH value which is inhibitory for cell growth (Duval *et al.*, 1992). Glucose also supplies a relatively small percentage of energy via the tricarboxylic acid (TCA) cycle and the pentose phosphate pathway (Fitzpatrick *et al.*, 1993; Petch and Butler, 1994).

The pentose phosphate pathway also serves to convert glucose into ribose-5-phosphate, a nucleotide precursor (Zielke *et al.*, 1976; Reitzer *et al.*, 1980). HeLa and mouse L cells can grow indefinitely in the absence of glucose if a pyrimidine riboside source is added suggesting that supplying nucleotide precursors is the only essential function of glucose in animal cell cultures (Wice *et al.*, 1981). Other cell lines however stop growing in the absence of sugar even with supplementation with a pentose source (Zielke *et al.*, 1976). Inhibition of cell growth in the absence of glucose may be due to the lack of substrates for anabolic reactions such as protein and lipid glycosylation (Zielke, 1984). Glucose serves as a precursor of UDP-N-acetyl hexosamine, a nucleotide pool involved in protein glycosylation (Ryll *et al.*, 1994).

Glutamine provides the majority of its energy via the TCA cycle by complete oxidation to CO_2 or partial oxidation to 3 or 4 carbon metabolites which include aspartate, lactate or alanine. This partial breakdown of glutamine is known as glutaminolysis (McKeehan, 1982; Lanks and Li, 1988). The general scheme of glutamine metabolism is shown in Fig. 1.4. Energy derived from glutamine has been shown to provide 30 - 95 % of the energy for mammalian growth depending on the cell line and substrate concentration

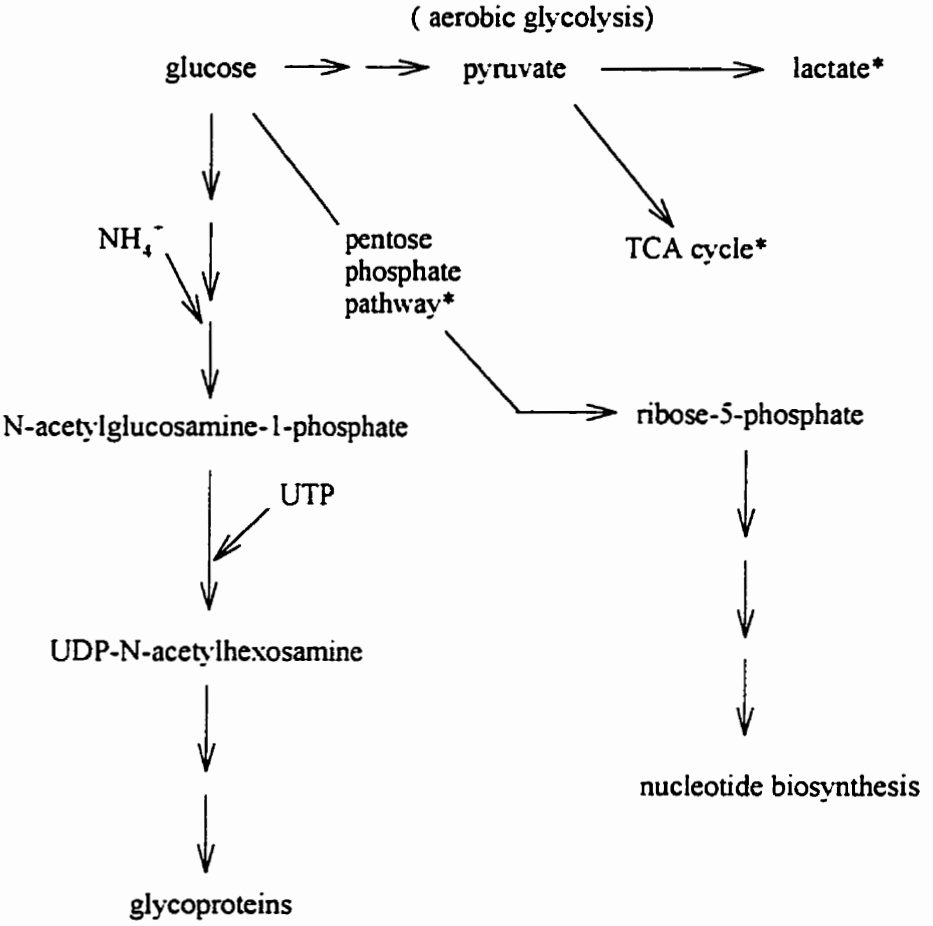

Figure 1.3 A general scheme of glucose metabolism in hybridoma cultures. * represents energy yielding pathways.

(Fitzpatrick *et al.*, 1993). Glutamine also has an essential role in the synthesis of nucleotides and proteins (Engstrom and Zetterberg, 1984)

One of the major by-products of glutamine metabolism is the ammonium ion which has been linked to cell growth inhibition in hybridomas (Doyle and Butler, 1990). Inhibition is possibly due to an intracellular rise in pH which may affect enzyme activity (Glacken, 1988). Alternatively, the channeling of energy towards maintaining ionic gradients over the cytoplasmic membrane rather than for cell biomass synthesis may inhibit growth (Martinelle and Haggstrom, 1993). Ryll *et al.* (1994) suggest that growth inhibition is due to the intracellular accumulation of UDP-N-acetyl hexosamine, a product of ammonium metabolism, which may alter glycosylation patterns of proteins.

Glucose and glutamine are extensively linked in maintaining nucleotide pools. Both substrates replenish energy reserves through catabolism in addition to providing the carbon and nitrogen backbones of newly synthesized nucleotide molecules.

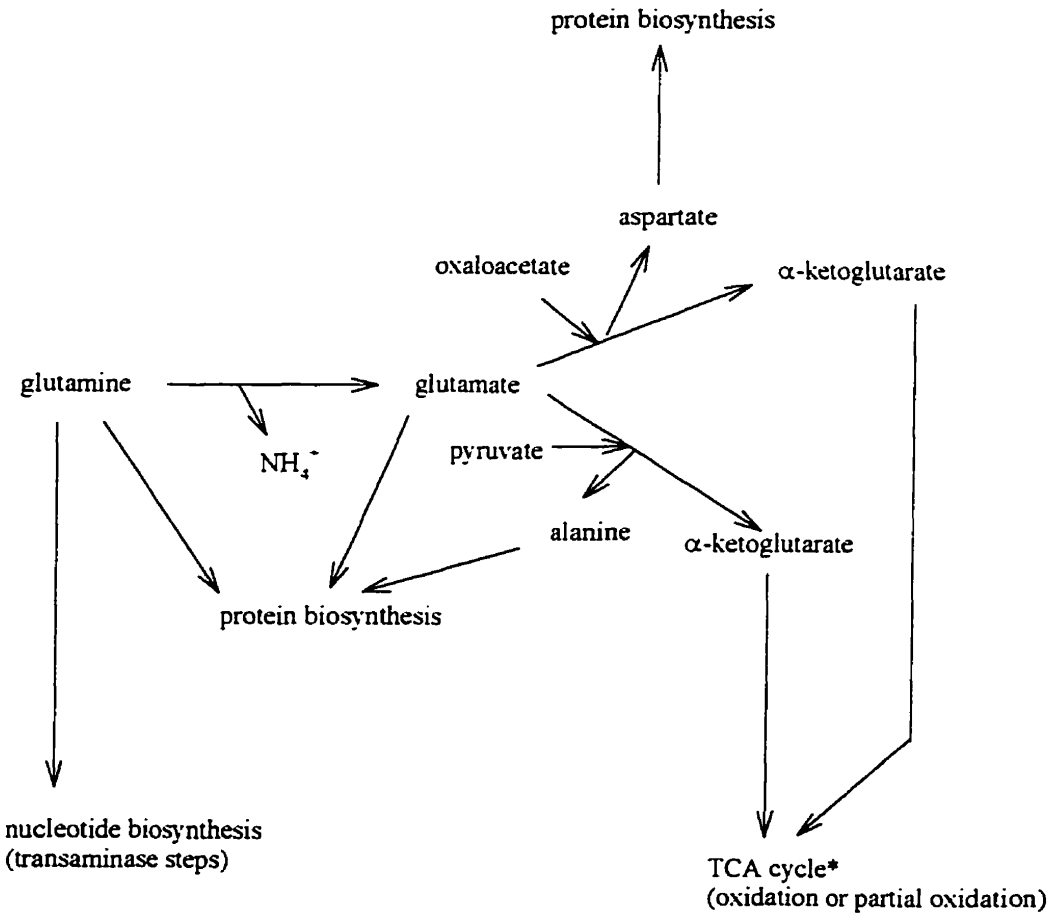

Figure 1.4 A general scheme of glutamine metabolism in hybridoma cell cultures.
* represents energy yielding pathways.

1.6 Monoclonal antibody production

Monoclonal antibodies have been shown to be produced in all four phases of a cell batch culture (Birch *et al.*, 1985; Velez *et al.*, 1986; Miller *et al.*, 1988a; Renard *et al.*, 1988). This indicates that hybridomas do not need to be dividing in order to produce and secrete monoclonal antibodies. Evidence that cell proliferation and Mab production can been uncoupled was also observed by using DNA synthesis inhibitors such as thymidine and cytoarabinoside (Hayter *et al.*, 1992; Modha *et al.*, 1992).

The productivity of hybridoma cultures is often measured as a total yield of Mab after several days of culture (Altschuler *et al.*, 1986; Velez *et al.*, 1986). Final Mab titers in batch and fed-batch cultures are determined by cell density, culture longevity and the specific Mab secretion rate. Total Mab yield however reflects the overall performance of the culture and does not indicate the changes in antibody secretion during the growth of the cells.

Although there is a general agreement that Mab is produced in all phases of growth there doesn't seem to be a consensus on whether Mab secretion rate is the same for all phases. Monoclonal antibody production appears to be constant throughout the growth of the cells in some cases (Velez *et al.*, 1986; Renard *et al.*, 1988). In other cases, there is an increased Mab accumulation during the stationary and death phases (Birch *et al.*, 1985; Emery *et al.*, 1987). There are two hypotheses regarding the increase in Mab during the late stages of growth. The increase may be due to the passive release of accumulated antibody in dead cells (Mohan and Lyddiatt, 1991; Leno *et al* .,1992) or due to an increase in the specific rate of antibody synthesis in viable cells (Birch *et al.*, 1985; Velez *et al.*,1986). The passive release theory is difficult to prove because of problems in distinguishing between active and passive release of antibodies.

Support for the active synthesis theory comes from studies that show that lower growth rates are concomitant with higher specific Mab production rates (qMab). Lower growth rates and higher qMab can be achieved by nutrient depletion, waste product accumulation, hyperosmotic stress, addition of DNA synthesis inhibitors or by lowering the dilution rate in chemostat and perfusion systems. (Birch *et al.*, 1985; Reuveny *et al.*,

1987; Dalili and Ollis, 1988; Hayter *et al.*, 1992; Martens *et al.*, 1993). Whether the lower growth rate is the direct cause of an increase in qMab is not known. However, some authors suggest that it is a stress related phenomenon (Miller *et al.*, 1988a; Oyaas *et al.*, 1989). The increase in Mab production at lower growth rates may be due to energy normally destined for growth processes being diverted toward non-essential protein synthesis or secondary metabolites (Modha *et al.*, 1992). Secondary metabolites such as antibiotics which are not essential for growth have been shown to be produced predominantly at low specific growth rates in microbial cultures (Martin and Demain, 1980).

Although hybridomas have been used extensively for the commercial production of monoclonal antibodies, predicting productivity is difficult. Commonly used parameters such as the rates of glucose and glutamine metabolism are unreliable (Glassy *et al.*, 1988, Costello, 1990). Other parameters such as dissolved oxygen level and ammonium accumulation correlate better with maximum cell density rather than antibody productivity (Reuveny *et al.*, 1986). Since antibody synthesis is an energy requiring process, evaluating the energetic/metabolic state of hybridomas may provide additional parameters in understanding growth and antibody kinetics of hybridomas. The metabolic state of cells may be evaluated by monitoring the intracellular adenine nucleotides levels as suggested by Atkinson (1977) or other pools such as pyrimidine or guanine nucleotides (Ryll *et al.*, 1994).

1.7 Intracellular nucleotides as a measurement of the cellular energetic/metabolic state of cells

Nucleotides are involved in many cellular reactions. In addition to being substrates for RNA and DNA synthesis, nucleotides act as energy carriers and play an important role in the regulation of cellular processes and pathways (Atkinson, 1977). Fluctuations in the nucleotide pools may therefore lead to changes in cell behavior such as cell transport, macromolecular synthesis, cell growth and viability.

1.7.1 Adenine nucleotides as metabolic regulators

The funneling of energy metabolism through the adenylate system has been developed extensively or retained throughout the evolution of all types of organisms (Atkinson, 1977). Cells utilize adenylates as common chemical intermediates to provide coupling between energy producing and energy consuming reactions (Lehninger, 1982). In hybridomas, 43-48 % of the total nucleotide pool can be accounted for by the adenylate fraction (Ryll *et al.*, 1991).

The adenylate fraction consists of adenosine triphosphate (ATP), adenosine diphosphate (ADP) and adenosine monophosphate (AMP). Of these three nucleotides, ATP has the central role in providing the driving force or "energy" for biosynthesis. By making the ATP-ADP couple part of a reaction pathway, the equilibrium position of a particular reaction may be displaced by several orders of magnitude depending on the relative concentrations of the adenylate nucleotides (Harold, 1986). This type of coupling permits the formation of products at physiologically useful concentrations (Atkinson, 1977).

For cells to function, the ratio of ATP/ADP must be kept high and relatively constant (Harold, 1986). To maintain this optimal ratio, cells increase the rate of ATP synthesis and reduce its consumption in response to intracellular adenylate concentrations. This regulation is provided by the allosteric inhibition or activation of key enzymes of ATP-regenerating and ATP-utilizing pathways by ATP, ADP and AMP (Atkinson, 1977). It is the ATP/ADP or ATP/AMP ratios that act as metabolic regulators rather than the actual adenylate concentrations. The binding sites of enzymes "sense" a ratio by having a high affinity for both nucleotides, with only one nucleotide causing the response (Harold, 1986). It is important to mention that adenylate control is only one of several regulatory inputs. Other controlling mechanisms may include feedback inhibition (Atkinson, 1968).

Enzymes involved in ATP synthesis pathways tend to be activated as the relative concentrations of ADP and AMP rise in the cell. Phosphofructokinase, pyruvate kinase, pyruvate dehydrogenase, citrate synthase and isocitrate dehydrogenase fall within this

category (Passonneau and Lowry, 1962; Atkinson, 1968; Shen and Atkinson, 1970). Enzymes involved in ATP consumption pathways exhibit the opposite type of control such that their activity is inhibited by increases in ADP or AMP relative concentrations. These enzymes include phosphoribosyl phosphate synthase, aspartate transcarbamylase and nucleoside diphosphokinase (Harold, 1986).

1.7.2 Adenylate energy charge

Because of the importance of all three adenylates in metabolism, Atkinson (1977) defined a mathematical expression (i.e. adenylate energy charge) to describe the energy status of the adenine nucleotide pool. The adenylate energy charge (or simply "energy charge") is an index of the fraction of the nucleotide pool that is charged with activated phosphoryl groups:

$$\text{energy charge} = \frac{\text{ATP} + 0.5\ \text{ADP}}{\text{ATP} + \text{ADP} + \text{AMP}} \qquad \text{(equation 1.1)}$$

Only ATP is present at a charge of 1, and only AMP is present at a charge of 0. At any intermediate value, there is a range of possible adenylate compositions. The actual relative concentrations of ATP, ADP and AMP at any given value of energy charge are determined by adenylate kinase which catalyses the following reaction (Atkinson, 1977; Harold, 1986)

$$2\ \text{ADP} \quad \text{<---------->} \quad \text{ATP} + \text{AMP} \qquad \text{(equation 1.2)}$$

Adenylate kinase catalyses the rapid return of the adenine nucleotide pool to equilibrium following a change in any one of its constituents. The equilibrium constant of the enzyme

is close to 1 and therefore does not alter the energy charge (Atkinson, 1977). Mutants lacking adenylate kinase are seriously impaired in growth and demonstrate the importance of maintaining a balanced adenylate system (Harold, 1986)

There are two types of enzymes that respond to changes in the energy charge (Atkinson, 1977). Enzymes that participate in sequences in which ATP is utilized respond to variations in the energy charge shown by curve U (Fig. 1.5). These sequences usually lead to the biosynthesis of cell components, storage compounds or secretory products (eg. Mabs). Enzymes participating in sequences in which ATP is regenerated respond to variations in the energy charge shown by curve R (Fig. 1.5). It is important to note that most energy charge responses are at the molecular level and depend on ATP/ADP or ATP/AMP ratios and not the ratio of all three adenylates (Atkinson, 1977).

Changes in the energy charge lead to the activation of pathways that in turn lead to its stabilization (Chapman *et al.*, 1971). Any tendency for the charge to fall would be resisted by the increases in the activity of ATP regenerating sequences (curve R) and decreases in the rates of ATP utilizing reactions (curve U). A tendency for the charge to rise would be opposed by the reverse processes.

In periods of metabolic stress when nutrient limitations prevent the generation of ATP, the energy charge may also be stabilized by adenylate deaminase in eukaryotic cells (Chapman *et al.*, 1976). Adenylate deaminase catalyses the production of inosine monophosphate (IMP) from the deamination of AMP (Chapman *et al.*, 1976). Removal of AMP would tend to raise the energy charge according to equation 1.1. Furthermore, removal of AMP will also tend to raise the ATP/ADP concentration ratio by the adenylate kinase reaction which is pushed to the right (equation 1.2). Adenylate kinase is activated when the energy charge falls and may be a useful means of limiting the extent of sudden drops in the nucleotide ratio (Chapman and Atkinson, 1973). Decreases in lymphocyte AMP have also been reported to be catalyzed by a membrane bound 5^{1}-nucleotidase which converts AMP to adenine (Matsumoto *et al.*, 1979).

A tabulation of values for various organisms shows that energy charge in generally stabilized near 0.85 in metabolizing cells (Chapman *et al.*, 1971). Energy charge values for tumorigenic cells, however, range for 0.64 for ovarian cancer cells to 0.92 for mouse

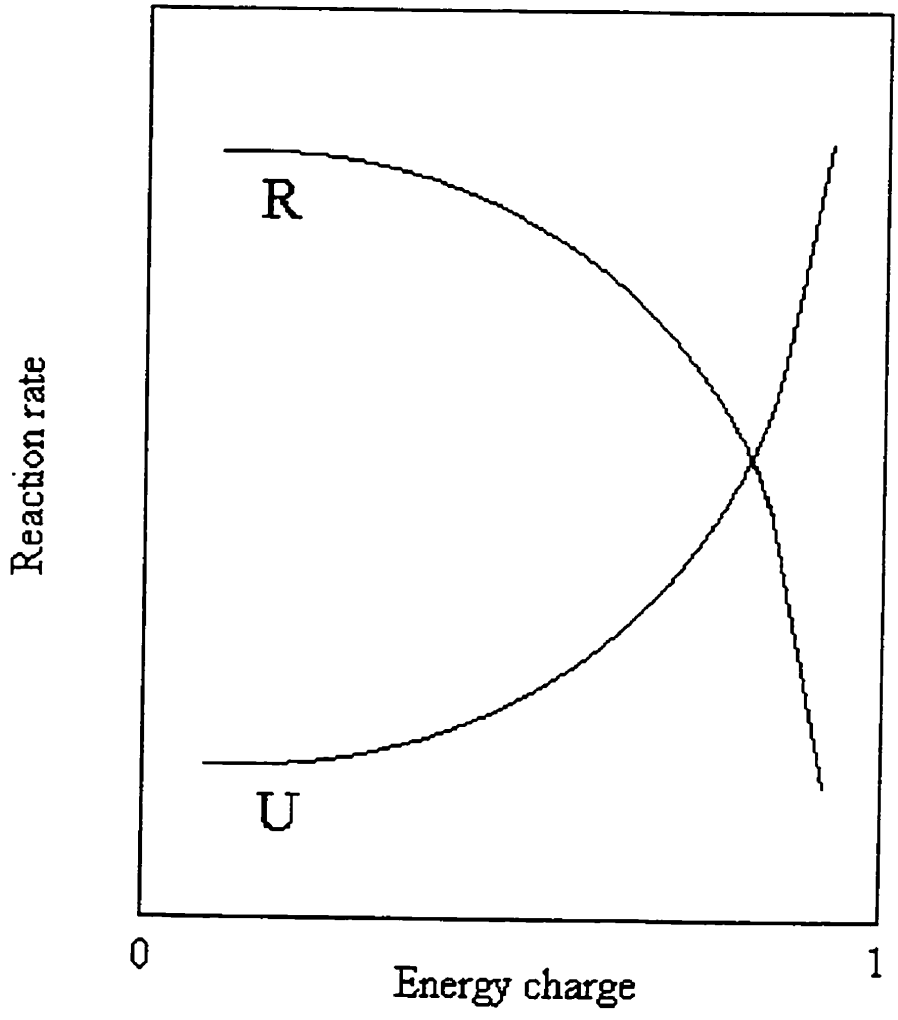

Figure 1.5. Responses of regulatory enzymes to energy charge (adapted from Atkinson, 1977). Curve R: Enzyme sequences where ATP is regenerated. Curve U: Enzyme sequences where ATP is utilized.

ascites tumor cells (Al-Wadi and Al-Bader, 1987). These values are probably not specific to particular cell types but may depend on the state of the cells in culture at the time of analysis. Findings suggest that energy charge is a more sensitive measure of changes in energy metabolism than adenine nucleotide content due to the energy charge's faster recovery after metabolic stress (Matsui *et al.*, 1994).

1.7.3 Adenylate nucleotides and energy charge parameters for monitoring growth, viability and protein synthesis

The importance of adenylates in metabolism has led to attempts to correlate energy charge values to cell culture behavior such as cell growth, cell survival (viability) and protein synthesis. Cellular growth in *E.coli* has been shown to be more sensitive to variations in energy charge than to the changes in the concentration of ATP or other intracellular nucleotides (Atkinson, 1977). Decreases in energy charge resulted in decreases in growth. However, this latter statement is not reciprocal since decreases in growth rate do not necessarily entail a decrease in energy charge. High energy charge values have been reported in the stationary phase of prokaryotes (Atkinson, 1977) and eukaryotes (Ryll *et al.*, 1991). Density inhibited Chinese hamster fibroblasts were shown to have the same energy charge as actively growing cells (Murphree *et al.*, 1974). Cell growth arrest with a DNA synthesis inhibitor also does not appear to alter the energy charge level in MAK 33 cells (Modha *et al.*, 1992).

Attempts have been made to correlate energy charge with cell viability or survival. It has been shown that a level of 0.5 was incompatible with life in most bacteria although a few types survived at energy charge values as low as 0.1 (Kristensen, 1989). Starvation studies with Chinese hamster ovary fibroblasts indicate that the regulation of energy charge is closely correlated with cell survival (Calderwood *et al.*, 1985). Other reports do not show this correlation as cells with energy charge levels as low as 0.26 (due to starvation) recuperated upon supplementation with glucose and glutamine (Live and Kaminska, 1975; Kristensen, 1989). The survival of cells in these experiments seem to correlate best with intracellular ATP levels. Cell death occurred below a critical low level

of ATP in human lung fibroblasts (Kristensen, 1989). Richter *et al.* (1996) proposed that the ATP level or energy charge are important determinants for the mode of cell death (i.e. apoptosis or necrosis). These conflicting reports lead to the conclusion that there is no simple correlation between energy charge, ATP and cell viability. The effect of energy charge and ATP on survival may depend on cell type. In addition, the compartmentalization of adenylates between the mitochondria and the cytosol in eukaryotes may complicate the assessment of the effect of energy charge on metabolism (Dawes, 1986).

Protein synthesis is an energy dependent process. Two high energy phosphate bonds of ATP are consumed in the synthesis of aminoacyl-tRNA (Lehninger, 1982). ATP is also required for binding of the 40S ribosomal subunit to mRNA and for the migration of the subunit toward the initiation codon (Rubin *et al.*, 1988). It is estimated that 60 % of cellular energy is used for amino acid polymerization (Stouthamer, 1979). The fraction of the total cellular energy required for Mab synthesis has also been estimated at 19.7 % for a high secreting hybridoma cell line (Butler, 1991).

The importance of ATP in protein synthesis has been demonstrated by several investigators who used metabolic inhibitors such as rhein and tributyltin-chloride (Castiglione *et al.*, 1990; Marinovich *et al.*, 1990). Inhibition of protein synthesis in these experiments was attributed to the impairment of ATP production. However, these studies do not explain the observation that protein synthesis can increase even though ATP concentration decreases (Swedes *et al.*, 1975). Rather, protein synthesis has been correlated to energy charge values. Metabolic studies with an *E.coli* mutant and Ehrlich ascites tumor cells demonstrated that decreases in protein synthesis parallel decreases in energy charge (Live and Kaminskas 1975; Swedes *et al.*, 1975). Changes in protein synthesis may be due to a hierarchy of ATP/ADP sensitivities among ATP utilizing reactions (Atkinson 1977; Brown, 1992). The anabolic and less essential processes such as the synthesis of polysaccharides, fats and non structural proteins would be shut down due to subtle changes in the ATP/ADP ratio in favor of more critical functions of the cell such as the biosynthesis of structural macromolecules and ion transport systems (Atkinson 1977; Brown, 1992). Changes in the energy charge alone, however, cannot fully explain

its effects on protein synthesis. Ehrlich ascite tumor cells with similar protein synthesis rates can have significantly different energy charge values (Live and Kaminskas, 1975).

Protein synthesis has also been shown to be inhibited by the accumulation of AMP or ADP which interferes with peptide chain elongation (Freudenberg and Mager, 1971). Since the accumulation of AMP and ADP results in a decreased energy charge, this is further evidence that energy charge is related to protein synthesis.

Although hybridomas have been used extensively for the commercial production of monoclonal antibodies, little information is published concerning their metabolism and even less concerning energy charge and ATP levels. Preliminary studies by Costello (1990) seem to indicate that the maximum level of monoclonal antibody production occurs during the death phase when the energy charge is also at its maximum. Modha *et al.*(1992) found that growth arrested hybridomas increased specific Mab production without affecting energy charge. It was suggested that the cessation of growth provided more available energy for the biosynthesis of non-structural or non-essential proteins such as Mabs (Modha *et al.*, 1992). Energy charge and energy levels (i.e. ATP concentration) may be a useful parameter for monitoring the productivity of hybridoma under different growth conditions.

1.7.4 Other nucleotide pools and ratios as metabolic parameters

Metabolic studies involving nucleotides have primarily focused on ATP, ADP and AMP because of their relative abundance in cells and their central role as energy carriers and regulators. Other nucleotides however are important in major biological processes. The uridine fraction (UTP + UDP-glucose + UDP-N-acetylhexosamine) which accounts for 30 - 35 % of the nucleotide pool in hybridomas supplies precursors for protein glycosylation (Ryll *et al.*, 1991). Increases in the UDP-N-acetylhexosamine pool has been correlated to the transformation of myelocytes and to the reduction in mammalian cell growth rates (De Korte *et al.*, 1987; Ryll and Wagner, 1991). Studies suggest that an imbalance in the uridine nucleotide pool may play a role in the regulation of glycosylation

by modulating glycosyltransferases (Sharma *et al.*, 1993). In mammalian cells, UTP also serves as a precursor of CTP, a nucleotide involved in phospholipid synthesis.

GTP acts as a regulator of lipid-mediated glycosylation reactions in animal cells (Bossuyt and Blankaert, 1993). Pall and Robertson (1988) propose that GTP provides energy for anabolic processes involved in growth and proliferation in eukaryotes and stimulates these processes by allosteric means. GTP-binding proteins also regulate intracellular vesicular trafficking and protein synthesis (Pall and Robertson, 1988; DeMatteis *et al.*, 1991; Stevens, 1993). GTP is essential for protein synthesis as it provides the primary source of energy for the initiation and elongation process (Rubin *et al.*, 1988).

Novel parameters such as the NTP ratio (ATP + GTP)/(UTP + CTP), U-ratio (UTP/UDP-N-acetylhexosamine) and the combined ratio NTP/U have been related to the different phases of growth cycle in hybridoma perfused batch cultures (Ryll and Wagner, 1992). The process for the production of recombinant interleukin-2 with Baby Hamster Kidney cells has been controlled by intracellular nucleotide pool measurements (Valley *et al.*, 1994). In this case, cultures were kept in an exponential growth phase by adjusting the perfusion rate of the bioreactor according to NTP and U ratio values. Other ratios such as the purine/pyrimidine, adenine/guanine, uracil/cytosine have been correlated to the transformation of myelocytes to the malignant state (De Korte *et al.*, 1987).

The regulatory potential of nucleotides in cell metabolism makes them good candidates for monitoring Mab productivity and cell viability in hybridomas. Understanding how antibody synthesis and cell death are regulated will ultimately lead to methods for enhanced productivity in large scale processes.

1.8 Aims of the Ph.D.

The amount of Mab that can be produced from a cell culture is dependent on factors such as the specific Mab production rate (qMab), the maintenance of cell viability (culture longevity) and the availability of nutrients. The main objective of this thesis was to determine whether these factors were related to the metabolic state of the cell.

Because of the broad role of nucleotides in cellular metabolism, intracellular levels and ratios of these metabolites were used to evaluate the metabolic state of the cells. Intracellular nucleotide levels have previously been shown to correlate to cell cycle phases, proliferation and transformation of animal cells (Rapaport *et al.*, 1979; De Korte *et al.*, 1987 Ryll and Wagner, 1991). It is therefore plausible that fluctuations in the nucleotide pools may also influence or depend upon other cell culture behavior.

The aims of the Ph.D. were to:

1) Test the hypothesis that specific Mab productivity is dependent upon the metabolic state of the hybridoma cell. (Re: Chapters 4 - 7)

Three approaches were used in investigating this hypothesis. First, the relationship between qMab and the metabolic state of the cells was determined. This was done by comparing intracellular nucleotide levels between hybridoma control cultures and hybridoma cultures with an altered qMab. It has been shown previously that the qMab can be altered by supplementing medium with a thymidine or sodium butyrate or by varying the cultivation temperature (Sureshkumar and Mutharasan, 1990; Hayter *et al.*, 1992; Oh *et al.*, 1993). In the second approach, the Mab-secreting hybridoma and non-Mab-secreting parent myeloma were compared for differences in intracellular nucleotide profiles. Differences in intracellular nucleotide pools between the two cell lines may be related to Mab synthesis. The third approach consisted of specifically altering the intracellular level of a nucleotide pool and determining the effects on the qMab. The specific nucleotide pool altered in these experiments (i.e. UDP-GNac) was chosen based on the results from the two first approaches.

Knowledge of the relationship between nucleotide pools and qMab was used to answer the following question: Can specific nucleotide levels or ratios be used as monitors of productivity?

2) Test the hypothesis that cell culture viability is dependent upon the metabolic state (intracellular nucleotide pools) of the hybridoma cell. (Re: Chapter 8)

To determine the relationship between nucleotide pools and cell culture viability, hybridomas were subjected to conditions that caused different rates of cell culture death. Intracellular nucleotide levels may give an early indication of loss of culture viability as defined by the ability of cells to exclude trypan blue. Trypan blue exclusion is a method of determining cell viability based on an assessment of the integrity of the cell membrane. Three question arose from these studies:

1. What is the predominant mode of cell death in hybridoma cultures (apoptosis or necrosis)
2. Can cultures be rescued once decreases in viability have begun.
3. Can intracellular nucleotides can be used as monitors of imminent cell death.

These questions were answered with respect to intracellular nucleotide levels.

3. Test the hypothesis that intracellular nucleotide levels are dependent upon the extracellular nutrient concentration. (Re: Chapter 9)

The ability of cells to derive energy from available nutrients is required for the maintenance of healthy cell cultures. Two major nutrients, glucose and glutamine are particularly important in hybridoma metabolism. Glucose and glutamine concentrations in the medium were compared to intracellular nucleotide levels in an effort to determine the contribution of each component to the cellular energetic state. Oxygen uptake at varying nutrient levels was evaluated to provide information on the contribution of substrate

oxidation to intracellular nucleotide maintenance. Understanding energy production in hybridomas can form the basis for the development of control strategies such as nutrient feeding which would ensure sufficient energy is available for maintaining culture viability and high antibody production.

4) Develop a serum-free medium for the culture of the CC9C10 hybridoma cell line. (Re: Chapter 3)

A chemically defined medium would eliminate problems associated with serum usage (i.e. variability of growth promoting properties, potential source of contamination, cost, etc.)

CHAPTER 2

Material and Methods

2.0 Chemicals and reagents

Chemicals and reagents used were obtained from Sigma Chemical Co. Ltd. unless otherwise stated. All aqueous solutions were prepared from purified water obtained after reverse osmosis followed by either distillation or Milli-Q (Millipore) filtration. Aseptic manipulations were carried out in a laminar flow cabinet (Nuaire Class II, Nuaire).

2.1 Growth media preparation

a) RPMI 1640 (Gibco)

Roswell Park Memorial Institute medium (RPMI 1640) was obtained as a glutamine-free (1x) strength liquid to which sterile glutamine was added prior to use. Glutamine was added at 2 - 4 mM from a 200 mM sterile stock solution (section 2.3).

b) DMEM (Gibco)

Dulbecco's Minimal Essential Medium (DMEM) was prepared in two ways. DMEM was originally obtained as a glutamine-free (1x) strength liquid to which sterile glutamine was added at 4 mM from a 200 mM sterile stock solution (section 2.3). In later studies, DMEM was obtained as a powder without glucose, glutamine, phenol red or sodium bicarbonate ($NaHCO_3$). DMEM powder was dissolved in 0.9x of the required volume of water and supplements were added: glucose, 4.5 g/L (25 mM); glutamine, 584

mg/L (4 mM); $NaHCO_3$, 3.7 g/L (44 mM) and phenol red, 15 mg/L. The medium was adjusted to pH 7.1 - 7.2 with 5M HCl prior to increasing to the final volume. The reconstituted powdered medium was sterilized by peristaltic pumping (pump model 5035, Watson-Marlow) through a 0.2 μm AcroCap filter (Gelman Sciences) into sterile bottles.

c) DMEM: Ham's F12 (1:1 mixture)

The 1:1 mixture of DMEM and Ham's F12 was prepared from powdered and liquid media as described in Table 2.1. DMEM powder (Gibco) was obtained without glucose, glutamine, $NaHCO_3$, or phenol red. Ham's F12 was obtained in three formats:

i. powder without $NaHCO_3$ (Gibco).

ii. powder without glucose and $NaHCO_3$ (Gibco).

iii. liquid without glutamine (Sigma).

The 1:1 mixture was dissolved in 0.9x of the required volume of water, adjusted to pH 7.1 - 7.2 and filtered sterilized as previously described (section 2.1.1b).

2.1.2 Serum-based media

Basal medium as prepared in section 2.1.1 was supplemented with 2 - 10 % (v/v) fetal bovine serum or iron-enriched calf serum (Gibco).

2.1.3 Commercial serum-free medium

Hybridoma Serum-Free Medium was purchased from Gibco as a ready to use (1x) strength liquid.

Table 2.1 Preparation of DMEM: Ham's F12 basal medium (1:1). Values are for preparing 1 liter of basal medium. All media contained final concentrations of $NaHCO_3$ (3.7 g/L) and phenol red (8.1 mg/L). According to needs, different glucose and glutamine concentrations were obtained by mixing media in the correct ratios or by removing/adding glucose and glutamine from original formulations.

DMEM/Ham's F12	1:1	1:1	1:1	1:1	1:1
Final glucose concentration (mM)	25	25	0	0	5
Final glutamine concentration (mM)	6	0.5	6	0.5	0
DMEM[a]	4.14 g	4.14 g	4.14 g	4.14 g	4.14 g
Ham's F12[b]	5.31 g	-----	-----	-----	-----
Ham's F12[c]	-----	4.41 g	4.41 g	4.41 g	-----
Ham's F12[d]	-----	-----	-----	-----	500 ml
$NaHCO_3$	3.70 g	3.70 g	3.70 g	3.70 g	2.52 g
Glucose	3.60 g	4.50 g	-----	-----	-----
Glutamine	805 mg	-----	805 mg	-----	-----
Phenol red	7.5 mg	7.5 mg	7.5 mg	7.5 mg	7.5 mg

[a]DMEM powder without glucose, glutamine, $NaHCO_3$ and phenol red.
[b]Ham's F12 powder without $NaHCO_3$ (contains glucose and glutamine).
[c]Ham's F12 powder without glucose and $NaHCO_3$ (contains glutamine).
[d]Ham's F12 powder without glutamine (contains glucose and $NaHCO_3$).

2.1.4 NB-SFM

NB-SFM consisted of DMEM: Ham's F12 in a 1:1 mixture supplemented with 10 μg/ml insulin, 10 μg/ml transferrin, 10 nm NaSe, 10 μM ethanolamine, 100 μM phosphoethanolamine and 0.1 % (w/v) Pluronic F-68. Supplements were added to the filter sterilized basal medium from stock solutions. All stock solutions were sterilized by filtration through a 0.2 μm syringe filter (Nalgene) or 0.2 μm AcroCap filter (Gelman Sciences). In standard NB-SFM, glucose and glutamine concentrations were 25 mM and 6 mM respectively.

Stock solutions

1) Insulin (5 mg/ml) - 30 mg bovine insulin was dissolved in 30 ml HCl (0.025 M). The solution was filter sterilized, aliquoted into 5 ml quantities and stored at -20°C.

2) Transferrin (5 mg/ml) - 30 mg bovine iron-saturated holo-transferrin was dissolved in 30 ml water. The solution was filter sterilized and stored at 4°C.

3) NaSe (10 μM) - 5.2 mg NaSe was dissolved in 30 ml water to make a solution of 1 mM. 250 μl of NaSe (1 mM) was diluted in 24.75 ml water to give 10 μM. The solution was filter sterilized and stored at 4°C.

4) Ethanolamine (4 mM) - 7.5 μl ethanolamine was diluted in 30 ml water. The solution was filter sterilized and stored at 4°C.

5) Phosphoethanolamine (50 mM) - 282.2 mg phosphoethanolamine was dissolved in 40 ml water. The solution was filter sterilized, aliquoted in 5 ml quantities and stored at -20°C.

6) Pluronic F-68 (10 % w/v) - 10 g Pluronic F-68 was dissolved in 100 ml water. The solution was filter sterilized and stored at 4°C.

2.2 Cell lines and stock culture maintenance

CC9C10 hybridoma and SP2/0 myeloma cell lines were obtained from the American Type Culture Collection, catalogue numbers HB123 and CRL1581, respectively. The CC9C10 hybridoma was produced by fusing lymph node cells of a bovine insulin immunized Balb/c mouse with the SP2/0 - Ag14 myeloma cell line (Schroer *et al.*, 1983). CC9C10 secretes an $IgG_{1\kappa}$ monoclonal antibody against bovine insulin. The SP2/0 myeloma cell line is a parent cell line of CC9C10 hybridomas and does not secrete monoclonal antibody.

Both cell lines were maintained in tissue culture flasks (T-flasks) containing growth medium. T-flasks were available in 25 cm^2, 75 cm^2, 150 cm^2 sizes and were typically used with 10, 30 and 50 ml medium respectively. Flasks were incubated in a humidified incubator (Nu2700 from NuAire) at 37°C with a 10 % CO_2 overlay. The caps of the flasks were left loose to allow for gaseous equilibration and pH stabilization of the medium. Routine subculturing of stock cells was done every 72 hours. Stock culture flasks were shaken to homogeneously suspend cells, a sample of cell suspension was then diluted 1:9 into a new flask. Alternatively, the viable cell density was determined (section 2.5.1) and the dilution factor was calculated to give a final cell density of 1 - 1.5 x 10^5 cells/ml.

Similar procedures as those described above were used for the preparation of T-flask cultures for growth and metabolic studies. Differences from this protocol are indicated for each experiment when necessary.

2.3 Cell culture feeding and pH adjustment

In experiments where it was desired to prevent glucose and glutamine limitation, cultures were fed daily starting on day 2 with 5 mM glucose/day and 1 μmol glutamine/10^6 cells per day. The addition of glutamine to flasks was based on the concentration of cells designated as control cultures for a particular experiment. This feeding regime was adapted from Reuveny *et al.* (1986). Glucose was added from a sterile stock solution of 1.5 M (stored at 4°C). Glutamine was added from a sterile stock solution of 200 mM (stored at -20°C). Stock solutions were sterilized by filtration through a 0.2 μm syringe filter (Nalgene).

The pH of cultures were adjusted visually to 6.8 - 7.0 (medium color: orange to red/orange) when needed by the dropwise addition of sterile sodium bicarbonate 1 M (pH 10.0). Within a given experiment, the same amount of $NaHCO_3$ was added to all flasks. The addition of $NaHCO_3$ to cultures typically raised the osmolarity from 335 mOsm/kg at the beginning of the culture to 374 mOsm/kg at the end of the culture.

2.4 Cryopreservation of cell lines and recovery from liquid nitrogen

Cells were frozen in liquid nitrogen for long periods of storage. A cell suspension from a mid-exponential phase culture was centrifuged at 200 x g for 5 min. The supernatant was discarded and the cell pellet was resuspended at 1 x 10^7 cells/ml in growth medium supplemented with 10 % (v/v) dimethylsulfoxide. The growth medium used for the resuspension was of the same formulation as the medium used to grow the cells. Aliquots (1 ml) of the cell suspension were transferred into cryogenic vials (Nalgene). Vials were placed at -80°C for 24 hours prior to transferring to a liquid nitrogen cylinder (Locator 8 Cryo Biological Storage System, Thermolyne).

For the recovery process, a vial of frozen cells was removed from the liquid nitrogen and thawed in a 37°C water bath. Pre-warmed growth medium (0.5 ml) was added to the vial, cells were suspended and then transferred to a sterile centrifuge tube

containing 10 ml growth medium. The cell suspension was centrifuged at 200 x g for 5 min. and the supernatant was decanted. The cell pellet was resuspended in 20 ml of fresh medium and transferred to two 25 cm^2 T-flasks for incubation at 37°C. After 24 hours, cells were counted (section 2.5.1) and subcultured as previously described (section 2.2).

2.5 Cell counting

2.5.1 Trypan blue exclusion method

Samples of cell suspension were diluted 1:1 with 0.2 % (w/v) trypan blue in Dulbecco's phosphate buffered saline (Gibco). Both grids of a Neubauer haemocytometer slide were loaded with the cell suspension and the number of cells present in four large squares of each grid were counted by microscopy. Cell counts were averaged from 8 squares and multiplied by 2.0 x 10^4 to give cells/ml. Cells which did not take up the dye were counted as viable, those that appeared blue were counted as non-viable. Total cell counts were calculated as the sum of viable and non-viable cells. The viability of a culture was determined by viable/total cells x 100 %.

2.5.2 Coulter counter

Total cell counts were made with a model Z_F Coulter Counter (Coulter Electronics Ltd.). The instrument was set to count particles greater than 10.0 μm. The aperture tube orifice was 100 μm and sampling volume was 0.5 ml. Cell samples (0.1 - 0.4 ml) were diluted in 20 ml of Isoton II buffer (Coulter Electronics Ltd.) in a Coulter cuvette. The cuvette was inverted for mixing prior to taking counts with the instrument. Isoton II buffer solution was used as a blank. Concentration of cells in the original sample were calculated as follows:

cell sample concentration = (diluted sample count - blank count)/ 0.5 ml x factor of dilution

2.6 Monoclonal antibody (Mab) analysis

2.6.1 Determination of Mab concentration by HPLC

Monoclonal antibody concentration was determined by affinity chromatography using the ProAna Mabs kit (Hyclone Lab Inc.). The kit consisted of the ProAna Mabs column (50 x 5 mm, 1ml), a pre-column filter and buffer concentrates. The ProAna Mabs column contained bacterial Fc receptor (Protein A) attached to a 10 μm silica support. The chromatographic system consisted of two HPLC pumps (Model 2150, LKB), a solvent conditioner (Model 2156, LKB), an HPLC controller (Model 2152, LKB) and a spectral detector (Model 2140, LKB). Sample injection was done through a manual valve fitted with a 1 ml loop. Chromatograms were collected by Wavescan software and analyzed using Model 2600 Chromatography software (PE Nelson). Both software programs were later replaced by EZChrom v.3.2 computer software (Shimadzu).

Binding buffer concentrate was diluted 1 in 20 in water and the pH adjusted to 5.0. Elution buffer concentrate was diluted 1 in 20 in water and the pH adjusted to 1.6. The pH was adjusted with 5M HCl or 10M NaOH. Water used for buffers was pre-filtered through a 0.2 μm AcroCap filter (Gelman Sciences) by peristaltic pumping. The gradient cycle for Mab detection is shown in Table 2.2.

Cell culture supernatant was diluted 1:1 or 1:2 in binding buffer prior to analysis. One ml of diluted sample was injected onto the column. Monoclonal antibody was detected by absorbance at 280 nm (Retention time: 2.9 min.). Quantitation of Mab was done by comparing the peak area to a standard peak area curve. Standards were prepared from polyclonal IgG (Hyclone Lab Inc.) diluted in binding buffer and ranging in concentration from 6.25 - 200 μg/ml.

Table 2.2 Gradient cycle for HPLC analysis of Mab

Time (min)	Binding buffer[a] (%)	Elution buffer[b] (%)	Flow rate (ml/min)
0 - 2	100	0	2
2 - 4	0	100	3
4 - 7	100	0	2

[a]Binding buffer concentrate (ProAna Mabs, Hyclone) diluted 1/20 in water, pH 5.0.
[b]Elution buffer concentrate (ProAna Mabs, Hyclone) diluted 1/20 in water, pH 1.6.

2.6.2 Mab purification

2.6.2.1 Affinity chromatography

Monoclonal antibody was purified with a protein A affinity column using a modified version of the manufacturer's protocol (Econo-Pac from BioRad Lab.). Three Econo-Pac protein A columns connected in series were attached to a Nalgene 0.2 μm pre-filter. The eluate was monitored by connecting the columns to a spectrophotometer (Ultrospec II, Pharmacia) equipped with a flow cell (Fisher) and a recorder (Model SE 120, ABB Goerz, AG). The columns were loaded with buffer or samples by a peristaltic pump (Model 101U, Watson Marlow). To equilibrate the system, binding buffer was run through the column assembly at 4 ml/min. for 10 minutes. Cell culture supernatant diluted with an equal volume of binding buffer was then loaded onto the affinity column at 1 ml/min. The column was subsequently washed with binding buffer (4 ml/min) until a stable absorbance at 280 nm was achieved. This was to ensure all unbound components were removed from the column. Monoclonal antibody was then eluted at 1 ml/min with 20 ml of elution buffer and collected as a peak at 280 nm. The Mab fraction was neutralized with 1.0 M Tris (pH 9.0) and dialyzed (section 2.6.2.2). The column was regenerated with 50 ml methanol (50 %) and re-equilibrated with binding buffer (4 ml/min). The column was cleaned periodically with 0.1 M NaOH. All buffer solutions were filtered with a 0.2 μm AcroCap filter (Gelman Sciences).

Buffer solutions

1) Binding buffer (0.1 M Tris; 1.5 M $(NH_4)_2SO_4$; pH 7.5)

12.11 g Tris base	
198.21 g $(NH_4)_2SO_4$	
~ 900 ml water	The pH was adjusted to 7.5 with 5 M HCl. The solution was made up to 1000 ml with water, filtered and stored at 4°C.

2) Elution buffer (0.1 M citrate-trisodium citrate dihydrate buffer, pH 5.0)

a) 5.76 g citrate was dissolved in 300 ml water.

b) 20.58 g trisodium citrate dihydrate was dissolved in 700 ml water.

Solution a) was added to 650 ml solution b) until the pH reached 5.0. The solution was filtered and stored at 4°C.

3) Neutralizing buffer (1.0 M Tris, pH 9.0)

12.11 g	Tris base	
~ 90 ml	water	The pH was adjusted to 9.0 with 5 M HCl. The solution was made up to 100 ml with water and stored at 4°C.

2.6.2.2 Dialysis

Neutralized Mab fractions were dialyzed against 4 liters of water containing 0.05 % (w/v) sodium azide at 4°C. Dialysis tubing with a molecular weight cutoff of 12 000 - 14 000 kD was used (Spectra/Por from Fisher). Dialyzed Mab was quantified by the bicinchoninic protein assay (section 2.11) and stored at -80°C in 5 ml aliquots. Samples were frozen in an angle to maximize surface area for lyophilization (section 2.6.2.3).

2.6.2.3 Lyophilization and reconstitution

Aliquots of monoclonal antibody prepared in section 2.6.2.2 were freeze dried by using a lyophilizer (Virtis). Caps from sample tubes were removed and replaced by parafilm. Three to four holes were punched through the parafilm to permit the escape of water vapor. Tubes were placed in a sealed dessicator unit and attached to the vacuum of the lyophilizer (-50°C) overnight. Lyophilized Mab was dissolved in water at a concentration of 0.5 - 5 mg/ml and stored at -80°C.

2.6.3 Mab deglycosylation

Monoclonal antibody was deglycosylated with N-glycosidase F (Boehringer-Mannheim Biochemica) following a modification of the manufacturer's protocol and Curling *et al.* (1990).

Add	21.3 µl	Purified Mab (5 mg/ml)
	1.2 µl	2-mercaptoethanol
	2.5 µl	10 % (w/v) SDS (sodium dodecyl sulfate)
	25 µl	

The Mab/mercaptoethanol/SDS solution was boiled for 3 minutes and then buffered with:

90 µl	phosphate buffer (275 mM Na_2HPO_4, 14 mM EDTA, pH 8.0)
10 µl	12.5 % Nonidet P-40

The buffered solution was mixed and aliquoted into 25 µl volumes. 1.5 µl N-glycosidase F (20 units/ml) or 1,5 µl water (control) was added to a 25 µl aliquot and the solution was incubated for 18 hours at 37°C.

2.6.4 SDS-PAGE

Electrophoresis of purified Mab was performed in a discontinuous polyacrylamide gel under reducing conditions according to the method of Laemmli (1970). The separating gel consisted of 8.55 % crosslinked polyacrylamide. The stacking gel consisted of 4 % crosslinked polyacrylamide. Minigels (7 cm x 8 cm) were run using the Mini-Protean II apparatus (BioRad Lab). The apparatus consisted of an electrophoretic cell, glass plates, combs and spacers (1.5 mm), and a casting stand assembly. Electrical current was supplied by an external power supply (Model 1000/500, BioRad).

2.6.4.1 Stock solutions

1) 30 % acrylamide/bis (BioRad)

14.6 g acrylamide

0.4 g N'N'-bis methylene acrylamide

Acrylamide was dissolved in water, made up to 50 ml, filtered and stored at 4°C in the dark.

2) 1.5 M Tris-HCl, pH 8.8

18.15 g Tris base was 70 ml water. The pH was adjusted to 8.8 with 1 M HCl. The solution was made up to 100 ml with water and stored at 4°C.

3) 0.5 M Tris-HCl, pH 6.8

6 g Tris base was dissolved in 60 ml water. The pH was adjusted to 6.8 with 1 M HCl. The solution was made up to 100 ml with water and stored at 4°C.

4) 10 % (w/v) SDS

10 g SDS was dissolved in water with gentle stirring and made up to 100 ml.

5) 0.05 % (w/v) Bromophenol blue

0.05 g Bromophenol blue was dissolved in 100 ml water.

6) Sample buffer

water	1ml
0.5 M Tris-HCl, pH 6.8	1 ml
glycerol	0.8 ml
10 % SDS	1.6 ml
2-mercaptoethanol	0.4 ml
0.05 % bromophenol blue	0.2 ml
	8 ml

7) 5x electrode buffer, pH 8.3

9 g Tris base

43.2 g glycine

3 g SDS

Added to 500 ml of water. The pH was adjusted to 8.3 with 1 M HCl. The solution was made up to 600 ml with water and stored at 4°C.

8) 10 % (w/v) ammonium persulfate (BioRad)

100 mg ammonium persulfate was dissolved in 1 ml water. The solution was prepared fresh daily.

2.6.4.2 Separating gel preparation (8.55 %)

4.5 ml	water
2.5 ml	1.5 M Tris-HCl, pH 8.8
0.1 ml	10 % SDS
2.85 ml	30 % acrylamide/bis

The 8.55 % acrylamide solution was deaerated under vacuum for at least 15 minutes. 50 µl of 10 % ammonium persulfate and 5 µl of TEMED (BioRad) were added after deaeration. The acrylamide/TEMED/persulfate mixture was immediately pipetted between the electrophoresis assembled glass plates so that the level was at least 1 cm below the expected level of the teeth of the comb. The acrylamide solution was overlaid with water-saturated isobutanol and allowed to polymerize for 45 minutes. After polymerization, the water-saturated isobutanol was rinsed off with distilled water and the top of the separating gel was dried with filter paper.

2.6.4.3 Stacking gel preparation (4 %)

6.1 ml	water
2.5 ml	0.5 M Tris-HCl, pH 6.8
0.1 ml	10 % SDS
1.3 ml	30 % acrylamide/bis

The 4 % acrylamide solution was deaerated under vacuum for at least 15 minutes. 50 µl of 10 % ammonium persulfate and 10 µl of TEMED (BioRad) were added after deaeration. The acrylamide/TEMED/persulfate mixture was immediately pipetted onto the separating gel and the comb placed between the plates making sure no air bubbles were trapped. The gel was allowed to polymerize for 45 minutes, the comb was then removed and the wells were rinsed with distilled water.

2.6.4.4 Sample and standard preparation

Molecular weight standards were purchased from Gibco-BRL: (myosin 200 kD; phosphorylase 97.4 kD; bovine serum albumin 68 kD; ovalbumin 43 kD; carbonic anhydrase 29 kD, B-lactoglobulin 18.4 kD and lysozyme 14.3 kD). Each standard was at a concentration of 1 mg/ml. Prior to use standards were diluted to 0.25 mg/ml in water. Samples (i.e. Mab at 0.5 mg/ml) or diluted standards were mixed 1:1 with sample buffer and boiled for 4 minutes.

2.6.4.5 Electrophoretic procedure

The lower and upper reservoirs of the electrophoretic cell were filled with 1x electrode buffer (i.e. combine 60 ml of 5x electrode buffer with 240 ml water). Sample

and standards were loaded into wells (25 µl/well). The MiniProtean II apparatus was set at 200 volts for 50 - 55 minutes.

2.6.4.6 Gel staining, MW determination and quantification

After the electrophoresis was complete, the gels were removed from the glass plates and placed for 30 min. in a staining and fixative solution (Coomassie blue R-250 in 40 % methanol/10 % acetic acid). Destaining of the gel to remove background coloration was done by placing the gel in 40 % methanol/10 % acetic acid for 1 - 3 hours. Gels were then placed on 3MM paper, covered in Saran wrap and dried in a slab gel dryer (Savant) at 70°C for 100 minutes. Gels were stored between glass plates.

Molecular weights were determined by comparison to the migration of protein standards. Stained gels were also analyzed with BioRad Gel Doc 1000 accompanied by Molecular Analyst Software (BioRad Lab.). Quantitative analysis of protein bands was based on the number of pixels in the bands subtracted by background values.

2.6.5 Western blot

Protein bands of unstained SDS-PAGE gels (section 2.6.4) were transferred to a 0.2 µm nitrocellulose paper by a modification of the method described by Towbin *et al.* (1979).

2.6.5.1 Stock solutions

1) 1.0 M Tris-HCl, pH 8.0

11.82 g Tris base was dissolved in 60 ml water. The pH was adjusted to 8.0 with 1 M HCl and the solution was made up to 75 ml with water.

2) Blotting buffer (25 mM Tris-192 mM glycine/ 20 % methanol, pH 8.3)

75 ml	1.0 M Tris-HCl, pH 8.0	
43.2 g	glycine	
600 ml	methanol	The solution was made up to 3 L with water. If necessary, the pH was adjusted to 8.3 with HCl or NaOH.

2.6.5.2 Preparation of the electrophoretic cell (BioRad)

1) Nitrocellulose paper (0.2 μm, Micron Separations Inc., USA) and 3MM paper were cut to match the size of the unstained polyacrylamide gel.

2) The polyacrylamide gel was pre-soaked in blotting buffer for a few minutes.

3) Two pieces of 3MM paper were briefly wet in blotting buffer and laid one on top of the other in the middle of the electrophoretic grid pad. Air bubbles were removed from the paper by rolling a Pasteur pipette over the surface of the paper.

4) The polyarylamide gel was placed "upside down" on the 2 pieces of 3MM paper and air bubbles were removed as in step # 3.

5) The nitrocellulose paper was wet briefly in blotting buffer and laid on top of the gel. Air bubbles were removed as in step # 3.

6) Two more pieces of 3MM paper were wet briefly in blotting buffer and laid on top of the nitrocellulose sheet. Air bubbles were removed as in step # 3 and the electrophoretic grid assembly was closed.

7) The electrophoretic cell chamber was filled with blotting buffer and the grid was submerged so that the acrylamide gel was facing the negative electrode and the nitrocellulose paper was facing the positive electrode.

8) The electrophoretic cell was connected to an external power supply (Model 1000/500, BioRad) and was run overnight at 5 volts.

9) The nitrocellulose sheet was air dried and stored at -20°C.

2.6.6 Glycosylation detection

Glycosylated proteins (i.e. Mab) were detected on nitrocellulose sheets with a carbohydrate detection kit (GlycoTrak from Oxford GlycoSystems). In brief, the carbohydrate moieties of glycoproteins are oxidized with periodate which generates aldehyde groups. These aldehyde groups react spontaneously with biotin-hydrazide and leads to the incorporation of biotin into the glycoprotein (Bayer *et al.*, 1990). The biotinylated glycoprotein is ligated to streptavidin-alkaline phosphatase conjugate and visualized with a substrate which reacts with the complexed enzyme to form a colored precipitate.

2.6.6.1 Stock solutions

1) Tris buffered saline (TBS), pH 7.2

6.05 g Tris was dissolved in 900 ml water and the pH was adjusted to 7.2 with 1 M HCl. NaCl (1.6 g) was added and the solution was made up to 1000 ml with water.

2) 200 mM sodium acetate buffer, pH 5.5

a) 6.80 g sodium acetate trihydrate was dissolved in 250 ml water

b) 600 µl acetic acid was diluted in 49.4 ml water

220 ml of solution a) was added to 30 ml solution b). The pH was checked and adjusted to 5.5 by adding dropwise amounts of solution a) or solution b)

3) 100 mM sodium acetate buffer, pH 5.5

Solution #2 was diluted 1:1 with water.

4) TBS/Mg, pH 9.5

1.21 g Tris base was dissolved in 80 ml water. The pH was adjusted to 9.5 with 0.1 M HCl. NaCl (0.58 g) and $MgCl_2.6H_2O$ (1.01 g) were added. The solution was made up to 100 ml with water.

6) Phosphate buffered saline (PBS), pH 7.2

575 mg	Na_2HPO_4
100 mg	NaH_2PO_4
800 mg	NaCl

Added to 400 ml water. The pH was adjusted to 7.2 with 1 M HCl or 1 M NaOH. The solution was made up to 500 ml with water.

7) Sodium acetate/ EDTA buffer

125 ml	200 mM sodium acetate, pH 5.5
465 mg	EDTA disodium salt

The solution was made up to 250 ml with water. The pH was not adjusted.

8) GlycoTrak solutions (A-F)

A. The contents of GlycoTrak vial A were emptied into 500 ml sodium acetate/EDTA to make 10 mM periodate.

B. 500 µl dimethylformamide was added to the contents of GlycoTrak vial B to make a biotin-hydrazide solution.

C. 0.5 g of GlycoTrak blocking reagent C was dissolved in 100 ml TBS by heating at 60°C for 45 min. (Some particulate material may not dissolve).

D. GlycoTrak Streptavidin-alkaline phosphatase, vial D- ready to use.

E. 1.3 ml 70 % (v/v) dimethylformamide was added to the contents of GlycoTrak vial D to make a nitroblue tetrazolium solution.

F. 1 ml dimethylformamide was added to the contents of GlycoTrak vial F to make a BCIP solution (5-bromo 4-chloro 3-indolyl phosphate). Some particulate material may not dissolve.

Stock solutions 1 - 7 and GlycoTrak solutions A - D were stored at 4°C. GlycoTrak solution E - F were stored in the dark at -20°C.

2.6.6.2 Labeling protocol

1) The nitrocellulose membrane blot was placed in a Petri dish and immersed in 15 ml PBS. The membrane was agitated at room temperature for 10 minutes. PBS was discarded after use.

2) The membrane was submerged in 15 ml of GlycoTrak solution A and agitated in the dark at room temperature for 20 minutes (i.e. The dish was wrapped in aluminum foil). The used solution was discarded

3) The membrane was washed 3 times using 15 ml fresh PBS. For each wash, the membrane was agitated at room temperature for 10 minutes. PBS was discarded after each wash.

4) 3 µl GlycoTrak solution B was added to 15 ml sodium acetate/EDTA buffer. The membrane was submerged in this solution and agitated at room temperature for 60 minutes. The TBS solution was discarded after use.

5) The membrane was washed 3 times using 15 ml fresh TBS. For each wash, the membrane was agitated at room temperature for 10 minutes. TBS was discarded after each wash.

6) The membrane was submerged in 15 ml GlycoTrak solution C and agitated at room temperature for at least 30 min or at 4°C overnight. The used solution was discarded and the membrane was washed as in step 5.

7) 7.2 µl GlycoTrak solution D was added to 12.5 ml TBS. The membrane was submerged in this solution and agitated at room temperature for 60 minutes. The used solution was discarded and the membrane was washed as in step 5.

8) 62.5 µl GlycoTrak solution E and 47 µl GlycoTrak solution F were added to 12.5 ml TBS/Mg and vortexed. This solution was made immediately prior to use. The membrane was submerged in this solution at room temperature and was not agitated. The blue-brown color was allowed to develop to the desired intensity (3 - 60 min). The membrane was rinsed several times with distilled water and allowed to air dry.

2.7 Nucleotide analysis

2.7.1 Nucleotide extraction

Samples of cell cultures (1 - 4 x 10^6 cells) were transferred to a 15 ml sterile centrifuge tube and sedimented at 350 x g for 8 minutes. The supernatant was aspirated and stored at -20°C. The cell pellet was resuspended in 120 - 150 µl ice-cold 6 % trichloroacetic acid, kept in an ice bath and sonicated for 15 seconds (Micron Ultrasonic Cell Disruptor, Mandel). The suspension was subsequently kept on ice for 15 - 20 min. The trichloroacetic acid/cell suspension was transferred to 1.5 ml centrifuge tube and sedimented at 14 000 x g for 10 minutes at 4°C. Supernatants were collected and neutralized with 27 µl Tris 0.5 M, pH 9.0 and 11.5 µl NaOH 2 M per 100 µl of trichloroacetic acid extract. Neutralized extracts were stored at -20°C.

2.7.2 Quantification of nucleotides by ion pair reverse phase HPLC

The HPLC hardware and computer software has been previously described (section 2.6.1). Instead of a manual injection valve, the system was linked to an autoinjector set to deliver 100 µl samples (Shimadzu SIL-9A). The spectral detector was set to read absorbances at 254 nm. An Adsorbosphere C-18 column (200 mm x 4.6 mm I.D., 5 µm particle size, Alltech) was used with a guard column containing the same adsorbant (Waters). Nucleotides were separated by using a gradient of two buffers modified from Ryll and Wagner (1991). Two gradient profiles were used (i.e. Gradient 1 and Gradient 2), both of which separated 11 nucleotides.

Gradient 1: 100 % buffer A for 2.5 min., 0 - 40 % buffer B for 14 min., 40 - 100 % buffer B for 8.5 min., 100 % buffer B for 12 min., 100 - 0 % buffer B for 4 min., 100 % buffer A for 9 min. Total run time: 50 min. Flow rate 1.5 ml/min.

Gradient 2: 0 - 20 % buffer B for 5 min., 20 - 24 % buffer B for 10 min., 24 - 60 % buffer B for 5 min., 60 - 100 % buffer B for 8.5 min., 100 % buffer B for 12 min, 100 - 0 % buffer B for 4 min., 100 % buffer A for 8 min. Total run time: 52.5 min. Flow rate 1.5 ml/min.

Nucleotide peaks were identified by comparing retention times with standard mixtures and by spiking samples with standards. Quantitation was performed by comparing the sample peak area to a standard peak area curve at 254 nm. A typical chromatogram of a cell extract is shown in Figure 2.1. Good separation of all nucleotides was achieved with a new column. As the column aged, the UTP and ADP peaks fused. In this case, the UTP peak area was determined by subtracting the calculated peak area of ADP concentration as determined by luminometry (section 2.7.3), from the fused peak area.

The possibility of interference with aromatic amino acids was considered by spiking with amino acid standards. Tryptophan was the only amino acid which coeluted with a nucleotide (UDP-GalNac). However, a positive identification of the nucleotide was made by determination of the characteristic absorbance ratio (A_{280}/A_{254}) of 0.33, which differed significantly from the corresponding ratio for tryptophan (1.98).

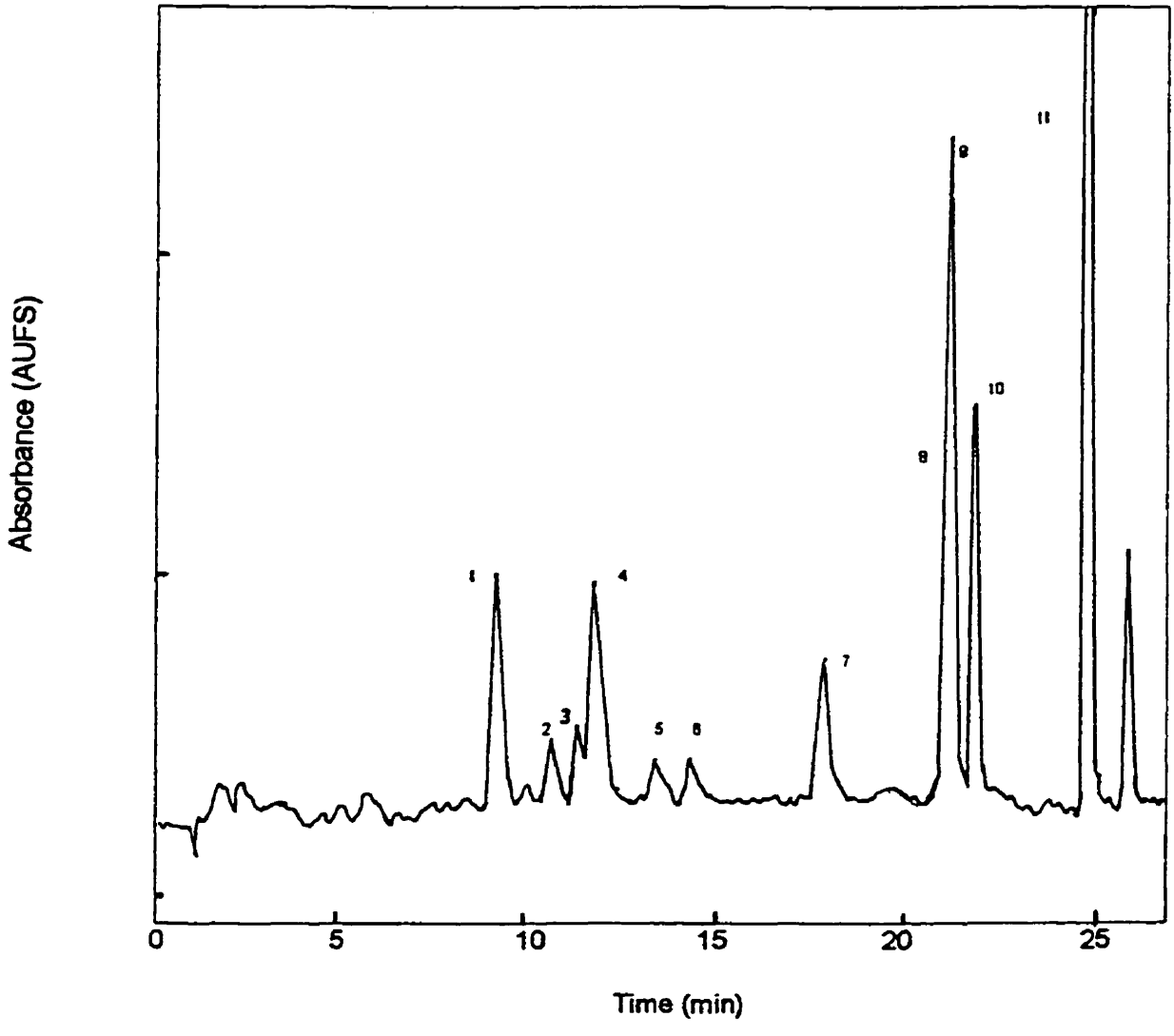

Figure 2.1 Gradient profile and chromatogram of a cell extract from a fed-batch culture of CC9C10 hybridomas. Peaks: 1 = NAD, 2 = UDP-Glucose (UDP-Glc), 3 = UDP-N-acetyl galactosamine (UDP-GalNac), 4 = UDP-N-acetyl glucosamine (UDP-GlcNac), 5 = AMP, 6 = GDP, 7 = CTP, 8 = ADP, 9 = UTP, 8 + 9 = ADP + UTP, 10 = GTP, 11 = ATP. All other peaks are unknown components.

2.7.2.1 HPLC buffers

1) Buffer A

46.8 g	KH_2PO_4	
9.6 g	K_2HPO_4	
10.88 g	tetrabutyl ammonium hydrogen sulfate	

Dissolved in 3.8 L water. The pH was adjusted 5.3 with 85 % (v/v) phosphoric acid. The solution was made up to 4 liters with water and filtered through a 0.2µm AcroCap filter.

2) Buffer B

1050 ml	buffer A	
450 ml	methanol (HPLC grade)	The pH was adjust to 5.9 with 2.5 M KOH.

2.7.2.2 Preparation of samples and standards

Nucleotide extracts were diluted 1:1 with a 50 % (v/v) solution of buffer A. Samples were mixed by vortex and centrifuged at 14 000 x g for 10 min at 4°C. Standards were prepared as follows:

1) standard 1 (2.78×10^{-5} M)

40 µl each of 1×10^{-3} M NAD, UDP-Glc, UDP-GalNac, AMP, GDP, CTP, UTP.

+ 440 µl	water	
+ 720 µl	50 % buffer A.	The solution was mixed and centrifuged as with samples.

2) standard 2 (5.56×10^{-6} M)

100 µl standard 1 + 200 µl water + 200 µl 50 % buffer A.

The solution was mixed and centrifuged as with samples.

3) standard 3 (2.78×10^{-5} M)

40 µl each of 10^{-3} M ADP, ATP, GTP, UDP-GlcNac.

+ 560 µl water

+ 720 µl 50 % buffer A. The solution was mixed and centrifuged as with samples.

4) standard 4 (5.56×10^{-6} M)

100 µl standard 3 + 200 µl water + 200 µl 50 % buffer A.

The solution was mixed and centrifuged as with samples.

5) standard mix

Standard 1 and standard 3 were mixed in a 1:1 ratio. The standard mix was used at the beginning of each multiple run to monitor retention time and column resolution.

2.7.2.3 HPLC column and autoinjector set-up

To avoid precipitation in the HPLC pumps and lines, water must be flushed through the system before the addition of buffer A and buffer B.

1) The C-18 column was connected to the HPLC system and the methanol content reduced in the column from 70 % to 0 % by replacement with 0.2 µm filtered water (Flow rate 1.5 ml/min). All lines were purged with water for 5 minutes.

2) The 20 % ethanol in the purging system of the autoinjector was replaced with 0.2 µm filtered water. Autoinjector lines were purged with water for 5 minutes.

3) The water in the solvent conditioner was replaced with buffer A and buffer B. The HPLC lines were then purged with both buffers. The flow rate was set at 1.5 ml/min. at 100 % buffer A. The HPLC system and autoinjector were now ready for sample loading and initiation of the gradient protocol (2.7.2)

2.7.2.4 Column storage

To store the column, buffer A and buffer B in the solvent conditioner were replaced with 0.2 μm filtered water. The system was flushed at 1.5 ml/min for 20 minutes with water. Buffer B was then replaced with 100 % methanol and a gradient was run from 0 - 100 % buffer B at 1.5 ml/min. (i.e. a step increase of 10 % buffer B each 10 minutes was used). 100 % buffer B was then run for 10 minutes and decreased to 70 % buffer B for another 10 minutes. The column was removed and stored at room temperature.

2.7.3 Quantification of adenylate nucleotides by luminometry

2.7.3.1 Principle

Adenyl nucleotides were quantified by using a modified bioluminescent assay (Lundin *et al.*, 1986). This assay is based upon the quantitative measurement of a stable level of light produced from the reaction catalyzed by firefly luciferase in the presence of ATP (equation 2.1). Light emission was measured with a luminescence photomoter (Luminometer 1250, LKB-Wallac) linked to a chart recorder (Model SE 120, ABB Goerz, AG).

$$ATP + luciferin + O_2 \xrightarrow[\text{luciferase}]{\text{firefly}} oxyluciferin + AMP + PPi + CO_2 + light \quad \text{(Reaction \# 1)}$$

The intensity of light emission is directly proportional to the ATP concentration ranging from 10^{-6} M to 10^{-13} M. ADP and AMP can quantified by the bioluminescent method after enzymatic conversion to ATP.

1) ADP conversion to ATP

2 ADP + 2 phosphoenolpyruvate ---------> 2 ATP + 2 pyruvate (Reaction # 2)
pyruvate kinase

2) AMP conversion to ATP

AMP + CTP ---------> ADP + CDP (Reaction # 3)
myokinase

ADP ---------> ATP (see Reaction # 2))

2.7.3.2 Stock solutions

1) 1.0 M potassium acetate

0.98 g potassium acetate was dissolved in 10 ml water and stored at 4°C.

2) Tris-acetate buffer (0.1M Tris, 6mM EDTA)

1.21g Tris base

0.06g. EDTA (free acid)

Dissolved in 80 ml water. The pH was adjusted to 7.75 with acetic acid (2 M). The solution was made up to 100ml and stored at 4°C.

3) ATP-MR (ATP monitoring reagent, luciferin-luciferase-Mg)

1 vial ATP monitoring reagent (LKB-Wallac) was reconstituted with 4200 µl Tris-acetate buffer and 1050 µl 1 M potassium acetate. Aliquots (1050 µl) were stored at - 20°C.

4) ATP standard (10^{-5} M)

1 vial ATP standard (LKB-Wallac) was reconstituted with 10 ml water. Aliquots (300 µl) were stored at - 20°C.

5) 0.2 M Phosphoenolpyruvate (PEP)

125 mg tricyclohexylammonium salt of phosphoenolpyruvate was dissolved in 1375 µl Tris-acetate buffer. Aliquots (60 µl) were stored at - 20°C.

6) Pyruvate kinase (2000 U/ml)

Pyruvate kinase (5000 U, Sigma P9136) was dissolved in 2.5 ml Tris-acetate buffer. Aliquots (60 µl) were stored at - 20°C.

7) Myokinase (1750 U/ml)

Myokinase (5000 U, Sigma M5520) was dissolved in 10-fold diluted Tris-acetate buffer. Aliquots (120 µl) were stored at - 20°C.

8) 110 mM CTP

25 mg CTP (Sigma C9274) was dissolved in 100 µl Tris 0.5 M pH 9 (Tris-buffer). 20 µl aliquots of Tris-buffer was then added until the pH was between 6 - 7. The solution was diluted up to 400 µl with water. Aliquots (12 µl) were stored at - 20°C.

2.7.3.3 Luminometry reagents (20 assays)

1) ATP-MR - 1 aliquot of 1050 µl kept on ice.

2) PK - 60 µl PEP (0.2 M) + 60 µl pyruvate kinase (2000 U/ml), kept on ice.

3) MK - 12 µl CTP (110 mM) + 120 µl myokinase (1750 U/ml) kept on ice.

4) ATP standard - 1 aliquot of 300 µl kept on ice.

5) TA buffer - Tris-acetate buffer (0.1M Tris, 6mM EDTA) kept at room temperature.

6) TCA blank - 100 µl 6% (v/v) TCA + 27 µl Tris (0.5 M, pH 9) neutralized with 2 M NaOH.

2.7.3.4 Luminometry assays

Assays were performed in luminometer polystyrene cuvettes. Solutions were mixed in cuvettes at the lowest vortex speed. Light emission were read after each step until a stable line was achieved. After each completed assay, the cuvette was rinsed immediately with distilled water. For more thorough cleaning, cuvettes were rinsed with distilled water and filled with 1 M HCl overnight.

a) Blank assay (Figure 2.2A)

1. Combine 430 µl TA buffer + 50 µl ATP-MR + 5 µl TCA blank .
2. Add 5 µl PK
3. Add 5 µl MK

b) standard assay (Figure 2.2B)

1. Combine 430 µl TA buffer + 50 µl ATP-MR + 5 µl TCA blank.
2. Add 10 µl ATP standard (ST1).
3. Add 5 µl PK.
4. Add 10 µl ATP standard (ST2).
5. Add 5 µl MK-CTP.
6. Add 10 µl ATP standard (ST3).

c) sample assay (Figure 2.2C)

1. Combine 430 µl TA buffer + 50 µl ATP-MR + 5 µl TCA blank.
2. Add 10 µl sample (TCA nucleotide extract -section 2.7.1)
3. Add 5 µl PK.
4. Add 5 µl MK.

2.7.3.5 Calculation of ATP, ADP and AMP concentration

Refer to Figure 2.2

$$\text{ATP in sample } (\mu M) = \frac{sATP\ (V)}{ST1\ (V)} \times \text{concentration of ATP standard.}$$

$$\text{ADP in sample } (\mu M) = \frac{sADP\ (V) - PK\ (V)}{ST2\ (V) - PK\ (V)} \times \text{concentration of ATP standard.}$$

$$\text{AMP in sample } (\mu M) = \frac{sAMP\ (V) - MK\ (V)}{ST3\ (V) - MK\ (V)} \times \text{concentration of ATP standard.}$$

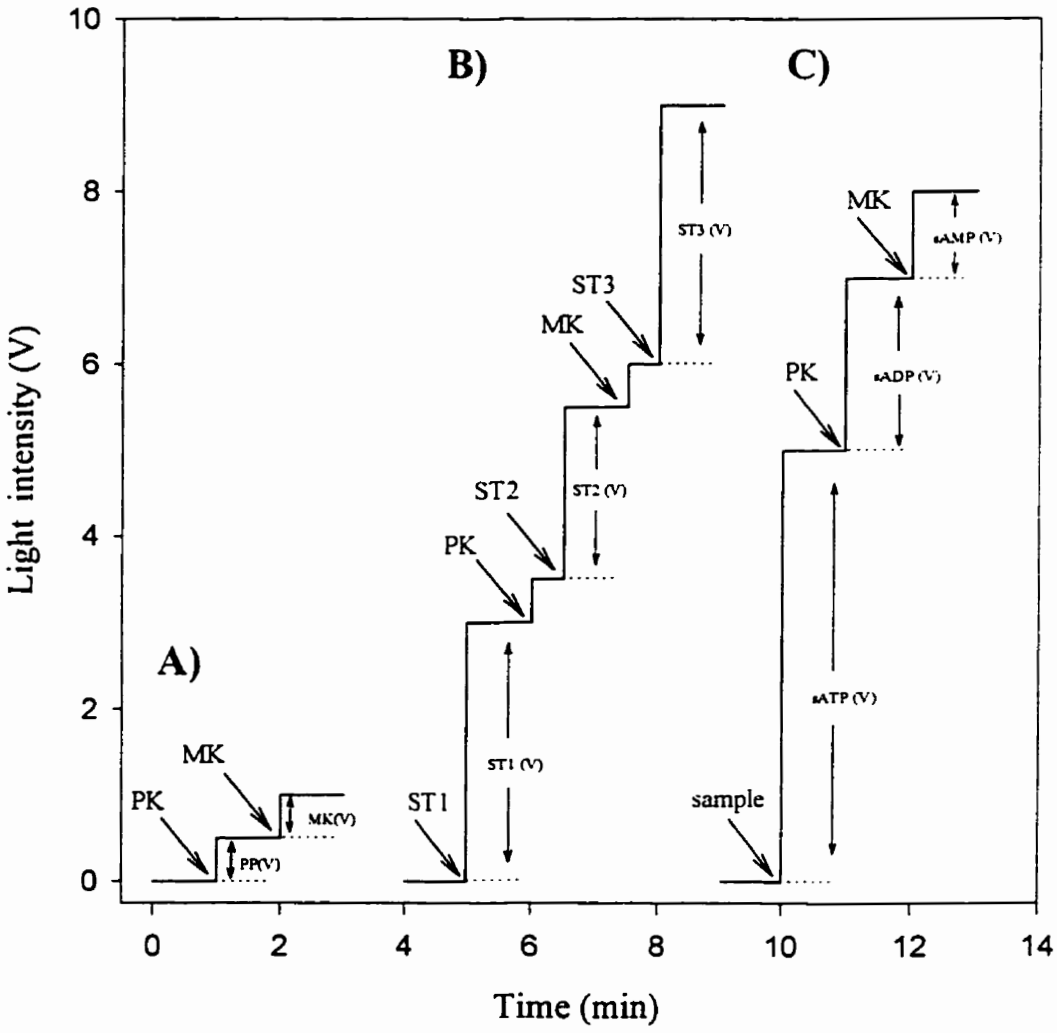

Figure 2.2 Measurement of ATP, ADP and AMP concentration with a bioluminescent assay. A) blank assay; B) standard assay; C) sample assay.
PK - pyruvate kinase + phosphoenolpyruvate; MK - myokinase + CTP; ST1 , ST2 and ST3 - ATP standards (10^{-5} M).

2.8 Glucose and lactate analysis

Cell culture supernatants (25 µl) were injected into a YSI Model 27 glucose/lactate analyzer (YSI Instruments) containing a glucose oxidase or lactate oxidase membrane. The analyzer was calibrated with either glucose standards (YSI Instruments, glucose 200 mg/ml or 500 mg/ml) or lactate standards (YSI Instruments, lactacte 15.00 mM). The analyzer was calibrated after every 5 - 6 samples. In cases where lactate concentrations exceeded detection limits, cell culture supernatants were diluted 1:2 with distilled water.

2.9 Glutamine analysis

2.9.1 Principle

The concentration of glutamine in cell culture supernatant was quantified by a modification of an enzymatic method described by Lund (1985). Glutamine was first converted to glutamate by glutaminase at pH 5.0 (Reaction # 1). In Reaction # 2, glutamate conversion to 2-oxoglutarate by glutamate dehydrogenase was coupled to the reduction of NAD+ to NADH. To overcome the unfavorable kinetics a high concentration of NAD, a low proton concentration (pH 9.0) and a trapping agent for 2-oxoglutarate (hydrazine hydrate) were used. The ADP in Reaction # 2 is a glutamate dehydrogenase activator. The formation of NADH is proportional to the concentration of glutamate and was measured by the change in absorbance at 340 nm.

$$\text{L-glutamine} + H_2O \xrightarrow[\text{glutaminase},\ H^+]{} \text{L-glutamate} + NH_4^+ \qquad \text{(Reaction \# 1)}$$

$$\text{L-glutamate} + NAD^+ + H_2O \xrightarrow[\text{ADP}]{\text{glutamate dehydrogenase}} \text{2-oxoglutarate} + NH_4^+ + NADH \qquad \text{(Reaction \# 2)}$$

2.9.2 Stock solutions

1) Acetate buffer (0.5M, pH 5.0)

a) 6.8 g sodium acetate trihydrate was dissolved in water and made up to 100 ml.

b) 2.9 ml acetic acid was diluted with 100 ml water

67.8 ml of solution (1a) was mixed with 32.2 ml solution (1b). The pH was checked and adjusted to pH 5.0 if necessary with solution (1a) or (1b).

2) Glutaminase (10 kU/L)

Glutaminase (Sigma G5382) was dissolved in 10 fold diluted acetate buffer to obtain 10kU/L. The solution was aliquoted into 250 µl quantities.

3) Hydroxylamine hydrochloride(20mM)

13.9 mg hydroxylamine hydrochloride was dissolved in 10 ml water

4) L-glutamine standard (100mM)

146 mg L-glutamine was dissolved in 10 ml water.

5) Tris-EDTA (Tris 0.25M, EDTA 5mM)

3g Tris base and 185 mg disodium EDTA was dissolved in 100 ml water.

6) Hydrazine hydrate 64% (w/v)

7) β-NAD (30mM)

200 mg β-NAD (free acid) was dissolved in 10 ml water. Aliquot were made in 1.5 ml quantities.

8) ADP (100mM)

48.0 mg ADP-sodium salt was dissolved in 800 ml water, neutralized with 50 - 100 µl NaOH (2M), and made up to 1 ml with water. Aliquot were made into 150 µl quantities.

9) Glutamate dehydrogenase (GDH)

Sigma G2626 , 2500 kU/L

10) Tris/Hydrazine buffer

9 ml Tris-EDTA (5) + 1.125 ml hydrazine hydrate (6) were mixed together and the pH adjusted to 9.0 with 5 M HCl. The solution was made up to 15 ml with water. The Tris/hydrazine buffer was stable for 1 week at 4°C.

Solutions 1, 3, 5 and 9 were stored in 4°C. Solutions 2, 4, 7, 8 are stored at -20°C.

2.9.3 Assay

The following solutions were made prior to use. Quantities were sufficient for one 96 well plate analysis.

Solution A: 2.16 ml acetate buffer (1)
1.08 ml hydroxylamine (3)
1.155 ml water

Solution A was kept in a 37°C water bath, and 108 µl glutaminase(2) was added prior to use.

Solution B: 2.16 ml acetate buffer (1)
1.08 ml hydroxylamine hydrate (3)
1.265 ml water

Solution B was kept in a 37°C water bath

Solution C: 9.6 ml Tris/ hydrazine (10)

3.1 ml water

This solution was put in a 37°C water bath for 15 min. 1.44 ml NAD (7) , 144 µl ADP (8) and 90 µl GDH (9) were then added to just prior to use.

Glutamine : standard stock solution (4) was diluted in water to give doubling dilutions ranging from 0.5mM to 0.03125mM

2.9.4 Procedure

A 96 well plate (NUNC) was divided into 2 sections. The first section (A) was treated with solution A (conversion of glutamine to glutamate). The second section (B) was treated with solution B (no conversion).

1) 70 µl samples were pipetted into wells. Each sample was present in both sections (A and B) of the 96 well plate. 70 µl standard glutamine solutions were pipetted on the solution A section (in duplicate).

2) 50 µl solution A was added to wells in section A. 50 µl solution B was added to wells in section B. The plate was covered with parafilm and incubated in a Thermomax multiplate reader (Molecular Devices) or in a CO_2 incubator for 75 min. at 37°C.

3) After the incubation period, 120 µl solution C was added to all of the wells. The plate was covered with parafilm and incubated in a Thermomax multiplate reader (Molecular Devices) or in a CO_2 incubator for 30 min at 37°C. After the incubation period, absorbance was read at 340 nm with the Thermomax multiplate reader and data was analyzed with Softmax software (Molecular Devices).

4) To calculate the concentration of glutamine in a sample, the absorbance at 340 nm was compared to the linear glutamine standard curve. Values for samples in section B (x) were then subtracted from values for samples in section A (glutamine + x). X was the background value of glutamate and interfering amino acids.

2.9.5 Preparation of samples

Samples to be treated with solution A had glutamine concentrations in the range of 0.05mM - 0.5mM for analysis. Samples were diluted with water to fall within this range. If the expected glutamine concentration was between 2 - 6 mM, samples were diluted 1/15 and 1/10. If the expected glutamine concentration was between 0 - 1 mM, samples were diluted 1/5, or not diluted.

Samples to be treated with solution B had glutamate concentrations in the range of 0.05mM - 0.5mM. Dilutions of 1/5 and no dilution of samples were found to be sufficient to fall within this range in batch culture samples.

2.10 Ammonium ion analysis

The concentration of ammonium ion (NH_4^+) in a sample was determined by converting NH_4^+ to ammonia gas (NH_3) by the addition of concentrated NaOH. The amount of NH_3 formed in the reaction was directly proportional to the NH_4^+ concentration and was measured with a specific ammonia probe (Orion 9512) connected to an electrode meter (accumet 25, Fisher). Quantification of NH_4^+ in a culture sample was done by comparing to a standard curve.

Standards (1 ml) ranging from 0.1 - 10 mM were put in test tubes containing a mini-magnetic stir bar. 10 µl NaOH (10 M) was added to the tubes just prior to inserting the probe. The ammonia probe was placed in the solution ensuring that no air bubbles were trapped under the electrode membrane and the solution was mixed at low speed. The

mV reading was allowed to stabilize (2 - 3 min.) and the final value was recorded. A computerized standard curve was generated by the electrode meter. Subsequent analysis of culture samples were displayed as mV or mM units. Cell culture samples (200 µl) were diluted with 800 µl distilled water. The 1 ml diluted samples were analyzed in the same manner as standards.

2.11 Bicinchoninic protein assay

The concentration of protein in a solution was determined by a modification of the bicinchoninic assay described by Smith *et al.* (1985). The reagents for the assay were available as a kit from Sigma.

2.11.1 Stock solutions

1) Bicinchoninic acid solution - Reagent A.

2) Copper sulfate pentahydrate 4 % solution - Reagent B

3) Protein standard solution

100 mg of bovine serum albumin was dissolved in 100 ml saline solution (0.15 M NaCl. 0.05 % sodium azide).

2.11.2 Assay

1) The required amount of protein determining reagent (PDR) was prepared by adding 1 part reagent B to 50 parts reagent A.

2) Protein standards ranging from 0.2 - 1.0 mg/ml were prepared by diluting stock solution (3) in distilled water. Distilled water (i.e. 0 mg/ml protein) was used as a blank.

3) Samples were prepared by diluting in distilled water so that the concentration would fall within the protein standard range.

4) 2.0 ml PDR was added to 100 µl sample, standards or blanks and vortexed. Tubes were incubated at 37°C for 30 minutes.

5) The tubes were cooled at room temperature for 1 hour. The absorbances were then read at 562 nm with a spectrophotometer (UltraSpec II, Pharmacia) using the tube containing 0 mg/ml protein to zero the instrument.

6) The concentrations of unknown samples were determined by comparing absorbances to a protein standard curve and then multiplying by the dilution factor of the unknown.

2.12 Quantitation of apoptosis and cell viability using fluorescent dyes (Mercille and Massie, 1994a)

2.12.1 Reagents

1) Dye mix working solution (100 µg/ml)

5 µl acridine orange (10 mg/ml) and 5 µl ethidium bromide(10 mg/ml) were diluted in 490 µl of Dulbecco's phosphate buffered saline (Gibco) and stored at 4°C. Both dyes were purchased from Molecular Probes.

2.12.2 Procedure

A volume of 4 µl of dye mix was added to 100 µl of cell suspension. The mixture was placed on a microscope slide and covered with a coverslip. The slide was examined at 400 x with a fluorescence microscope using a mercury lamp as source of illumination. The fluorescence microscope was fitted with a filter combination suitable for observing fluorescein (i.e. exciter filter B and barrier filter 515W).

Acridine orange (AO) is a membrane permeable dye that intercalates into double stranded DNA (dsDNA) and makes it appear green. Ethidium bromide (EB) is a membrane impermeable dye that intercalates into dsDNA and makes it appear orange. The integrity of the membrane was therefore determined by the color of the chromatin. Cells with intact membranes had green chromatin due to AO. Cells with damaged membranes had orange chromatin due to both EB and AO intercalation (In this case EB fluorescence overwhelmed AO fluorescence).

The morphology of cellular chromatin was used to distinguish between apoptotic and nonapoptotic cells. Non apoptotic nuclei showed a diffuse fluorescent intensity reflecting the distribution of the chromatin. Apoptotic nuclei, in contrast, exhibited highly condensed chromatin that was uniformly stained. The condensed chromatin appeared as groups of spherical beads or in the form of crescents around the periphery of the nucleus. This type of condensation was easily distinguishable from that observed during cell division which was more ordered.

A minimum of 200 total cells were counted per cell culture sample. Four distinct type of cells were recorded according chromatin morphology and membrane integrity:

1) Viable cells (V) - green chromatin with diffuse fluorescence intensity (Fig. 2.3)

2) Apoptotic cells with intact membranes (Apm^+) - condensed green chromatin in the shape of beads or crescents (Fig. 2.3)

3) Apoptotic cells with damaged membranes (Apm^-) - condensed orange chromatin in the shape of beads or crescents (Fig. 2.3)

4) Non-viable or necrotic cells (N) - orange chromatin with diffuse fluorescence intensity (Fig. 2.3)

The percentage of each type of cell was determined in relation to total cells counts (i.e. % V = V/ total cell x 100 %). Apoptotic cells with intact membranes (Apm^-) were considered to be cells in the early stages of death and were included in calculations of the total dead cell population (i.e. total dead cells = Apm^- + Apm^- + N). Photographs of cells were taken with camera mounted on the fluorescence microscope. Kodak Ektachrome daylight color slide 400 film was used with exposure times ranging from 5 - 20 seconds.

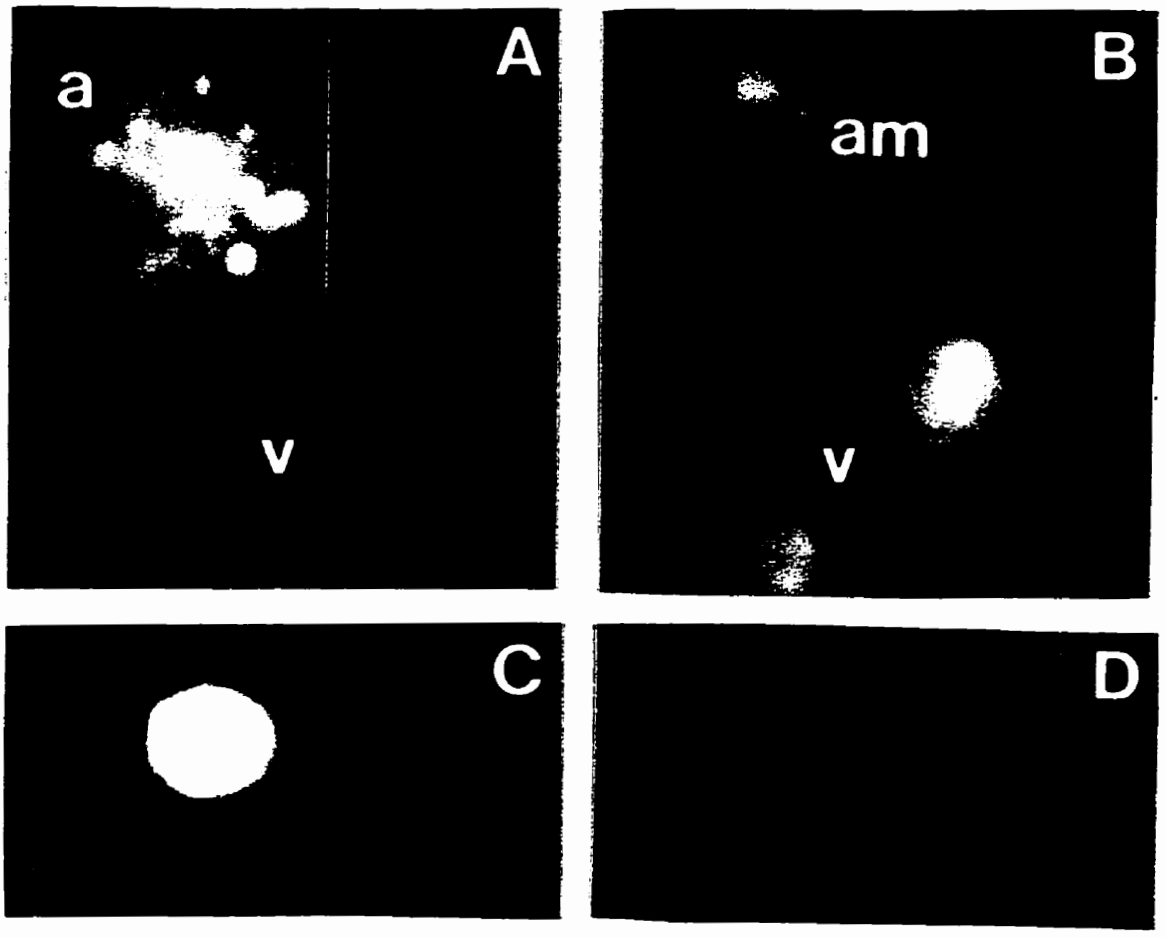

Figure 2.3 Fluorescent photomicrographs of CC9C10 hybridomas stained with acridine orange and ethidium bromide.
(A) Viable cell (v) and apoptotic cell with damaged membrane (a).
(B) Viable cells (v) and apoptotic cell with intact membrane (am).
(C) Necrotic cell.
(D) Mitotic cell.

2.13 Determination of oxygen consumption rate (Wohlpart *et al.*, 1990)

Oxygen concentration was determined with an oxygen probe (YSI Model 5331) connected to a biological oxygen monitor (YSI Model 5300) and a chart recorder (Model SE 120, ABB Goerz AG). Filtered air was bubbled in 37°C distilled water and used to calibrate the probe to 100 % dissolved oxygen at air saturation. The biological oxygen monitor had an electronic zero. Calibration was done every 7 samples.

The calibrated probe was inserted into a YSI glass chamber containing 10 ml of cell suspension (5 x 10^5 cells/ml) and a 20 mm Teflon coated magnetic stir bar. The probe was inserted making sure that all the air was removed from the chamber. The assembly was put in a 37°C stirred water bath containing a submergible stir plate set at 700 rpms. Oxygen depletion was monitored for 10 - 15 minutes. The specific oxygen uptake rate (OUR) was calculated from the slope of the oxygen concentration (expressed as % of air saturation) versus time. It was assumed that an air saturation value was 224.7 μM at 37°C.

$$\underset{(\mu\text{mol } O_2/\text{hour per } 10^6 \text{ cells})}{\text{OUR}} = \frac{\%\ O_2 \text{ depletion}}{\text{time}} \times \frac{224.7\ \mu\text{mol } O_2}{(100\ \%)(1000\ \text{ml})} \times \frac{10^6 \text{ cells}}{\text{cell concentration}}$$

where time is expressed in hours and cell concentration is expressed in cells/ml.

Simplified formula:

$$\underset{(\mu\text{mol } O_2/\text{hour per } 10^6 \text{ cells})}{\text{OUR}} = \frac{\%\ O_2 \text{ depletion} \times 2247}{(\text{time})(\text{cell concentration})}$$

2.14 Mathematical formulae

2.14.1 Maximum specific growth (μ_{max})

The maximum specific growth rate (μ_{max}) is defined as:

$$\mu_{max}\ (h^{-1}) = \frac{\ln (N/N_O)}{(t - t_O)}$$

Where N and N_O are cell concentrations at time points t and t_O during the exponential growth phase

2.14.2 Viability index (V_I)

The viability index (V_I) is defined as:

$$V_I\ (x\ 10^6\ \text{cell-days/ml}) = \int_0^t X_v dt$$

Where X_v is the viable cell concentration at time point t. The V_I was calculated from the integration of the viable cell density curve versus time curve by the trapezoidal rule (SigmaPlot software).

2.14.3 Specific production and consumption rates

The specific consumption/production rate of media components during batch culture (q_C) was calculated from the slope of the viability index (V_I) versus component concentration:

$$q_C = \frac{C - C_O}{V_I - V_{I,O}}$$

Where C and C_O are concentrations of media components at time t and t_O. Where V_I and $V_{I,O}$ are the viability index values at time points t and t_O. (Note: t and t_O are chosen in the linear part of the curve). Q_C is measured in $\mu g/10^6$ cell-days or $\mu mol/10^6$ cell-days.

CHAPTER 3

3. Development of a serum-free medium

3.1 Introduction

Hybridomas are designed for the purpose of producing large quantities of monoclonal antibodies which have become important tools in biological research and medical applications. Traditionally, basal nutrient medium has been supplemented with animal serum (5 - 10 % v/v) in order to sustain the growth of hybridomas as well as many other cell types (Barnes and Sato, 1980; Bjare, 1992). Basal nutrient medium is a complex isotonic mixture of chemically defined components such as amino acids, carbohydrates, vitamins and salts (Eagle, 1955; Lambert and Birch, 1985). Serum, the supernatant of clotted blood, however contains many ill-defined growth factors and compounds essential for cell growth (Shacter, 1989). This chemically undefined soup of proteins may also vary between batches resulting in inconsistencies in cell growth and adds to the difficulty of product purification (Glassy *et al.*, 1988). Depending on the source, serum can account for more than half of overall medium cost. These disadvantages as well as concerns over serum's safety in producing medical products for humans has led researchers to find alternative medium additives. Media which exclude animal serum from its formulation is commonly known as serum-free. Serum can be replaced by purified proteins, lipids, trace elements, peptides and other nutrients (Lambert and Birch, 1985; Murakami, 1989). The first objective of this research project was therefore to develop a serum-free medium for the CC9C10 hybridoma cell line.

3.2 Results

3.2.1 Establishment of a suitable serum-based medium for CC9C10 growth

Upon receipt from the American Type Culture Collection, CC9C10 hybridomas were cultured in RPMI 1640 basal medium (Gibco) supplemented with 10 % fetal calf serum as suggested by the supplier. Fetal calf serum was subsequently replaced with iron enriched calf serum (Fe-CS), a cheaper serum source, with no significant effect on cell growth (data not shown). The basal medium was also eventually replaced by DMEM (Gibco), which exhibited similar growth promoting properties as RPMI 1640 (data not shown). The switch to DMEM was initially due to the benefits of using a single basal medium in the laboratory (i.e. sharing of supplies and reduction of costs). CC9C10 hybridomas were routinely maintained in serum supplemented DMEM until a suitable serum-free formulation was found. The typical maximum viable cell density obtainable in DMEM (+ 10 % Fe-CS) was 2.0 x 10^6 cells/ml in batch culture over 4 days and following an inoculation of 1 x 10^5 cells/ml.

3.2.2 Adaptation to a commercial serum-free medium

CC9C10 hybridomas grown in DMEM (+ 10 % Fe-CS) were easily weaned to a serum level of 2 % by a gradual reduction of supplemented serum over 6 passages. After 6 passages at the 2 % serum level, cells were transferred directly to H-SFM (Gibco), a commercial serum-free medium designed for hybridomas. CC9C10 hybridomas were passaged 5 times in H-SFM before comparing growth profiles with cells grown in DMEM (+ 2 % Fe-CS). Exponentially growing cells from each stock culture were collected by centrifugation and resuspended at 1.3 x 10^5 cells/ml in 30 ml of each medium. Experiments were carried out in duplicate in 75 cm^2 T-flasks over 174 hours. As shown in Fig.3.1, hybridomas grown in H-SFM reached a 26 % higher maximum viable cell density (1.32 x

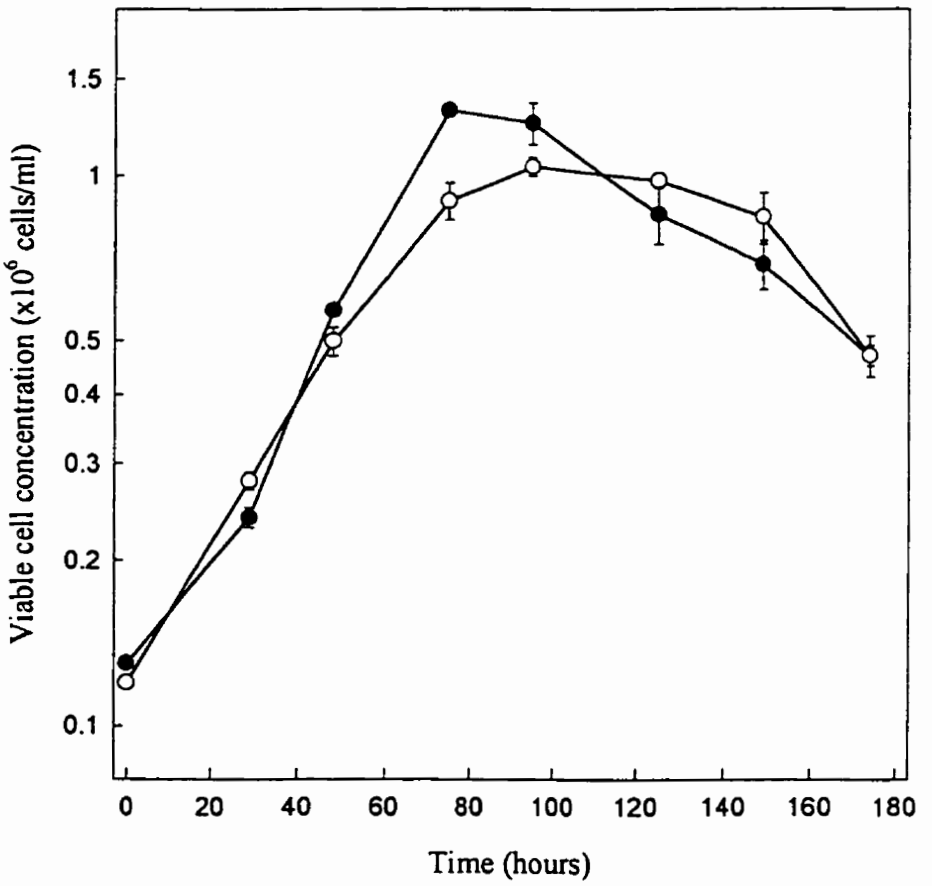

Figure 3.1 Growth profiles of CC9C10 hybridomas in serum-supplemented and serum-free media. Hybridomas previously adapted to DMEM (+ 2 % Fe-CS) or H-SFM were inoculated into T-flasks (75 cm^2) containing 30 ml of each respective medium. Cultures were inoculated at 1.3 x 10^5 cells/ml in DMEM supplemented with 2 % Fe-CS, (O); or H-SFM (●). Viable cell concentration values are the mean ± S.E.M. from two identical flasks inoculated from the same cell stock.

10^6 cells/ml) compared to 2 % serum-based cultures (1.04 x 10^6 cells/ml). The cell density of cultures grown in 2 % serum-based medium was consistently lower than cell density of cultures grown in 10 % serum-based medium. H-SFM cultures also had a 20 % higher μmax (0.031 h^{-1}) compared to cultures grown in 2 % serum (0.026 h^{-1}). Cells grown in serum-based medium however had a prolonged stationary phase (50 -70 hours) while H-SFM cultures had a relatively short stationary phase (20 hours).

3.2.3 Development and optimization of a serum-free medium specific for CC9C10 cells

The first step taken in developing a "homemade" serum-free medium was to find a suitable starting formulation. A literature search revealed a promising formulation which had shown success with several hybridoma cell lines including SP2/0 derived cells. This medium developed by Tharakan *et al.* (1986), abbreviated in this text as T-SFM, was composed of DMEM, insulin, transferrin, NaSe, ethanolamine and 2-mercaptoethanol (Table 3.1). After it was established that CC9C10 cells were growing well in H-SFM, they were gradually shifted to the T-SFM formulation. The H-SFM medium was replaced in steps of 50, 75, 88 and 94 % T-SFM over a 3 week period. Adaptation to 100 % T-SFM was however not successful. Passaging CC9C10 hybridomas in T-SFM resulted in elevated cell death (> 60 %) within the first 24 hours of incubation and reduced cell growth. A maximum of 3 passages in T-SFM was possible before total cell death occurred. The elimination of NaSe from the T-SFM formulation did not alleviate this problem. The removal of 2-mercaptoethanol from the formulation however did prevent cell death in the first 24 hours of incubation and improved cell growth. Reduction of the ethanolamine concentration from 20 μM to 10 μM also improved cell yields slightly. However continuous passaging in this modified T-SFM (mT-SFM) was not successful and ultimately led to CC9C10 culture death.

The mT-SFM formulation was improved further to the medium formulation, J-SFM, by Dr. Jan in our laboratory (Table 3.1). The addition of 100 μM

Table 3.1 The composition of serum-free formulations. All media contained 25 mM glucose, 3.7 g/L $NaHCO_3$ and 8.1 mg/L phenol red

Serum-free medium	T-SFM[a]	mT-SFM	J-SFM	NB-SFM
basal medium	DMEM[b]	DMEM[b]	DMEM[c]	DMEM: Ham's F12[c]
insulin (μg/ml)	10	10	10	10
transferrin (μg/ml)	10	10	10	10
NaSe (nM)	1	----	----	10
ethanolamine (μM)	20	10	10	10
phosphoethanolamine (μM)	----	----	100	100
2- mercaptoethanol (μM)	50	----	----	----
Pluronic F-68 (% w/v)	----	----	0.1	0.1

a- Tharakan *et al.* (1986)
b - contains 4 mM glutamine
c - contains 6 mM glutamine

phosphoethanolamine, 0.1 % (w/v) Pluronic F-68 and 6 mM glutamine was sufficient to allow continuous passaging of CC9C10 cells.

Further optimization upon J-SFM was made by changing the DMEM basal medium to a 1:1 mixture of DMEM: Ham's F12 and by adding 10 nM NaSe. The comparison of growth of CC9C10 cells in the different media is shown in Fig.3.2. CC9C10 hybridomas which had been growing in 6 % H-SFM: 94 % J-SFM were collected by centrifugation and resuspended at 2 x 10^5 cells/ml in 10 ml serum-free medium differing in basal medium and NaSe content. Cultures were grown in 25 cm^2 T-flasks in duplicate. As seen in Fig.3.2, serum-free medium composed of DMEM: Ham's F12 and NaSe was optimal for growth. NaSe caused a 32 % and 6 % increase in the maximum viable cell density in DMEM and DMEM: Ham's F12 basal medium respectively. Maximum cell densities were also maintained for a prolonged period in cultures grown in serum-free media containing DMEM: Ham's F12 instead DMEM. Serum-free medium containing DMEM: Ham's F12 and NaSe was also optimal in independent experiments in which CC9C10 cells were directly transferred from H-SFM (data not shown).

The last step in medium optimization was the increase in the glucose concentration of the DMEM: Ham's F12 which normally contains 17.5 mM glucose. The comparison of growth and metabolism of CC9C10 hybridomas in serum-free medium containing 17.5 mM or 25 mM glucose is shown in Fig.3.3. Hybridomas which had been growing in modified J-SFM (DMEM:Ham's F12, insulin, transferrin, ethanolamine, phosphoethanolamine, Pluronic F-68 and NaSe) were inoculated at 1.2 x10^5 cells/ml by dilution in media containing 17.5 mM (low) or 25 mM (high) glucose. The 30 ml cultures were grown in duplicate in 75 cm^2 T-flasks. Cell growth in both media was similar for the first 72 hours. At 96 hours, cultures in the high glucose medium reached a 30 % higher maximum cell density than cultures inoculated in the low glucose medium. A reduction in the viable cell density was observed in the low glucose medium at 120 hours and this was concomitant with the total depletion of the carbohydrate. A decrease in the viable cell density of the high glucose medium culture however only occurred at 168 hours, 48 hours later than the low glucose culture. Cell death in the high glucose culture was also

coincident with glucose exhaustion. Analysis of both media indicates that glutamine may also have been a limiting factor after 120 hours (data not shown).

The DMEM: Ham's F12 based serum-free medium containing 25 mM glucose was shown to be optimal for cell growth and yield. This medium was used for routine CC9C10 stock culture maintenance and in all subsequent experimental procedures. The formulation of this "homemade" serum-free medium is shown in Table 3.1 and was designated as NB-SFM.

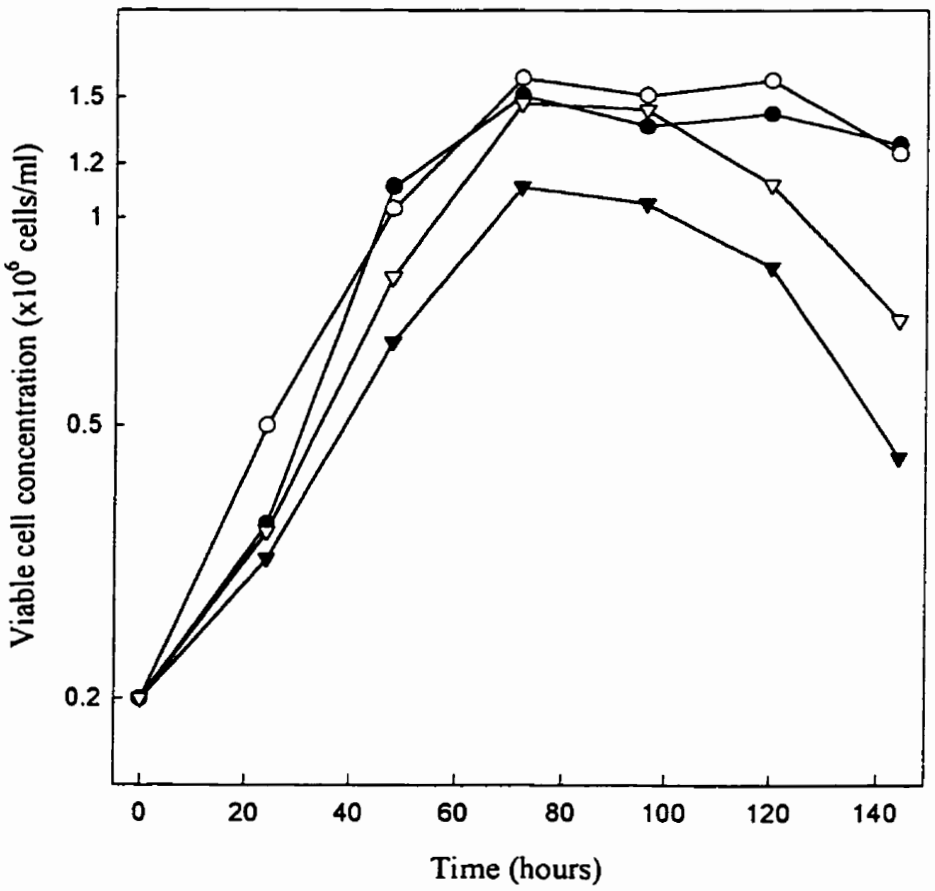

Figure 3.2 The effect of basal medium and NaSe on the growth of CC9C10 hybridomas. Hybridomas previously adapted to 6 % H-SFM: 94 % J-SFM were inoculated into T-flasks (25 cm^2) containing 10 ml of modified J-SFM. J-SFM formulations differed in basal medium and NaSe content: DMEM: Ham's F12, (●), DMEM: Ham's F12 supplemented with 10 nM NaSe, (O); DMEM, (▼); DMEM supplemented with 10 nM NaSe, (▽). Initial cell density was 2.0 x 10^5 cells/ml. Viable cell concentration values are the mean from two identical flasks inoculated from the same cell stock. Errors were less than 10 % of the mean.

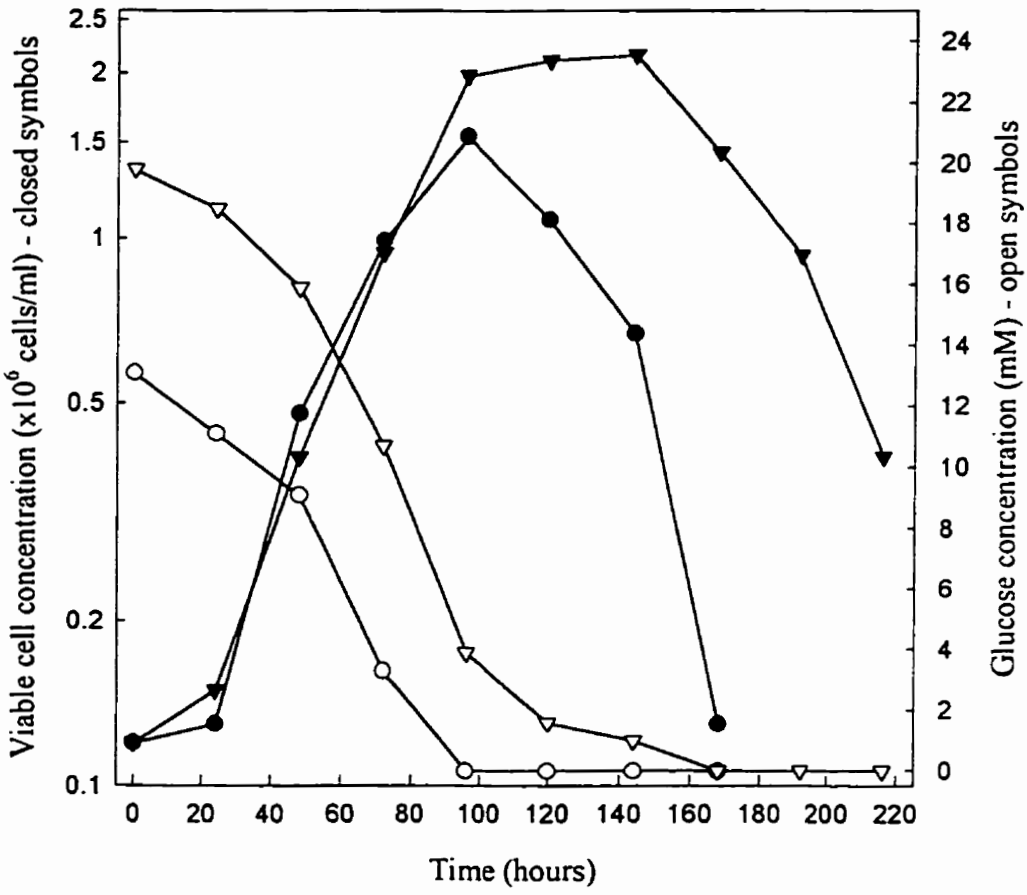

Figure 3.3 The effect of initial medium glucose concentration on the growth of CC9C10 hybridomas. Hybridomas previously adapted serum-free medium (DMEM: Ham's F12, insulin, transferrin, ethanolamine, phosphoethanolamine, Pluronic F-68 and NaSe) were inoculated by dilution into T-flasks (75 cm^2) containing the same medium but with different glucose levels: 17.5 mM glucose, (●, O); 25 mM glucose, (▼,▽). Initial cell density was 1.3 x 10^5 cells/ml in 30 ml total volume. Glucose concentration is represented by open symbols. Viable cell concentration is represented by closed symbols. Viable cell density and glucose concentration are the mean from two identical flasks inoculated from the same cell stock. Errors were less than 10 % of the mean.

3.3 Discussion

There are several advantages in using serum-free medium rather than serum-supplemented medium in animal cell cultures. Serum-free medium is a chemically defined mixture which can be prepared consistently. In contrast, supplements such as serum render the medium chemically undefined. Serum is a complex mixture of known and unknown constituents subject to variations according to genetic, dietary and veterinary history of the animal from which it was obtained (Shacter, 1989). Serum-free medium also reduces the risk of infectious agent contamination and simplifies purification of protein products (Glassy *et al.*, 1988).

In this study, CC9C10 hybridomas which were traditionally grown in serum-supplemented medium were conditioned to grow in low serum and serum-free media by adaptation. The adaptation consisted of a weaning procedure in which serum in the medium was decreased gradually. Low serum containing medium was then replaced by a commercial serum-free medium, H-SFM (Gibco). The reduction of serum concentration in the medium from 10 % to 2 % resulted in a 50 % decrease in the maximum viable cell density obtainable. This is consistent with findings from other labs and is probably due to a dilution of essential growth factors (Tharakan *et al.*, 1986). Cells adapted to low serum (2 %) were then successfully transferred to H-SFM without any further loss of cell yield. H-SFM gave slightly higher maximum viable cell densities but shortened the stationary phase compared to 2 % serum supplemented cultures. Although cells grew well in H-SFM, the medium formulation was proprietary and essentially undefined. Growing CC9C10 hybridomas in H-SFM was therefore used as a stepping stone in the adaptation of cells to a "homemade" serum-free medium.

There are numerous published serum-free media formulations that have been developed for the in vitro growth and productivity of hybridoma cell lines (Kawamoto *et al.*, 1983; Tharakan *et al.*, 1986; Murakami, 1989; Kimata *et al.*, 1991). Most of these formulations consist of commonly available commercial media such as DMEM, RPMI 1640 or Ham's F12 which have been supplemented with ITES (i.e. insulin, transferrin, ethanolamine and selenium). Insulin is a small hormonal polypeptide that stimulates

glucose uptake and synthesis of RNA, protein and lipids (Schubert, 1979). Insulin is included in most serum-free formulations. Transferrin, an iron-binding glycoprotein, facilitates the transport of the metal ion across the plasma membrane and may also act to detoxify trace metals (Trowbridge and Omary, 1981; Bretscher, 1985). Ethanolamine has been shown to optimize hybridoma growth in serum-free medium (Murakami, 1989). Its exact function is unknown but it is likely associated with lipid synthesis (Glassy *et al.*, 1988). Selenium is a co-factor of glutathione peroxidase, an important metabolic detoxifier (Nielsen, 1981).

Tharakan *et al.*'s medium formulation (1986) which consists of DMEM, ITES and 2-mercaptoethanol has been shown to be successful with a SP2/0 derived hybridoma. (Note: CC9C10 is a SP2/0 derivative, Schroer et. al. 1983). Attempts to adapt CC9C10 hybridomas to Tharakan *et al*'s formulation (T-SFM) were not successful. As is the case with many published formulations it was necessary to modify components to meet specific needs. It has been observed in other laboratories that different hybridomas (even when they are closely related) may vary slightly in their growth requirements and as a consequence individual optimization for each cell line is essential (Fazekas de St.Groth, 1983; Glassy *et al.*, 1988; Shacter, 1989). Several modifications to T-SFM were needed to adapt CC9C10 cells to the serum-free medium. It was found that the removal of 2-mercaptoethanol from the medium increased cell culture survival. This is in contrast to other cell lines in which the presence of 2-mercaptoethanol has been shown to stimulate cystine uptake, restore the reduced form of glutathione and facilitate the transition from G_1 to S phase of the cell cycle (Broome and Jeng, 1973). Other modifications to the formulation included reducing the ethanolamine concentration; increasing the glucose, glutamine and NaSe concentration; and adding phosphoethanolamine and Pluronic F-68. Phosphoethanolamine probably has the same function as ethanolamine (Murakami *et al.*, 1989). Pluronic F-68, a synthetic co-polymer of propylene oxide and ethylene oxide, is effective in preventing cell damage during cell culture suspension, mixing and aeration (Michaels *et al.*, 1991; Chattopadhyay *et al.*, 1995).

Replacing DMEM with a 1:1 mixture of DMEM and Ham's F12 also resulted in better cell yields. This difference in cell yield may be related to the additional components

present in Ham's F12 such as Cu^{+2}, Zn^{+2}, biotin and vitamin B_{12}. In particular, Zn^{+2} has been shown to be important in the biological activity of insulin, a major component of serum-free formulations (Butler, 1992).

3.4 Conclusion

CC9C10 hybridomas were conditioned to grow in "homemade" serum-free designated as NB-SFM by an adaptation procedure (Table 3.1). NB-SFM was used in all subsequent experiments and any modifications to the formulation (i.e. glucose or glutamine concentration) are indicated for each experiment.

CHAPTER 4

4. Effect of temperature on nucleotide pools and monoclonal antibody production in CC9C10 hybridoma[1].

4.1 Introduction

The increased commercial importance of monoclonal antibodies (Mabs) has resulted in attempts to optimize their yield in cell culture systems. The amount of Mab that can be produced from a cell culture is dependent on factors such as the specific Mab production rate (qMab) and maintenance of culture viability. Various reports have indicated that high antibody productivity occurs under conditions that are not optimal for hybridoma cell growth. Culture conditions of hyperosmolarity, high temperature or the addition of growth inhibitors have all been shown to cause an increase in specific monoclonal antibody production rates (Sureshkumar and Mutharasan, 1990; Ozturk and Palsson, 1991b; Modha *et al.*, 1992). This suggests the possibility of dissociating the conditions of optimal qMab from the conditions that are optimal for cell growth in the development of culture strategies that maximize the final volumetric titer of Mab (Oh *et al.*, 1993). The rationale is to attain a high cell density prior to establishing conditions for optimal qMab.

Optimization of hybridoma cell culture productivity depends on a better understanding of how antibody synthesis is regulated. In some cases, higher qMab at reduced growth rates can be explained by cells remaining in the G_1 phase of the cell cycle for relatively longer time periods. (Borth *et al.*, 1992). However, such an explanation is not applicable to all experimental data (Bloemkolk *et al.*, 1992). Monoclonal antibody production has also been monitored in relation to culture parameters such as nutrient consumption and waste accumulation. These parameters however are insufficient in explaining differences in Mab production rates.

[1]The contents of this chapter were included in a paper: Barnabé, N., and Butler, M (1994) Effect of temperature on nucleotide pools and monoclonal antibody production in a mouse hybridoma. *Biotechnol. Bioeng.* 44: 1235 - 1245.

Analysis of intracellular nucleotides may prove to be more useful because they are involved in all areas of metabolism. In addition to being substrates, products and energy carriers, nucleotides play an important role in the regulation of cellular processes and pathways (Atkinson, 1977). Fluctuations in the nucleotide pools can therefore lead to changes in cell behavior. One study has shown that imbalances in nucleotide pools correlate with cell cycle phases, proliferation, differentiation and transformation of myelocytes (De Korte *et al.*, 1987). Other studies have demonstrated that nucleotide pools are good indicators of growth behavior in mammalian and plant cells (Meyer and Wagner, 1985; Ryll and Wagner, 1991).

In this chapter, we investigate the relationship between incubation temperature, Mab production and nucleotide pool imbalances. Increases in Mab productivity coincident with temperature increases in the range of 33 to 39°C have been reported previously in mouse hybridomas (Reuveny *et al.*, 1986; Sureshkumar and Mutharasan, 1990). In other hybridoma cell lines incubation temperature has no effect on qMab (Bloemkolk *et al.*, 1992). The purpose of our investigation was to determine whether culture temperature affected qMab in the CC9C10 hybridoma which has been well characterized in our laboratory (Petch and Butler, 1994) and to determine whether such changes could be correlated with changes in intracellular nucleotide pools.

4.2 Experimental set-up and analysis

CC9C10 hybridomas taken from the mid-exponential phase of stock cultures were inoculated by dilution into 150 cm^2 T-flasks containing NB-SFM (25 mM glucose, 6 mM glutamine). The 90 ml cultures were incubated for 7 days at various temperatures with daily removal of samples (2- 4 ml) for analysis. Three incubation temperatures were used: 33°C, 37°C and 39°C . Due to limited space, only one incubator chamber was set at a non-standard temperature (33 or 39°C) at a given time. Each experiment was compared to a control culture at 37°C and prepared in duplicate from the same cell inoculum. For the temperature shift experiment, cells were grown at 37°C for 2 days and then transferred to

33°C or 39°C. To prevent glucose and glutamine limitation in the medium, all cultures were fed daily starting on day 2 with 5 mM glucose/day and 1 μmol glutamine/10^6 cells per day as previously described (section 2.3) The pH of cultures were also adjusted with sodium bicarbonate when necessary (section 2.3).

Viable cell density was determined by the trypan blue exclusion method and Mab concentration by HPLC (section 2.5.1 and section 2.6.1). Glucose, lactate and glutamine concentrations were determined enzymatically (section 2.8 and 2.9). The concentration of ammonia was determined with a specific probe (section 2.10). Two methods were used to evaluate the intracellular nucleotide pools of the CC9C10 hybridomas during culture growth. Trichloroacetic acid extracted nucleotides were quantified by ion pair reverse phase liquid chromatography (section 2.7.2). Adenyl nucleotides (ATP, ADP, AMP) were also analyzed by luminometry (section 2.7.3). The two analytical methods gave similar values for ATP and AMP (less than 10 % difference).

4.3 Results

4.3.1 Growth profile and Mab production

The growth profiles for the CC9C10 cells at various temperatures are shown in Figure 4.1 and Figure 4.2. The 33°C culture and corresponding control showed an apparent lag phase in the first 24 hours, although this may be due to an unexplained low sample count on day 1 (Fig. 4.1). Similar maximum viable cell densities (0.93 - 0.97 x 10^6 cells/ml) were attained at 33°C and 37°C on day 3 of the incubation period. Cells grown at 33°C also remained at a higher cell density for a prolonged period compared to the control culture. In contrast, the maximum viable cell density decreased by 45% (to 0.52 x 10^6 cells/ml) at 39°C compared to the corresponding 37°C control (Fig. 4.2). After 4 days of incubation, cell death was more rapid at 39°C than at 37°C.

The maximum specific growth rates (μ_{max}) are presented in Table 4.1. The μ_{max} values were not significantly different for cultures at 33°C and 37°C (0.032 - 0.035 h^{-1}), as

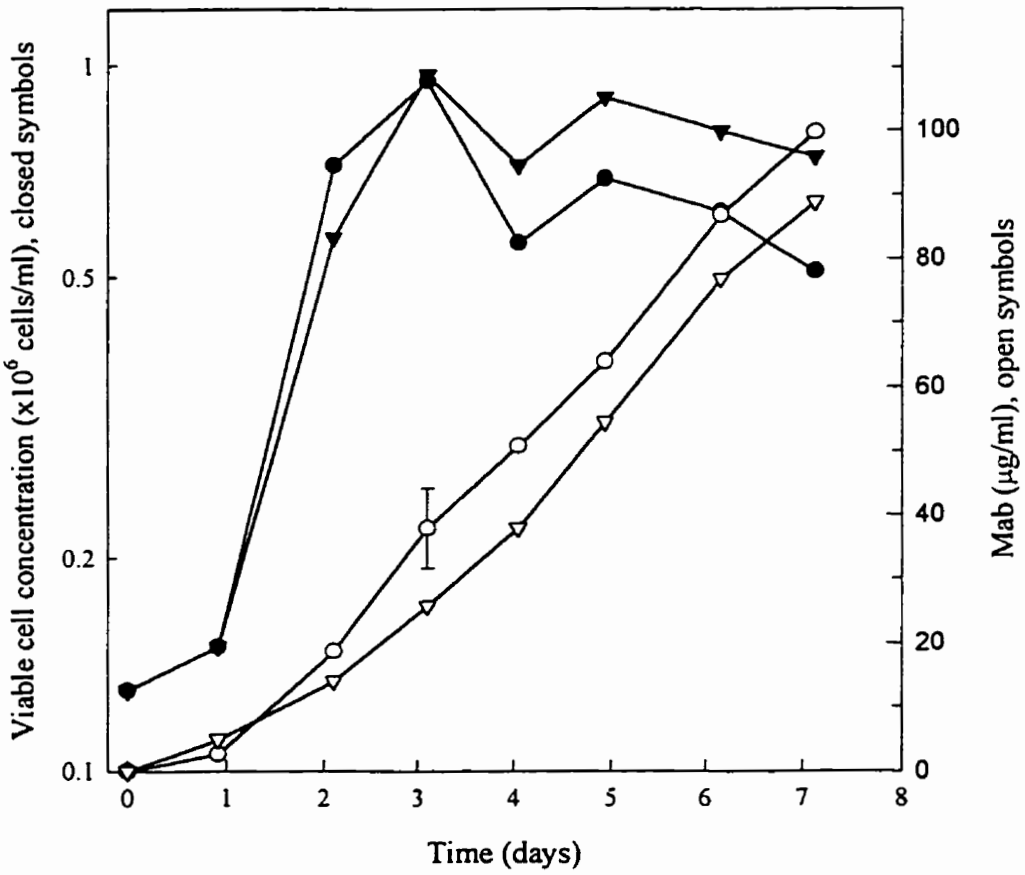

Figure 4.1 Growth and monoclonal antibody profiles of CC9C10 hybridomas at 37°C and 33°C: 37°C (● ,O) and 33°C (▼,∇). Hybridomas from the mid-exponential phase were inoculated at 1.3 x 10^5 cells/ml into T-flasks (150 cm^2) containing 90 ml NB-SFM. Viable cell and Mab concentration values are the mean from two identical flasks inoculated from the same stock culture. Errors were less than 10 % of the mean unless otherwise indicated.

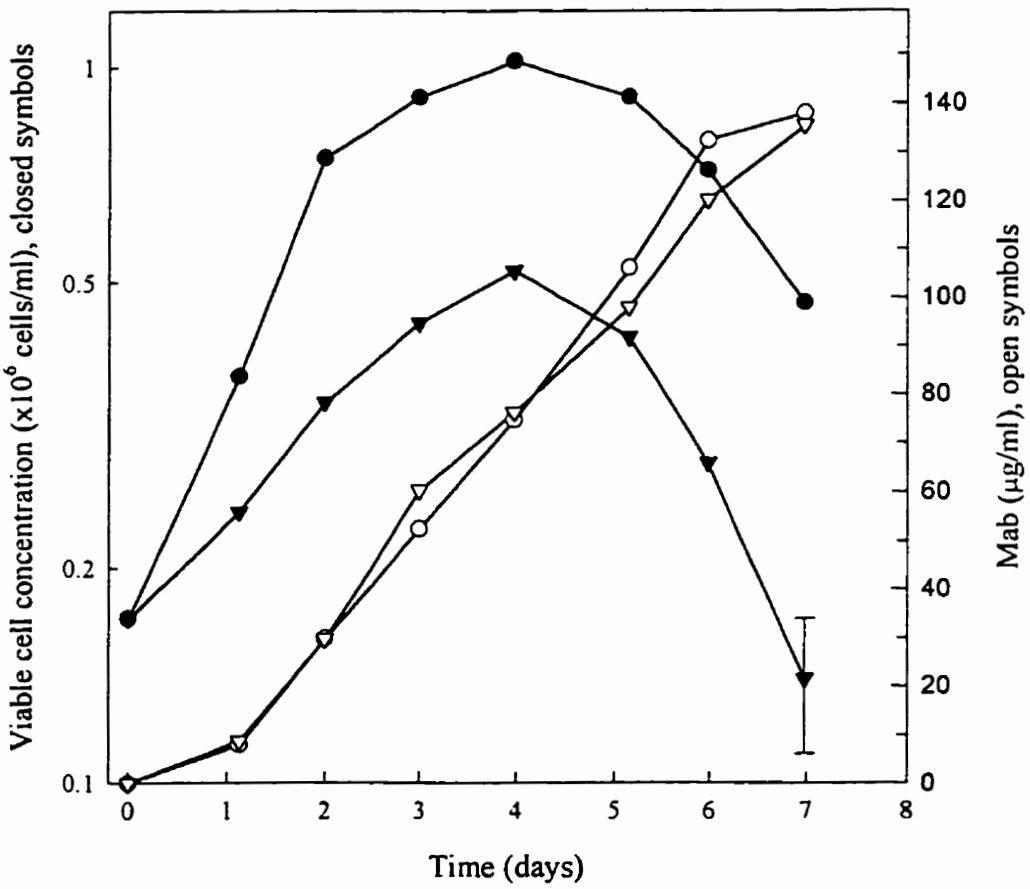

Figure 4.2 Growth and monoclonal antibody profiles of CC9C10 hybridomas at 37°C and 39°C: 37°C (● ,O) and 39°C (▼,∇). Hybridomas from the mid-exponential phase were inoculated at 1.7 x 10^5 cells/ml into T-flasks (150 cm^2) containing 90 ml NB-SFM. Viable cell and Mab concentration values are the mean from two identical flasks inoculated from the same stock culture. Errors were less than 10 % of the mean unless otherwise indicated.

calculated from day 1 to day 3 (i.e. exponential phase). At 39°C, the μ_{max} was 59% lower (0.013 h^{-1}) than at the control temperature (day 0 to day 2). The reduction in growth at 39°C is also reflected in the viability index, the integral of cell density-time, which was 52% lower than the control (Table 4.1).

The final Mab concentration (volumetric production) was not significantly different at 39°C compared to the control (136 μg/ml). However, a small reduction (11%) in Mab yield occurred at 33°C (Table 4.1). The specific Mab production rate (qMab) calculated from the slope of the viability index (V_I) versus Mab concentration was linear at all temperatures (Fig. 4.3). Under standard conditions at 37°C the mean qMab value was 26.0 μg/10^6 cell-days. The qMab however increased with an increase in culture temperature(Table 4.1, Fig. 4.3). Cultures grown at 33°C had a qMab 21% lower than the control at 37°C, whereas the resulting qMab at 39°C was 97% higher than the control.

4.3.2 Temperature shift

In the previous section, it was found that qMab was enhanced at 39°C. This enhanced qMab however did not result in an improvement in Mab yield due to a concomitant reduction in μ_{max} and viable cell density. An attempt was therefore made to improve Mab yield by shifting to a nonstandard temperature (39°C) once the culture had attained a high cell density. Hybridomas were inoculated into NB-SFM, grown at 37°C for 2 days and then transferred to 39°C as previously described (section 4.2). Controls for temperature shift experiments remained at 37°C. For comparative purposes, a temperature shift to 33°C after 2 days was also done with an independent culture. The shift to 33°C did not significantly affect the maximum cell density when compared to 37°C (0.91- 0.95 x 10^6 cells/ml), although the cells were maintained at a high density for a longer period at the lower temperature (Fig. 4.4). In contrast, the shift to 39°C resulted in an immediate decrease in viable cell concentration (Fig. 4.5).

Table 4.1 Effect of temperature on the maximum specific growth rate (μ_{max}) ,viability index (V_I), Mab concentration,[a] and specific Mab production rate (qMab).

Temperature (°C)	μ_{max} (h^{-1})	V_I (day7) (x10^6 cell days/ml)	Mab production (μg/ml)	qMab (μg /10^6 cell days)
33	0.035 ± 0.001	4.65 ± 0.08	89 ± 6	18.9 ± 0.4
37[b]	0.035 ± 0.001	4.10 ± 0.08	100 ± 4	24.0± 0.5
37[c]	0.032 ± 0.001	4.99 ± 0.16	138 ± 14	28.1 ± 0.9
39	0.013 ± 0.001	2.36 ± 0.01	136 ± 1	55.4 ± 2.6

Values are means from two independent cultures. The errors of qMab was determined from the slope of the curve drawn as the best straight line through eight points, each of which was based on duplicate determinations.

[a]Mab produced from day 0 to day 7.

[b]Same cell stock culture used for 33 °C experiment.

[c]Same cell stock culture used for 39 °C experiment.

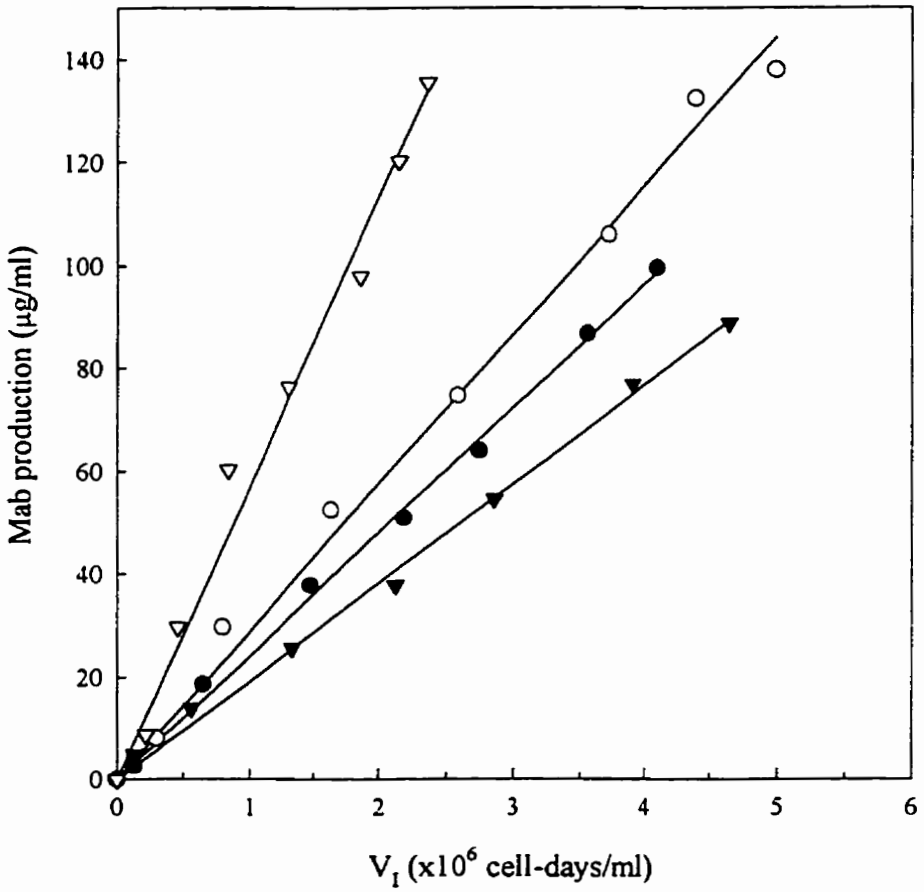

Figure 4.3 Effect of temperature on specific monoclonal antibody production: 37°C (●) and 33°C (▼); 37°C (O) and 39°C (▽). Controls (37°C) were set-up for each non standard temperature. The control for the 33°C culture is represented by closed circles whereas the control for the 39°C culture by open circles. Values were calculated from Figures 4.1 and 4.2.

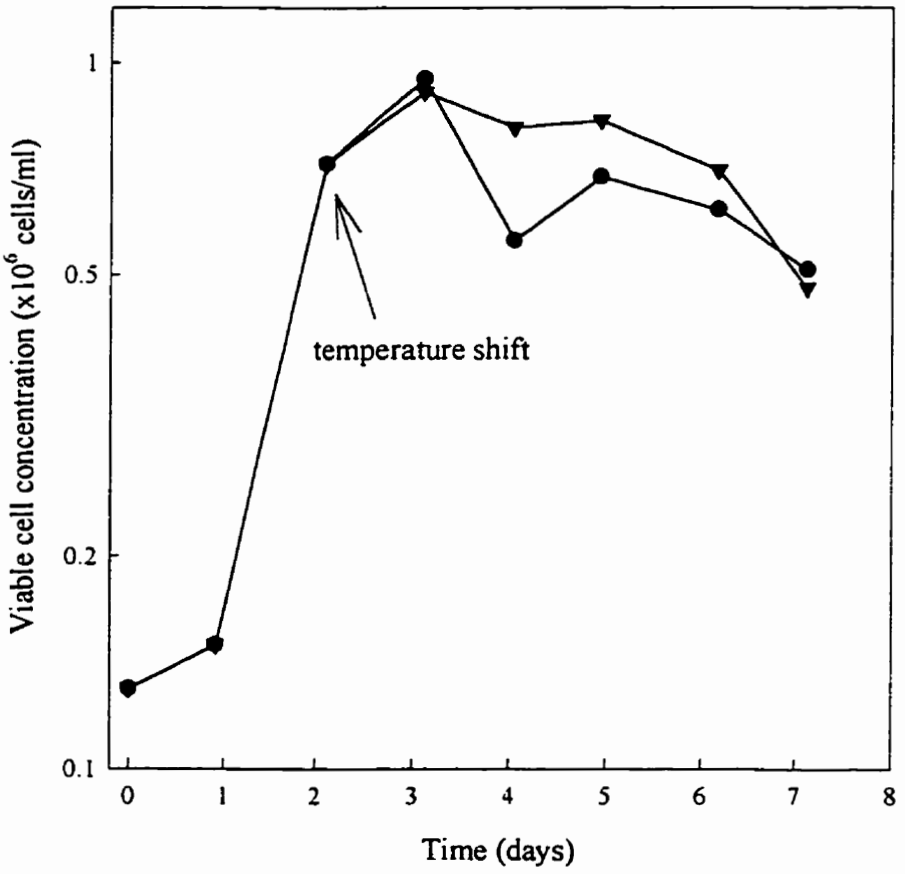

Figure 4.4 Growth profiles of CC9C10 hybridomas shifted to 33°C after 2 days: 37°C (●) and 33°C (▼). Hybridomas from the mid-exponential phase were inoculated at 1.3 x 10^5 cells/ml into T-flasks (150 cm^2) containing 90 ml NB-SFM. Controls remained at 37°C for the incubation period. Controls were done in duplicate with errors less than 10 % of the mean. Cultures at 33°C were done in simplicate from the same cell stock.

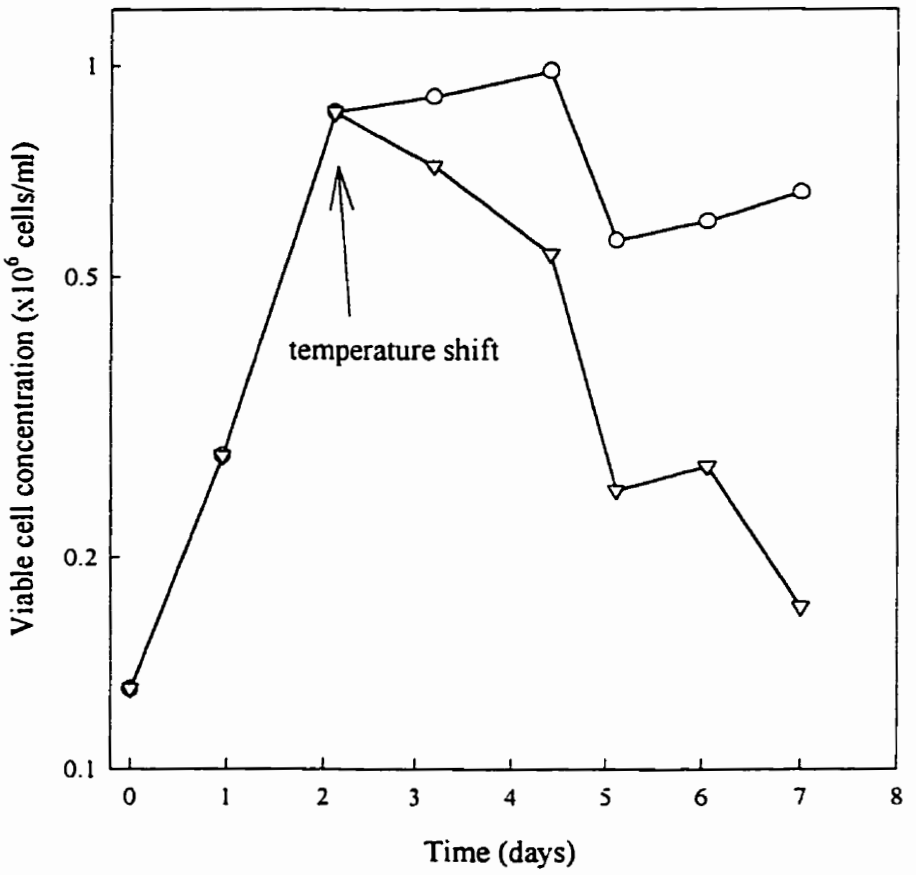

Figure 4.5 Growth profiles of CC9C10 hybridomas shifted to 39°C after 2 days: 37°C (O) and 39°C (∇). Hybridomas from the mid-exponential phase were inoculated at 1.3 x 10^5 cells/ml into T-flasks (150 cm^2) containing 90 ml NB-SFM. Controls remained at 37°C for the incubation period. Viable cell concentration values are the mean from two identical flasks inoculated from the same stock culture. Errors were less than 10 % of the mean.

The specific Mab production rates (qMab) are shown in Figure 4.6. Control cells (37°C) demonstrated a constant rate of production over the course of the cultivation period (24.8 ± 2.5 $\mu g/10^6$ cell-days). The temperature shift to 39°C increased Mab productivity by 53% (38.0 ± 3.3 $\mu g/10^6$ cell-days), whereas the temperature shift to 33°C lowered productivity to a value of 18.5 ± 1.0 $\mu g/10^6$ cell-days. However, the effect on the final volumetric yield of Mab was insignificant between the 37°C and 39°C cultures, although higher Mab concentrations at 39°C occurred at earlier time points. Higher volumetric yields were observed at 37°C (107 μg/ml) compared to 33°C (85 μg/ml).

4.3.3 Cell metabolism

The concentrations of glucose, glutamine, lactate and ammonia were determined for cultures grown at different temperatures. It was found that glucose and glutamine were not limiting in any cultures due to the feeding regimen. Maximum cell density in 33°C and 37°C cultures coincided with by-product accumulation: lactate 20 and 26 mM; and ammonia, 3.5 and 4.2 mM respectively. Maximum cell density in 37°C and 39°C cultures coincided with a lactate and ammonia accumulation of 31 mM and 5.2 mM respectively for both cultures.

The specific rates of consumption or production of these substrates and metabolic by-products during cell growth are presented in Table 4.2. Rates were determined from plots of substrate (or product) concentration against the integral of cell concentration and time (section 2.14.3). An increase in temperature resulted in an increase of specific rates of glucose uptake (q_G) and lactate production (q_L). The glucose uptake rate was 85% higher at 39°C and 13% lower at 33°C. Similar variations were found with the lactate production rate. The amount of lactate produced per unit of glucose, the lactate yield ($Y_{Lac/Glc}$), was between 1.6-1.9 in all cultures.

The specific rate of glutamine uptake (q_Q) and ammonia production (q_A) at 39°C increased by 103 % and 114 % respectively when compared to cells at 37°C (Table 4.2). Ammonia yield from glutamine ($Y_{Amm/Gln}$) however did not vary in the range of 37-39°C.

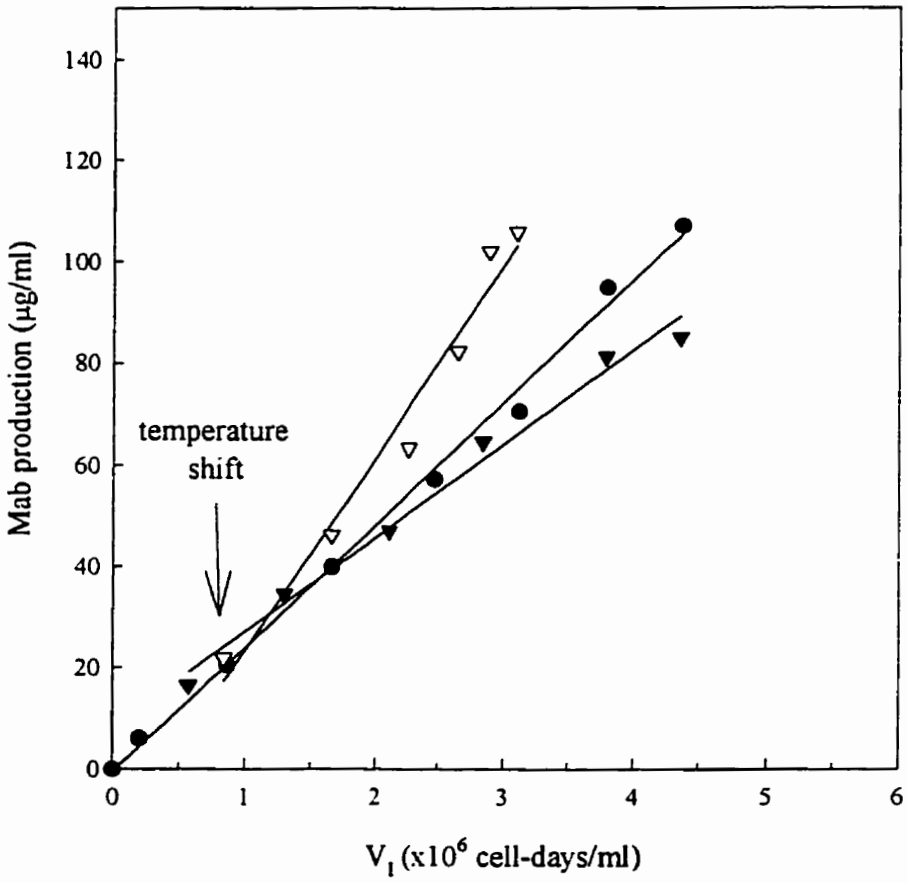

Figure 4.6 Effect of temperature on specific monoclonal antibody production after a temperature shift: 37°C, average of two separate experiments (●); 33°C, shift on day 2 (▼); and 39°C, shift on day 2 (▽). Values were calculated from Figures 4.4 and 4.5.

Table 4.2 Metabolic rates at different temperatures (exponential phase)

Temperature (°C)	Specific glucose uptake rate (q_G)	Specific lactate production rate (q_L)	Lactate yield, $Y_{Lac/Glc}$ (mol/mol)	Specific glutamine uptake rate (q_Q)	Specific ammonia production rate (q_A)	Ammonia yield, $Y_{NH4+/Gln}$ (mol/mol)
33	7.5 ± 0.5	12.3 ± 0.3	1.6	2.2 ± 0.1	1.5 ± 0.1	0.68
37[a]	8.6 ± 0.2	15.7 ± 0.4	1.8	2.2 ± 0.1	2.1 ± 0.2	0.95
37[b]	9.2 ± 0.5	17.9 ± 1.0	1.9	2.7 ± 0.2	2.8 ± 0.2	1.04
39	17.0 ± 0.6	29.7 ± 0.8	1.7	5.5 ± 0.2	5.8 ± 0.2	1.05

Metabolic rates are in μmol/10^6 cell days

[a]Same cell stock culture used for 33 °C experiment.

[b]Same cell stock culture used for 39 °C experiment.

At 33°C, no significant change in q_Q was observed while the q_A decreased when compared to controls. This resulted in a decrease in ammonia yield at 33°C. Both the q_Q and q_G decreased during the decline phase even though specific Mab production rate remained constant (data not shown).

4.3.4 Nucleotide analysis

One of the goals of this study was to determine if a relationship exists between intracellular nucleotide pools and Mab production. The nucleotide content of cells at 33°C, 37°C and 39°C was determined from pooled daily samples taken over a 6 day cultivation period for the cultures indicated in Figure 4.1 and 4.2 and also from pooled samples taken after the temperature shift (Fig. 4.4 and 4.5). The total intracellular nucleotide concentration of cells was not significantly different between 33°C and 37°C (Tables 4.3 and 4.4). However, at 39°C there was a significant increase in the concentration of all identified nucleotides which included ATP, GTP, CTP, UTP, ADP, GDP, UDP-GalNac, UDP-GlcNac, UDP-Glc, AMP and NAD (data not shown). The imbalance of the nucleotide content at different temperatures is better reflected in the relative concentrations of specific nucleotides, which is expressed as a percentage of the total intracellular nucleotide content in Tables 4.3 and 4.4. Only the values at maximal cell density or after a 24 hour exposure to different temperatures are shown but statistical analysis was performed on multiple points from daily samples to include all phases of cultures. Statistical analysis was done with a one-tailed paired *t*-test (Appendix A2).

The main component of the nucleotide pool at all temperatures was ATP which accounted for about 34 - 40 % of total nucleotide concentration (Tables 4.3 and 4.4). The relative concentration of ATP decreased with a rise in temperature. Despite the decrease in ATP, no significant differences in the adenylate energy charge (ATP+0.5ADP)/ATP+ADP+AMP) were found (Tables 4.5 and 4.6). Values were maintained above 0.81 for all cultures during the 6 day cultivation period (Fig. 4.7).

Table 4.3 Relative quantities of nucleotides compared to the total nucleotide content at maximum cell density. Statistical evaluation was performed with a one tailed paired *t*-test. The total measured nucleotide content is equal to 100 %.

Temperature (°C)	Total (nmol/ 10^6 cells)	NAD (%)	UDP-Glc (%)	UDP-GalNac (%)	UDP-GlcNac (%)	UTP (%)	CTP (%)	GTP (%)	ATP (%)	ADP (%)	AMP (%)	GDP (%)
33	9.3	6.7	2.1	2.2[a]	7.3[a]	13.8[b]	6.1	7.4[a]	43.9[a]	6.8	2.5[b]	1.2
37[c]	8.8	7.0	1.4	3.7	13.6	11.1	4.4	8.5	41.5	5.7	1.8	1.3
37[d]	7.9	7.5	1.3	4.5	15.8	8.2	6.7	8.0	40.3	5.4	1.1	1.1
39	12.8[a]	8.2[a]	0.8	6.5[a]	22.0[a]	7.2	5.8	8.1	34.2[a]	4.3[a]	1.8	0.9

[a]Represents significant differences ($P < 0.1$) determined from day 1 to 6 ($n = 5$) when compared to controls (37 °C).
[b]Represents significant differences ($P < 0.1$) determined from day 3 to 6 ($n = 3$) when compared to controls (37 °C).
[c]Same cell stock culture used for 33 °C experiment.
[d]Same cell stock culture used for 39 °C experiment.

Table 4.4 Relative quantities of nucleotides compared to the total nucleotide content from the temperature shift experiments. Representative values were taken 24 hours after the temperature shift. Statistical evaluation was performed with a one tailed paired *t*-test. The total measured nucleotide content is equal to 100 %.

Temperature (°C)	Total (nmol/ 106 cells)	NAD (%)	UDP-Glc (%)	UDP-GalNac (%)	UDP-GlcNac (%)	UTP (%)	CTP (%)	GTP (%)	ATP (%)	ADP (%)	AMP (%)	GDP (%)
33	11.5	6.5[a]	1.8	2.5[a]	11.4[a]	13.2	5.2	8.5	41.8[a]	5.4	2.5	1.1
37[b]	8.8	7.0	1.4	3.7	13.6	11.1	4.4	8.5	41.5	5.7	1.8	1.3
37[c]	12.2	7.7	1.4	4.1	15.5	9.7	4.1	8.0	37.9	5.7	4.3	1.6
39	13.2[a]	8.3[a]	1.3	5.9[a]	18.9[a]	7.4	4.9	7.4	34.8[a]	6.9	1.8	2.3

[a]Represents significant differences ($P < 0.1$) determined from day 3 to 5 ($n = 3$) when compared to controls (37 °C).
[b]Same cell stock culture used for 33 °C experiment.
[c]Same cell stock culture used for 39 °C experiment.

Table 4.5 Nucleotide ratios at maximum cell density. Statistical evaluation was performed with a one tailed paired *t*-test.

Temperature (°C)	SA/SU	Purine/ pyrimidine	ATP/GTP	UTP/CTP	Energy charge	NTP ratio	U-ratio	NTP/U
33	2.09[a]	1.96[b]	5.92[a]	2.27	0.89	2.59[a]	1.44[a]	1.79[b]
37[c]	1.65	1.72	4.86	2.51	0.90	3.23	0.64	5.03
37[d]	1.57	1.53	5.01	1.21	0.92	3.25	0.40	8.09
39	1.10[b]	1.17[b]	4.21[a]	1.26	0.90	3.26	0.25[a]	12.81[a]

[a]Represents significant differences ($P < 0.1$) determined from day 1 to 6 ($n = 5$) when compared to controls (37 °C).

[b]Represents significant differences ($P < 0.1$) determined from day 3 to 6 ($n = 3$) when compared to controls (37 °C).

[c]Same cell stock culture used for 33 °C experiment.

[d]Same cell stock culture used for 39 °C experiment.

Table 4.6 Nucleotide ratios from the temperature shift experiments. Representative values were taken 24 hours after the temperature shift. Statistical evaluation was performed with a one tailed paired *t*-test.

Temperature (°C)	SA/SU	Purine/ pyrimidine	ATP/GTP	UTP/CTP	Energy charge	NTP ratio	U-ratio	NTP/U
33	1.72[a]	1.74	4.92[a]	2.53	0.90	2.73	0.93	2.86
37[b]	1.65	1.72	4.86	2.51	0.90	3.23	0.64	5.03
37[c]	1.56	1.66	4.74	2.38	0.85	3.32	0.50	6.68
39	1.30[a]	1.38[a]	4.71[a]	1.49	0.88	3.42	0.30	11.50

[a]Represents significant differences ($P < 0.1$) determined from day 3 to 5 ($n = 3$) when compared to controls (37 °C).

[b]Same cell stock culture used for 33 °C experiment.

[c]Same cell stock culture used for 39 °C experiment.

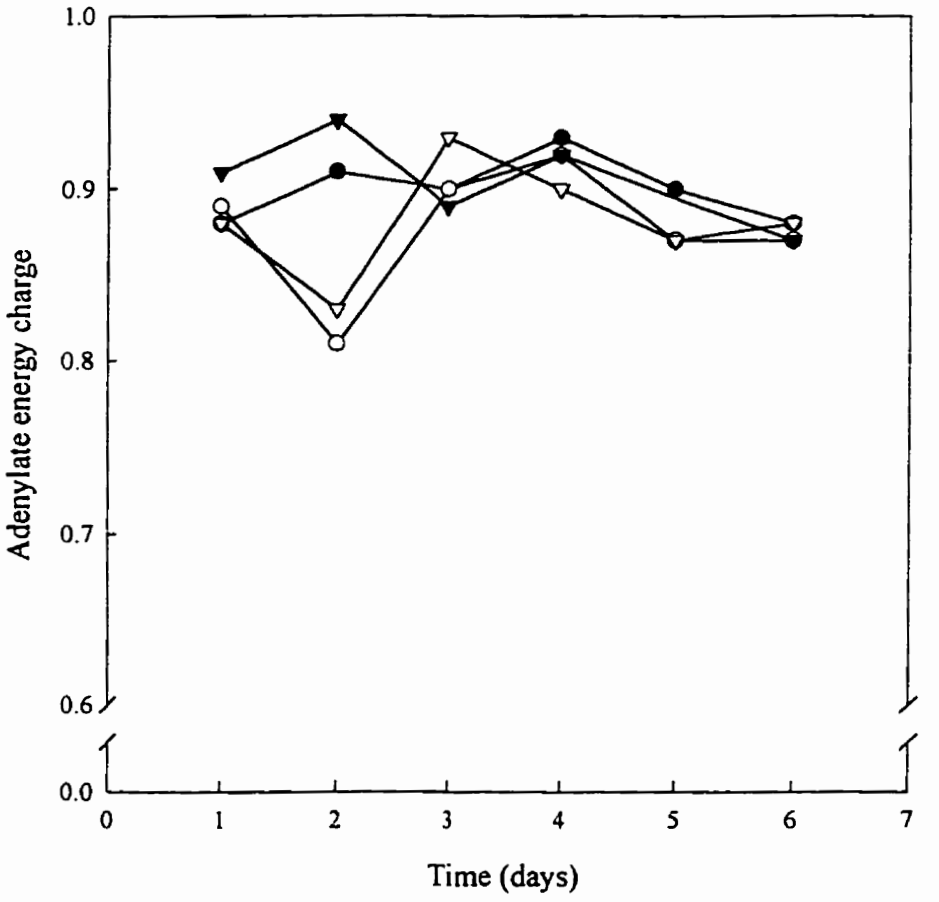

Figure 4.7 Effect of temperature on adenylate energy charge: 37°C (●) and 33°C (▼) ; 37°C (O) and 39°C (∇). Control cultures (37°C) were set-up for each nonstandard temperature. The control for the 33°C culture is represented by closed circles whereas the control for the 39°C culture by open circles.

The relative concentration of UDP-sugars (UDP-GalNac and UDP-GlcNac) increased significantly with temperature from 33 - 39°C (Tables 4.3 and 4.4). At 39°C, the relative UDP-GNac pool increased 23 - 40 % compared to cultures at 37°C. UDP-GlcNac was the predominant sugar - nucleotide at all temperatures and accounted for more than 60 % of UDP-sugar content. It was also observed that cells regardless of the temperature accumulated UDP-GNac (UDP-GalNac + UDP-GlcNac) as the cell culture progressed through the exponential and decline phases (Fig. 4.8 and Fig. 4.9). A corresponding decrease in the relative content of UTP was also found during the progress of each culture. The relative concentration of UTP was also significantly higher at 33°C than at 37°C (Fig. 4.8), although no significant differences were found at 39°C. Other significant changes in nucleotide levels include a decrease in the relative concentration of GTP at 33°C and an increase in NAD at 39°C. The UDP-Glc, CTP, GDP pools did not change with temperature (Table 4.3 and Table 4.4).

The imbalance of the intracellular nucleotide content is also reflected in nucleotide ratios as seen in Tables 4.5 and 4.6. For the CC9C10 hybridoma, characteristic changes were observed in nucleotide ratios during the course of culture. The U-ratio, (UTP/UDP-GNac) decreased from an initial value of 1.8 - 2.5 in control cultures to 0.5 at maximum cell density, after which there was a further decrease to 0.1 (Fig. 4.10). The NTP ratio, (ATP + GTP)/(UTP + CTP), of control cultures increased from an initial value of 1.2 to 3.2 at maximum cell density and increased further to 3.8 - 4.3 at the end of culture (Fig.4.11). The NTP/U ratio, (i.e. NTP ratio/ U-ratio), increased from 0.5 - 0.7 initially to 5 - 8 at maximum cell density and then increased further to a value of 16 - 25 (Fig. 4.12). These trends in nucleotide ratio fluctuations (i.e. U-ratio decrease, NTP ratio and NTP/U ratio increase) were also observed at 33°C and 39°C.

Some significant differences were however observed in the ratio values with respect to culture temperature. The SA/SU (adenyl nucleotides/uridine nucleotides), purine/pyrimidine, ATP/GTP and U-ratios all decreased with increased culture temperature (Table 4.5). The decrease in SA/SU and purine/pyrimidine ratios are due to a rise in relative concentrations of UDP-GlcNac and a fall in ATP (Table 4.3). The ATP/GTP ratio was constant (4.79 ± 0.05; n=10) at 37°C over a 6 day cultivation period

(Table 4.5, Fig. 4.13). At 33°C and 39°C, the ATP/GTP ratio stabilized after 2 days of incubation to values of 4.86 and 4.18 respectively. In contrast, the pyrimidine triphosphate ratio (UTP/CTP) did not show any significant differences with respect to time or culture conditions. It was also found that the NTP/U ratio also increased with higher culture temperatures. Similar patterns in nucleotide ratios were observed in the temperature shift experiment (Table 4.6).

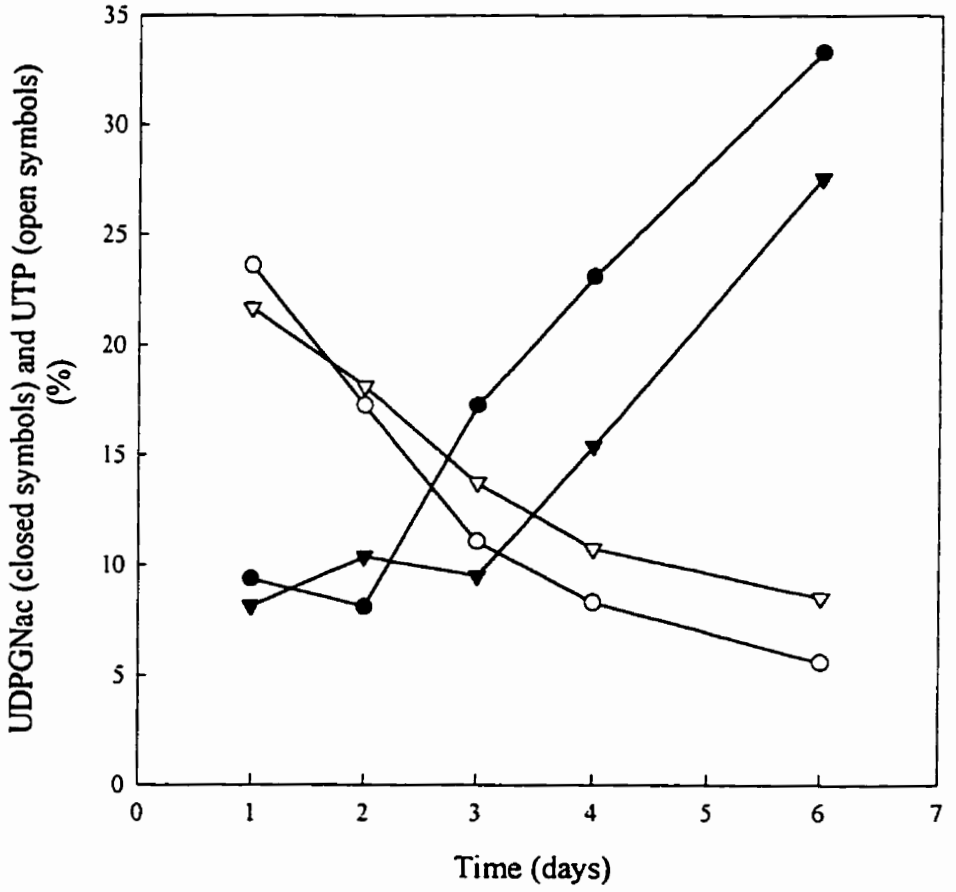

Figure 4.8 Changes in the relative quantities of UDP-GNac and UTP at 37°C and 33°C: The UDP-GNac and UTP fractions are referred to the total amount of identified nucleotides. UDP-GNac is defined as the sum of UDP-GalNac and UDP-GlcNac: 37°C (●, O) and 33°C (▼;▽). UTP and UDP-GNac values at 37°C and 33°C were statistically different based on one tailed paired *t*-tests (Re: Table 4.3).

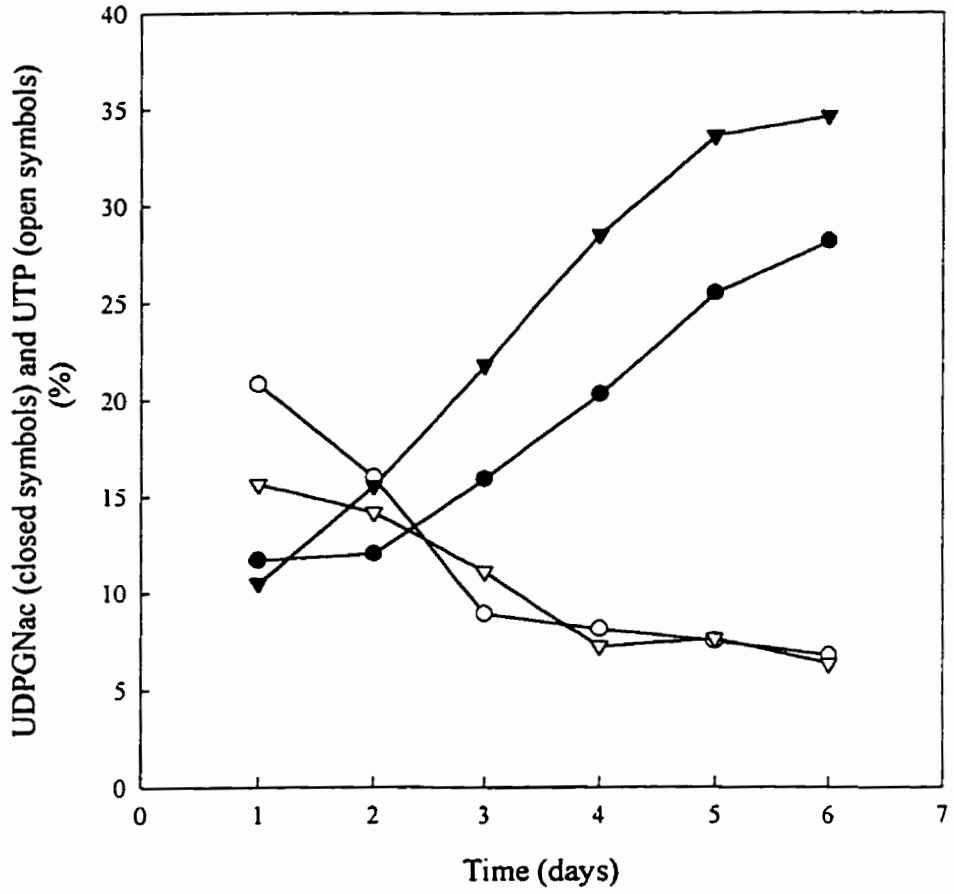

Figure 4.9 Changes in the relative quantities of UDP-GNac and UTP at 37°C and 39°C: The UDP-GNac and UTP fractions are referred to the total amount of identified nucleotides. UDP-GNac is defined as the sum of UDP-GalNac and UDP-GlcNac: 37°C (●, O) and 39°C (▼;▽). UDP-GNac values at 37°C and 39°C were statistically different based on a one tailed paired *t*-test (Re: Table 4.3).

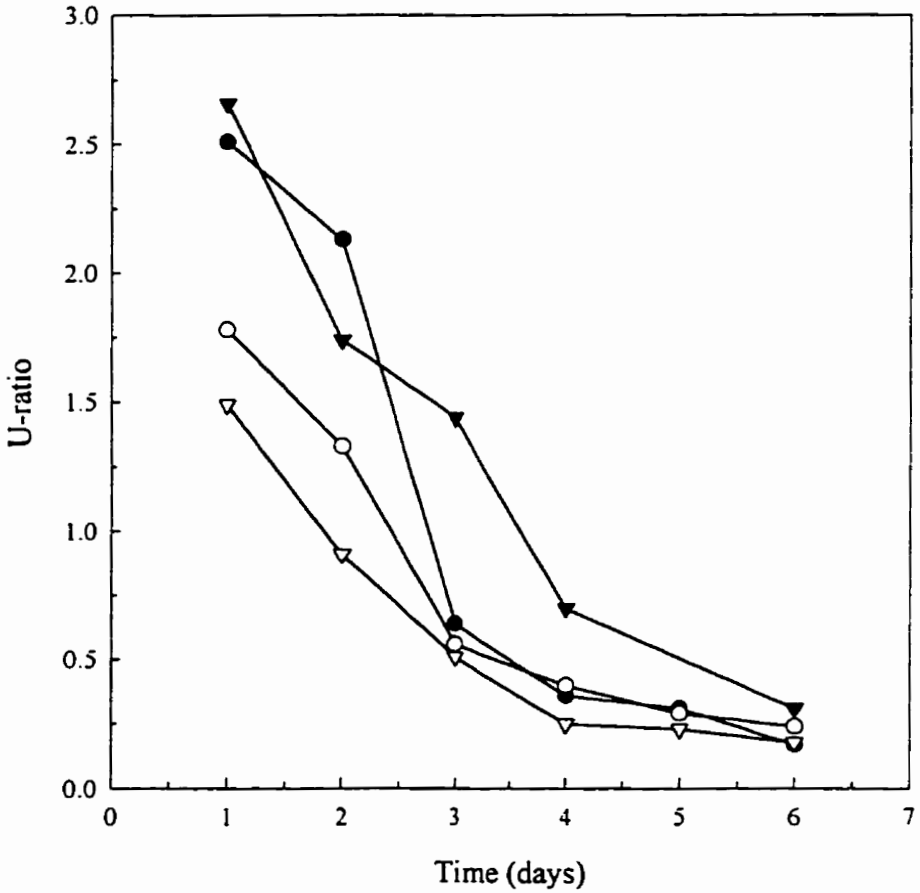

Figure 4.10 Effect of temperature on the U-ratio: 37°C (●) and 33°C (▼); 37°C (O) and 39°C (∇). Control cultures (37°C) were set-up for each nonstandard temperature. The control for the 33°C culture is represented by closed circles whereas the control for the 39°C culture by open circles. The U-ratio is defined as (UTP/UDP-GNac). U-ratios at 33°C and 39°C were statistically different from values at 37°C based on one tailed paired *t*-tests (Re: Table 4.5).

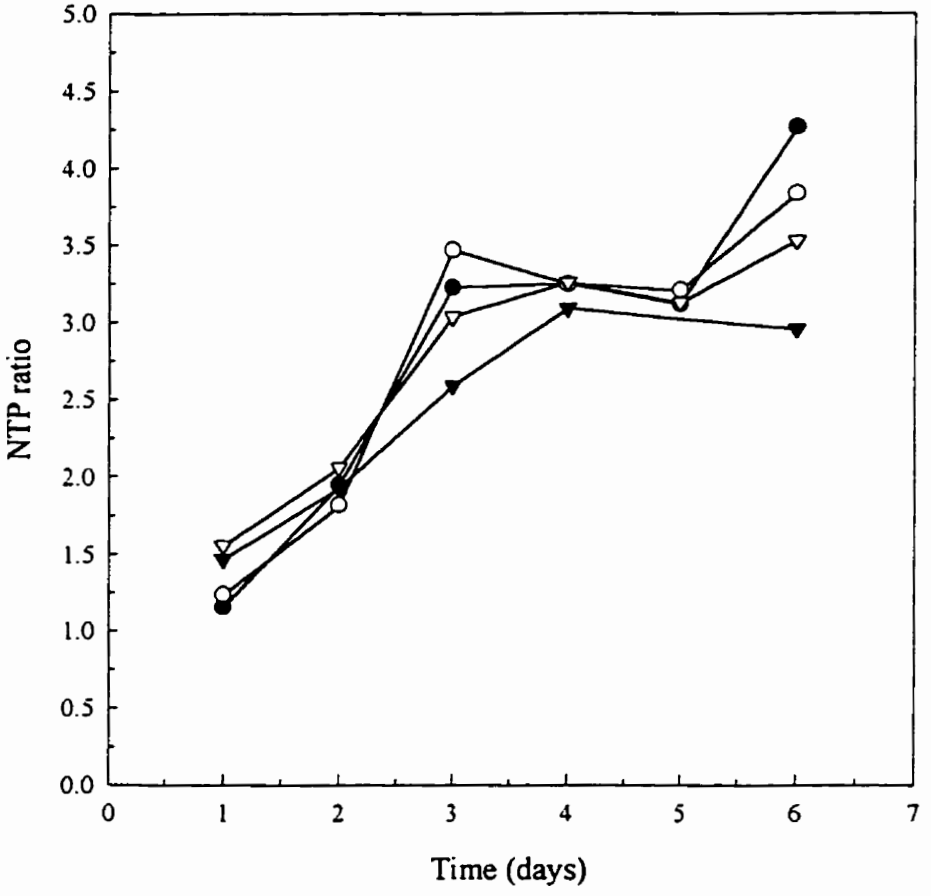

Figure 4.11 Effect of temperature on the NTP ratio: 37°C (●) and 33°C (▼); 37°C (O) and 39°C (▽). Control cultures (37°C) were set-up for each nonstandard temperature. The control for the 33°C culture is represented by closed circles whereas the control for the 39°C culture by open circles. The NTP ratio is defined as (ATP + GTP)/(UDP + CTP). The NTP ratios at 33°C were statistically different from values at 37°C based on a one tailed paired *t*-test (Re: Table 4.5).

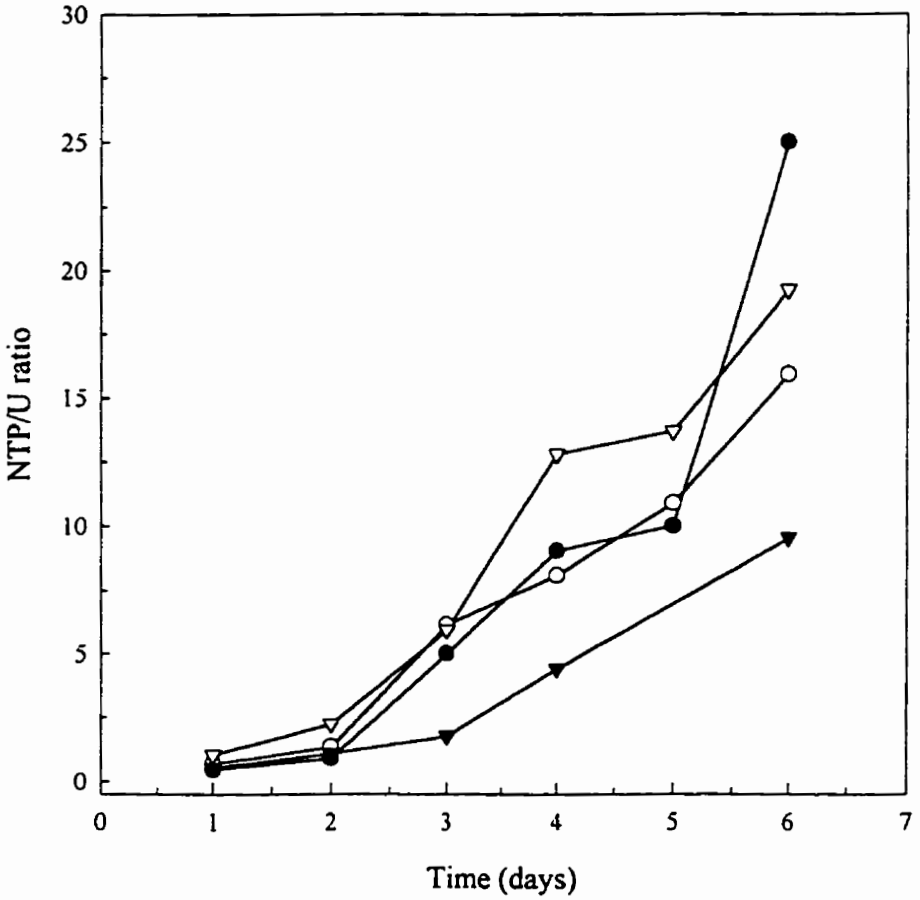

Figure 4.12 Effect of temperature on the NTP/U ratio: 37°C (●) and 33°C (▼); 37°C (O) and 39°C (∇). Control cultures (37°C) were set-up for each nonstandard temperature. The control for the 33°C culture is represented by closed circles whereas the control for the 39°C culture by open circles. The NTP/U ratio is defined as (NTP ratio/ U-ratio). The NTP/U ratios at 33°C and 39°C were statistically different from values at 37°C based on one tailed paired *t*-tests (Re: Table 4.5).

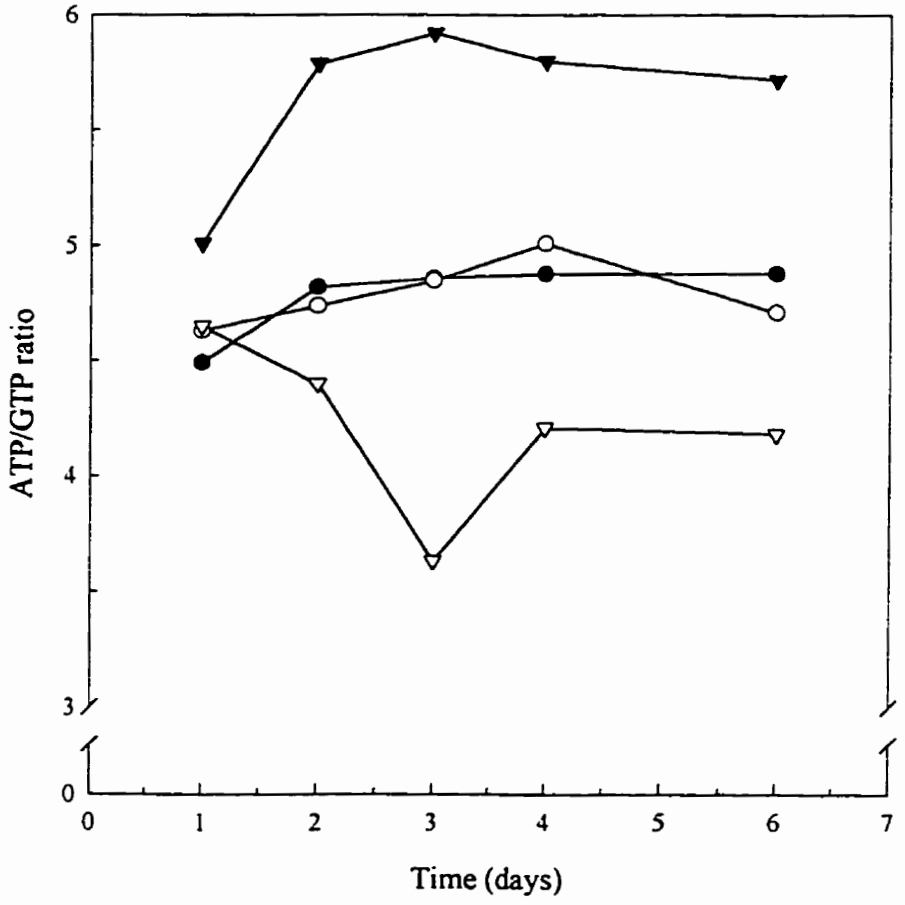

Figure 4.13 Ratio between ATP and GTP at various temperatures: 37°C (●) and 33°C (▼); 37°C (O) and 39°C (▽). Control cultures (37°C) were set-up for each nonstandard temperature. The control for the 33°C culture is represented by closed circles whereas the control for the 39°C culture by open circles. The ATP/GTP ratios at 33°C and 39°C were statistically different from values at 37°C based on one tailed paired *t*-tests (Re: Table 4.5).

4.4 Discussion

The objective of the work described in this chapter was to determine whether changes in the specific monoclonal antibody production rate (qMab) could be correlated with changes in intracellular nucleotide pools. To achieve differential rates of qMab, CC9C10 hybridomas were cultured in temperatures ranging from 33°C - 39°C.

Similar maximum viable cell densities and μ_{max} were attained at 33°C and 37°C. At 39°C, however the maximum viable cell density and μ_{max} decreased significantly 2-fold compared to controls. It is interesting to note that, although the maximum cell densities attained at 37°C and 39°C were significantly different, growth ceased at the same time point. Lactate and ammonia concentrations at this time point were the same in both 37°C and 39°C suggesting that similar factors may have been involved in limiting cell yields in both cultures. High accumulations of lactate and ammonia at 39°C despite reduced μ_{max} and viable cell densities were due to increased rates of cell metabolism. Previous analysis of hybridoma growth with respect to temperature range showed a similar decrease in maximal cell density at 39°C, lower μ_{max} values at 33°C and unchanged or higher μ_{max} values at 38-39°C compared to controls at 37°C (Sureshkumar and Mutharasan, 1990; Bloemkolk *et al.*, 1992). The effect of temperature on μ_{max} therefore appears to be cell line specific.

The qMab was linear at all temperatures indicating constant productivity during the course of each culture. The qMab was therefore independent of cell growth, an observation which has been made previously for hybridomas (Renard *et al.*, 1988; Sureshkumar and Mutharasan, 1990; Ozturk and Palsson, 1991b). An increase in temperature however was concomitant with an increase in qMab. The qMab for the control cultures ranged from 24 - 28 $\mu g/10^6$ cells. The variable qMab values for the controls are attributed to a slight loss in antibody productivity with cell passage which is not uncommon for hybridoma cell lines (Schmid *et al.*, 1990). The observation of increased qMab at elevated temperatures is also compatible with findings from other laboratories (Reuveny *et al.*, 1986; Sureshkumar and Mutharasan, 1990; Borth *et al.*, 1992). Furthermore, human peripheral blood lymphocytes show enhanced DNA synthesis

and proliferation at higher-than-normal temperatures, an effect which has been related to the immune response of lymphocytes in vivo during fever (Smith *et al.*, 1978; Wooten *et al.*, 1993).

In an effort to improve Mab yield, CC9C10 hybridomas were grown to a high cell density before shifting to a qMab enhancing temperature (i.e. 39°C). This strategy did not improve the maximum Mab titer as expected. Shifting the temperature to 39°C did cause a significant increase in the qMab however this was accompanied by a significant decrease in viable cell concentration, an effect which was also noted by Sureshkumar and Mutharasan (1990). Comparisons between cultures inoculated at 39°C and cultures shifted to 39°C after two days of incubation indicates that CC9C10 cells are less susceptible to temperature when they are in the exponential phase of growth. This suggests that thermotolerance is achieved during the growth phase perhaps due to the synthesis of heat shock proteins (HSP's). It has been shown that hyperthermia can induce the expression of HSP's which confer tolerance to stressful environments in mammalian cell cultures (Subjeck *et al.*, 1982; Passini and Gochee, 1989). In Ehrlich ascites tumor cells, it is the exponential phase rather than stationary phase cells that are more sensitive to hyperthermia (Gabai *et al.*, 1995).

An increase in temperature resulted in an increase in the specific rate of glucose uptake and lactate production, a finding consistent with other hybridoma cell lines (Reuveny *et al.*, 1986; Sureshkumar and Mutharasan, 1990). The amount of lactate produced per unit of glucose was relatively constant in the temperature ranges tested. This suggests that the catabolic pathway of glucose utilization does not change with temperature, a result which concurs with a previous report (Borth *et al.*, 1992). This is however in contrast to Sureshkumar and Mutharasan (1990) who reported a 2.4 fold increase in the lactate yield in the same temperature range (33 - 39°C).

The specific glutamine uptake rate q_Q increased at 39°C with no change in ammonia yield compared to controls at 37°C. At 33°C, q_Q was the same as at 37°C whereas the ammonia yield was lower. These observations were attributed to changes in cell metabolism as opposed to changes in the spontaneous degradation rate of glutamine. The rate of spontaneous degradation of glutamine occurs at 10% per day, which would be

reflected in an increase of 0.6 mM ammonia per day at 37°C in the culture medium used in these experiments (Tritsch and Moore, 1962). The degradation rate is affected by temperature with an increase of 12% at 39°C and decrease of 20% at 33°C. Although these rates affect the determined values of q_Q and q_G, they are not sufficient to account for the significant differences observed between culture temperatures, which must therefore be related to metabolic effects.

Once it was established that increasing the temperature resulted in a higher per cell formation of Mab, intracellular nucleotides were examined for a possible correlation to this phenomenon. Fluctuations in nucleotide pool size have been shown in the past to affect enzyme activities and to correlate with cell cycle phases, proliferation, differentiation and transformation (De Korte *et al.*, 1987; Sharma *et al.*, 1993). Fluctuations in nucleotide pool size are also indicators of growth behavior in mammalian and plant cell cultures (Meyer and Wagner, 1985; Ryll and Wagner, 1992).

The main component of the nucleotide pool at all temperatures was ATP which accounted for about 35 - 40 % of total nucleotide concentration. The absolute cell concentration of ATP increased at higher temperatures, in line with the increase in total intracellular nucleotide concentration and concurring with previous data that ATP concentration correlated with qMab (Modha *et al.*, 1992). However, the relative concentration of ATP, expressed as a percentage of total nucleotides, decreased with a rise in temperature and qMab. This decrease in ATP may have been related to the observed increase in NAD which is synthesized from ATP via NAD pyrophosphorylase (Williams *et al.*, 1987). The adenylate energy charge which is a good indicator of the energy status of the cell (Atkinson, 1977) was maintained above 0.81 in all cultures. These results agree with Modha *et al.* (1992) who reported unchanged energy charge values with increased qMab in hybridoma cultures in which DNA synthesis was inhibited.

The most pronounced change in relative nucleotide pool concentrations was the fluctuation of the acetylated UDP-sugars (UDP-GalNac and UDP-GlcNac) which increased significantly with temperature from 33 - 39°C and was concurrent with an increase in qMab. The UDP-sugars are precursors of the carbohydrate side chains of glycoproteins (including Mab). Rates of intracellular glycosylation and subsequent

glycoprotein secretion may well be related to the availability of the appropriate UDP-sugars. This is supported by evidence that higher glycosyltransferase activities are associated with elevated Mab productivity (Cole *et al.*, 1993). However, any hypothesis relating UDP-sugar pools and qMab must take into account the observed accumulation of the nucleotide-sugars at an apparently constant qMab during the progress of each culture. This event is also accompanied by a corresponding decrease in the relative content of UTP, a relationship previously observed in hybridomas (Ryll and Wagner, 1992). This decrease in UTP is probably directly related to its conversion to the sugar-nucleotide pool (amino sugar + UTP $\rightarrow$ UDP-GNac + Pi). UDP-GNac accumulation during cell culture has been observed in the past but has been associated with reduced growth rates (Ryll and Wagner, 1992) and transformation of neutrophiles (De Korte *et al.*, 1987).

The NTP, U- and NTP/U ratios have been suggested as tools for monitoring the physiological state of mammalian cells in vitro and as early predictors of the entry of cells into a reduced growth phase (Ryll and Wagner, 1992). Decreases in nucleotide ratios were also shown during the transformation of myelocytes (De Korte *et al.*, 1987). For the CC9C10 hybridoma, characteristic changes were observed in these nucleotide ratios during the course of culture regardless of temperature. For example, the U-ratio decreased whereas the NTP and NTP/U ratios both increased as the cultures progressed through the exponential, stationary and decline phases. This is consistent with trends in ratios observed by Ryll and Wagner (1992) for hybridomas entering the stationary phase in perfused reactors. Comparisons with viable cell densities also indicate that a significant increase in the NTP/U ratio after day 2 (39°C) or day 3 (33°C) coincided with the end of the exponential phase of growth of CC9C10 hybridomas. This concurs with a previous report (Ryll and Wagner, 1992).

On the other hand some significant differences were observed in nucleotide ratios with respect to culture temperature. The SA/SU (adenyl nucleotides/uridine nucleotides), purine/pyrimidine, ATP/GTP and U-ratios all decreased with increased culture temperature and correlated with increased qMab. Each temperature was associated with a specific ATP/GTP ratio. The ATP/GTP ratio reflects the division of purine nucleotide synthetic pathways into guanine and adenine nucleotides and has been shown to be

regulated by the nutritional state in a lower eukaryote (Pall and Robertson, 1988). A constant ATP/GTP ratio was also reported by Ryll and Wagner (1992) for a perfused culture of murine hybridomas with no indication of its effect on Mab production rates.

4.5 Conclusion

The specific monoclonal antibody productivity (qMab) of CC9C10 hybridoma increased with incubation temperature in the range 33°C to 39°C. qMab was constant at each temperature and was independent of the phase of culture. The qMab increased by 97 % at 39°C and decreased by 21% at 33°C compared to controls at 37°C. The μ_{max} was 59 % lower at 39°C compared to control cultures (37°C). Specific rates of substrate (glucose and glutamine) utilization and by-product (lactate and ammonia) formation also increased with temperature but the yield coefficient, $Y_{Lac/Glc}$ was constant for 33-39°C and $Y_{Amm/Gln}$ was constant for 37-39°C. $Y_{Amm/Gln}$ at 33°C was lower than the control.

The increased qMab at elevated temperatures correlated with certain parameters related to the intracellular nucleotide pool. These included the relative content of UDP-N-acetyl galactosamine, UDP-N-acetyl glucosamine, NAD and NTP/U ratio which increased with qMab whereas the relative ATP content, SA/SU ratio, ATP/GTP ratio and purine/pyrimidine ratio and U-ratio all decreased with qMab. In particular, the relative UDP-GNac pool was increased by 23 - 40 % compared to controls at 37°C. The correlation of these nucleotide parameters with qMab indicates the possibility that they may have a regulatory role with respect to antibody synthesis or secretion.

Several changes in nucleotide pool ratios were also associated with progression of cultures through exponential, stationary and death phases. The NTP and NTP/U ratios increased whereas the U-ratio decreased during the course of each culture. The adenylate energy charge however remained relatively constant at a value >0.8 during all phases.

Conclusions on the effects of temperature on qMab, cell metabolism, nucleotide pools and their interrelationships were supported by duplication of the experiments with CC9C10 cultures inoculated from different cell stocks (data not shown).

CHAPTER 5

5.0 The effect of thymidine or sodium butyrate supplementation on nucleotide pools and monoclonal antibody production

5.1 Introduction

In previous experiments it was shown that an increase in the cultivation temperature was concomitant with an increase in the qMab and specific changes in the nucleotide pool (chapter 4). To determine if these nucleotide pool fluctuations were consistent with qMab enhancement other methods of increasing Mab production in hybridomas were investigated. Two methods were employed: supplementation of cultures with thymidine or supplementation of cultures with sodium butyrate.

Supplementation of cultures with thymidine can increase the specific rate of antibody production in hybridomas (Hayter *et al.*, 1992). It is believed that the enhanced qMab is due to the thymidine-induced cell growth arrest. Other factors such as cAMP supplementation or hyperosmolarity which perturb cell growth can also enhance productivity (Oyaas *et al.*, 1989; Dalili and Ollis, 1988). Perturbation of cell growth may result in energy normally destined for building cell mass for replication being directed toward non-essential protein synthesis.

Sodium butyrate supplementation has been shown to enhance the production of proteins in several cell lines including Chinese hamster ovary cells, HeLa and hybridomas (Oh *et al.*, 1993). The increase in protein production due to sodium butyrate may be linked to the hyperacetylation of histones which leads to increased accessibility of DNA to RNA polymerase. Alternatively, an increase in protein production may also be due to the growth arresting properties of sodium butyrate (Bruce *et al.*, 1992).

5.2 Results

5.2.1 The effect of thymidine on growth, productivity and intracellular energy charge of CC9C10 hybridomas[1]

The aim of this experiment was to determine if the specific monoclonal antibody production rate (qMab) could be enhanced by thymidine supplementation and whether this could be correlated with changes in intracellular nucleotide pools.

CC9C10 hybridomas from the mid-exponential phase of stock cultures were inoculated at 1.5 x 10^5 cells/ml by dilution into 150 cm^2 T-flasks containing NB-SFM (25 mM glucose, 6 mM glutamine). Starting on day 2, cultures were fed daily with glucose and glutamine and the pH was adjusted as previously described (section 2.3). Thymidine (0 - 8 mM) was added to cultures on the second day of incubation from a concentrated stock solution (400 mM). To prepare this concentrate, thymidine was first dissolved in 0.65 M NaOH to give a final thymidine concentration of 625 mM. The solution was filter sterilized and stored at - 20°C. When needed the basic thymidine solution was thawed and neutralized with 1 M HCl and 1 M $NaHCO_3$ to give a final thymidine concentration of 400 mM. Each culture condition was done in duplicate from cells inoculated from the same cell stock.

The growth profiles for CC9C10 cells supplemented with varying levels of thymidine are shown in Fig. 5.1. Viable cell concentrations were determined by the trypan blue exclusion method (section 2.5.1). Cell growth was partially arrested upon addition of thymidine (> 4 mM) to CC9C10 cultures. Similar maximum viable cell densities were reached in control cultures (0 mM thymidine) and those supplemented with 4 - 6 mM thymidine (i.e. 1.01 - 1.11 x 10^6 cells/ml). Cultures supplemented with 8 mM thymidine however reached a maximum viable cell density of 0.76 x 10^6 cells/ml, a value 25 % lower

[1]The content of section 5.2.1 were included in a poster presentation at the CSM/SIM Joint Meeting, 1993, Toronto, Ontario.

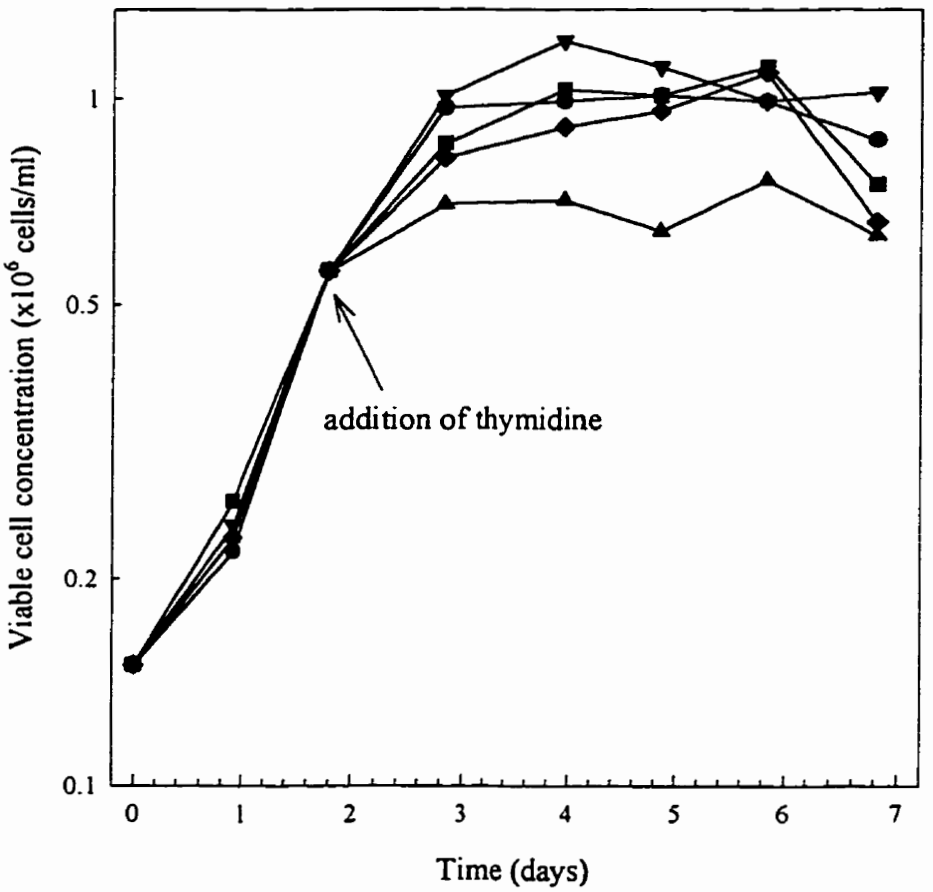

Figure 5.1 The effect of thymidine on CC9C10 cell growth. Hybridomas were inoculated into T-flasks (150 cm^2) containing 90 ml NB-SFM at 1.5 x 10^5 cells/ml. After 2 days of incubation, thymidine was added to the cultures: 0 mM, (●); 2 mM, (▼); 4 mM, (■); 6 mM, (◆); 8 mM (▲). Viable cell concentration values are the mean from two identical flasks inoculated from the same cell stock. Errors were less than 11 % of the mean.

than controls. Cultures supplemented with 2 mM thymidine reached a maximum cell density of 1.21 x 10^6 cells/ml, significantly higher (20 %) than controls. Total cell densities increased daily in all cultures until day 6 (data not shown).

Intracellular adenylate nucleotides were analyzed with a bioluminescent assay (section 2.7.3). It was found that the addition of thymidine after 2 days of incubation caused a significant decrease in the adenylate energy charge compared to control values (Fig.5.2). Energy charge values were stabilized in all cultures after 4 days of incubation and were inversely proportional to the amount of thymidine in the medium (Table 5.1). Control culture energy charge remained at 0.83 ± 0.01 from day 4 - 7. This is in contrast to 8 mM thymidine supplemented cultures in which energy charge was 0.13 units lower than the controls during the same period.

The monoclonal antibody concentration of cultures was determined by HPLC (section 2.6.1). The Mab yield after 7 days of incubation was approximately the same for controls and thymidine supplemented cultures (95 - 106 μg/ml) despite the differences in the viable cell density. A plot of the Mab concentration versus the viability index showed that the qMab (i.e. slope of the curve) increased significantly when cultures were supplemented with 8 mM thymidine (Fig. 5.3). A comparison of the qMab during the period of stable energy charge levels is shown in Table 5.1. The addition of 6 and 8 mM caused a 26 % and 61 % increase in the qMab respectively compared to control cultures (18.8 μg/10^6 cell days) This increase in qMab coincided with a decrease in energy charge levels.

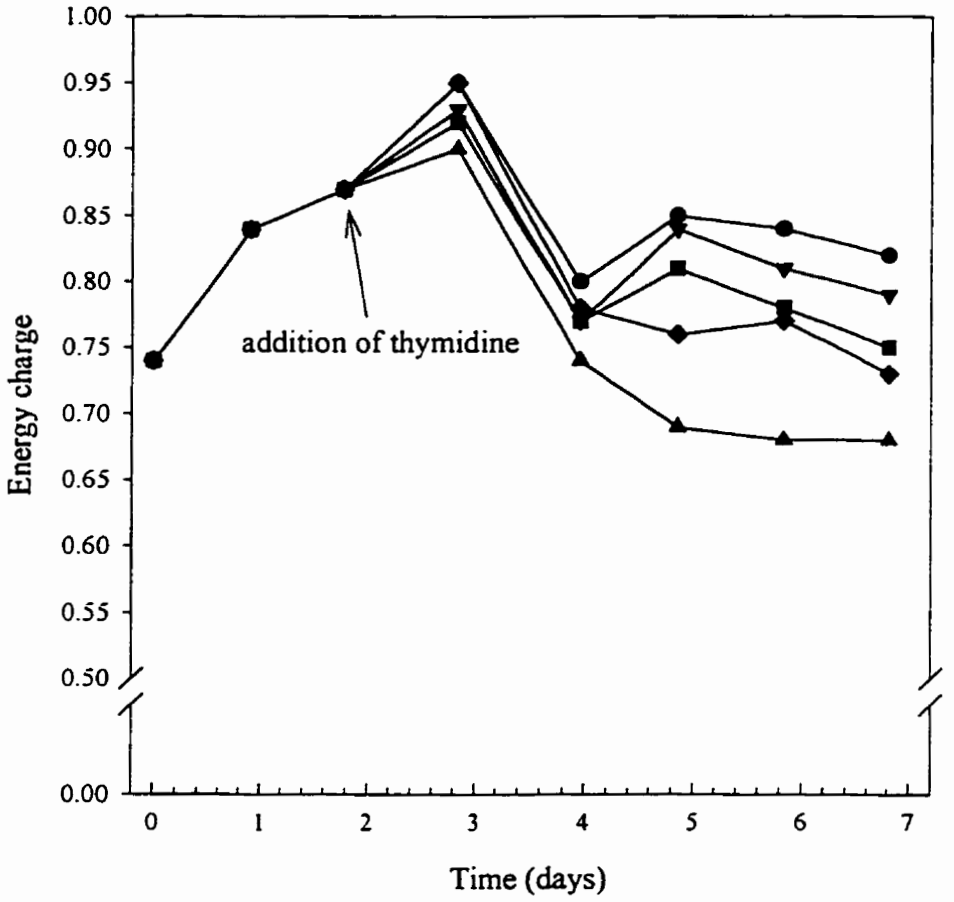

Figure 5.2 The effect of thymidine on CC9C10 intracellular energy charge. Hybridomas were inoculated into T-flasks (150 cm^2) containing 90 ml NB-SFM at 1.5 x 10^5 cells/ml. After 2 days of incubation, thymidine was added to the cultures: 0 mM, (●); 2 mM, (▼); 4 mM, (■); 6 mM, (◆); 8 mM (▲). Energy charge values are the mean from two identical flasks inoculated from the same cell stock. Errors were less than 0.01 units.

Table 5.1 The effect of thymidine on the intracellular energy charge and the specific Mab production rate (qMab). The qMab was determined from the slope of the viability index versus Mab concentration from days 4 to 7. The error on the qMab was calculated from the standard error of the best straight line through 4 points.

Thymidine (mM)	Average energy charge (days 4 - 7)	qMab (days 4 - 7) - $\mu g/10^6$ cells-days
0	0.83 ± 0.01	18.8 ± 0.8
2	0.80 ± 0.01	17.4 ± 0.8
4	0.78 ± 0.01	19.0 ± 0.8
6	0.76 ± 0.01	23.6 ± 2.0
8	0.70 ± 0.01	30.3 ± 1.5

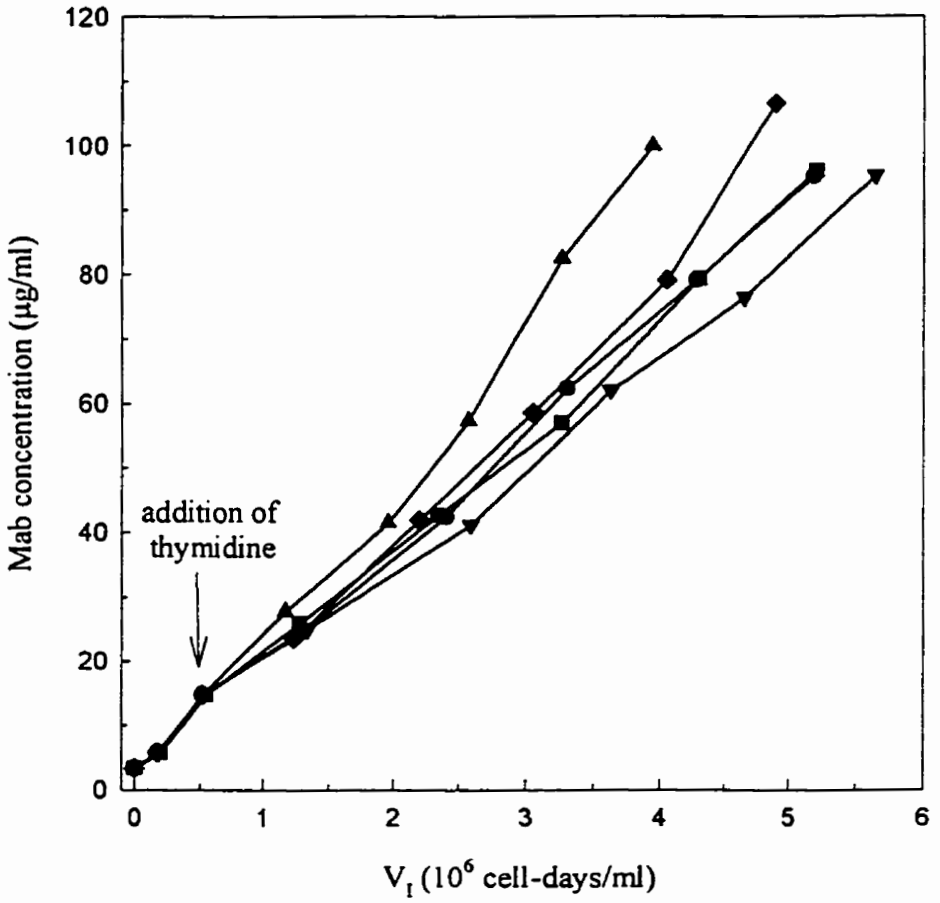

Figure 5.3 The effect of thymidine on specific monoclonal antibody production. Hybridomas were inoculated into T-flasks (150 cm^2) containing 90 ml NB-SFM at 1.5 x 10^5 cells/ml. After 2 days of incubation, thymidine was added to the cultures: 0 mM, (●); 2 mM, (▼); 4 mM, (■); 6 mM, (◆); 8 mM (▲).Mab concentration and the viability index (V_I) values are the mean from two identical flasks inoculated from the same cell stock. Errors were less than 11 % of the mean.

5.2.2 The effect of thymidine on intracellular nucleotide pools

It was found in preliminary experiments (section 5.2.1) that the supplementation of CC9C10 cultures with 8 mM thymidine caused a decrease in the adenylate energy charge which was concomitant with an increase in qMab. In this experiment, the investigation of the effect of thymidine (8 mM) was expanded to include other nucleotide pools which have been previously associated with enhanced qMab (chapter 4). CC9C10 cells were inoculated at 1.5 x 10^5 cells/ml in NB-SFM, supplemented with either 0 or 8 mM thymidine, and cultured as described previously (section 5.2.1). The effect of thymidine supplementation on cell growth, energy charge and qMab was consistent with findings from previous experiments (section 5.2.1). For example, supplementation with 8 mM thymidine caused a 25 % decreased in maximum viable cell density, a 0.11 - 0.12 unit decrease in energy charge and 65 % increase in qMab.

Additional data on the effect of thymidine on nucleotide pools was obtained by ion pair reverse phase liquid chromatography (section 2.7.2) from pooled daily samples taken over a 6 day cultivation period. It was found that the total intracellular nucleotide pool was significantly higher in 8 mM thymidine supplemented cultures compared to control cultures (Table 5.2). The increase in total nucleotides was due to a broad increase in all detectable nucleotides. The imbalance in nucleotide content was also seen in the relative concentration of nucleotides pools which is expressed as a percentage of total nucleotides. The addition of 8 mM thymidine caused a significant decrease in the relative ATP concentration (Table 5.3, Fig. 5.4). Paired daily observations shows that relative concentration of ATP was consistently 14 - 16 % lower in thymidine supplemented cultures. The addition of 8 mM thymidine however had the opposite effect on the two other adenylate nucleotides, ADP and AMP, in addition to GDP (Table 5.3). The mono- and diphosphonucleotides pools increased significantly ($P < 0.1$) when compared to control cultures. In both the 0 and 8 mM thymidine supplemented cultures the relative concentration of acetylated UDP-sugars increased and the relative concentration of UTP decreased as the cultures progressed through the exponential, stationary and decline phases (Fig. 5.5). The relative UDP-GNac of thymidine supplemented cultures was 13 -

Table 5.2 Relative quantities of nucleotides compared to the total nucleotide content (%) from thymidine supplementation experiments (CC9C10 hybridomas). Representative values were taken after 4 days of incubation. Statistical evaluation was performed with a one-tailed paired *t*-test. The total measured nucleotide content is equal to 100 %.

Thymidine (mM)	Total (nmol/ 106 cells)	NAD (%)	UDP-Glc (%)	UDP- GNac (%)	UTP (%)	CTP (%)	GTP (%)	ATP (%)	ADP (%)	AMP (%)	GDP (%)
0	7.9	7.4	1.3	20.3	8.2	6.7	8.0	40.3	5.4	1.1	1.1
8	10.9[a]	7.6	1.3	23.6[a]	8.4	2.5	6.8	34.7[a]	8.9[b]	4.4[b]	1.8[a]

[a] Represents significant differences ($P < 0.05$) determined from day 3 to 6 ($n = 4$) when compared to control cultures (0 mM thymidine).

[b] Represents significant differences ($P < 0.1$) determined from day 3 to 6 ($n = 4$) when compared to control cultures (0 mM thymidine).

Table 5.3 Nucleotide ratios of CC9C10 hybridomas from thymidine supplementation experiments. Representative values were taken after 4 days of incubation. Statistical evaluation was performed with a one-tailed paired *t*-test.

Thymidine (mM)	SA/SU	Purine/ pyrimidine	ATP/GTP	UTP/CTP	Energy charge	NTP ratio	U-ratio	NTP/U
0	1.57	1.53	5.01	1.21	0.92	3.25	0.40	8.09
8	1.44	1.58	4.42[a]	3.28	0.81[a]	3.79	0.35	10.70

[a] Represents significant differences ($P < 0.06$) determined from day 3 to 6 ($n = 4$) when compared to control cultures (0 mM thymidine).

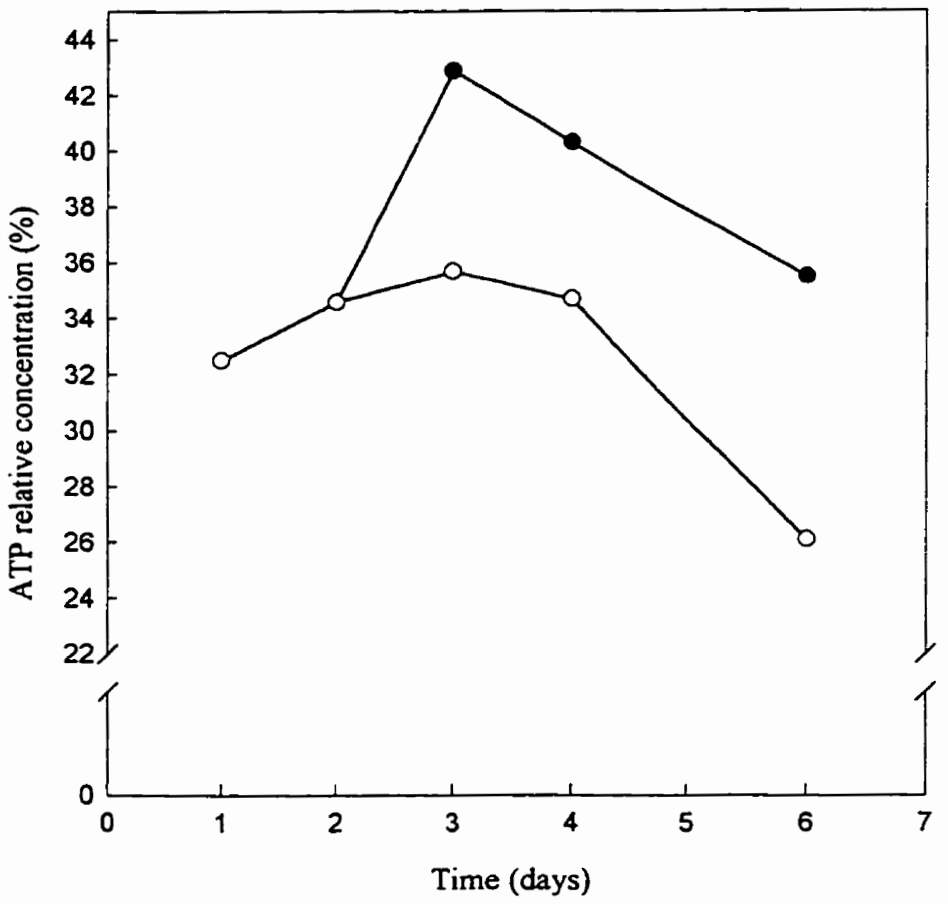

Figure 5.4 The effect of thymidine on the relative quantity of ATP. Hybridomas were inoculated into T-flasks (150 cm^2) containing 90 ml NB-SFM at 1.5 x 10^5 cells/ml. After 2 days of incubation, thymidine was added to the cultures: 0 mM, (●) or 8 mM (O). ATP values are the result of pooled daily samples and are relative to the total amount of identified nucleotides.

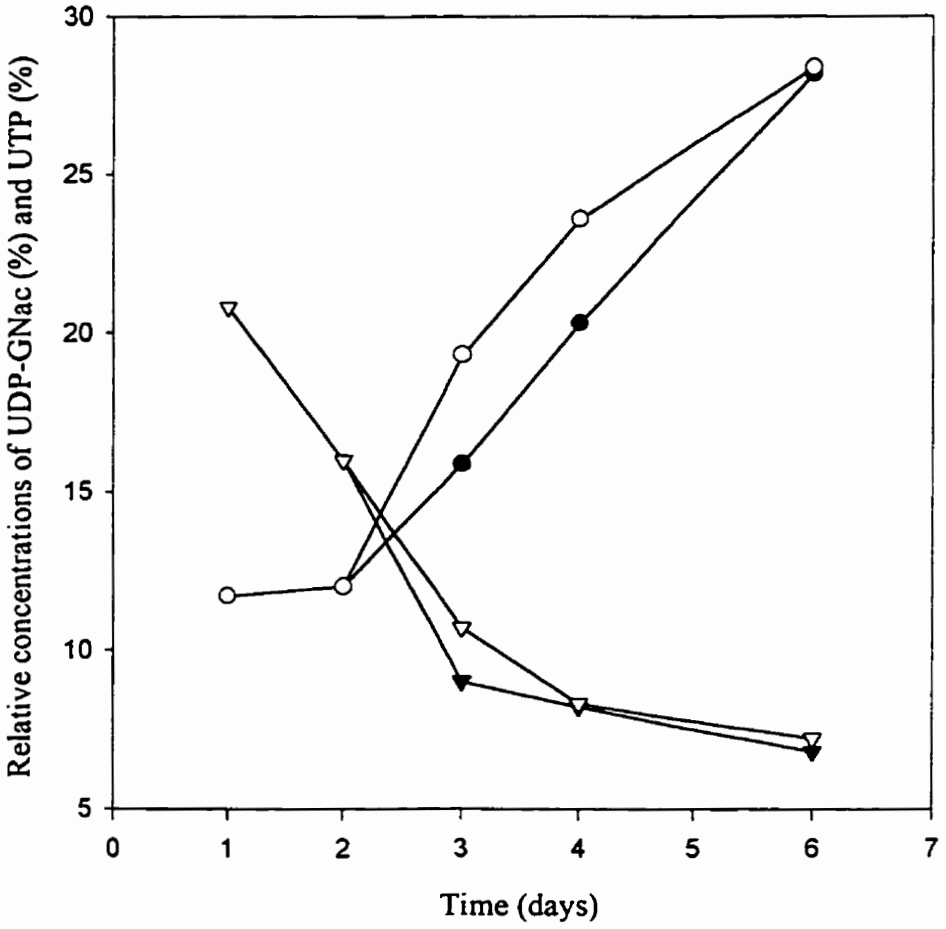

Figure 5.5 The effect of thymidine on the relative quantity of UDP-GNac and UTP. Hybridomas were inoculated into T-flasks (150 cm^2) containing 90 ml NB-SFM at 1.5 x 10^5 cells/ml. After 2 days of incubation, thymidine was added to the cultures: 0 mM, (●, ▼) or 8 mM (O, ∇). UDP-GNac and UTP relative values are represented by circles and triangles respectively. Values are the result of pooled daily samples and are relative to the total amount of identified nucleotides.

16 % higher than controls on days 3 and 4 of incubation. Both cultures eventually attained similar UDP-GNac levels on day 6. The relative concentrations of NAD, UDP-Glc, UTP, CTP, GTP did not change with the addition of thymidine.

Some significant differences were observed in nucleotide ratios (Table 5.3). Energy charge as mentioned previously decreased with the addition of thymidine. The ATP/GTP ratio was also significantly lower in thymidine supplemented cultures (Table 5.3 and Fig.5.6). After day 2, control culture ATP/GTP ratios ranged between 4.7 - 5.0 compared to 3.5 - 4.4 for thymidine supplemented cultures. No significant differences in other nucleotide ratios such as SA/SU, purine/pyrimidine, NTP ratio, U-ratio and NTP/U were observed between controls and thymidine supplemented cultures.

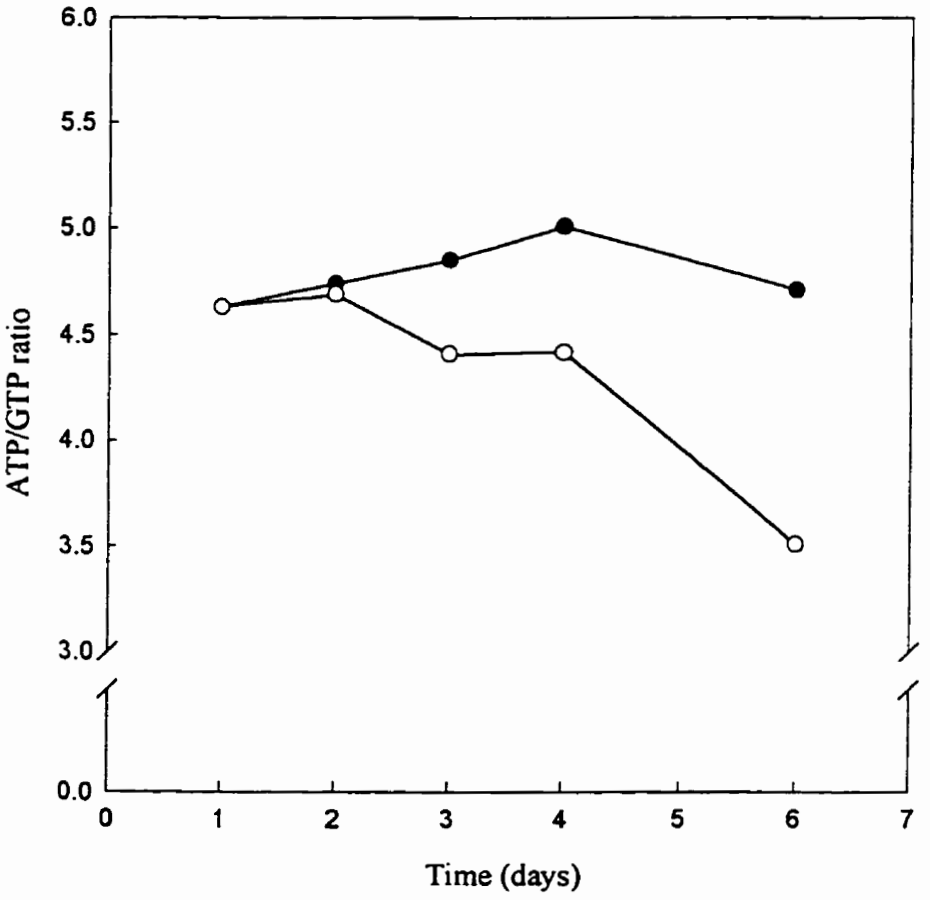

Figure 5.6 The effect of thymidine on the ATP/GTP ratio. Hybridomas were inoculated into T-flasks (150 cm^2) containing 90 ml NB-SFM at 1.5 x 10^5 cells/ml. After 2 days of incubation, thymidine was added to the cultures: 0 mM, (●) or 8 mM (O). ATP/GTP values are the result of pooled daily samples.

5.2.3 The effect of sodium butyrate on cell growth, intracellular nucleotide pools and monoclonal antibody production

The aim of this experiment was to determine if the specific monoclonal antibody production rate (qMab) could be enhanced by sodium butyrate supplementation and to determine if a correlation existed with intracellular nucleotide pools. CC9C10 hybridomas from the mid-exponential phase of stock cultures were inoculated at 1.5 x 10^5 cells/ml by dilution into 150 cm^2 T-flasks containing NB-SFM (25 mM glucose, 6 mM glutamine). Starting on day 2, cultures were fed daily with glucose and glutamine and the pH was adjusted as previously described (section 2.3). The NB-SFM was supplemented on day 0 with varying levels of sodium butyrate (0 mM, 0.2 mM and 0.4 mM) from a concentrated stock solution (200 mM). In another set of flasks, 0.4 mM sodium butyrate was added after 2 days of incubation. Each culture condition was done in duplicate from cells inoculated from the same cell stock.

The growth profiles for CC9C10 cells supplemented with varying levels of sodium butyrate are shown in Figure 5.7. Viable cell concentrations were determined by trypan blue exclusion. The addition of 0.2 and 0.4 mM sodium butyrate on day 0 caused a significant reduction in cell growth compared to control cultures. Maximum specific growth rates were reduced by 22 % when compared to controls (Table 5.4). Despite the decrease in μ_{max} all cultures reached similar maximum cell densities (1.0 - 1.1 x 10^6 cells/ml). Controls reached maximum cell density on day 3 after which cell numbers declined. Sodium butyrate supplemented cultures (0.2 mM and 0.4 mM) reached maximum cell density on day 3 and day 4 respectively. In both latter cultures, high cell density was maintained for 3 - 4 days before declining. Cultures in which 0.4 mM sodium butyrate was added after 2 days of incubation did not have an altered growth profile compared to control cultures (data not shown). All cultures had similar values for the viability index after 8 days of incubation (Table 5.4).

Analysis of Mab production by HPLC revealed a significant difference between 0.2 and 0.4 mM sodium butyrate supplemented cultures compared to controls (Fig. 5.8). Control cultures had a constant qMab as indicated by the slope of the Mab concentration versus viability index curve (qMab = 19.9 ± 0.6 $\mu g/10^6$ cell days). The qMab slope for

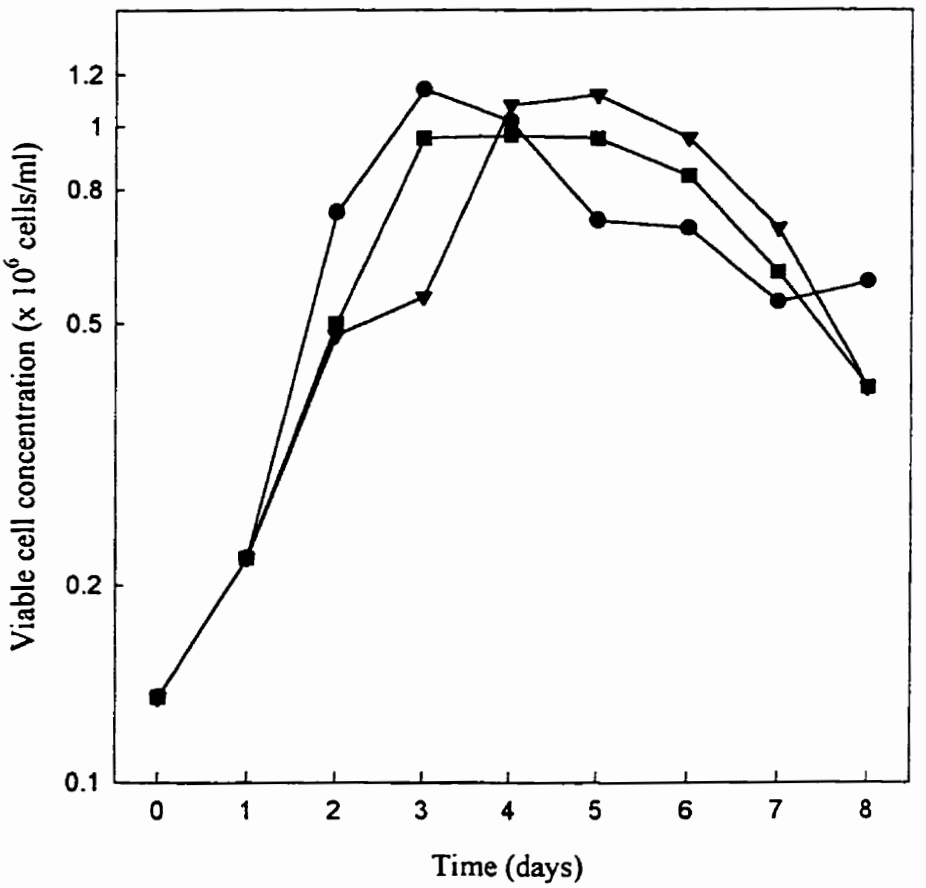

Figure 5.7 The effect of sodium butyrate on CC9C10 cell growth. Hybridomas were inoculated into T-flasks (150 cm^2) containing 90 ml NB-SFM at 1.5 x 10^5 cells/ml. NB-SFM contained varying concentrations of sodium butyrate: 0 mM, (●); 0.2 mM, (■); 0.4 mM, (▼). Viable cell concentration values are the mean from two identical flasks inoculated from the same cell stock. Errors were less than 10 % of the mean.

Table 5.4 Effect of sodium butyrate on the maximum specific growth rate (μ_{max}) ,viability index (Vi), Mab concentration[a] and specific Mab production rate (qMab).

Culture	μ_{max} (h^{-1})	V_I (day8) (x10^6 cell days/ml)	Mab production (μg/ml)	qMab (day 0 - 8) (μg/ 10^6 cell-days)	qMab (day 0 - 4) (μg/ 10^6 cell-days)	qMab (day 4 - 8) (μg/ 10^6 cell days)
control	0.036 ± 0.002	5.38 ± 0.01	114 ± 2	19.9 ± 0.6	18.7 ± 1.4	22.5 ± 1.4
0.4mM	0.028 ± 0.001	5.38 ± 0.03	137 ± 3	25.3 ± 1.2	34.6 ± 1.4	20.6 ± 1.1
0.2mM	0.028 ± 0.005	5.31 ± 0.12	130 ± 3	23.4 ± 0.7	28.1 ± 1.4	21.5 ± 1.2
0.4mM[b]	0.036 ± 0.002	5.87 ± 0.45	114 ± 1	18.7 ± 0.8	17.7 ± 1.2	21.2 ± 2.2

[a]Mab produced from day 0 to day 8

[b]Cultures were supplemented with sodium butyrate after 2 days of incubation

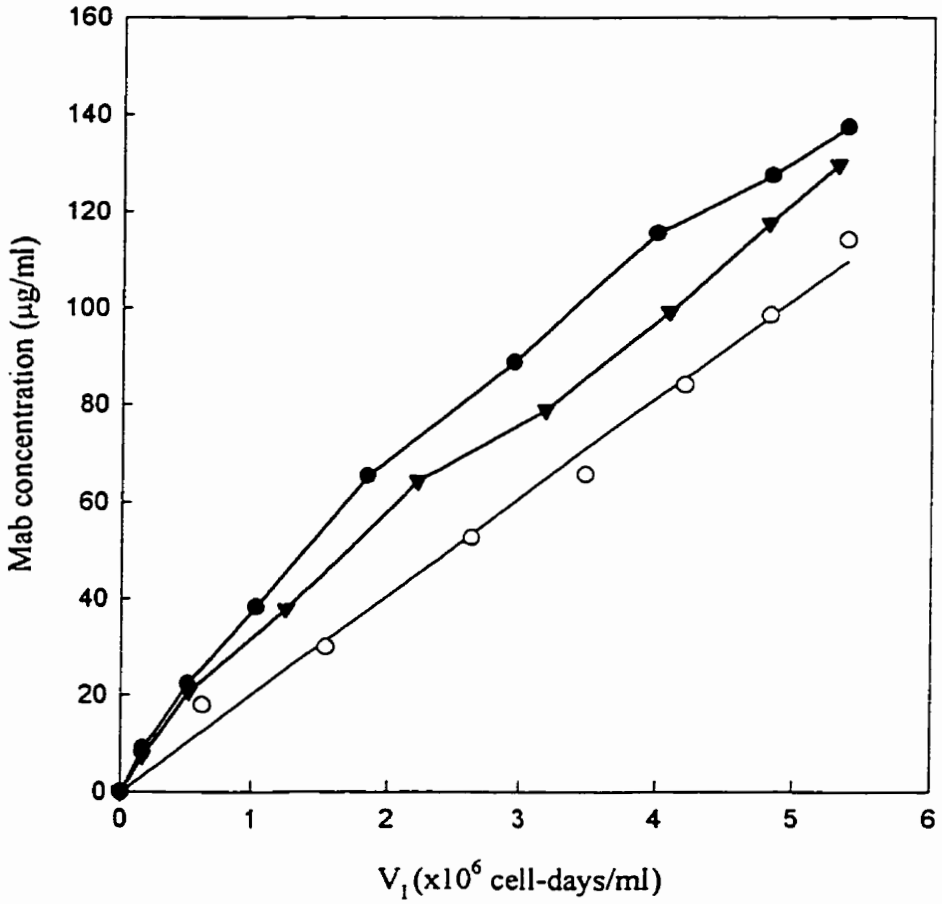

Figure 5.8 The effect of sodium butyrate on CC9C10 productivity. Hybridomas were inoculated into T-flasks (150 cm^2) containing 90 ml NB-SFM at 1.5 x 10^5 cells/ml. NB-SFM contained varying concentrations of sodium butyrate: 0 mM, (O); 0.2 mM, (▼); 0.4 mM, (●). Mab production and viability index (V_I) values are the mean from two identical flasks inoculated from the same cell stock.

sodium butyrate supplemented cultures in contrast was not constant during the cultivation period (Fig. 5.8). Two phases of production were present in these cultures (Table 5.4). The first phase of qMab occurred between day 0 - 4. In 0.2 mM sodium butyrate supplemented cultures the qMab was 50 % higher than controls during this period. In 0.4 mM sodium butyrate supplemented cultures the qMab was 85 % higher than controls. In the second phase of Mab production (days 4 - 8), the qMab in sodium butyrate supplemented cultures was equal to control values (22.5 ± 1.4 $\mu g/10^6$ cell days). Volumetric production of Mab was 14 - 20 % higher in cultures supplemented on day 0 with 0.2 and 0.4 mM sodium butyrate (Table 5.4) Cultures in which 0.4 mM sodium butyrate was added after 2 days of incubation did not have different qMab or Mab yield compared to controls.

Nucleotide analysis of 0 and 0.4 mM sodium butyrate supplemented cultures was done by a combination of luminometry and chromatography (section 2.7). It was found that the relative concentration of ATP was 2 - 9 % lower during the first 3 days of incubation in sodium butyrate supplemented cultures when compared to controls (Fig.5.9).

The relative concentration of NAD was also significantly lower compared to controls from day 2 - 4. The first four days of incubation corresponded to the high production phase of sodium butyrate supplemented cultures. Analysis of the relative UDP-GNac concentration during this period showed that this nucleotide pool was 21 - 40 % higher in sodium butyrate supplemented in the first 2 days of incubation (Fig. 5.10). The relative UTP concentration was significantly higher in sodium butyrate cultures in the latter 3 days of the high production phase when compared to controls (day 2 - 4).

Nucleotide ratios were also monitored. It was found that a lower SA/SU and a higher UTP/CTP ratios coincided with the high production phase of sodium butyrate supplemented cultures when compared to controls (not shown). No significant differences were observed in other nucleotide ratios such as ATP/GTP, energy charge and NTP/U (not shown).

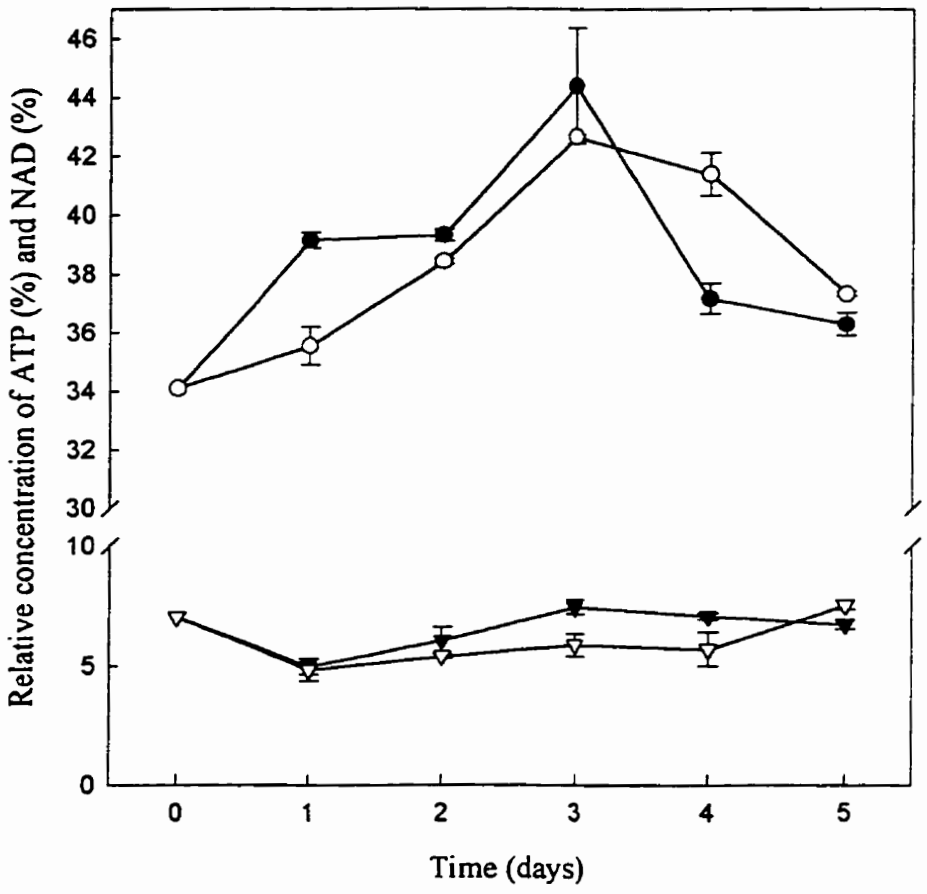

Figure 5.9 The effect of sodium butyrate on the relative quantity of ATP and NAD. Hybridomas were inoculated into T-flasks (150 cm^2) containing 90 ml NB-SFM at 1.5 x 10^5 cells/ml. NB-SFM contained varying concentrations of sodium butyrate: 0 mM, (●,▼) or 0.4 mM,(O, ∇). ATP and NAD relative values are represented by circles and triangles respectively. Values are the mean ± S.E.M. from two identical flasks inoculated from the same cell stock and are relative to the total amount of identified nucleotides.

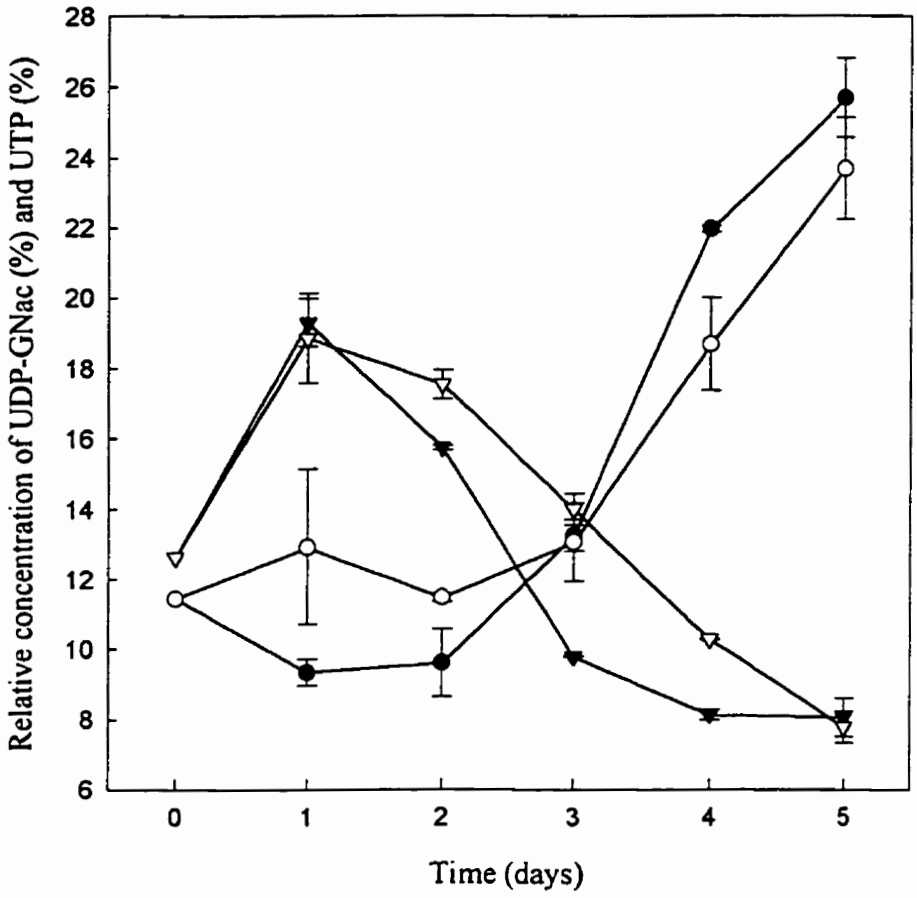

Figure 5.10 The effect of sodium butyrate on the relative quantity of UDP-GNac and UTP. Hybridomas were inoculated into T-flasks (150 cm^2) containing 90 ml NB-SFM at 1.5 x 10^5 cells/ml. NB-SFM contained varying concentrations of sodium butyrate: 0 mM, (●, ▼) or 0.4 mM,(O, ∇). UDP-GNac and UTP relative values are represented by circles and triangles respectively. Values are the mean ± S.E.M. from two identical flasks inoculated from the same cell stock and are relative to the total amount of identified nucleotides.

5.3 Discussion

The objective of the work described in this chapter was to determine if the qMab could be altered by thymidine or sodium butyrate supplementation. Nucleotide analysis of cultures with altered qMab would then be used for comparisons with nucleotide profiles from other conditions which affect Mab productivity (i.e. incubation temperature).

Thymidine arrests cell growth by inhibiting the formation of dCDP, a DNA precursor. Thymidine is normally taken up by cells and rapidly converted to dTTP, an allosteric inhibitor of ribonucleotide reductase (Adams, 1980).

The effect of thymidine on CC9C10 cell growth was dose-dependent. A concentration of 8 mM thymidine reduced the growth rate and inhibited viable cell density increases. Cell growth however was not completely arrested as total cell density continued to increase in thymidine supplemented cultures. Lower concentrations of 4 and 6 mM thymidine also reduced the growth rate but allowed cultures to reach similar viable cell densities as controls. In contrast, a thymidine concentration of 2 mM caused a modest but significant increase in the viable cell concentration. Substantially lower thymidine levels in the culture medium (i.e. in the μM range) have been shown to improve cell yields in cultured cell lines (Morton, 1981; Lambert and Birch, 1985).

The partial cell growth arrest at 4 - 8 mM thymidine and growth stimulation at 2 mM thymidine is inconsistent with reports in which 2 - 5 mM thymidine were sufficient for complete cell growth arrest in cultured cell lines (Adams, 1980). The inability of thymidine to completely arrest DNA synthesis indicates a possible deficiency exists in the conversion of thymidine to dTTP in CC9C10 hybridomas. It has been shown that cells deficient in thymidine kinase, an enzyme that converts thymidine to dTMP, are not inhibited by extracellular thymidine (Bjursell and Reichard, 1973).

Supplementation of CC9C10 cultures with 6 - 8 mM thymidine caused a decrease in the adenylate energy charge concomitant with an increase in the qMab. The decrease in energy charge however is probably an artifact of thymidine addition and is not related to Mab productivity. This comes from the observation that energy charge is not reduced under other conditions which enhance productivity (i.e. cultivation temperature and

sodium butyrate supplementation). The reduction in energy charge is neither a consequence of reduced cell growth as several other growth inhibitors do not alter energy charge values in hybridomas (Modha *et al.*, 1992). It is postulated here that energy charge may be reduced in thymidine supplemented cultures due to the formation of excess dTMP. Excess dTMP would cause a reduction in ATP levels via the thymidylate kinase reaction:

$$ATP + dTMP \underset{\text{thymidylate kinase}}{\overset{\rightarrow}{\underset{\leftarrow}{}}} ADP + dTDP$$

It has been suggested that increased Mab productivity may occur as a result of decreased cell growth brought about by thymidine addition (Hayter *et al.*, 1992). This observation is consistent with the data presented here however it does not explain why control CC9C10 cells do not have an increased qMab during periods of reduced growth (i.e. stationary and death phase).

The analysis of nucleotides from thymidine supplemented cultures showed that an increase in qMab was also concomitant with a decrease in the relative ATP concentration and ATP/GTP ratio; and concomitant with an increase in the relative UDP-GNac concentration and total nucleotides. These fluctuations in nucleotide pools have been seen previously under temperature conditions which affect Mab productivity in CC9C10 hybridomas (chapter 4).

The inoculation of CC9C10 cells in sodium butyrate supplemented NB-SFM caused a significant decrease in the maximum growth rate and resulted in the appearance of two Mab production phases. The first phase of Mab production occurred between day 0 - 4 and corresponded to the exponential and early stationary phase of growth. The qMab of sodium butyrate cultures during this phase was 50 - 85 % higher than control cultures. The second phase of Mab production occurred between day 4 - 8. The qMab during this period was equivalent to control values which remained constant during the 8 days of incubation. Unlike the other method which enhanced qMab (i.e. temperature increases or thymidine supplementation), the addition of sodium butyrate to the NB-SFM resulted in a

significant increase in the volumetric Mab production compared to control cultures. Sodium butyrate can therefore be used to maximize Mab yield in batch cultures.

In contrast, the addition of sodium butyrate after 2 days of incubation did not affect cell growth, qMab or Mab yield. These observations suggest that sodium butyrate lost its qMab enhancing properties in the later stages of culture. A loss of sodium butyrate effectiveness may be linked to cell density or cell culture phase at the time of inoculation. Further studies are needed to determine if the loss of effectiveness can be reversed by increasing the dosage of sodium butyrate in the culture. Daily feeding with sodium butyrate may prove to prolong the high qMab phase of cultures thus enhancing the Mab yield.

The exact mechanism of the sodium butyrate qMab enhancing properties are not yet clear. Sodium butyrate has been shown to be capable of regulating gene expression and cell growth by hyperacetylation of histones (Bruce *et al.*, 1992). Hyperacetylated histones detach from DNA thus rendering segments of chromatin more accessible to RNA polymerases. Elevated mRNA expression of certain proteins has been reported after treatment with butyrate (Oh *et al.*, 1993). Bruce *et al* (1992) also suggest that the qMab enhancing properties of sodium butyrate are related to a reduction in cell growth.

A correlative relationship between enhanced qMab and nucleotide pools in sodium butyrate supplemented was not conclusive. Reasons for the inconclusiveness may be due to the short term effect of sodium butyrate on qMab and to errors in defining the end of the high production phase. Nevertheless, certain trends in nucleotide pool fluctuations previously associated with enhanced qMab have been identified in sodium butyrate supplemented cultures albeit only for the first 2 or 3 days of incubation. These fluctuations included an increase in the relative UDP-GNac pool and a relative decrease in the ATP pool. No significant changes in the ATP/GTP pool were observed in sodium butyrate cultures. This latter finding is not consistent with other qMab enhancing protocols in which the ATP/GTP ratio decreased concomitantly with an increase in qMab (section 4.0 and 5.2.2).

5.4 Conclusion

The specific monoclonal antibody productivity (qMab) of CC9C10 hybridomas increased upon supplementation with thymidine which also caused partial cell growth arrest. The increased qMab correlated with an increase in the relative content UDP-GNac, a decrease in the relative ATP content, ATP/GTP ratio and energy charge. A decrease in energy charge may have been due to the action of thymidylate kinase.

The qMab of CC9C10 hybridomas also increased upon supplementation with sodium butyrate but was limited to the exponential and early stationary phase of cultures. The enhanced qMab phase loosely correlated with a relative increase in UDP-GNac and a decrease in the relative ATP content and growth rate.

CHAPTER 6

6.0 An intracellular nucleotide comparison between CC9C10 hybridoma and SP2/0 myeloma

6.1 Introduction

The purpose of the following study was to determine if differences existed between the intracellular nucleotide profile of a Mab secreting cell line and the profile of a Mab-deficient cell line. Differences between these cell types may indicate which nucleotides are important for Mab production, assembly or secretion. It was with this objective in mind that CC9C10 and SP2/0 cells were chosen for the following study. CC9C10 cells are hybridomas produced from the fusion of lymph node cells of a bovine insulin immunized Balb/c mouse with the SP2/0 - Ag14 myeloma cell line (Schroer *et al.*, 1983). CC9C10 cells secrete an $IgG_{1\kappa}$ monoclonal antibody against bovine insulin. SP2/0 used in this study is the parent cell line of CC9C10 and does not secrete monoclonal antibody.

6.2 Results

CC9C10 and SP2/0 taken from the mid-exponential phase of stock cultures were inoculated at 1.5 x 10^5 cells/ml by dilution into 150 cm^2 T-flasks containing NB-SFM (25 mM glucose, 6 mM glutamine). The 90 ml cultures were incubated for 7 days at 37°C with daily removal of samples for analysis. Cultures were fed glucose and glutamine and the pH adjusted daily starting on day 2 as previously described (section 2.3). Metabolite and nucleotide concentrations of CC9C10 cells were determined from independent cultures (n = 2) inoculated from different cell stocks. Metabolite and nucleotide concentrations of SP2/0 cells were determined from independent cultures (n = 2) from the same cell stock. Statistical analysis was done with a one-tailed paired t-test (Appendix A2).

6.2.1 Growth and metabolism

Viable cell density was determined by the trypan blue exclusion method. As shown in Fig 6.1, CC9C10 and SP2/0 cells had similar growth profiles. Both cell lines attained a maximum viable cell density of 1 x 10^6 cells/ml after 3 days of incubation. The maximum growth rates of SP2/0 and CC9C10 cells were not significantly different (Table 6.1).

Glucose, lactate, glutamine and ammonia concentrations in the cell culture supernatant were analyzed as previously described (section 2.8 - 2.10) and the specific production and consumption rates of the metabolites were determined. CC9C10 had a 28 ± 2 % higher glucose uptake rate (q_G) and lactate production rate (q_L) than SP2/0 myelomas. Lactate yield was the same in both cell lines (1.8 mol lactate/ mol glucose) as was the specific glutamine uptake (q_Q). The ammonia yield from glutamine however was approximately 1 mol/mol for CC9C10 compared to 0.7 mol/mol for SP2/0. The qMab rate of CC9C10 hybridomas was 19 - 26 $\mu g/10^6$ cells-days depending on the passage number. SP2/0 did not secrete any monoclonal antibody.

6.2.2 Nucleotide analysis

Intracellular nucleotide analysis of cultures was done by a combination of luminometry and chromatography (section 2.7). It was found that each cell type had a characteristic nucleotide pattern and this was reflected by significant differences in the relative nucleotide concentrations (Table 6.2). Over a 4 day period which included the mid-exponential and death phases, CC9C10 cultures had a lower relative concentration of UDP-Glc and CTP and a higher relative concentration of ATP, ADP and GTP compared to SP2/0 cultures ($P < 0.05$). Significant differences were also observed in the UDP-GNac and UTP relative pools (Fig. 6.2). The relative UTP content of CC9C10 cultures decreased during the incubation period from 22 to 8 % whereas in SP2/0 the same nucleotide pool increased from 3 to 15 %. In both hybridoma and myeloma cultures the UDP-GNac content was stable in the early to mid-exponential phase after which the

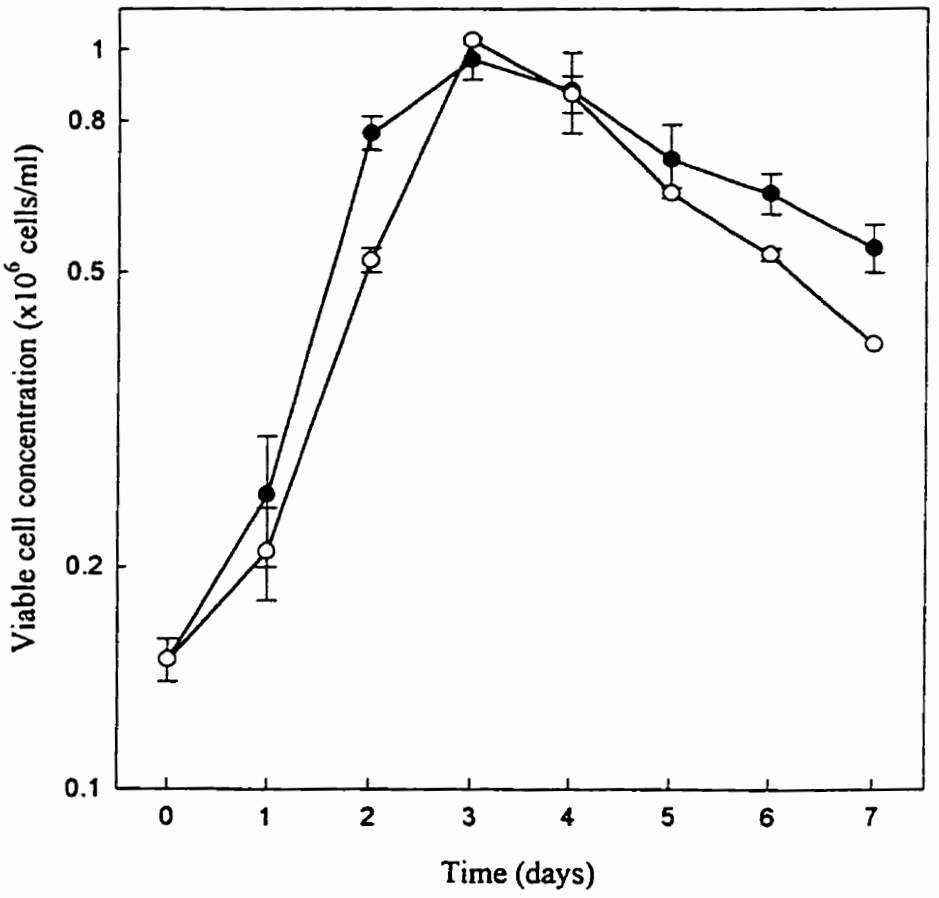

Figure 6.1 Growth profiles of CC9C10 hybridoma and SP2/0 myeloma. Both cell lines were inoculated into 90 ml NB-SFM at 1.5 x 10^5 cells/ml in 150 cm^2 T-flasks: CC9C10 hybridoma, (●); SP2/0 myeloma, (O). Viable cell concentrations are the mean S.E.M. from independent cultures inoculated from different cell stocks.

Table 6.1. A metabolic comparison between two related cell lines: CC9C10 hybridoma and SP2/0 myeloma. Metabolic rates for CC9C10 are the mean ± S.E.M. from independent cultures inoculated from different stock cells (n = 2). Metabolic rates for SP2/0 are the mean ± S.E.M. from two identical flasks inoculated from the same cell stock (n = 2). Metabolic rates (μmol/10^6 cell-days) were calculated for the exponential phase of growth.

cell line	μ_{max} (h^{-1})	qMab (μg/10^6 cell-days)	Specific glucose uptake rate (q_G)	Specific lactate production rate (q_L)	Lactate yield, $Y_{Lac/Glc}$ (mol/mol)	Specific glutamine uptake rate (q_Q)	Specific ammonia production rate (q_A)	Ammonia yield $Y_{NH4+/Gln}$ (mol/mol)
CC9C10	0.035 ± 0.002[a]	19 - 26[c]	8.9 ± 0.3	16.8 ± 1.1	1.8 ± 0.1	2.5 ± 0.3	2.4 ± 0.4	0.99 ± 0.04
SP2/0	0.031 ± 0.002[b]	NA	7.0 ± 0.6	12.9 ± 0.1	1.8 ± 0.1	2.5 ± 0.1	1.7 ± 0.1	0.68 ± 0.06

[a]Values are the mean from independent cultures inoculated from four different cell stocks (n = 4).
[b]Values are the mean from independent cultures inoculated from two different cell stocks (n = 2).
[c]qMab values are dependent on passage number.
NA - not applicable

Table 6.2 Relative quantities of nucleotides in CC9C10 and SP2/0 cultures compared to the total nucleotide content (%). Representative values were taken after 4 days of incubation. Statistical evaluation was performed with a one-tailed paired *t*-test. The total measured nucleotide content is equal to 100 %.

Cell line	Total (nmol/ 10^6 cells)	NAD (%)	UDP-Glc (%)	UDP- GNAc (%)	UTP (%)	CTP (%)	GTP (%)	ATP (%)	ADP (%)	AMP (%)	GDP (%)
CC9C10	11.3	7.8	1.3	21.7	8.2	6.3	7.9	39.4	4.9	1.0	1.1
SP2/0	7.0	7.8	2.3[a]	16.5[b]	15.5[b]	10.2[a]	7.1[a]	32.9[a]	4.8[a]	1.4	1.1

[a] Represents significant differences ($P < 0.05$) determined from day 2 to 5 ($n = 4$) when compared to CC9C10.
[b] Represents significant differences ($P < 0.05$) determined from day 3 to 5 ($n = 3$) when compared to CC9C10.

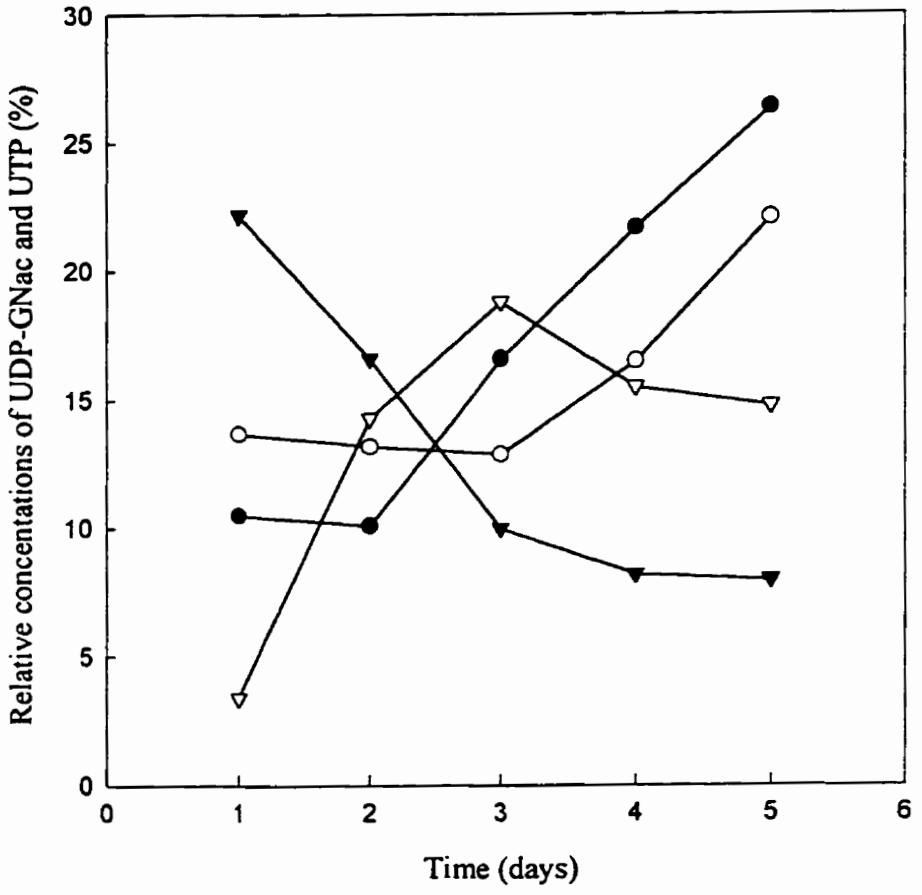

Figure 6.2 Relative quantities of UDP-GNac and UTP compared to the total nucleotide content in CC9C10 and SP2/0 cell lines. Cells were inoculated into 90 ml NB-SFM at 1.5 x 10^5 cells/ml in 150 cm^2 T-flasks: CC9C10 hybridoma, (●,▼); SP2/0 myeloma, (O, ∇). UDP-GNac and UTP relative concentrations are represented by circles and triangles respectively.

relative sugar-nucleotide content increased daily. The UDP-GNac relative pool in the latter days of the culture was significantly higher in the Mab-secreting hybridoma as opposed to the Mab-deficient myeloma ($P < 0.05$).

Other characteristic changes were observed in the nucleotide ratios during the course of culture growth (Fig.6.3). In CC9C10 cultures the U-ratio decreased from 2.1 to 0.2 over a 5 day period whereas in SP2/0 cultures the U-ratio increased from 0.2 to 1.5 at maximum cell density before declining to 0.7. The NTP ratio of CC9C10 cultures increased from 1.2 to 3.3 during the exponential phase before stabilizing at the latter value. In SP2/0 cultures, the NTP ratio decreased from 2.2 to 1.5 during the same period. The ATP/GTP ratio was relatively constant in both cultures. CC9C10 cultures had an ATP/GTP ratio of 4.8 - 4.9 compared to a value of 4.2 - 4.7 for SP2/0 cultures.

As seen in Fig.6.4, the NTP/U ratio was also significantly different between the Mab secreting hybridoma and non-secreting myeloma. The NTP/U ratio increased from an initial value of 0.6 in CC9C10 cultures to more than 20 after 5 days. The NTP/U ratio of SP2/0 cultures decreased from an initial value of 9 to 2 during the same period. Other nucleotide ratios such as SA/SU and purine/pyrimidine were significantly lower in SP2/0 compared to CC9C10 (Table 6.3). Energy charge was not significantly different between the two cell lines.

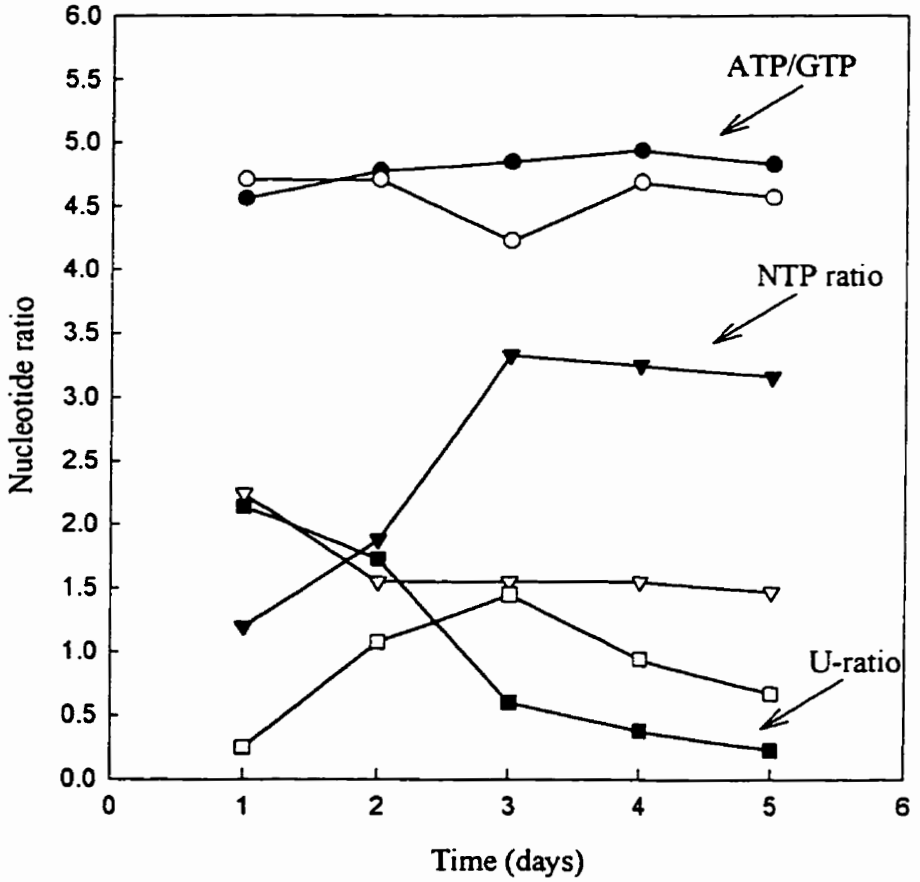

Figure 6.3 Nucleotide ratios in CC9C10 and SP2/0 cell lines. Cells were inoculated into 90 ml NB-SFM at 1.5 x 10^5 cells/ml in 150 cm^2 T-flasks: CC9C10 hybridoma, (●,▼,■); SP2/0 myeloma, (O, ∇, □). ATP/GTP. NTP ratio and U-ratio are represented by circles, triangles and squares respectively.

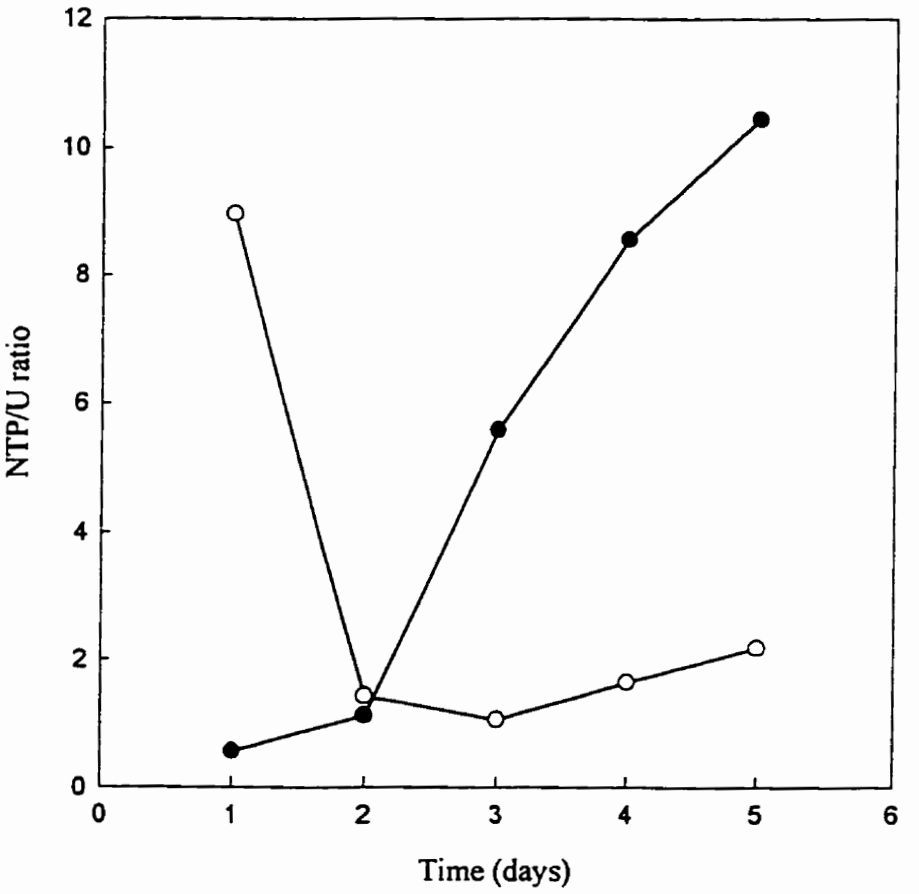

Figure 6.4 NTP/U ratio in CC9C10 and SP2/0 cell lines. Cells were inoculated into 90 ml NB-SFM at 1.5 x 10^5 cells/ml in 150 cm^2 T-flasks: CC9C10 hybridoma, (●); SP2/0 myeloma, (O).

Table 6.3 Nucleotide ratios of CC9C10 and SP2/0 culture. Representative values were taken after 4 days of incubation. Statistical evaluation was performed with a one-tailed paired *t*-test.

cell line	SA/SU	Purine/ pyrimidine	ATP/GTP	UTP/CTP	Energy charge	NTP ratio	U-ratio	NTP/U
CC9C10	1.46	1.45	4.94	1.29	0.92	3.25	0.38	8.57
SP2/0	1.14[a]	1.06[a]	4.69[a]	1.53	0.90	1.55[a]	0.94[a]	1.65[a]

[a] Represents significant differences ($P < 0.05$) determined from day 2 to 5 ($n = 4$) when compared to CC9C10.

6.3 Discussion

CC9C10 hybridomas may share as much as 50 % of its genes with the SP2/0 myeloma, its parental cell line. It was therefore expected that their metabolism would be similar. CC9C10 and SP2/0 cells had a similar growth profile and shared several metabolic characteristics. Both cell lines had a similar lactate yield from glucose despite the higher glucose consumption rate in CC9C10 hybridomas. This was consistent with comparative studies between CC9C10 and SP2/0 cell lines using the same serum-free formulation (Petch, 1994). A similar glutamine uptake rate between the cell lines was also consistent with the previously reported work. It was however found that ammonia yield from glutamine was significantly lower in SP2/0 cultures compared to CC9C10. This finding is in contrast to Petch (1994) who reported no differences in the ammonia yield between the cell lines. Changes in ammonia yield may be linked to differences in medium glucose concentration which was significantly higher in the work presented here (25 mM versus 17.5 mM). Glucose and glutamine metabolism are interrelated and are subject to the concentration of each substrate in the medium (Medina and Nunez de Castro, 1990)

The major observable difference in cell metabolism between CC9C10 cells and SP2/0 cells is the production of monoclonal antibody. In CC9C10 cells, the qMab ranged from 19 - 26 $\mu g/10^6$ cells-days depending on passage number whereas the SP2/0 is a Mab-deficient cell line. Comparative analysis of nucleotide pools has revealed many differences between the cell lines which may be correlated to the production of Mab. It was found that CC9C10 hybridomas had significantly higher UDP-GNac levels than SP2/0 myelomas in the latter stages of the cultures. The larger UDP-GNac pool accumulation in the CC9C10 cells may be correlated to the greater need of this nucleotide pool in the Mab secreting cell line compared to the myeloma. The UDP-GNac pool supplies precursors to the carbohydrate side chains of proteins such as monoclonal antibodies. An elevated UDP-GNac pool in Mab producing cells is consistent with previous studies using hybridomas with altered qMab (section 4.0 and 5.0).

CC9C10 hybridomas also had a higher relative intracellular level of purine triphosphates (ATP + GTP) and a lower relative level of pyrimidine triphosphates (UTP + CTP) than SP2/0 myelomas. The higher purine triphosphate levels in hybridomas may be

reflective of the importance of these nucleotides in Mab synthesis. ATP and GTP are essential for protein synthesis as they are required for the translation of eukaryotic mRNAs (Rubin *et al.*, 1988). GTP hydrolysis provides the primary source of energy for the initiation and elongation process of protein synthesis. ATP is required for binding of 40S to the mRNA and for the migration of the ribosomal subunit toward the initiation codon. ATP is also essential for the formation of aminoacyl-tRNA, an activated intermediate which is incorporated into a growing peptide chain (Lehninger, 1982). The GTP levels may also affect protein glycosylation. The intracellular concentration of GTP has been shown to stimulate the incorporation of GlcNac into intermediate lipid acceptors (Bossuyt and Blanckaert, 1993).

The purine and pyrimidine triphosphate imbalances is better reflected in the NTP ratio which correlates the relation between these two important nucleotide pools. The NTP ratio (ATP + GTP)/ (CTP + UTP) was significantly higher in CC9C10 hybridomas compared to SP2/0 myelomas. The NTP ratio as well as U- and NTP/U ratios have been suggested as tools for monitoring the physiological state of mammalian cells in vitro and as early predictors of the entry of cells into a reduced growth phase (Ryll and Wagner, 1992). In this study, these nucleotide ratios were more characteristic of the cell type rather than physiological state of the cells. The NTP, NTP/U ratio increased in CC9C10 cells as the cultures progressed through the exponential phase and remained at high levels during the stationary and death phases. The opposite behavior was observed in SP2/0 myelomas. The U-ratio profile during the course of cell culture was also dependent on cell type.

The ATP/GTP ratio was significantly lower in the SP2/0 myeloma compared to the CC9C10 hybridoma. The lower ATP/GTP ratio for the Mab-deficient cell line is not consistent with studies in which a low ATP/GTP ratio was correlated with a high qMab. This suggests that the ratio is not directly related to the qMab. The ATP/GTP ratio has been shown to be regulated by the nutritional state in lower eukaryotes (Pall and Robertson, 1988). The slight difference in nutrient metabolism between SP2/0 and CC9C10 may have contributed to differences observed in the ATP/GTP ratio.

6.4 Conclusion

CC9C10 hybridoma and SP2/0 myeloma differ in their nucleotide profiles and this may be related to differences in Mab synthesis. The Mab-secreting cell line (CC9C10) had a higher purine triphosphate and UDP-GNac levels and lower pyrimidine triphosphate levels than the Mab-deficient cell line (SP2/0). The NTP, NTP/U and U-ratio fluctuations during the course of the culture were dependent on cell type.

CHAPTER 7

7.0 The relationship between intracellular UDP-N-acetyl hexosamine nucleotide pool and monoclonal antibody production in a mouse hybridoma[1]

7.1 Introduction

Most proteins important as biotechnological products and secreted from mammalian cells have a carbohydrate moiety which is added following protein synthesis by the metabolic process of glycosylation which occurs in the Golgi apparatus. An understanding of the cellular process associated with glycosylation is essential to ensure adequate metabolic control and management of the cells used in large-scale production of a glycoprotein.

Intracellular pools of UDP-N-acetylhexosamine are of major importance in the provision of precursors for the glycosylation of secreted proteins. UDP-N-acetylhexosamine is present as two major structural isomers within the cell, namely UDP-N-acetylglucosamine and UDP-N-acetylgalactosamine, collectively abbreviated to UDP-GNac. The two forms of UDP-GNac can be interconverted by an isomerase enzyme. In addition to its role as a precursor, the animal cell intracellular sugar-nucleotide pool has been correlated to several cellular events. Increases in UDP-N-acetylhexosamine levels are concomitant with the inability of human colon cancer cells to differentiate (Wice *et al.*, 1985), growth inhibition (Ryll *et al.*,1994; Krug *et al.*, 1984) and cell ultrastructure modifications such as endoplasmic reticulum distentions (Morin *et al.*,1983).

It has been observed that the intracellular UDP-GNac pool of several mammalian cell lines can be significantly increased by the addition of ammonium ions to the culture medium (Ryll *et al.*,1994). This accumulation is due to the increased synthesis of the sugar

[1]The contents of this chapter were included in a paper: Barnabé, N., and Butler, M (1998) The relationship between intracellular UDP-N-acetyl hexosamine nucleotide pool and monoclonal antibody production in a mouse hybridoma. *J.Biotechnol.* in press.

-nucleotide. Ammonium is incorporated into fructose-6-phosphate, derived from glycolysis, to form glucosamine-6-phosphate, a UDP-GNac precursor (Ryll *et al.*,1994).

Another method by which UDP-GNac can accumulate in the cell is by a reduced rate of utilization. Tunicamycin, an antibiotic whose structure is comprised of N-acetylglucosamine, tunicamine, uracil and a variable fatty acid residue, specifically inhibits the enzyme associated with the transfer of GNac from UDP-GNac to dolichol phosphate, a lipid carrier involved in the N-linked glycosylation of proteins (Tkacz and Lampen, 1975; Ito *et al.*, 1980). Inhibition of the enzyme leads to a reduced rate of utilization of UDP-GNac and its subsequent accumulation in cells (Morin *et al.*, 1983). Prevention of the assembly of the dolichol-linked oligosaccharide also results in the inhibition of asparagine-linked protein glycosylation (Hickman *et al.*, 1977).

In a previous section we showed that a temperature-induced enhancement of the monoclonal antibody production rate (qMab) of the hybridoma cell line, CC9C10 was correlated with an increase in the intracellular UDP-GNac pool (chapter 4). It was postulated that the level of UDP-GNac in the cell may have affected Mab glycosylation and ultimately Mab production. Alternatively, the UDP-GNac pool may act as regulator of the antibody synthesis pathway. In order to test these postulates we grew the hybridomas under conditions favorable for the sugar-nucleotide accumulation and monitored the rate of synthesis and characteristics of the secreted antibody. Two agents were used to raise intracellular UDP-GNac levels - ammonium and tunicamycin.

7.2 Experimental set-up and analysis

Cells were grown routinely at 37 °C under a 10% CO_2 humidified atmosphere in NB-SFM (25 mM glucose, 6 mM glutamine). Special media differing from this mixture are indicated in the text. Cultures (50 and 90 ml) were routinely contained in 150 cm^2 T-flasks. In fed-batch experiments, cells were fed daily starting on day 2 with glucose and glutamine and the pH was adjusted when required with sodium bicarbonate as previously described (section 2.3). Samples (1.5 - 5.0 ml) were taken daily for cell counts,

supernatant collection and nucleotide extraction. On the final day of incubation the remaining supernatant was collected for Mab purification (section 2.6.2).

Cells from multi-well plate experiments were enumerated with a Coulter counter (section 2.5.2). In all other experiments, cells were counted using a hemocytometer and the viability determined by the trypan blue exclusion method (section 2.5.1). Glucose, glutamine, lactate and ammonium were analyzed as previously described (sections 2.8 - 2.10). Monoclonal antibody concentrations from unpurified cell culture supernatants were quantified by HPLC with a Protein A/G column (section 2.6.1).

Monoclonal antibody was deglycosylated with N-glycosidase F (section 2.6.3). The deglycosylated Mab was used to establish SDS-PAGE parameters for the separation of deglycosylated versus glycosylated IgG heavy chain. SDS-PAGE was performed in a discontinuous polyacrylamide gel under reducing conditions according to the method of Laemmli (section 2.6.4). Quantitative analysis of stained protein bands was based on the number of pixels in the band subtracted by background values (section 2.6.4.5). Protein bands of unstained gels were transferred to 0.2 μm nitrocellulose paper according to the method of Towbin (section 2.6.5). Glycosylated proteins on the nitrocellulose sheets were detected with a carbohydrate detection kit (section 2.6.6). Nucleotides were quantified by an ion pair reverse-phase liquid chromatography or by an enzymatic bioluminescent assay (section 2.7).

Tunicamycin used in experiments consisted of a mixture of isomers A, B, C, and D from a *Streptomyces* species (Sigma Chemical Co.). A stock solution of 250 μg/ml was prepared in 70 mM NaOH and filter sterilized. Tunicamycin solutions were stored at - 20 °C until needed. NH_4Cl and NaCl stock solutions (2 M) were prepared in distilled water and filter sterilized.

7.3 Results

7.3.1 The effect of tunicamycin

7.3.1.1 Cell growth

The effect of tunicamycin on the growth of CC9C10 hybridoma cells was determined in 24 well plates with three different media. The purpose of this was to determine a sublethal dose of the tunicamycin that would allow a study of the effect of perturbations in metabolite levels. Cultures were inoculated at 1.5 x 10^5 cell/ml (2.2 ml per well) and assayed for total cell density and viability after 3 days. Results are the mean of duplicate experiments from independent cultures inoculated from a same cell stock.

As shown in Fig.7.1, supplementation of cultures with tunicamycin caused a significant decrease in cell yield even at low concentrations. This effect was pronounced in the NB-SFM which was found to be ineffective in promoting cell growth at all tunicamycin concentrations tested. Supplementation of the NB-SFM with bovine serum albumin (BSA) or iron-enriched calf serum (Gibco) however resulted in significant cell growth in the presence of 0.001 μg/ml tunicamycin. Cell density in these cultures were 16 - 19 % lower than controls in which no tunicamycin was added. The viability of the cells in BSA and serum supplemented cultures was not affected by the presence of 0.001 μg/ml tunicamycin. However, a tunicamycin concentration of 0.01 μg/ml or higher prevented substantial cell growth and caused a significant decrease in cell viability after 3 days. Further analysis showed that there was no significant difference in cell yield in tunicamycin-treated cultures supplemented with 0.1 % instead of 0.5 % BSA.

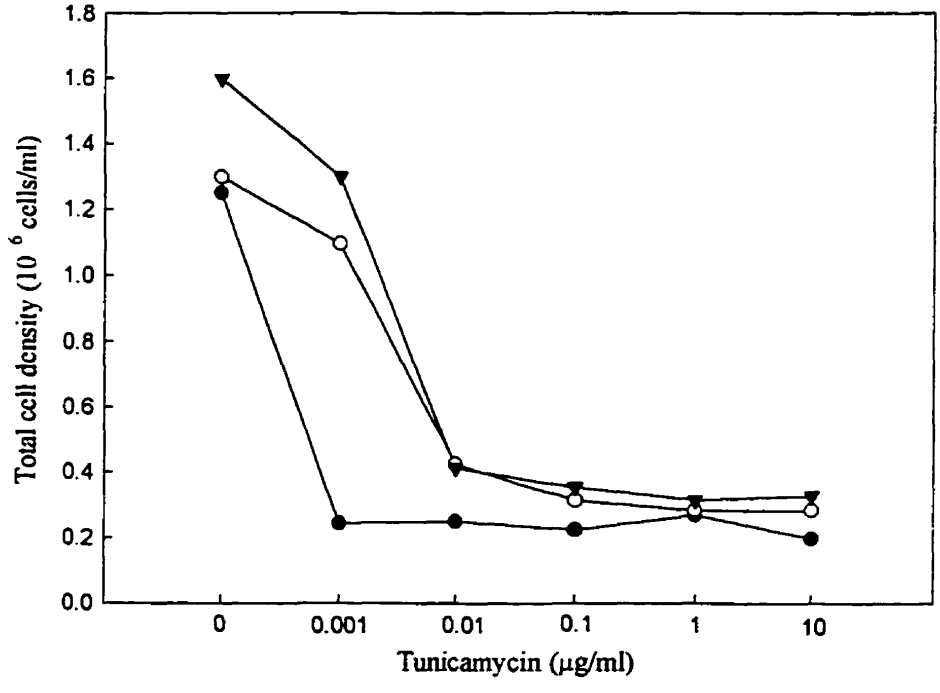

Figure 7.1 The effect of tunicamycin on cell yield. The cultures contained NB-SFM, (●); NB-SFM supplemented with 0.5 % BSA, (O) and NB-SFM supplemented with 10 % serum, (▼). Cultures were inoculated with cells from the mid-exponential phase. Cell densities were determined in cultures (2.2 ml) which were inoculated at 1.5 x 10^5 cells/ml and were incubated in 24 well plates for 3 days at 37°C.

7.3.1.2 Mab production rates

The effect of tunicamycin on Mab production was determined by exposing hybridomas to varying concentrations of the antibiotic. All the tunicamycin-treated cultures were inoculated with exponentially growing cells harvested by centrifugation and resuspended in NB-SFM supplemented with 0 - 1 μg/ml tunicamycin. The hybridomas were pre-incubated in culture medium for 4 h at 37 °C prior to the establishment of each experimental culture to allow sufficient time for secretion of the intracellular Mab synthesised before tunicamycin treatment (Leatherbarrow and Dwek, 1983; Walker *et al.*, 1989). Control cultures (0 μg/ml tunicamycin) were set up in parallel for each of the tunicamycin concentrations tested. Results from tunicamycin-treated cultures are representative of two independent cultures inoculated from the same cell stock. Results from control cultures are representative of three independent cultures inoculated from different cell stocks.

The effect of a low concentration of tunicamycin (0.001 μg/ml) was determined in stationary cultures (90 ml) inoculated at 1.3 x 10^5 cells/ml and maintained at a near normal growth rate in serum-free media (+ 0.1 % BSA). Since 0.001 μg/ml tunicamycin did not completely inhibit cell division, monoclonal antibody synthesis could be monitored in actively growing cell cultures. These cultures were maintained for 6 days by daily feeding from day 2 as previously described (section 7.4.2). Cultures treated with higher concentrations of tunicamycin (0.01 - 1 μg/ml) were inoculated at a cell density of 10^6 cells/ml in 50 ml serum-free media (+ 0.1 % BSA) and maintained for 3 days. The high inoculation density ensured a sufficient antibody and cell concentration for analysis.

The specific Mab production rate (qMab) was calculated from the slope of a plot of the viability index (V_I) versus the Mab concentration. The viability index is defined as the integral of the cell concentration and time as determined from the growth curve (Renard *et al.*, 1988). This plot was linear in all cases, showing that Mab production was directly proportional to the number of viable cells in culture. No significant difference was observed in the Mab production rate of cells grown with 0.001 μg/ml tunicamycin compared to control cultures (20.3 ± 2.0 μg per 10^6 cells per day). The Mab production

rates for 0.01 - 1 μg/ml tunicamycin-treated cultures incubated at high cell density for 2-3 days are shown in Table 7.1. The qMab values determined for 0.01 - 0.1 μg/ml tunicamycin-treated cultures were not significantly different from control cultures. The qMab for 1 μg/ml tunicamycin-treated cultures was significantly higher at 26.4 ● 2.0 μg per 10^6 cells per day. However, at this high tunicamycin concentration the cell viability decreased to less than 50% within 2 days of incubation.

7.3.1.3 Mab glycosylation

The state of glycosylation of the immunoglobulin secreted from the tunicamycin-treated cells was examined. Antibodies were purified from supernatants collected after 6 days of incubation for 0.001 μg/ml tunicamycin-treated cultures and after 3 days for 0.01 - 1 μg/ml tunicamycin- treated cultures. It is to be noted that the Protein A columns used in the purification have the same affinity for glycosylated and non-glycosylated immunoglobulins (Leatherbarrow and Dwek, 1983; Nose and Wigzell, 1983).

The purified antibody samples were electrophoresed under reducing conditions and compared to protein markers. For control cultures the Mab separated into 2 bands (Fig. 7.2). The low molecular weight band corresponded to the IgG light chain with an approximate molecular weight of 26 kD. The high molecular weight band corresponded to the IgG heavy chain at 51 kD. The electrophoresis pattern of Mab purified from 0.001 μg/ml tunicamycin-treated cultures was identical to that from control cultures (Fig.7.2a). Cells treated with 0.01 and 0.1 μg/ml tunicamycin produced two forms of the heavy chain band as evidenced by the presence of two bands close together on the SDS-PAGE (Fig.7.2b and 7.2c, lanes 4 and 5). Cells treated with 1 μg/ml tunicamycin produced only 1 heavy chain band that migrated further than the control heavy chain band (Fig.7.2d, lane 4 and 5). The difference in migration distance between the control heavy chain and the faster migrating heavy chain of tunicamycin treated cultures corresponded to 0.65 - 0.80 kD indicating a possible loss of the carbohydrate moiety of the IgG heavy chain.

Table 7.1 The specific Mab production rate, state of glycosylation and maximum UDP-GNac concentration of tunicamycin-treated cultures.

Tunicamycin (μg/ml)	qMab[a] (μg per 10^6 cells per day)	% glycosylated Mab	% non - glycosylated Mab	Maximum UDP-GNac concentration (nmol per 10^6 cells)
0	20.3 ± 2.0	100	0	2.1 ± 0.1
0.01	18.4 ± 0.6	81	19	2.9 ± 0.1
0.1	20.5 ± 0.5	12	88	9.2 ± 1.2
1	26.4 ± 2.0	0	100	8.9 ± 0.3

[a]The qMab was determined from the slope of the best straight line through data points of the viability index (V_I) versus Mab concentration. These values were calculated for cultures maintained for 3 days except for 0.1 - 1 μg/ml where qMab was calculated for 2 days of incubation. Controls data points were the average of multiple determinations (n=3). Other points were taken from duplicate determinations (n=2).

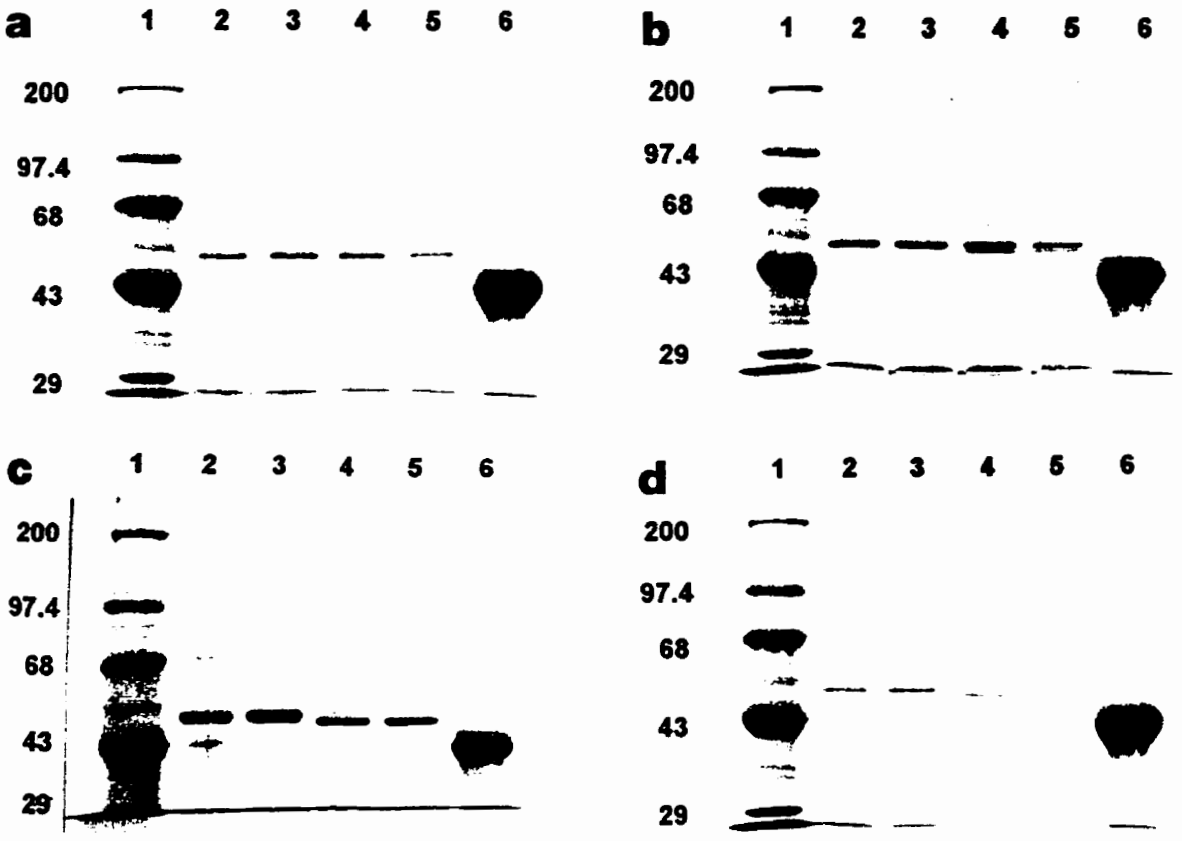

Figure 7.2 Electrophoresis of purified Mab from cultures treated with tunicamycin. Proteins were electrophoresed on a 8.55% cross-linked polyacrylamide gel under reducing conditions.

Lane 1: molecular weight standards (x 10^3). *Lanes 2 and 3*: Mab from cultures without a tunicamycin supplement . *Lanes 4 and 5*: Mab purified from cultures treated 0.001 μg/ml tunicamycin (a), 0.01 μg/ml tunicamycin (b), 0.1 μg/ml tunicamycin (c) or 1 μg/ml tunicamycin (d). Lane 6: ovalbumin.

The carbohydrate content of each band was determined by glycosylation analysis of Western blots. Analysis of control culture Mab shows that the heavy chain of IgG was glycosylated as evidenced by the staining of the 51 kD band (Fig.7.3, lanes 1, 2, 5 and 6). Light chains of IgG were not glycosylated. For the tunicamycin-treated cells only one of the heavy chain bands (with the slower migration) was detected by the carbohydrate-sensitive stain. This is shown in Fig.7.3 by the very faint band for the sample from 0.1 μg/ml tunicamycin-treated cultures (lanes 3 and 4). The faster migrating heavy chain bands of Mab purified from 0.01 - 1 μg/ml tunicamycin supplemented cultures were not detected by carbohydrate staining confirming a lack of glycosylation. Absence of staining of Mab purified from 1 μg/ml tunicamycin supplemented cultures indicates a total inhibition of glycosylation (not shown).

An analysis of the Mab populations based on electrophoresis band intensities is shown in Table 7.1. This shows a decrease in the level of Mab glycosylation with increase in tunicamycin concentration addition to the cultures. At 1 μg/ml tunicamycin, the hybridomas secreted only the non-glycosylated form of the Mab. In 0.1 μg/ml tunicamycin, hybridomas secreted 7 times more non-glycosylated Mab than glycosylated Mab. In 0.01 μg/ml tunicamycin, 4 times more glycosylated Mab was secreted than non-glycosylated Mab.

7.3.1.4 Nucleotide analysis

By analysis of the cell lysates extracted from the hybridoma cells, we examined the possibility that tunicamycin affected the intracellular nucleotide pools. The cell lysates were extracted from cultures described previously in the analysis of monoclonal antibody production. No significant differences in nucleotide pools were found in cultures treated with 0.001 μg/ml tunicamycin when compared to control cultures. However, supplementation of cultures with a tunicamycin concentration of 0.01 μg/ml or higher resulted in a pronounced increase in the UDP-GNac pool which consists of UDP-GalNac and UDP-GlcNac (Fig.7.4 and 7.5). The increase of these two UDP-sugars was dependent

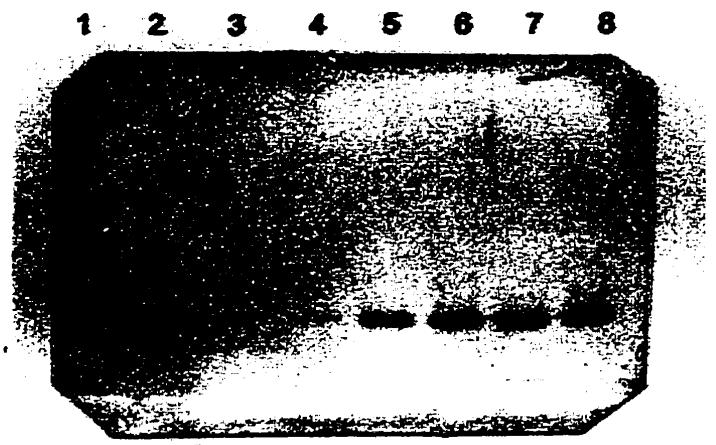

Figure 7.3 Glycosylated protein detection on a nitrocellulose membrane. Electrophoresed proteins were transferred to a nitrocellulose membrane by Western blotting. Glycoproteins were detected on the membrane with a glycosylation detection kit (GlycoTrak from Oxford GlycoSystems).

Lanes 1 and 2: Mab purified from control cultures. *Lanes 3 and 4*: Mab purified from 0.1 μg/ml tunicamycin-treated cultures. *Lanes 5 and 6*: Mab purified from control cultures. *Lanes 7 and 8*: Mab purified from 0.001 μg/ml tunicamycin-treated cultures.

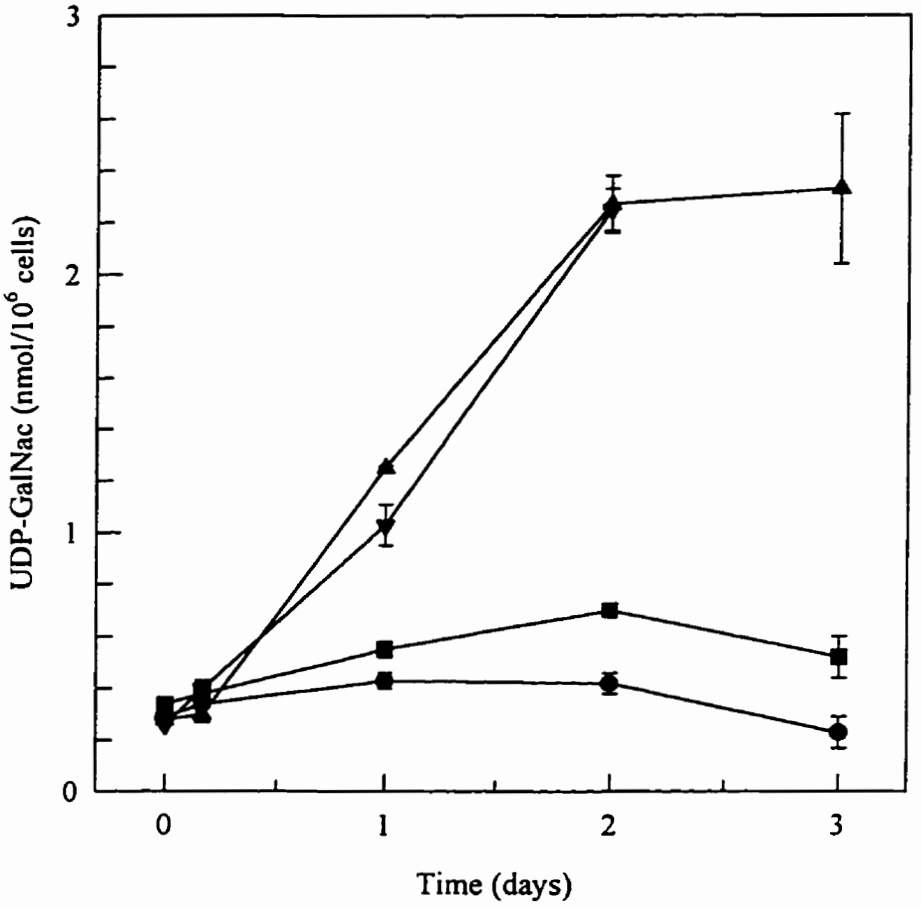

Figure 7.4 Effect of tunicamycin on intracellular concentrations of UDP-GalNac. Cultures were supplemented with 0 μg/ml tunicamycin (control) (●), 0.01 μg/ml tunicamycin (■), 0.1 μg/ml tunicamycin (▲) or 1 μg/ml tunicamycin (▼). Cultures (50 ml) were established in 150 cm^2 T-flasks by inoculating cells from mid-exponential phase at 1.0 x10^6 cells/ml. Daily samples (1-4 x 10^6 cells) were taken for nucleotide analysis by HPLC. Each point is a mean (± SEM) determination from 2 (+tunicamycin) or 3 (control) independent cultures.

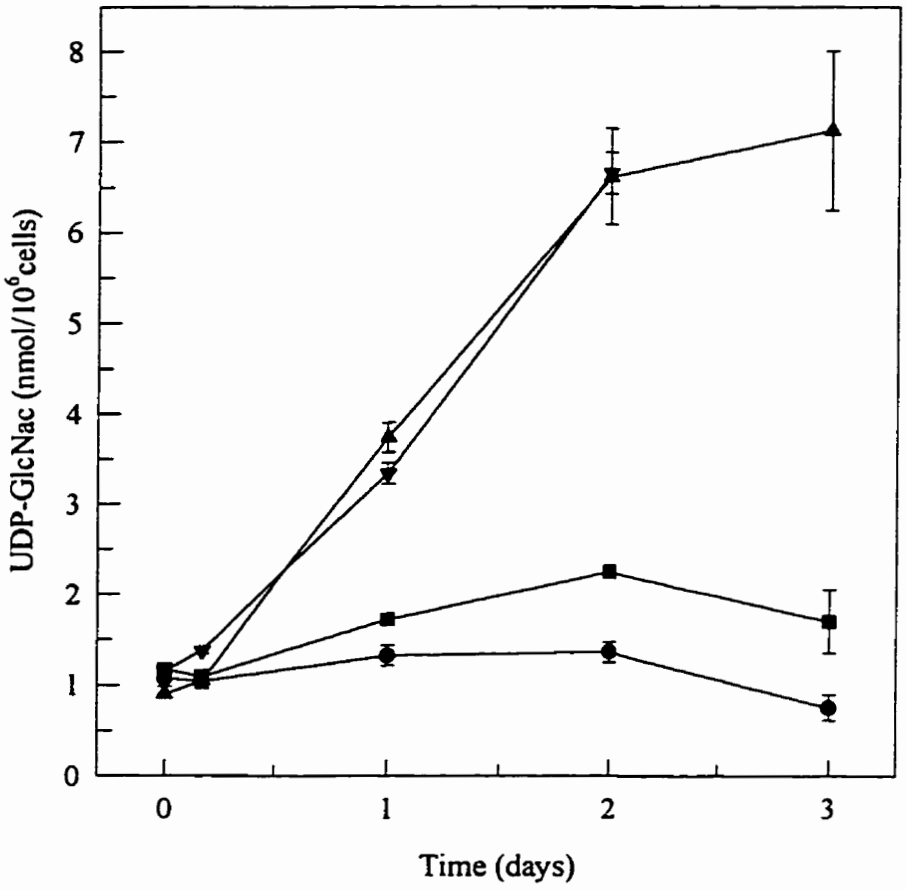

Figure 7.5 Effect of tunicamycin on intracellular concentrations of UDP-GlcNac. Cultures were supplemented with 0 μg/ml tunicamycin (control) (●), 0.01 μg/ml tunicamycin (■), 0.1 μg/ml tunicamycin (▲) or 1 μg/ml tunicamycin (▼). Cultures (50 ml) were established in 150 cm^2 T-flasks by inoculating cells from mid-exponential phase at 1.0 $x10^6$ cells/ml. Daily samples (1-4 x 10^6 cells) were taken for nucleotide analysis by HPLC. Each point is a mean (± SEM) determination from 2 (+tunicamycin) or 3 (control) independent cultures.

on the dose of tunicamycin. The maximum concentration of both UDP-GalNac and UDP-GlcNac in 0.1 - 1.0 μg/ml tunicamycin treated cultures was 4.9 - 5.5 greater than control cultures. In 0.01 μg/ml tunicamycin treated cultures, the sugar-nucleotide pool was 1.6 - 1.7 fold greater than control cultures.

The ratio of UDP-GlcNac/ UDP-GalNac was constant in all tunicamycin-treated and control cultures with UDP-GlcNac amounting to 76 ± 5 % of the total UDP-GNac pool. The UDP-GNac pool of 0.1 and 1 μg/ml tunicamycin treated cultures accounted for 24 - 52 % of total nucleotides compared to 12 - 25 % for the control cultures. The UDP-GNac pool of cells treated with 0.01 μg/ml tunicamycin accounted for 16 - 28 % of total nucleotides. The total intracellular nucleotide pool was significantly higher in cells containing an elevated level of UDP-GNac.

The UDP-GNac pool was directly proportional to the percentage of non-glycosylated Mab secreted by the cells (Table 7.1). Cellular UDP-GNac levels of 9 nmol per 10^6 cells were accompanied by over 88 % of the Mab population being in the non-glycosylated form. UDP-GNac levels of 2.9 nmol per 10^6 cells were accompanied by 19% of Mab population being non-glycosylated. Mab was fully glycosylated in the presence of a UDP-GNac level of 2.1 nmol per 10^6 cells or lower. Although both qMab and UDP-GNac increased at high tunicamycin concentration, there was no evidence for a direct relationship between qMab and UDP-GNac levels (Table 7.1).

7.3.2. Effect of ammonium chloride

Ammonium chloride has also been shown to perturb the intracellular UDP-GNac concentration (Ryll *et al.*, 1994). Therefore, it was decided to compare the metabolic effects observed with tunicamycin to those of NH_4Cl. Ammonium chloride differs from tunicamycin in the proposed mechanism of enhancement of the UDP-GNac pool, causing an increased synthesis of the nucleotides rather than a decreased rate of utilization.

All cultures used to investigate the effect of NH_4Cl were inoculated at 1.3 x 10^5 cells/ml in 90 ml of medium and maintained for 6 days by daily feeding from day 2. Exponentially growing cells were inoculated into NB-SFM containing 0, 5 or 10 mM NH_4Cl. Cultures supplemented with 10 mM NaCl were used as a control for the increase in osmolarity due to the addition of ammonium and chloride ions. Results are representative of two independent cultures inoculated from the same cell stock (5 mM NH_4Cl and 10 mM NaCl supplemented cultures) or from different cell stocks (0 mM NH_4Cl and 10 NH_4Cl).

7.3.2.1 Growth and ammonium ion concentrations

Growth curves of NH_4Cl and NaCl treated cells are shown in Fig.7.6. Cultures treated with 10 mM NH_4Cl showed a lower growth rate (0.020 h^{-1}) compared to the control cultures (0.034 h^{-1}) and a 37 % lower maximum cell density. A concentration of 5 mM NH_4Cl did not significantly affect the growth rate. However, the maximum cell density was 18 % lower than the control value. NaCl-treated cells had similar growth characteristics as in control cultures. Glutamine metabolism resulted in ammonium production which caused an increased concentration in the medium of up to 4.5 mM for control cultures. Maximum ammonium ion concentration for 5 mM and 10 mM NH_4Cl - treated cultures were 9.2 mM and 13.1 mM respectively.

7.3.2.2 Mab glycosylation and production rates

Mab production rates are shown in Table 7.2. Culture supplementation with NaCl (10 mM) or NH_4Cl (5 mM) did not result in a significant increase in qMab compared to the control value (23.1 μg per 10^6 cells per day). However, supplementation of medium with 10 mM NH_4Cl resulted in a 36 % increase in qMab when compared to the control.

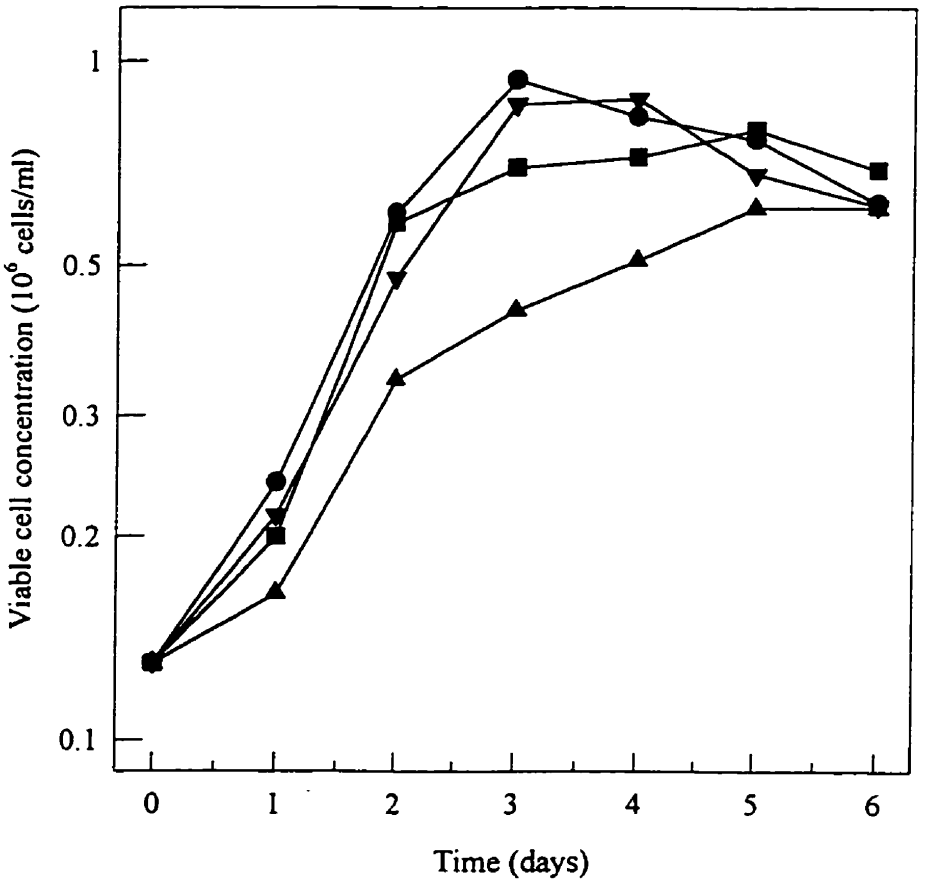

Figure 7.6 Effect of NH_4Cl or NaCl on cell growth. Cultures were supplemented with 0 mM NH_4Cl (control) (●), 5 mM NH_4Cl (■); 10 mM NH_4Cl (▲) or 10 mM NaCl (▼). Cell concentrations were determined from daily samples of cultures (90 ml) established in 150 cm^2 T-flasks by inoculating cells from mid-exponential phase at 1.3 $x10^5$ cells/ml. Each point is a mean determination from 2 independent cultures. The error was less than 10 % of the mean in all cases.

Table 7.2 The specific Mab production rate, state of glycosylation and maximum UDP-GNac concentration of cultures supplemented with NH_4Cl or NaCl.

NH_4Cl or NaCl* (mM)	qMab[a] (μg per 10^6 cells per day)	% glycosylated Mab	% non - glycosylated Mab	maximum UDP-GNac concentration (nmol per 10^6 cells)
0	23.1 ± 0.5	100	0	3.0 ± 0.3
5	26.8 ± 0.6	100	0	5.9 ± 0.2
10	33.1 ± 0.8	100	0	10.1 ± 0.5
10*	25.5 ± 0.7	100	0	3.5 ± 0.5

[a]The qMab was determined from the slope of the best straight line through data points of the viability index (Vi) versus Mab concentration. These values were calculated for cultures maintained for 6 days. Controls and 10 mM NH_4Cl data points were means of multiple determinations (n=4). Other points were taken from duplicate determinations (n=2).

Monoclonal antibodies purified from cell culture supernatants were electrophoresed and analyzed for the presence of carbohydrate chains. All heavy chain bands of Mab samples from NH_4Cl and NaCl supplemented cultures were fully glycosylated as shown by carbohydrate-specific staining on the nitrocellulose membrane. There was no evidence of non-glycosylated heavy chain bands as observed in the tunicamycin-treated cultures.

7.3.2.3 Nucleotide analysis

Cell lysates from cultures treated with NH_4Cl were also analyzed for nucleotide concentrations by HPLC. The UDP-GalNac and UDP-GlcNac pools increased significantly as a result of supplementing the cultures with NH_4Cl (Fig.7.7 and 7.8). The values appeared to increase to a maximum at day 3 in the NH_4Cl -supplemented cultures, although the drop in value for all samples at day 2 is unexplained. The increase of the UDP-GNac pool was dependent on the NH_4Cl concentration (Table 7.2). An addition of 5 mM NH_4Cl resulted in a 2.1 - 2.4 fold increase in the maximum UDP-GalNac and UDP-GlcNac concentrations when compared to control cultures. An addition of 10 mM NH_4Cl resulted in a 3.7 - 4.0 fold increase in the sugar-nucleotide pools. NaCl did not affect significantly the UDP-GNac pool (Table 7.2).

The ratio of UDP-GlcNac/ UDP-GalNac was constant in all the ammonia-treated and control cultures with UDP-GlcNac amounting to 76 $\pm$ 1 % of the total UDP-GNac pool. This was consistent with the data from the tunicamycin experiments. The percentage of UDP-GalNac and UDP-GlcNac compared to total nucleotides was significantly higher in NH_4Cl supplemented cultures compared to controls. The UDP-GNac pool of cells treated with 5 mM NH_4Cl accounted for up to 37 % of total nucleotides compared to 26 % for control cultures. In 10 mM NH_4Cl supplemented cultures the UDP-GNac pool consisted of up to 41 % of all nucleotides. The total intracellular nucleotide pool was significantly higher in cells containing an elevated level of UDP-GNac.

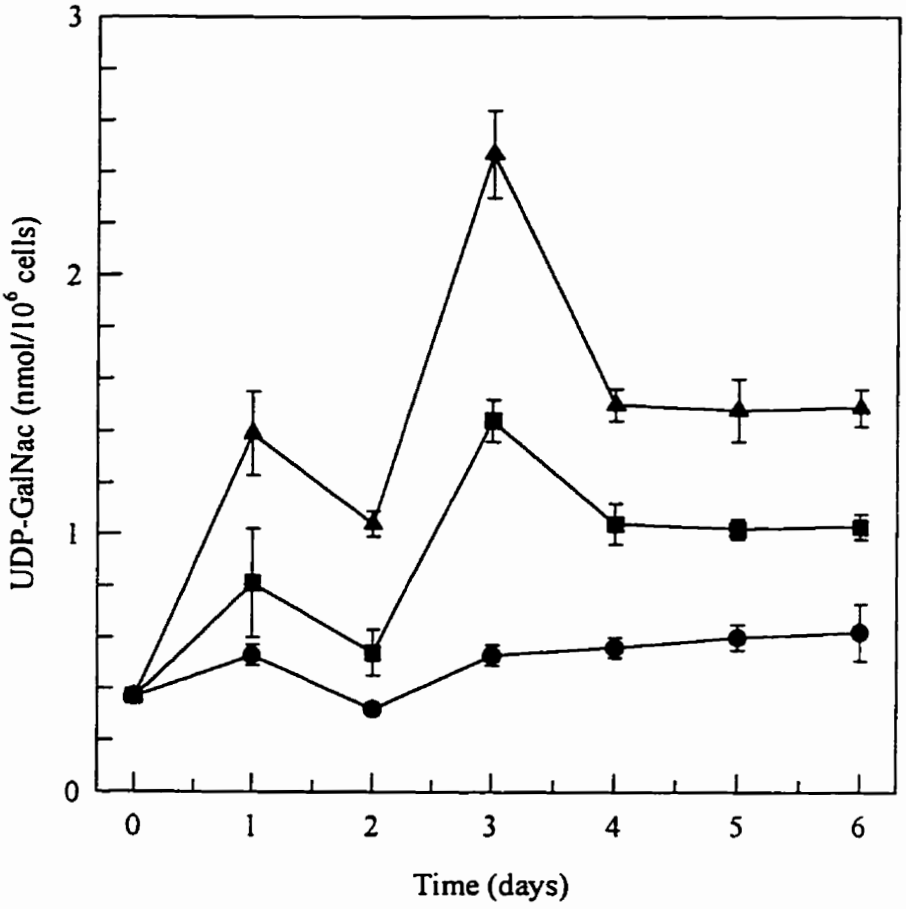

Figure 7.7 Effect of NH_4Cl on intracellular concentrations of UDP-GalNac. Cultures were supplemented with 0 mM NH_4Cl (control) (●), 5 mM NH_4Cl (■) or 10 mM NH_4Cl (▲). Cultures (90 ml) were established in 150 cm^2 T-flasks by inoculating cells from mid-exponential phase at 1.3 x10^6 cells/ml. Daily samples (1-4 x 10^6 cells) were taken for nucleotide analysis by HPLC. Each point is a mean (± SEM) determination from 2 independent cultures.

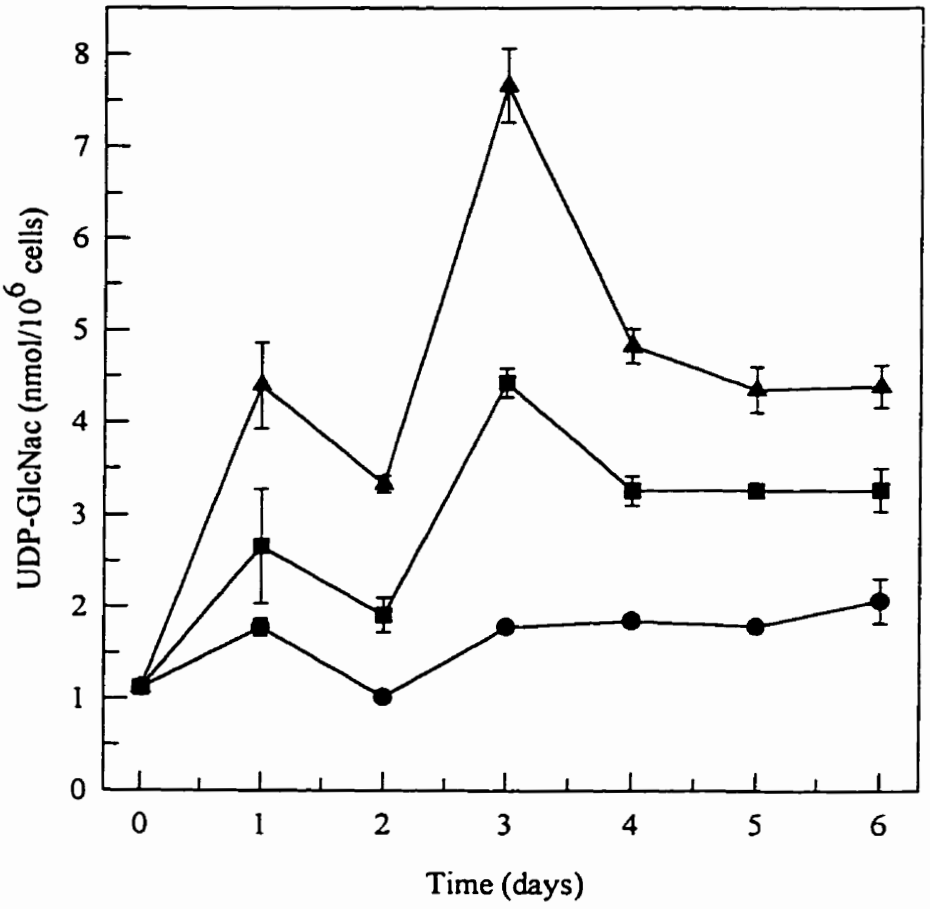

Figure 7.8 Effect of NH_4Cl on intracellular concentrations of UDP-GlcNac. Cultures were supplemented with 0 mM NH_4Cl (control) (●), 5 mM NH_4Cl (■) or 10 mM NH_4Cl (▲). Cultures (90 ml) were established in 150 cm^2 T-flasks by inoculating cells from mid-exponential phase at 1.3 x10^6 cells/ml. Daily samples (1-4 x 10^6 cells) were taken for nucleotide analysis by HPLC. Each point is a mean (± SEM) determination from 2 independent cultures.

7.4 Discussion

The availability of an intracellular pool of UDP-GNac is necessary to ensure full glycosylation of secreted glycoprotein from cultured mammalian cells. Previous work has implicated the intracellular concentration of UDP-GNac as a key regulator of cell viability and productivity. Ryll *et al.* (1994) suggested that an elevated intracellular concentrations of UDP-GNac is a mediator of loss of cell viability induced in cultures following the accumulation or addition of ammonia. In a previous report from our laboratory we showed that elevated culture temperatures induced an increase in UDP-GNac and a concomitant enhancement of specific antibody productivity, qMab (section 4.0).

The purpose of the work presented here was to determine whether the intracellular level of UDP-GNac in a murine hybridoma has a significant role in monoclonal antibody production or in the degree of antibody glycosylation. The hybridoma (CC9C10) was grown under conditions favorable for UDP-GNac intracellular accumulation. Two approaches were used. The first involved the addition of tunicamycin which has previously been shown to result in reduced UDP-GNac utilization and inhibition of protein glycosylation (Morin *et al.*, 1983). Tunicamycin is a structural analogue of UDP-GNac and its mechanism of intracellular action involves competitive inhibition of the transfer of GNac to the dolichol phosphate carrier during the cellular glycosylation process (Tkacz and Lampen, 1975). The second approach involved the addition of NH_4Cl which has previously been shown to result in increased UDP-GNac synthesis (Ryll *et al.*,1994). This is thought to occur by promoting the activity of the enzyme, glucosamine phosphate isomerase which affects the amination of fructose 6-phosphate to glucosamine 6-phosphate by ammonia . Glucosamine 6-phosphate is a precursor for the synthesis of UDP-GNac.

In our experiments with murine hybridoma cultures it was important to establish concentrations of tunicamycin and ammonia that perturbed the metabolism of UDP-GNac without causing a significant rate of cell death. Previous reports have shown that tunicamycin concentrations of 1-10 μg/ml arrested protein glycosylation without inhibiting

protein synthesis in cell culture (Leatherbarrow *et al.*,1985; Walker *et al.*, 1989). However, these studies were conducted in serum-supplemented cultures. In the serum-free medium used to culture the CC9C10 hybridomas described in our report (NB-SFM), tunicamycin at >0.01 μg/ml arrested cell growth and reduced cell viability significantly. Supplementation of the NB-SFM cultures with serum or bovine serum albumin reduced significantly the growth inhibitory effect of tunicamycin and improved culture viability. This protective effect may be due to the potential binding between serum albumin and the fatty acid residue of tunicamycin (Ashbrook *et al.*,1975).

The experimental data showed that concentrations of tunicamycin up to 0.1 μg/ml did not significantly alter the Mab production rate (qMab) when compared to the control cultures, although at 1 μg/ml tunicamycin there was a modest but significant increase in the qMab. From this we conclude that tunicamycin does not significantly affect the rate of Mab production in viable cells. At the high concentration of tunicamycin tested there was a significant population of non-viable cells in the culture which increased to more than 50 % after only 2 days. It is probable that the apparently higher qMab observed at the highest tunicamycin concentration tested was due to passive antibody release by non-viable cells (Mohan and Lyddiatt, 1991).

Secreted proteins from mammalian cells show variable glycosylation patterns which depend upon a range of parameters including the metabolic state of the cells as well as the conditions of culture (Jenkins *et al.*, 1996). Murine immunoglobulin IgG_1 of the type secreted by the CC9C10 cells has two CH2 heavy chain domains each of which contains a conserved glycosylation site at Asn297 to which are linked complex biantennary oligosaccharides (Rudd and Dwek., 1997). Additional sites may be present in some IgG molecules but these are likely to be of minor structural importance. Tunicamycin caused a decrease in the molecular weight of the heavy chain of the Mab from the CC9C10 hybridomas. This lower molecular weight heavy chain as well as the light chain was non-glycosylated as shown by Western blot analysis. The decrease in molecular weight of the heavy chain corresponded to the approximate size of previously analyzed carbohydrate groups from IgG (Hamako *et al.*, 1993).

A comparison between the data for Mab glycosylation and production rates indicates that the non-glycosylated Mab was secreted at the same rate as the glycosylated Mab. Thus, qMab is not affected by the extent of glycosylation in these cells. This is consistent with findings that glycosylation is not necessary for intracellular transport, assembly or secretion of IgG isotype antibodies (Weitzman and Scharff, 1976). However, cells secreting other immunoglobulin isotypes (IgA and IgE) have these functions impaired in the absence of glycosylation (Hickman *et al.*,1977; Sidman, 1981). This may suggest that there are differences in the mechanism or rates of synthesis and glycosylation related to the isotype of the secreted immunoglobulin.

Tunicamycin caused a dose dependent increase in the intracellular UDP-GNac pool of CC9C10 cells up to a concentration of 0.1 μg/ml. This may indicate feedback inhibition of hexosamine synthesis by the sugar-nucleotides (Kornfield *et al.*, 1964). Similar nucleotide accumulations have been observed in a leukemic cell line (Morin *et al.*, 1983). A compilation of results indicate that tunicamycin induces UDP-GNac accumulation without affecting the qMab. This finding suggests that temperature induced UDP-GNac accumulation and the concomitant qMab enhancement found in previous studies may be independent events (section 4.0).

A second method of increasing UDP-GNac intracellular concentrations was by supplementing cultures with ammonium chloride. This results in an increased rate of sugar-nucleotide synthesis as reported in other studies (Ryll *et al.*, 1994). Although NH_4Cl is growth inhibitory (Doyle and Butler, 1990; McQueen and Bailey, 1991), it is less toxic than tunicamycin thus allowing cells to grow exponentially during a period when UDP-GNac accumulates significantly. Ryll *et al.* (1994) suggest that growth inhibition is mediated by UDP-GNac accumulation.

Supplementation of hybridoma cultures with NH_4Cl up to 10 mM resulted in a concentration-dependent increase in intracellular UDP-GNac to a level comparable with that observed with tunicamycin. However, the NH_4Cl-induced UDP-GNac accumulation could not be directly correlated with the specific antibody production (qMab). The treatment of cultures with 5 mM NH_4Cl did not affect the qMab whereas a treatment of 10 mM NH_4Cl resulted in a 36 % increase compared to control cultures. The increase in

qMab at 10 mM NH_4Cl may be attributed to other effects of ammonium supplementation and related more directly to a reduction in growth rate. Reductions in growth rate have been associated in other studies with an increase in Mab production (Miller *et al.*, 1988a; Hayter *et al.*, 1992).

Analysis of Mab purified from NH_4Cl treated cultures by gel electrophoresis and Western blotting shows that ammonia did not prevent glycosylation. In previous reports ammonium chloride has been shown to prevent terminal sialylation of oligosaccharides in plasma and Chinese hamster ovary cell glycoproteins (Thorens and Vassalli, 1986; Borys *et al.*, 1994; Anderson and Goochee, 1995). Similar changes may have occurred in the Mab from the ammonia-treated CC9C10 cells. However, such small changes in the heterogeneity of the glycosylation pattern would have been undetectable from the gel electrophoresis used in our analysis.

7.5 Conclusion

We have shown that supplementation of a hybridoma culture with tunicamycin or ammonium chloride caused up to a 5 fold increase in intracellular concentrations of UDP-GalNac and UDP-GlcNac. The resulting high sugar-nucleotide levels did not affect significantly the specific monoclonal antibody production rate showing that the availability of UDP-GNac is not a limitation to higher productivity. Tunicamycin, but not ammonium chloride, inhibits the glycosylation of Mab. However, the non-glycosylated Mab was secreted at the same rate as the glycosylated form showing that the glycosylation process does not appear to limit productivity in these cells. We conclude that UDP-N-acetyl hexosamine does not act as a mediator of enhanced rates of monoclonal antibody synthesis in the hybridoma cell culture system. These results are important in the further understanding of the inter-relationship of measurable metabolic parameters in high producer mammalian cell lines used in large-scale bioprocesses.

CHAPTER 8

8.0 The relationship between intracellular nucleotides levels and culture viability

8.1 Introduction

Intracellular nucleotides have been implicated in all areas of metabolism. They act as substrates, products and energy carriers in many cellular reactions. Nucleotides also play an important role in the regulation of cellular processes and pathways (Atkinson, 1977). Studies have shown that imbalances in nucleotide pools correlate with viable cell processes such as cell cycle phases, proliferation, differentiation and transformation (Rapaport *et al.*, 1979; De Korte *et al.*, 1987; Ryll and Wagner, 1992). It is therefore plausible that fluctuations in the nucleotide pools may also influence or depend upon other cell behaviors such as cell death.

Cell death is a critical factor limiting the productivity of hybridoma cultures. This is due to the observation that Mab production is related to the number of viable cells (Renard *et al.*, 1988). Conditions that would sustain viability for an extended period of time would therefore improve product yield. For many years, animal cell death was considered to be a passive uncontrolled phenomenon referred to as necrosis. It is now widely accepted that under certain circumstances animal cells may actually play an active role in their own demise. This cell "suicide" known as apoptosis is regulated by gene expression (Mosser and Massie, 1994; Hale *et al.*, 1996). The two modes of cell death can be distinguished morphologically. Apoptotic cells are characterized by the condensation of nuclear chromatin into the shapes of crescents or spherical beads (Mercille and Massie, 1994a). It has even been speculated that condensation during apoptosis may be due to the sharing of common pathways with mitosis (Meikrantz and Schlegel, 1995). No condensation of chromatin is apparent however in necrotic cells.

Other morphological and biochemical changes often associated with apoptotic cells are the reduction in cell volume, blebbing of the plasma membrane, fragmentation of the

cell into apoptotic bodies and cleavage of DNA at the linker region between nucleosomes. The internucleosomal cleavage of the chromatin in apoptotic cells can be visualized by agarose gel electrophoresis as a DNA ladder having multiples of 180 - 200 base pairs (Wyllie, 1980; Sokolova *et al.*, 1992). There is however evidence questioning this technique for identifying apoptotic cells. For example, not all apoptotic cell deaths are characterized by the typical DNA ladder and cells undergoing massive necrosis have been shown to exhibit internucleosomal cleavage (Cohen *et al.*, 1992; Collins *et al.*, 1992).

Lymphoid cell lines die by a combination of apoptosis and necrosis when grown in batch cultures. A balance between the two modes of cell death may be due to the simultaneous presence of different inducers. Studies indicate that apoptosis is induced by glucose, glutamine or oxygen limitations while necrosis is caused by the accumulation of metabolic by-products such as lactate and ammonium.(Mercille and Massie, 1994a, 1994b; Singh *et al.*, 1994). Other studies however have demonstrated that glucose deprivation may cause significant cell death by necrosis (Petronini *et al.*, 1996).

The purpose of this investigation was to determine if a relationship exists between hybridoma culture viability, mode of cell death and nucleotide pools. Comparing these parameters may give insights into how cell death is regulated or induced and lead to the development of strategies aimed at optimizing culture productivity.

8.2 Preparation of stock cultures and flasks prior to experiments

Stock cultures of CC9C10 hybridomas were inoculated at 1.2 x 10^5 cells/ml in T-flasks (150 cm^2) containing a total of 50 ml NB-SFM. Cultures were incubated at 37°C for 66-67 hours before use in experiments. This treatment of cells gave consistently high density cultures (0.9 - 1.3 x 10^6 cells/ml) in the mid-exponential phase of growth. Exponentially growing cells were collected by centrifugation at 190 g for 5 minutes and the supernatant was decanted. Tissue culture flasks (25 cm^2) with loosened caps were pre-incubated overnight in a CO_2 incubator at 37°C prior to use.

8.3 Results

8.3.1 The effect of inoculation density on viability and intracellular nucleotide levels of CC9C10 hybridomas

The aim of this experiment was to investigate if decreases in culture viability would coincide to specific changes in nucleotide pools. In order to obtain varying death profiles, cultures were inoculated at different cell densities. Exponentially growing cells as prepared in section 8.2 were suspended in 10 ml NB-SFM (25 mM glucose, 6 mM glutamine) in replicate T-flasks (25 cm^2) at three different inoculation densities: 1.25; 2.5 and 5.0 x 10^5 cells/ml. Cultures were incubated at 37°C in a CO_2 incubator. Cells were counted using a hemocytometer and viability determined by the trypan blue exclusion method (section 2.5.1). Intracellular nucleotides were extracted and quantified by ion pair reverse phase chromatography (gradient 2) and by luminometry as previously described (section 2.7). Flasks were sacrificed for each sampling time point until a significant decrease in viability was observed. Experiments were done in duplicate with cultures inoculated from a different cell stock. The data was averaged to give a mean and standard error of the mean where n = 2.

8.3.1.2 Growth and viability

As shown in Fig.8.1, cultures inoculated at different densities reached similar maximum viable cell numbers (1.5 ± 0.1 x 10^6 cells/ml). The time that the cultures reached maximum values however was dependent on the initial inoculum density. Cultures inoculated at 1.25; 2.5 and 5.0 x 10^5 cells/ml attained maximum viable cell numbers after 78, 53 and 42 hours respectively. The maximum cell growth rate (μ_{max}) calculated from the slope of the growth curve was the same for the two cultures inoculated at the lower cell densities (0.035 ± 0.002 h^{-1}). Cultures inoculated at 5 x 10^5 cells/ml had a 23 % lower μ_{max} (0.027 ± 0.001 h^{-1}).

For the purposes of this study, the beginning of the death phase of a culture was defined as the first decrease in cell population viability. Culture viability was over 92 % for all cultures at the time of inoculation. After 36 hours of incubation, the viability of the

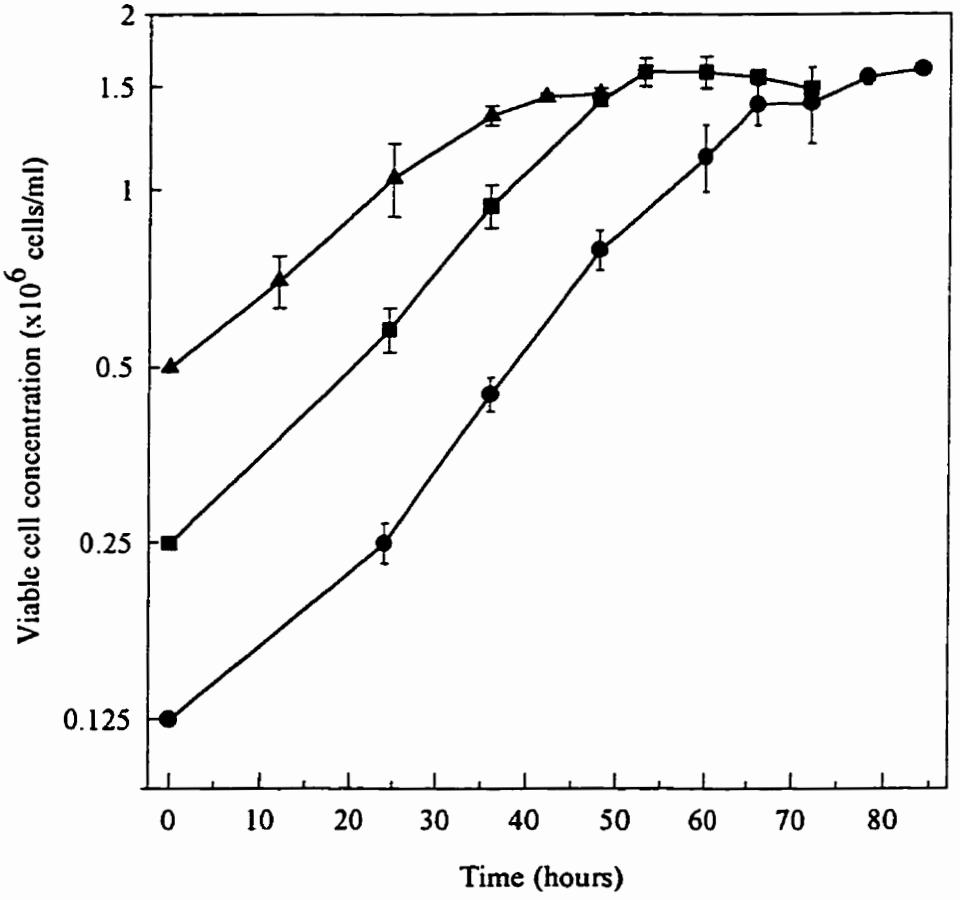

Figure 8.1 The effect of initial inoculation density on CC9C10 growth. Hybridomas were inoculated into T-flasks (25 cm^2) containing 10 ml NB-SFM (25 mM glucose, 6 mM glutamine) at the following densities: 1.25 x 10^5 cells/ml, (●); 2.5 x 10^5 cells/ml, (■); 5.0 x 10^5 cells/ml, (▲). Values are the mean from two independent cultures inoculated from different cell stocks.

culture inoculated at 5.0 x 10^5 cells/ml began to decline (Fig.8.2). The time of the onset of the death phase for cultures inoculated at 2.5 and 1.25 x 10^5 cells/ml was 60 and 72 hours respectively. The onset of death for the two latter cultures was within 7 hours of attaining the maximum viable cell density. Cultures inoculated at 5.0 x 10^5 cells/ml exhibited a decrease in viability 7 hours prior to reaching its maximum viable cell density.

8.3.1.3 Metabolite analysis

Nutrient concentrations in the medium at the beginning of the death phase were determined for each culture. Glucose levels were greater than 6 mM when all cultures exhibited a decrease in viability. Glutamine concentrations at these time points were 0.3 - 0.5 mM in cultures inoculated at 1.25 and 2.5 x 10^5 cells/ml. Higher concentrations of glutamine (1.3 ± 0.1 mM) were observed at the onset of death in cultures inoculated at 5 x 10^5 cells/ml. Glutamine was totally depleted in cultures inoculated at 1.25 and 2.5 x 10^5 cells/ml after 78 and 72 hours respectively.

8.3.1.4 Nucleotide analysis

Nucleotide profiles were compared to decreases in the viability of the cell cultures. The results showed that the intracellular UTP concentrations increased in cells during the first 24 hours of exponential growth (Fig.8.3). During this period maximum UTP values of 1.9 - 2.8 nmol/10^6 cells were attained in all cultures. After 24 hours of incubation, UTP levels decreased. In cultures inoculated at 1.25 and 2.5 x 10^5 cells/ml, the UTP concentration was depleted to 1.0 nmol/10^6 cells 6 -7 hours prior to a decrease in viability (Table 8.1). The level of UTP remained below this value for the remainder of the culture period as viability continued to decline. In cultures inoculated at 5 x 10^5 cells/ml, UTP concentrations did not go below 1.0 nmol/10^6 cells until 7 hours after the onset of the death phase.

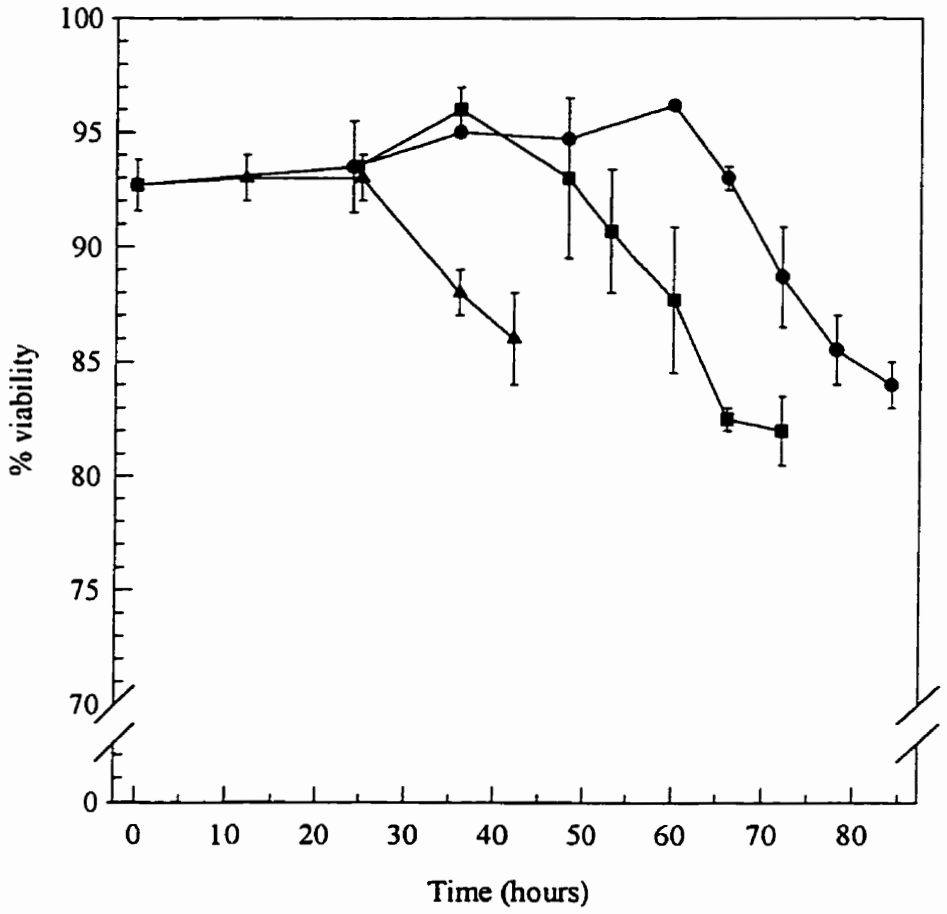

Figure 8.2 The effect of initial inoculation density on CC9C10 viability. Hybridomas were inoculated into T-flasks (25 cm^2) containing 10 ml NB-SFM (25 mM glucose, 6 mM glutamine) at the following densities: 1.25 x 10^5 cells/ml, (●); 2.5 x 10^5 cells/ml, (■); 5.0 x 10^5 cells/ml, (▲);. Values are the mean from two independent cultures inoculated from different cell stocks.

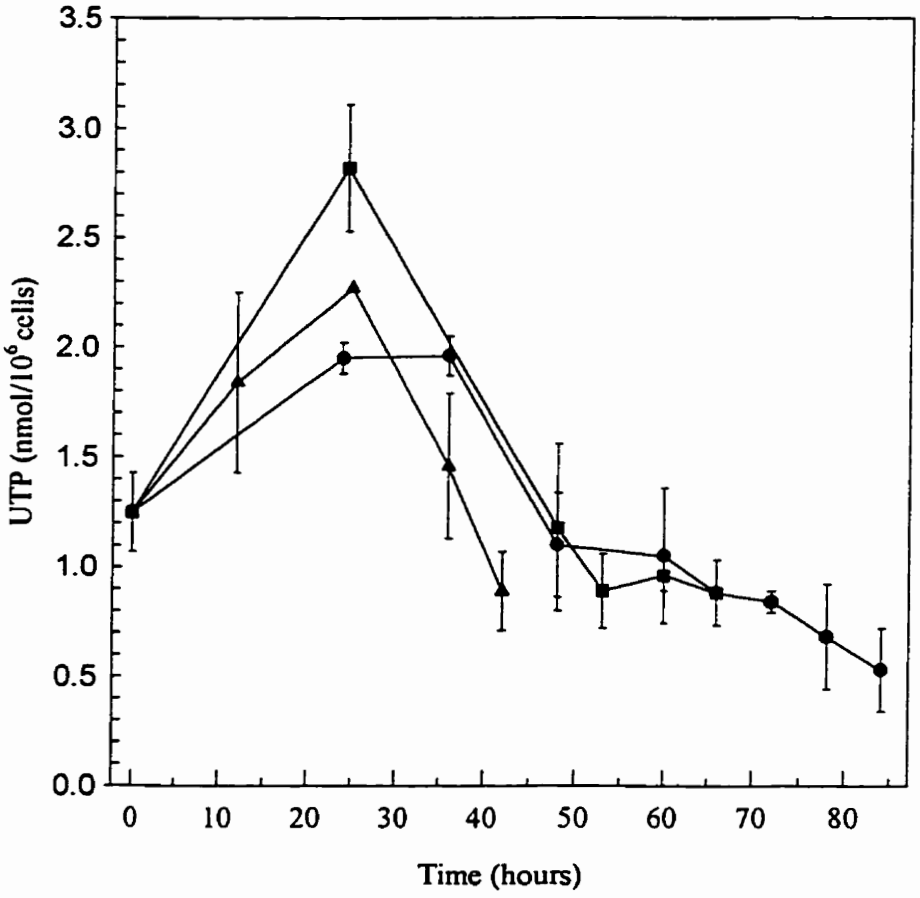

Figure 8.3 The effect of initial inoculation density on CC9C10 intracellular UTP levels. Hybridomas were inoculated into T-flasks (25 cm^2) containing 10 ml NB-SFM (25 mM glucose, 6 mM glutamine) at the following densities: 1.25 x 10^5 cells/ml, (●); 2.5 x 10^5 cells/ml, (■); 5.0 x 10^5 cells/ml, (▲). Values are the mean from two independent cultures inoculated from different cell stocks.

Table 8.1 Correlation between decreases in pyrimidine levels and the time of the first decrease in viability. N_{max} is the maximum viable cell density.

Initial inoculum density ($\times 10^5$ cells/ml)	Time when cultures attain N_{max} (hours)	Time of the first decrease in viability (hours)	Time when UTP levels fall below 1 nmol/10^6 cells (hours)	Time when CTP becomes undetectable (hours)
1.25	72	72	66	60
2.50	53	60	53	53
5.00	42	36	42	42

A decrease in cell culture viability was accompanied by a significant depletion of the CTP pool. The resulting low concentrations of CTP in the cellular extracts and the low resolution of the HPLC CTP peak made it difficult to accurately quantify this nucleotide. CTP levels for the purpose of this study were therefore characterized as detectable or undetectable. Detectable limits of CTP were set at 0.2×10^{-5} M as determined by HPLC detection of nucleotide standards. A cell extract concentration of 0.2×10^{-5} M translates to approximately 0.4×10^{-6} nmol/10^6 cells.

Decreases in CTP values to undetectable levels was concomitant with the onset of the death phase (Table 8.1). In cultures inoculated at 1.25 and 2.5×10^5 cells/ml, CTP was undetectable 7 - 12 hours prior to a decrease in viability. Once CTP levels were depleted the intracellular pool of this nucleotide did not recuperate and remained undetectable. In cultures inoculated at 5.0×10^5 cells/ml, the CTP pool was not depleted until 7 hours after the onset of the death phase.

Analysis of purine nucleotide triphosphates, ATP and GTP, did not reveal any correlation between the onset of death and decreased intracellular levels for all inoculation densities tested. Intracellular ATP concentrations remained between 3 - 5 nmol/10^6 cells prior to and after decreases in viability. GTP values during this same culture period were in the range of 0.6 - 1.2 nmol/10^6 cells. The adenylate energy charge of all cultures did not fluctuate significantly and remained higher than 0.8 at all time point measurements.

8.3.2 The effect of initial glucose concentration on viability and intracellular nucleotide levels of CC9C10 hybridomas

To complement the previous experiment (section 8.3.1), the variation in glucose concentration was used as a second method to obtain differential death profiles. This method has the advantage over using different inoculation densities because the inducer of cell death is known (i.e. glucose starvation). Experimental methods were the same as in section 8.3.1 with the following modification: exponentially growing cells were inoculated into replicate flasks containing NB-SFM supplemented with 0, 1, 5, 10 or 25 mM

glucose. Inoculation density was 5 x 10^5 cells/ml and initial glutamine concentration was 6 mM.

8.3.2.1 Growth and viability

As shown in Fig.8.4 and Table 8.2, culture growth and yield was dependent on the initial glucose concentration. Hybridoma cells inoculated into NB-SFM containing 0 mM glucose did not multiply. The inoculation density (5.0 x 10^5 cells/ml) was therefore the maximum cell density in these cultures. In the presence of 1 and 5 mM glucose, cultures reached maximum viable cell densities of 6.3 and 8.5 x 10^5 cells/ml respectively. Maximum viable cell densities of 1.03 and 1.44 x 10^6 cells/ml were attained in NB-SFM containing 10 mM and 25 mM glucose respectively.

In addition to decreased yield of cells, cultures grown in low glucose concentrations also had reduced growth rates (Table 8.2). In the absence of glucose, no growth (μ_{max} = 0) was recorded in the hybridoma cultures. Glucose concentrations of 1 and 5 mM caused μ_{max} rates of 0.019 ± 0.001 h^{-1}. Glucose concentrations of 10 and 25 mM glucose gave μ_{max} rates of 0.027 ± 0.001 h^{-1}.

The beginning of the death phase was determined by monitoring the cell population for the first decrease in viability. Culture viability was over 92 % for all cultures at the time of inoculation. The time of the onset of the death phase was proportional to the initial glucose concentration (Fig.8.5). After 7 - 9 hours of incubation, the viability of cultures grown in the absence of glucose began to decline. Cultures grown in 1, 5, 10 and 25 mM glucose experienced reductions in viability after 19, 26, 30 and 36 hours respectively. The onset of death for cultures grown in 0 - 10 mM glucose was within 7 hours of attaining the maximum viable cell density (Table 8.2). Cultures grown in NB-SFM containing 25 mM glucose however showed a decrease in viability 7 hours prior to reaching the maximum viable cell density.

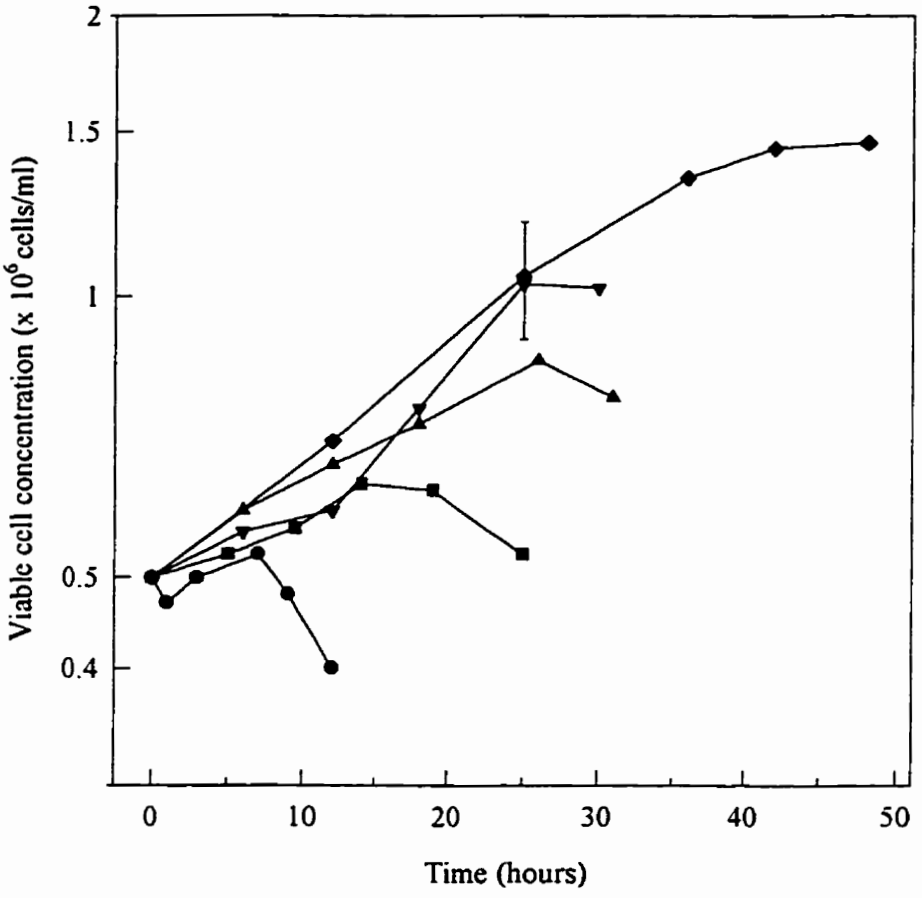

Figure 8.4 The effect of initial glucose concentration on CC9C10 growth. Hybridomas were inoculated into T-flasks (25 cm^2) containing 10 ml NB-SFM (6 mM glutamine) containing varying initial glucose concentrations: 0 mM, (●); 1 mM, (■); 5 mM, (▲); 10 mM, (▼); 25 mM, (◆). Values are the mean from two independent cultures inoculated from different cell stocks. Errors were less than 11 % of the mean except where indicated by the error bars.

Table 8.2 The effect of initial glucose concentration of cell growth and viability. N_{max} is the maximum viable cell density.

Initial glucose concentration (mM)	N_{max} (x 10^6 cells/ml)	Time when cultures attain N_{max} (hours)	μ_{max} (h^{-1})	Time of the first decrease in viability (hours)	Time of glucose depletion (hours)
0	0.50 ± 0.03	0	0	7 - 9	0
1	0.63 ± 0.03	14	0.018 ± 0.001	19	9
5	0.85 ± 0.05	26	0.020 ± 0.003	26	18
10	1.03 ± 0.07	25	0.028 ± 0.003	30	30
25	1.44 ● 0.02	42	0.027 ± 0.001	36	NA

NA- not applicable

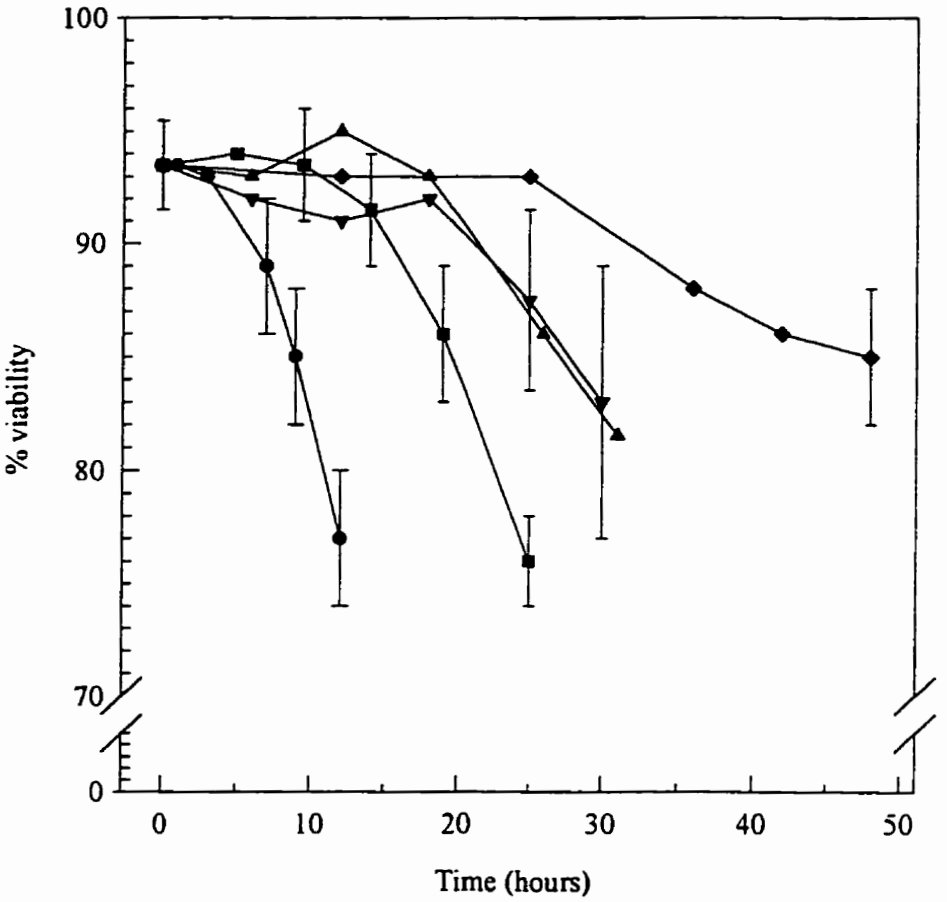

Figure 8.5 The effect of initial glucose concentration on CC9C10 viability. Hybridomas were inoculated into T-flasks (25 cm^2) containing 10 ml NB-SFM (6 mM glutamine) containing varying initial glucose concentrations: 0 mM, (●); 1 mM, (■); 5 mM, (▲); 10 mM, (▼); 25 mM, (◆). Values are the mean from two independent cultures inoculated from different cell stocks. Errors were less than 3 % of the mean except where indicated by the error bars.

8.3.2.2 Metabolite analysis

Glucose levels were totally depleted before or at the onset of the death phase in all cultures except for the NB-SFM containing an initial concentration of 25 mM (Table 8.2). The glucose level in the latter culture was 10.2 ± 1.2 mM at the first time point where a decrease in viability had occurred. Glutamine levels were greater than 1.1 mM in all cultures prior to a decline in culture viability.

8.3.2.3 Nucleotide analysis

The four nucleotide triphosphates pools (CTP, UTP, GTP and ATP) decreased in relation to the glucose concentration. In cultures grown in the absence of glucose, CTP pools were undetectable after only 3 hours of incubation. In the presence of 1 - 10 mM glucose, CTP pools reached undetectable values as glucose was depleted from the medium and prior to a decrease in culture viability (Table 8.3). Cells grown in an initial glucose concentration of 25 mM did not exhibit depleted CTP pools until after a decrease in viability had occurred. UTP pools decreased significantly within 5 hours of incubation in NB-SFM containing 0 or 1 mM glucose (Fig.8.6). UTP levels dropped to 0.45 nmol/10^6 cells or lower from an original value of 1.21 nmol/10^6 cells (a 61 % decrease). In cultures grown in an initial glucose concentration of 5 and 10 mM, UTP values started to decline after 12 - 18 hours of incubation. After 26 - 30 hours, UTP had dropped to less than 0.51 nmol/10^6 cells. Cultures grown in NB-SFM containing 25 mM glucose did not experience similar drastic drops in UTP levels. Intracellular concentrations of UTP did however decrease to 0.89 nmol/10^6 cells after a decrease in viability had occurred at 42 hours. Comparison of UTP values at the first decrease in viability time point are shown in Table 8.3. Almost all UTP values were lower or equal to 0.51 nmol/10^6 cells at the onset of the death phase. The only exception was the culture grown in an initial glucose concentration of 25 mM. In this culture glucose was not limiting during the incubation period.

Table 8.3 Nucleotide levels at the first decrease in culture viability.

Initial glucose concentration (mM)	CTP	UTP (nmol/10^6 cell)	GTP (nmol/10^6 cells)	ATP (nmol/10^6 cells)	Energy charge
0	ND	0.21 ± 0.07	0.19 ± 0.01	0.71 ± 0.14	0.34 ± 0.03
1	ND	0.43 ± 0.12	0.29 ± 0.06	0.84 ± 0.05	0.26 ± 0.03
5	ND	0.51 ± 0.30	0.35 ± 0.10	1.29 ± 0.30	0.32 ± 0.05
10	ND	0.51 ± 0.03	0.39 ± 0.17	1.25 ± 0.24	0.28 ± 0.03
25	D	1.46 ± 0.33	1.10 ± 0.03	4.75 ± 0.36	0.93 ± 0.01

ND - not detectable
D - detectable

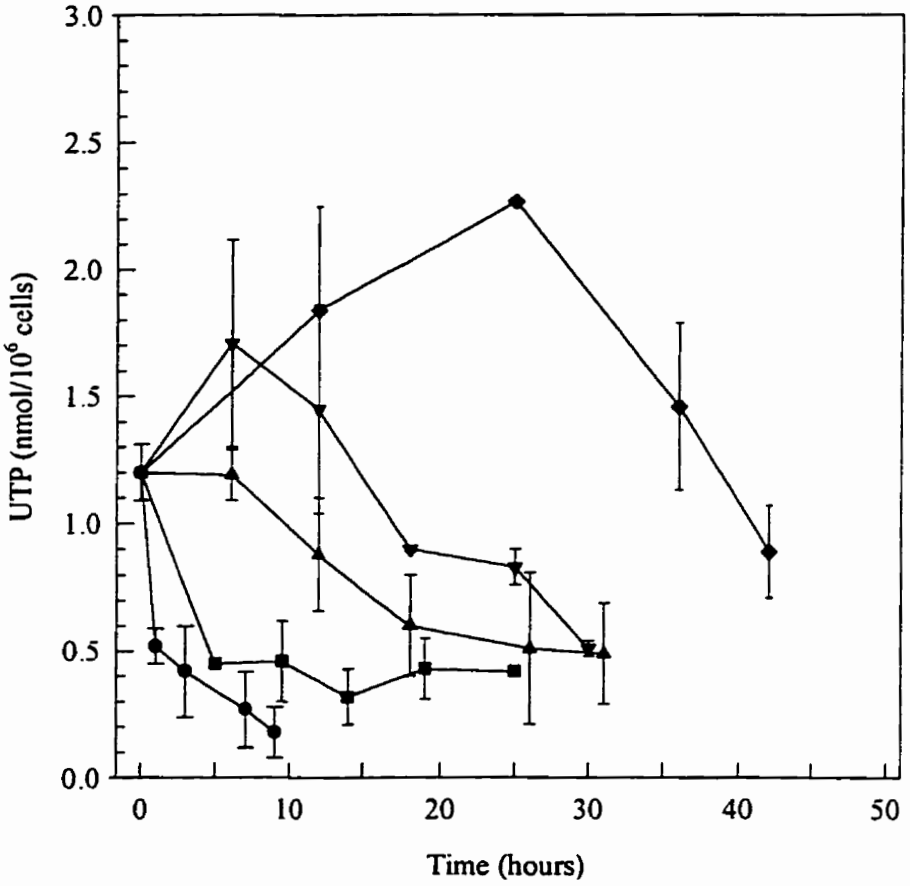

Figure 8.6 The effect of initial glucose concentration on CC9C10 intracellular UTP levels. Hybridomas were inoculated into T-flasks (25 cm^2) containing 10 ml NB-SFM (6 mM glutamine) containing varying initial glucose concentrations: 0 mM, (●); 1 mM, (■); 5 mM, (▲); 10 mM, (▼); 25 mM, (◆). Values are the mean from two independent cultures inoculated from different cell stocks.

Profiles of GTP and ATP pools during the growth and death of CC9C10 hybridomas were similar to UTP profiles (Fig.8.7 and Fig.8.8). Cultures grown in NB-SFM containing 0 and 1 mM glucose exhibited significant drops in the purine triphosphates after 5 hours of incubation. GTP levels decreased to less than 0.29 nmol/10^6 cells from an original value of 0.75 nmol/10^6 cells (61 % decrease). ATP levels dropped to 1.0 nmol/10^6 cells or lower from an original value of 3.4 nmol/10^6 cells (70 % decrease). In cultures grown in 5 and 10 mM glucose, purine triphosphate levels started to decline after 6 and 18 hours respectively. Cultures grown in 25 mM glucose did not exhibit similar decreases in the ATP and GTP intracellular concentrations. Comparisons of ATP and GTP values at the first decrease in viability time point are shown in Table 8.3. Except for the cells grown in an initial concentration of 25 mM glucose, all cultures had GTP values of 0.39 nmol/10^6 cells or lower and ATP values of 1.29 nmol/10^6 cells or lower when viability began to decline.

An analysis of nucleotide ratios shows that the cultures in which glucose was depleted had significantly reduced energy charge levels (Fig 8.9). All energy charge values were less than 0.34 at the time of a decrease in viability in cultures inoculated into 0 - 10 mM glucose. In cultures grown in 25 mM glucose, the energy charge levels remained high prior to and after a decrease in viability.

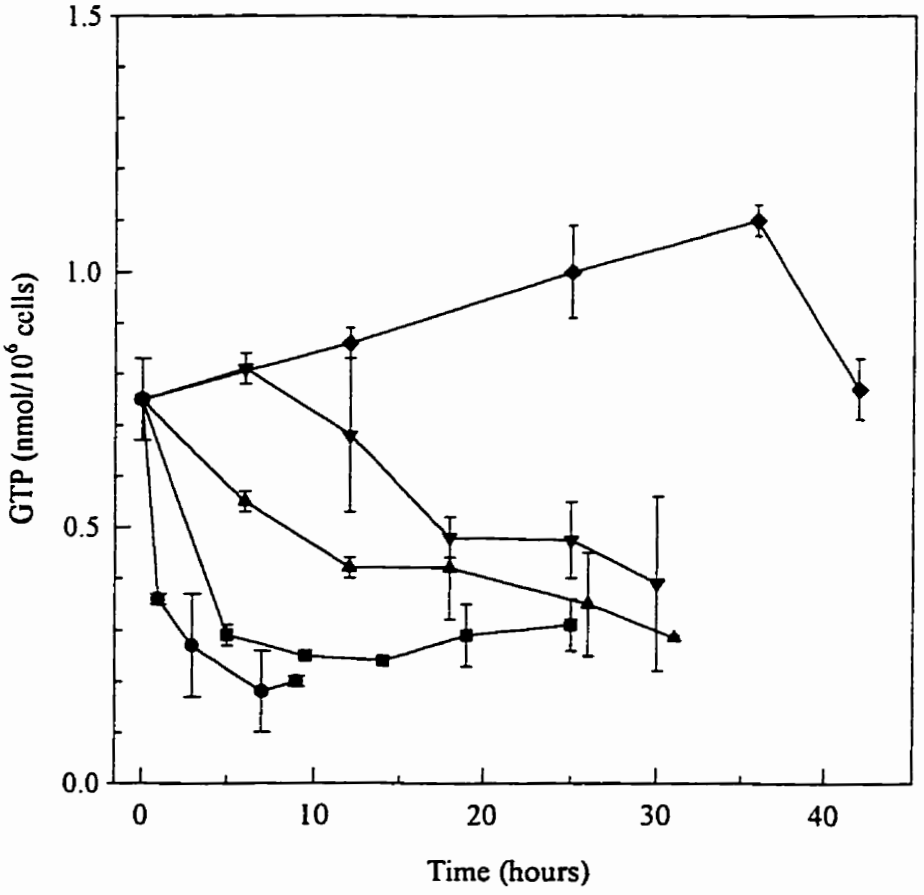

Figure 8.7 The effect of initial glucose concentration on CC9C10 intracellular GTP levels. Hybridomas were inoculated into T-flasks (25 cm^2) containing 10 ml NB-SFM (6 mM glutamine) containing varying initial glucose concentrations: 0 mM, (●); 1 mM, (■); 5 mM, (▲); 10 mM, (▼); 25 mM, (◆). Values are the mean from two independent cultures inoculated from different cell stocks.

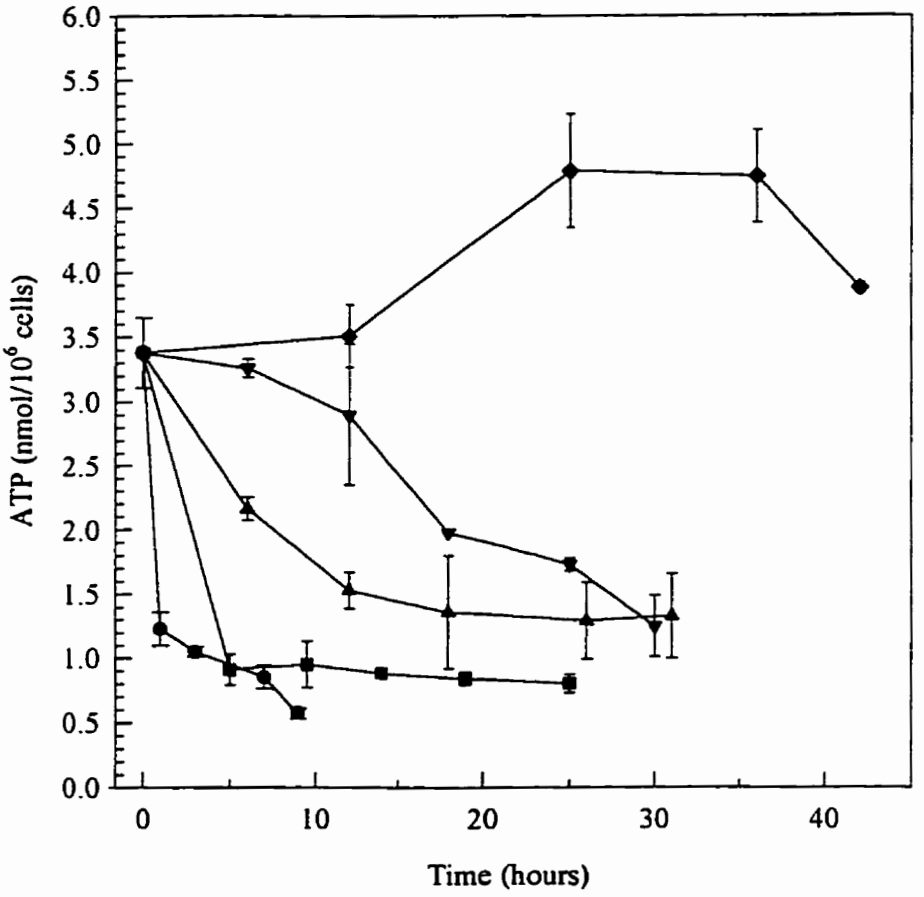

Figure 8.8 The effect of initial glucose concentration on CC9C10 intracellular ATP levels. Hybridomas were inoculated into T-flasks (25 cm^2) containing 10 ml NB-SFM (6 mM glutamine) containing varying initial glucose concentrations: 0 mM, (●); 1 mM, (■); 5 mM, (▲); 10 mM, (▼); 25 mM, (◆). Values are the mean from two independent cultures inoculated from different cell stocks.

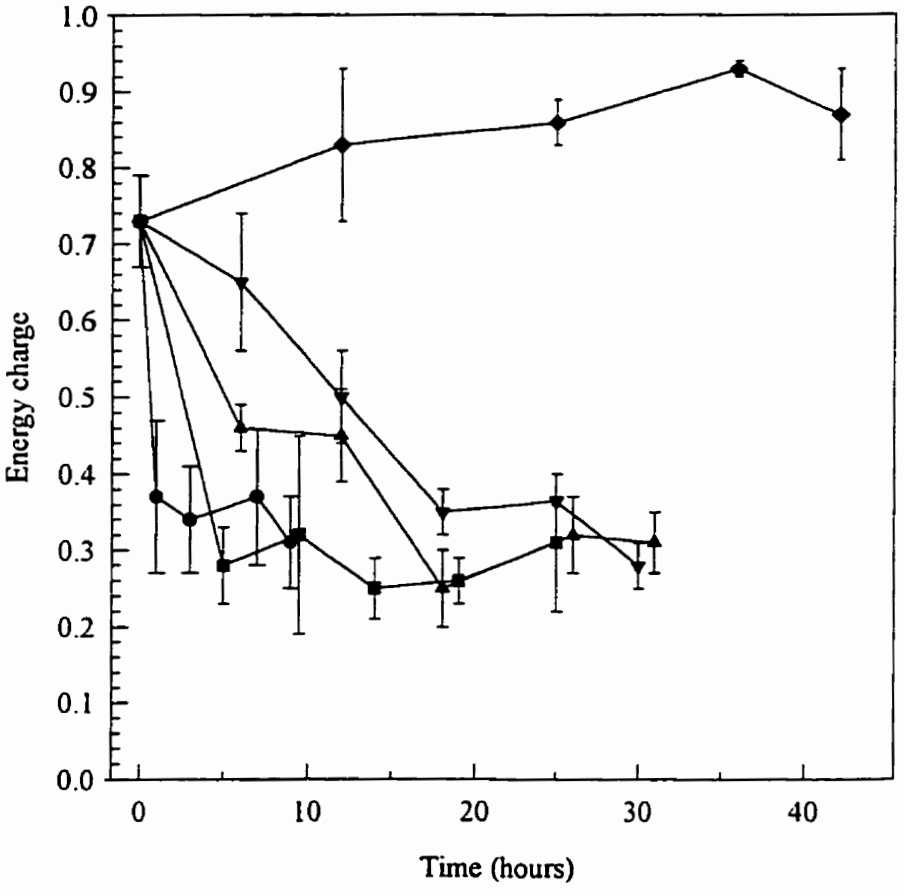

Figure 8.9 The effect of initial glucose concentration on CC9C10 intracellular energy charge. Hybridomas were inoculated into T-flasks (25 cm^2) containing 10 ml NB-SFM (6 mM glutamine) containing varying initial glucose concentrations: 0 mM, (●); 1 mM, (■); 5 mM, (▲); 10 mM, (▼); 25 mM, (◆). Values are the mean from two independent cultures inoculated from different cell stocks.

8.3.3 Determination of the method of cell death in normal batch culture

It was found in previous studies that in batch cultures, UTP and CTP pools decrease prior to a decline in cell culture viability. To better understand the role of these nucleotide changes in this context it is necessary to determine the method of cell death. The aim of this experiment was therefore to measure the fraction of cells that die by apoptosis or necrosis during the early stages of cell culture death. Experimental methods were the same as in section 8.3.1 with the following modification: exponentially growing cells were inoculated into replicate flasks containing NB-SFM (25 mM glucose, 6 mM glutamine) at an inoculation density of 1.2×10^5 cells/ml. The fraction of viable, apoptotic and necrotic cells were determined by fluorescent microscopy (section 2.12).

8.3.3.1 Relative contribution of apoptosis and necrosis to cell death in CC9C10 batch cultures

The evolution of cell death in normal batch culture is shown in Fig.8.10. Cells grew exponentially for the first 72 hours at a rate of 0.031 ± 0.002 h^{-1} and reached maximum cell density of $1.21 \bullet 0.15 \times 10^6$ cells/ml. Initial viability of the cell culture was greater than 90 % as determined by fluorescent microscopy. As the culture approached 72 hours of incubation, the number of apoptotic cells began to increase. No significant changes in necrotic cell numbers were observed in the early stages of cell culture death. At the 120 hour time point, 24 % of all cells were apoptotic thus representing 94 % of total dead cells. Apoptotic cells can be subdivided into two distinct groups based on membrane integrity (Fig.8.11). Apoptotic cells with intact membranes (Apm^+) or with permeable membranes (Apm^-) were both present at time of inoculation and represented 1.9 % and 3.0 % of the cell population respectively. In the first 50 hours of incubation, both levels of apoptotic cell types remained relatively constant. After 50 hours, the increase in Apm^- was faster than Apm^+. This resulted in Apm^- making up over 75 % of the apoptotic cell population at 120 hour time point.

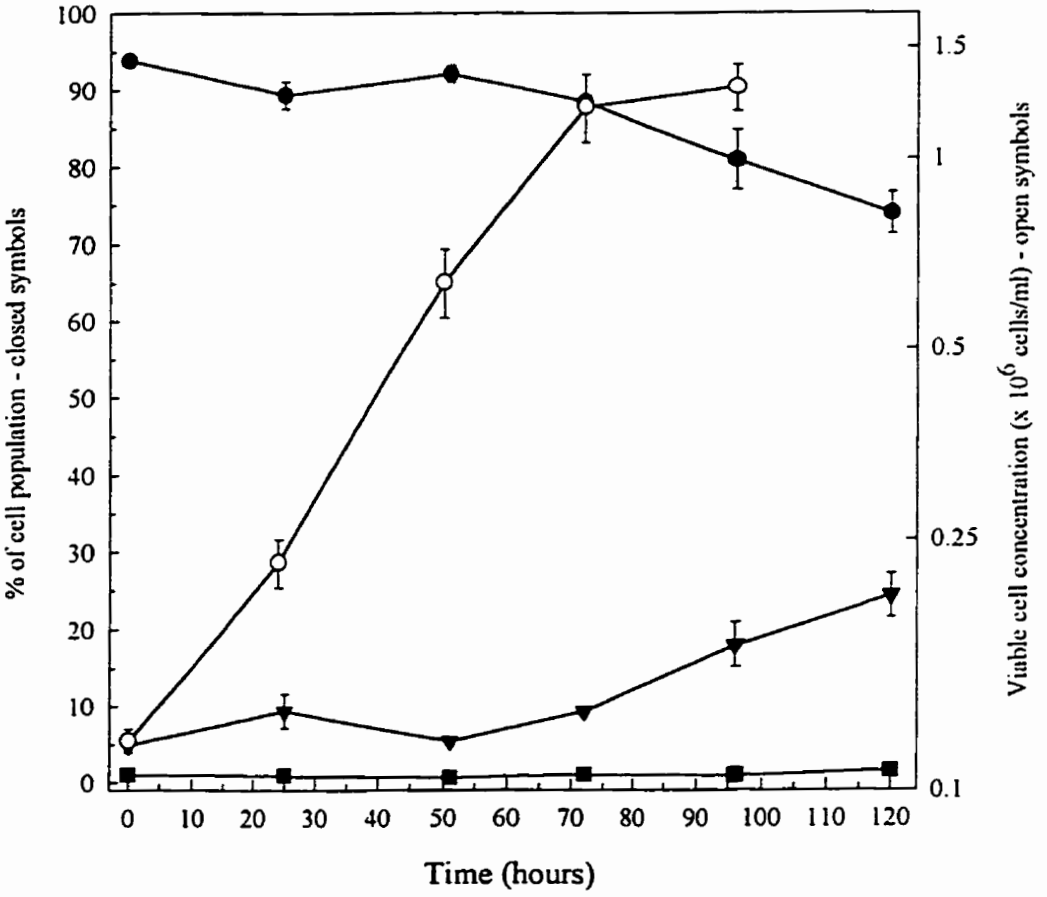

Figure 8.10 The evolution of cell death in CC9C10 normal batch culture. Hybridomas were inoculated into T-flasks (25 cm^2) containing 10 ml NB-SFM (25 mM glucose, 6 mM glutamine) at 1.2 x 10^5 cells/ml. The viable cell density (O) was determined with the use of a hemocytometer (n=4). The fraction of viable (●), apoptotic (▼), and necrotic (■) cells were determined by fluorescent microscopy. Values are the mean from two independent cultures inoculated from different cell stocks.

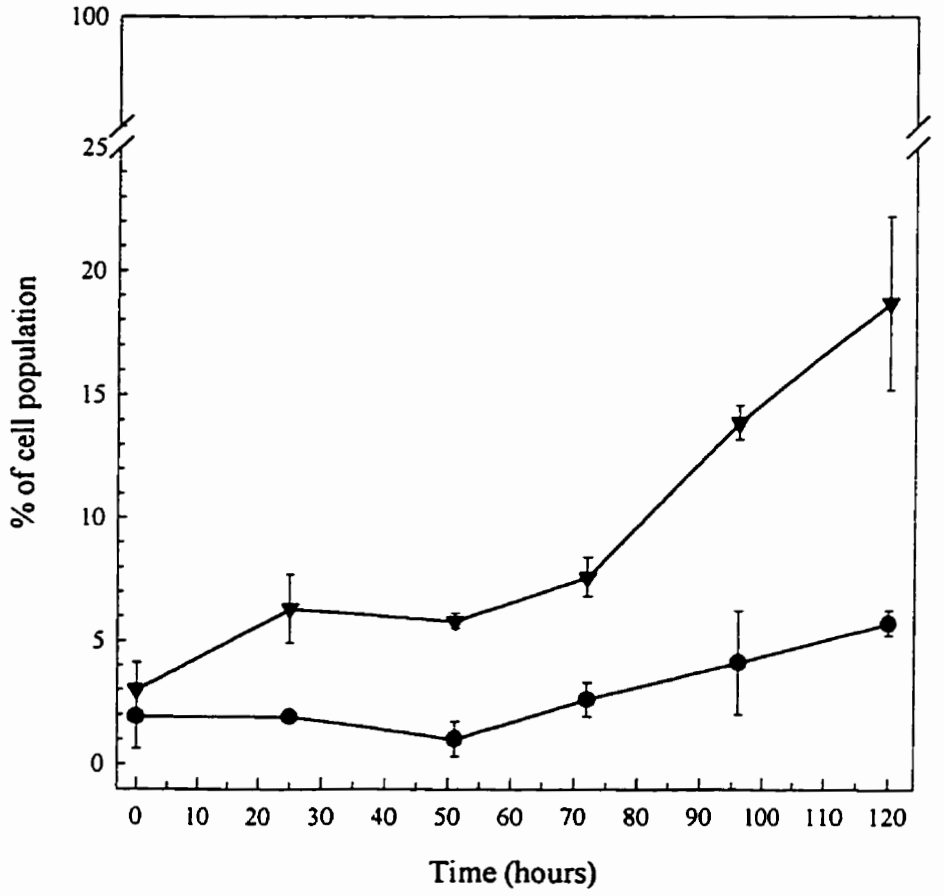

Figure 8.11 The distribution of apoptotic cell types in CC9C10 normal batch culture. Hybridomas were inoculated into T-flasks (25 cm^2) containing 10 ml NB-SFM (25 mM glucose, 6 mM glutamine) at 1.2 x 10^5 cells/ml. The fraction of apoptotic cells with intact membranes, Apm^+, (●) and permeable membranes, Apm^-, (▼) were determined by fluorescent microscopy. Values are the mean from two independent cultures inoculated from different cell stocks.

8.3.4 Determination of the method of cell death in glutamine-limited cultures

Previous analysis of batch cultures (section 8.3.1) has shown that the beginning of cell culture death coincides with a significant decrease in glutamine levels. As cell death progressed, glutamine was totally depleted. Further studies (section 8.3.3) revealed that the major cause of cell death in batch culture was apoptosis. The following experiment therefore investigates whether glutamine limitation can induce apoptosis. Experimental methods were the same as in section 8.3.3 with the following modification: exponentially growing cells were inoculated into replicate flasks containing NB-SFM (25 mM glucose, 0.5 mM glutamine) at an inoculation density of 5×10^5 cells/ml.

8.3.4.1 Relative contribution of apoptosis and necrosis to cell death in glutamine-limited CC9C10 cultures

The evolution of cell death in glutamine-limited cultures is shown in Fig.8.12. Cells grew to a maximum cell density of 6.6×10^5 cells/ml after 15 hours of incubation and remained at that level for another 10 hours before a significant decline was observed. Culture viability was greater than 90 % for the first 10 hours of incubation. A decline in viability at 20 hours coincided with a total depletion of glutamine and an increase in the apoptotic cell population. After 48 hours of incubation 49.7 % of the cell population was apoptotic, 45.6 % viable and 4.6 % necrotic. Apoptosis accounted for 91 % of total dead cells.

Analysis of the apoptotic cell distribution indicates an initial increase in the Apm^- cells after 20 hours of incubation and an apparent plateau at approximately 10 % (Fig.8.13). The fraction of Apm^- cells rapidly increases in comparison to Apm^+ cells after 20 hours of incubation..

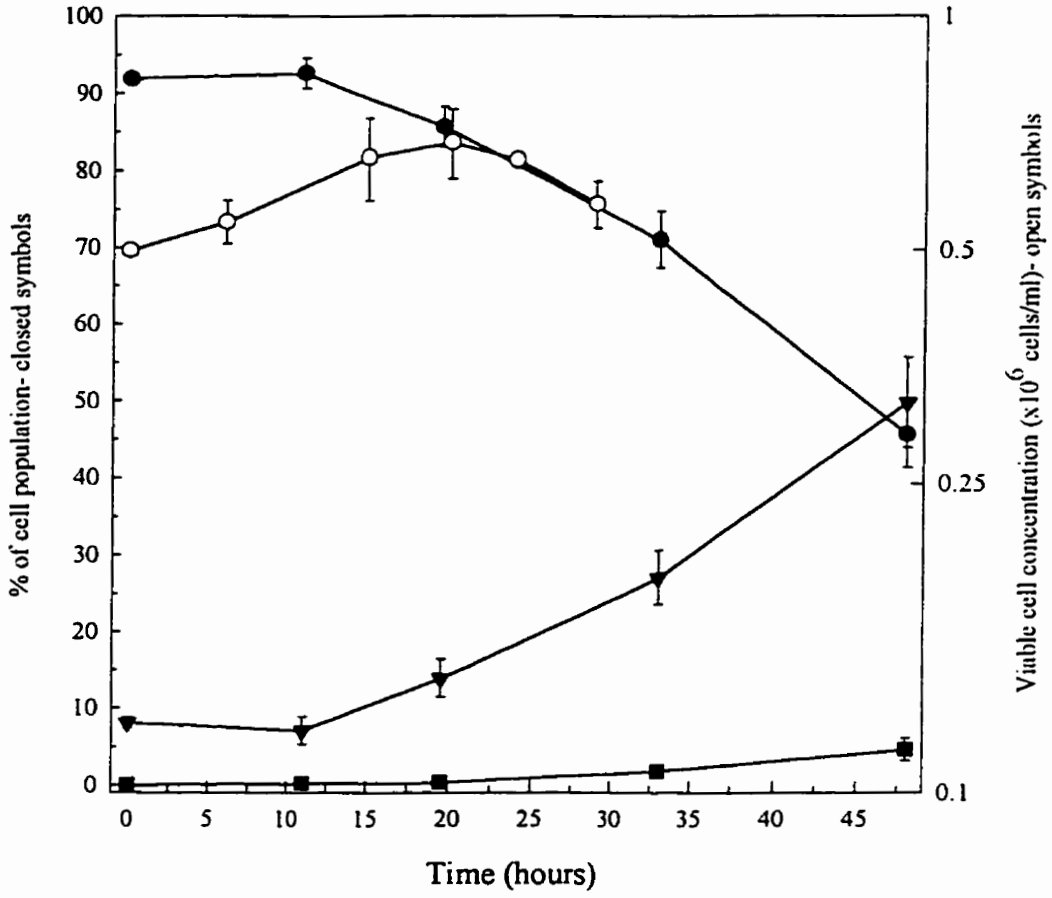

Figure 8.12 The evolution of cell death in a glutamine-limited CC9C10 culture. Hybridomas were inoculated into T-flasks (25 cm^2) containing 10 ml NB-SFM (25 mM glucose, 0.5 mM glutamine) at 5 x 10^5 cells/ml. The viable cell density (O) was determined with the use of a hemocytometer. The fraction of viable (●), apoptotic (▼), and necrotic (■) cells were determined by fluorescent microscopy. All values are the mean from two independent cultures inoculated from different cell stocks.

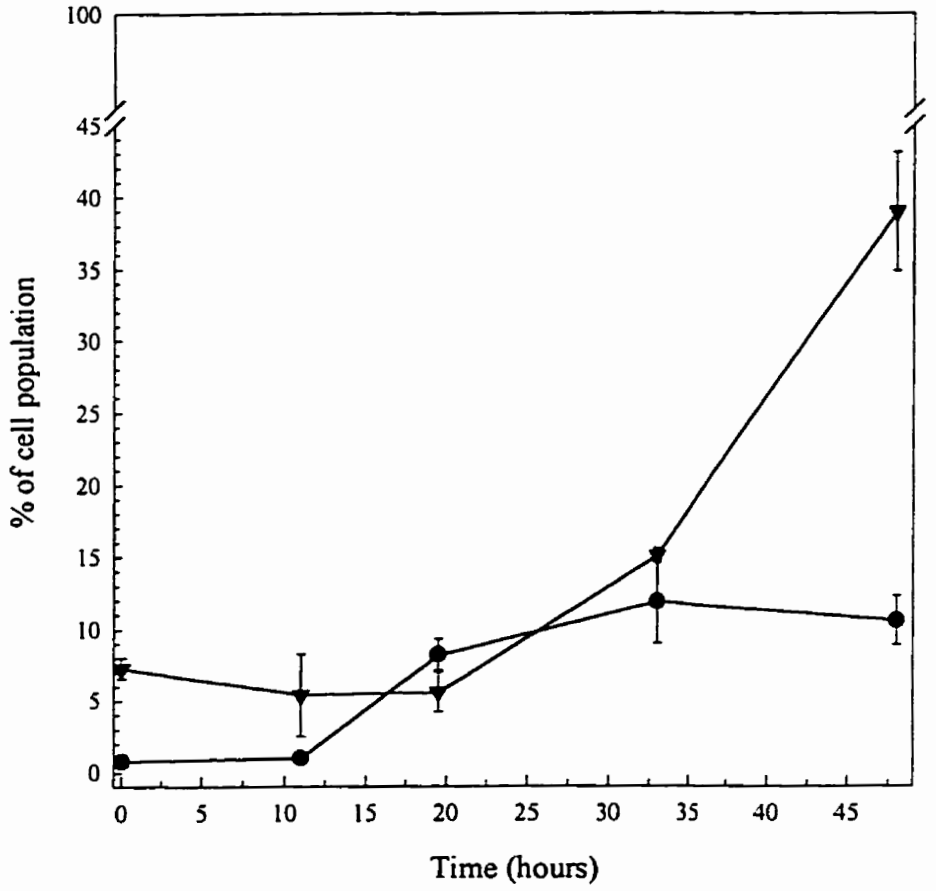

Figure 8.13 The distribution of apoptotic cell types in a glutamine-limited CC9C10 culture. Hybridomas were inoculated into T-flasks (25 cm^2) containing 10 ml NB-SFM (25 mM glucose, 0.5 mM glutamine) at 5 x 10^5 cells/ml. The fraction of apoptotic cells with intact membranes, Apm^+, (●) and permeable membranes, Apm^-, (▼) were determined by fluorescent microscopy. Values are the mean from two independent cultures inoculated from different cell stocks.

8.3.5 Determination of the method of cell death in glucose-limited cultures

Previous studies had shown that glucose limitation caused a severe drop in nucleotide triphosphate pools and a rapid induction of cell death. In order to assess the role of nucleotides in the decline of culture viability, the mode of cell death was evaluated. Experimental methods were the same as in section 8.3.3 with the following modification: exponentially growing cells were inoculated into replicate flasks containing NB-SFM (0 mM glucose, 6 mM glutamine) at an inoculation density of 5×10^5 cells/ml.

8.3.5.1 Relative contribution of apoptosis and necrosis to cell death in glucose-depleted CC9C10 cultures

The evolution of cell death in glucose-deprived cultures is shown in Fig.8.14. Cell density remained at 5×10^5 cells/ml for 10 hours before a decline was observed. Viability which was greater than 90 % initially remained at this level until a significant decrease to 83 % at 10 hours. The decrease in viability was due to a concomitant increase in the number of apoptotic cells. After 19 hours of incubation, 36 % of the cell population was apoptotic, 57 % viable and 6 % necrotic. Apoptotic cells made up more than 85 % of total dead cells.

Analysis of the apoptotic cell distribution shows similar levels of Apm^+ and Apm^- cells (2 - 3 %) during the first 6 hours of incubation (Fig. 8.15). At 10 hours there is a significant increase in Apm^+ cells compared to the Apm^- cells which remained at a constant level. A further incubation resulted in a rapid rise in the Apm^- cell fraction and leveling off of the Apm^+ cell fraction at 12 - 14 %.

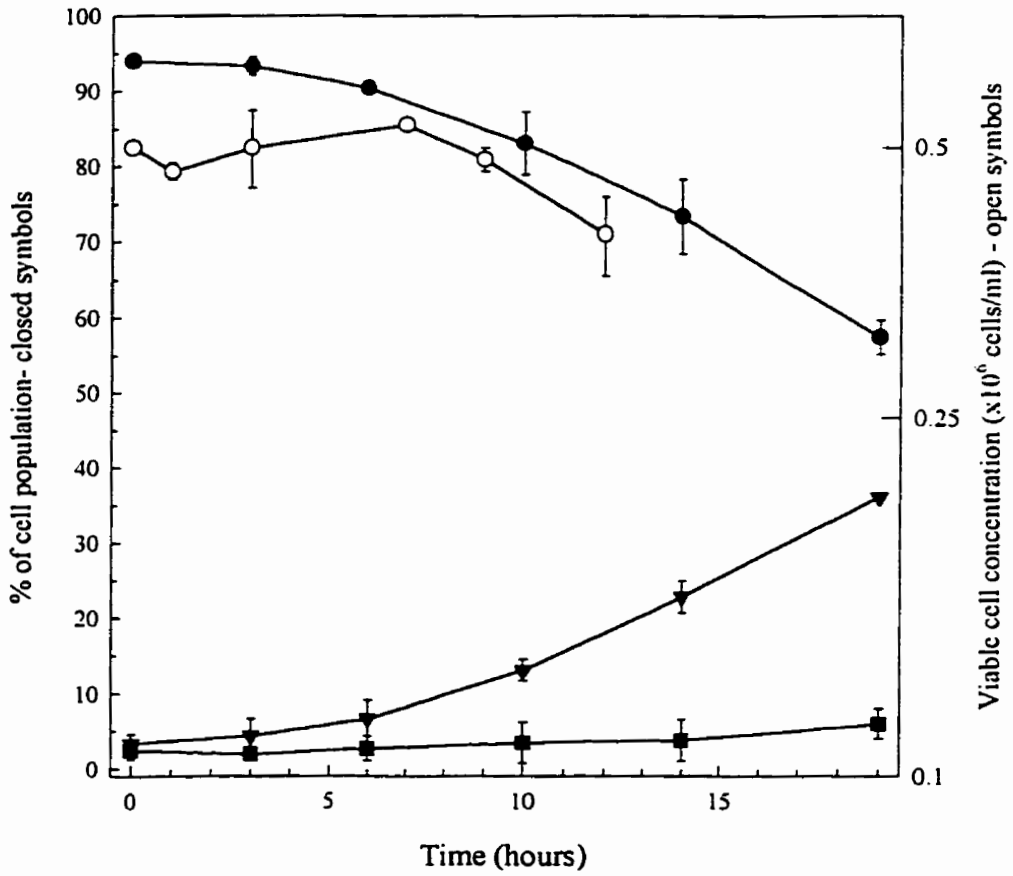

Figure 8.14 The evolution of cell death in a glucose-depleted CC9C10 culture. Hybridomas were inoculated into T-flasks (25 cm^2) containing 10 ml NB-SFM (0 mM glucose, 6 mM glutamine) at 5 x 10^5 cells/ml. The viable cell density (O) was determined with the use of a hemocytometer. The fraction of viable (●), apoptotic (▼), and necrotic (■) cells were determined by fluorescent microscopy. All values are the mean from two independent cultures inoculated from different cell stocks.

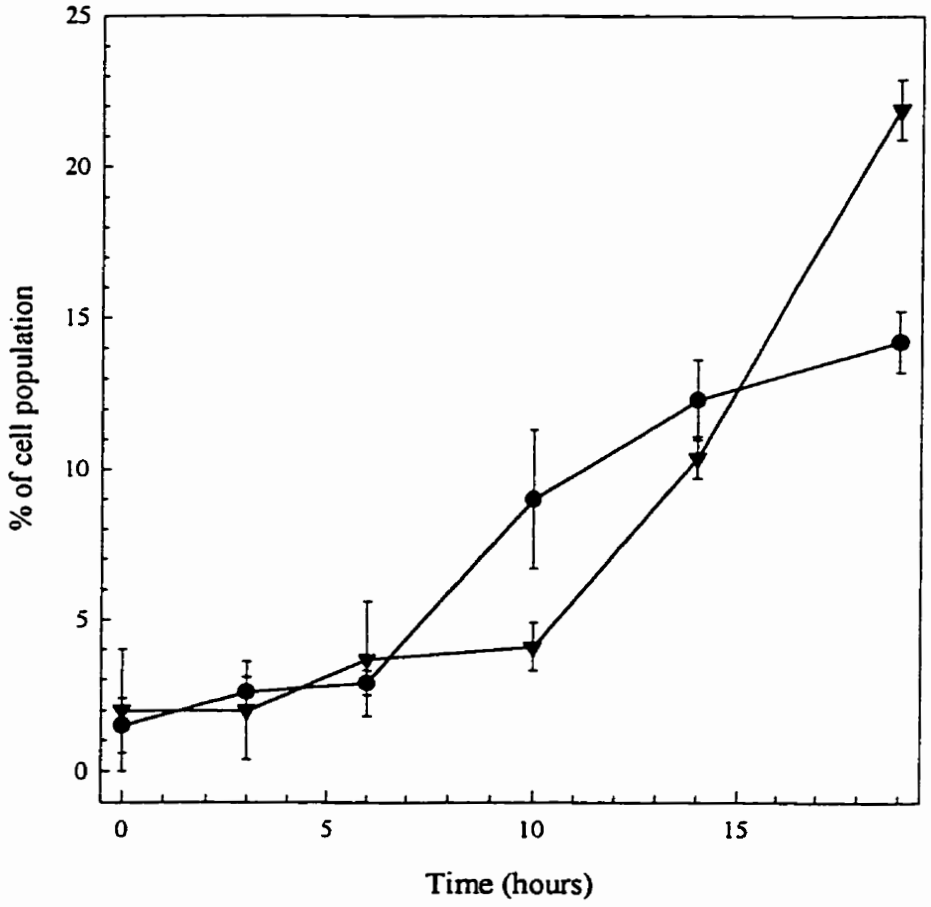

Figure 8.15 The distribution of apoptotic cell types in a glucose-depleted CC9C10 culture. Hybridomas were inoculated into T-flasks (25 cm^2) containing 10 ml NB-SFM (0 mM glucose, 6 mM glutamine) at 5 x 10^5 cells/ml. The fraction of apoptotic cells with intact membranes, Apm^+, (●) and permeable membranes, Apm^-, (▼) were determined by fluorescent microscopy. Values are the mean from two independent cultures inoculated from different cell stocks.

8.3.6 Rescuing a glucose-limited culture that has begun apoptosis

Apoptosis can be induced in CC9C10 hybridoma cultures by glucose deprivation (section 8.3.5). In an attempt to stop apoptosis induction, glucose was fed at different time intervals. Glucose feeding times were varied in order to determine if cultures can be rescued after a prolonged exposure to an apoptotic inducer. Energy charge was used as a nucleotide parameter because of its correlation to glucose-limited induced cell death. Experimental methods were the same as in section 8.3.3 with the following modification: exponentially growing cells were inoculated into replicate flasks containing NB-SFM (0 mM glucose, 6 mM glutamine) at an inoculation density of 5×10^5 cells/ml. Control cultures were not supplemented with glucose. Other cultures were fed with 25 mM glucose at 5, 10, 15 or 22 hours.

8.3.6.1 The effects of glucose feeding on viable cell density, viability and energy charge

Glucose deprivation caused a significant decrease in viable cell number and viability after 15 hours of incubation (Fig.8.16 and 8.17). After 30 hours, viability was down to 37 % from an initial value of 94 %. Feeding with glucose at 5 hours however prevented any significant decline in viable cell number and viability. In fact, the cell culture doubled in cell density and maintained a high viability after 30 hours. Feeding with glucose at 10 hours did not prevent a 22 % and 10% decrease in culture density and viability respectively at the 15 hour time point. After 15 hours, cell numbers did not decline any further and growth was reinitiated in the later stages of the culture (Fig.8.16). Cultures could be similarly rescued with glucose feeding at 15 or 22 hours. As was the case at 10 hours, the feeding at 15 or 22 hours did not immediately prevent a significant decrease in viable cell number and viability (Fig.8.16 and 8.17). Cultures did manage however to recuperate as shown by the increase in cell density and viability after 50 hours of incubation. Analysis of adenylate nucleotides during the incubation of cultures shows that after only 1 hour, the energy charge decreases significantly to 0.50 from an initial value of

0.84 (Fig.8.18). Energy charge values remained below 0.50 until glucose was added to the medium. Glucose supplementation at 5, 10, 15 and 22 hours restored the energy charge to 0.86 or higher.

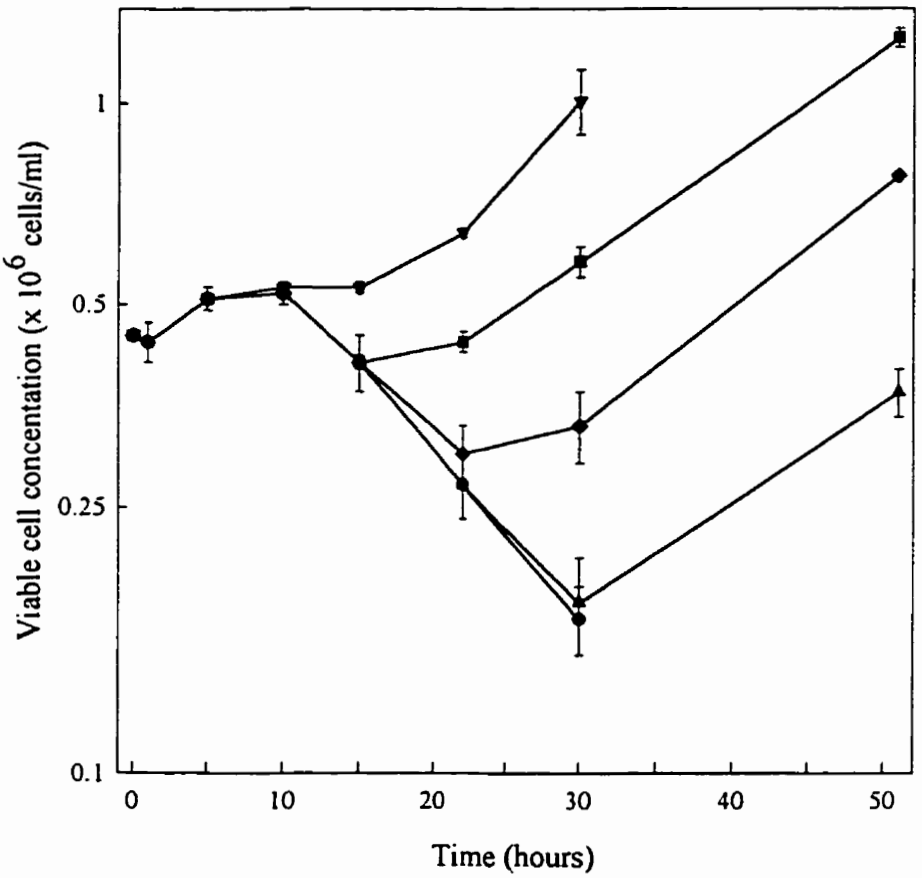

Figure 8.16 The effect of glucose feeding on the viable cell density of glucose-depleted CC9C10 cultures. Hybridomas were inoculated into T-flasks (25 cm^2) containing 10 ml NB-SFM (0 mM glucose, 6 mM glutamine). Control cultures were not supplemented with glucose (●). Other cultures were fed with 25 mM glucose at 5 hours (▼); 10 hours (■); 15 hours (◆) and 22 hours (▲). Values are the mean from two independent cultures inoculated from different cell stocks.

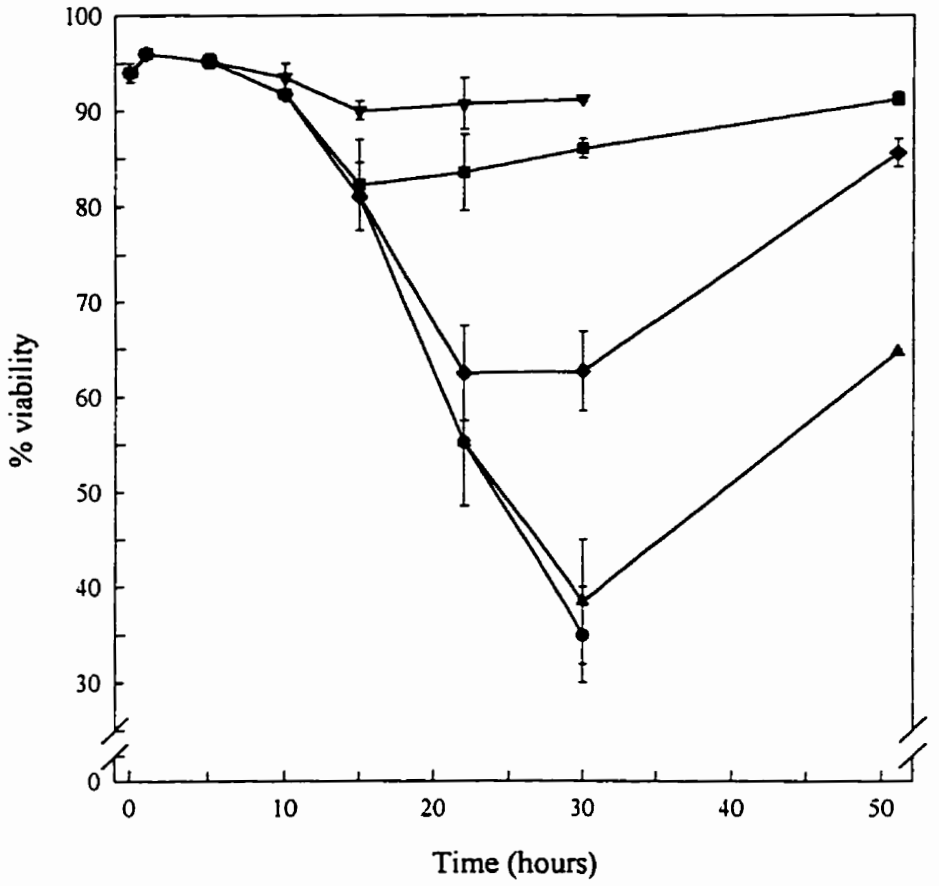

Figure 8.17 The effect of glucose feeding on the viability of glucose-depleted CC9C10 cultures. Hybridomas were inoculated into T-flasks (25 cm^2) containing 10 ml NB-SFM (0 mM glucose, 6 mM glutamine). Control cultures were not supplemented with glucose (●). Other cultures were fed with 25 mM glucose at 5 hours (▼); 10 hours (■); 15 hours (◆) and 22 hours (▲). Values are the mean from two independent cultures inoculated from different cell stocks.

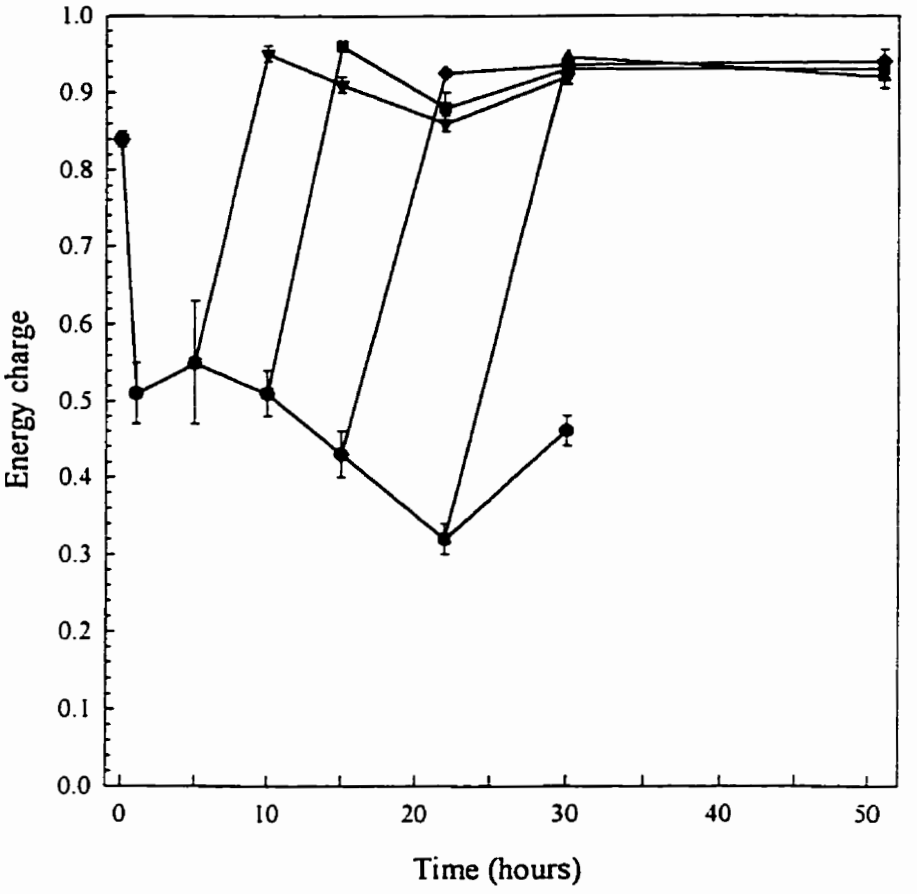

Figure 8.18 The effect of glucose feeding on the energy charge of glucose-depleted CC9C10 cultures. Hybridomas were inoculated into T-flasks (25 cm^2) containing 10 ml NB-SFM (0 mM glucose, 6 mM glutamine). Control cultures were not supplemented with glucose (●). Other cultures were fed with 25 mM glucose at 5 hours (▼); 10 hours (■); 15 hours (◆) and 22 hours (▲). Values are the mean from two independent cultures inoculated from different cell stocks.

8.4 Discussion

To assess the relationship between nucleotide pools and culture viability, hybridomas were grown in conditions that caused variable death profiles. Two approaches were used: (a) hybridomas were inoculated at different cell densities and (b) hybridomas were inoculated in varying concentrations of glucose. The inoculation of cultures at high cell densities (5 x 10^5 cells/ml) caused a 23 % reduction in maximum growth rate (μ_{max}) compared to cultures inoculated at lower densities (1.25 - 2.5 x 10^5 cells/ml). Reasons for a decreased μ_{max} are not known but it is probable that in high density cultures a reduction in nutrient availability is quicker thus impeding cell growth. Other studies have found that an increase in cell density is concomitant with a decrease in the oxygen consumption rate (Wohlpart *et al.*, 1990). The reduction in oxygen consumption has been linked to lower growth rates in bioreactors (Miller *et al.*, 1988b).

Despite differences in growth rate, all cultures attained a similar maximum cell density (N_{max}) albeit at different times indicating perhaps a common limitation. This same limitation probably caused the viability to decrease within a 7 hour time frame of reaching N_{max}. Analysis of the two major nutrients, glucose and glutamine, indicates that neither were completely depleted prior to a decrease in viability. Glutamine however may have been sufficiently low (0.3 - 0.4 mM) in the cultures to induce growth arrest and death (Petronini *et al.*, 1996). The possibility that other nutrient limitations or inhibitors may have caused decreases in viability was not investigated. One interesting study however proposes that a small molecular weight inhibitor (< 3000 Da) in the supernatant the concentration of which is dependent on cell number may cause cell death in batch cultures (Lee *et al.*, 1995).

Cell death in batch culture was mainly due to apoptosis as opposed to necrosis as determined by the morphological appearance of cells under fluorescent microscopy. This is consistent with other studies involving hybridomas and lymphoid cell lines.(Vomastek and Franek, 1993; Mercille and Massie, 1994a; Singh *et al.*, 1996). Apoptotic hybridomas exhibited the typical collapse of chromatin into dense spheres while necrotic and viable cells did not display any significant condensation of the DNA. Two types of apoptotic

cells emerged from this study: apoptotic cells with intact membranes (Apm^+) and apoptotic cells with damaged membranes (Apm^-). The presence of Apm^+ cells indicates that apoptosis occurs prior to a loss in membrane integrity. During the death phase, the fraction of Apm^- cells increases more rapidly than the fraction of Apm^+ cells suggesting that once the apoptotic pathway is induced the integrity of the membrane is not maintained for a prolonged period of time. Destruction of the membrane after apoptosis induction is referred to as secondary necrosis (Kerr *et al.*, 1991; Mercille and Massie, 1994a).

Glutamine limitation was found to cause apoptosis in CC9C10 hybridoma cultures and this is consistent with other hybridoma and lymphoid cell lines (Mercille and Massie, 1994a; Petronini *et al.*, 1996). The appearance of apoptotic cells however did not occur until after a total glutamine depletion. This is in contrast to batch cultures where apoptosis was induced in the presence of low levels of glutamine (0.3 - 0.4 mM) suggesting that limitation of the amino acid was not the initial cause of cell death in these cultures.

The rate of culture death was also determined by inoculating hybridomas in different glucose concentrations. It was found that the initial glucose concentration was directly proportional to cell yield, growth rate and the time of the onset of cell culture death. Total glucose depletion was found to be the cause of cell death in cultures inoculated into 10 mM glucose or less. The onset of death for glucose-limited cultures was also within 7 hours of reaching maximum cell density, an observation made previously with batch cultures in complete medium. Analysis of the death phase of glucose-limited cultures indicates that apoptosis is the prevalent mode of cell death accounting for 85 % of dead cells. Other studies have shown that apoptosis is the major mode of cell death in glucose-starved hybridomas but only after a brief period of necrosis (Mercille and Massie, 1994a). This was not found for the CC9C10 cultures studied here. In contrast, leukemia/lymphoma cell lines die only by necrosis when deprived of glucose indicating that the susceptibility to apoptotic induction is cell line specific (Petronini *et al.*, 1996). Differences in apoptotic susceptibility has been observed by Singh *et al.* (1994). This research group demonstrated that Chinese hamster ovary (CHO) cells and insect cells did not die by apoptosis when subjected to the same conditions that cause apoptosis in hybridoma cell lines.

The relationship between cell death and the metabolic state of the hybridoma was determined by monitoring intracellular nucleotide pools of batch and glucose-limited cultures. Fluctuations in nucleotide pool size have been shown in other studies to affect enzyme activities and to correlate with the cell cycle and growth behavior (Rapaport *et al.*, 1979; Ryll and Wagner, 1992; Sharma *et al.*, 1993). It has been postulated in this study that cell death may also influence or be caused by nucleotide pool imbalances.

Of the four nucleotide triphosphates (NTPs), CTP is preferentially exhausted during the decline phase in both batch and glucose-limited cultures. One possible reason for this is that during normal growth the basal level of CTP in CC9C10 hybridoma cultures is lower than other NTPs (chapter 4). Depletion of CTP is due to the presence of intrinsically lower concentrations of the nucleotide. CTP has also been shown to be the least abundant of the NTPs in a variety of other mammalian cell lines (Jackson *et al.*, 1980; Smith *et al.*, 1992; Snyder *et al.*, 1994). This observation may be a reflection of the less important role of CTP as an energy source compared to other NTPs.

A decrease in CTP may be due to an attempt of the hybridoma cell to maintain an elevated ATP level for a longer period of time. Nucleoside diphosphokinase, an enzyme with a broad specificity, can transfer the high energy phosphate from CTP to ADP thus replenishing ATP pools (equation 8.1).

$$\text{CTP} + \text{ADP} \xleftrightarrow[\text{diphosphokinase}]{\text{nucleoside}} \text{CDP} + \text{ATP} \qquad \text{(equation 8.1)}$$

CTP may also be depleted due to the excessive formation of CDP-choline, a precursor to phospholipids, generated in times of stress to repair mammalian plasma membranes. This latter hypothesis however is probably not relevant to hybridoma cells which die by apoptosis, a mechanism in which membranes remain intact several hours after the cell dies.

It has been shown in other studies that a specific depletion of the CTP pool by metabolic inhibitors leads to cell death (Slingerland *et al.*, 1995; Viola *et al.*, 1995; Heinemann *et al.*, 1995). CTP depletion may cause cell death by two methods. The loss

of CTP in the cell may induce a shortage of RNA precursors therefore impairing RNA synthesis which ultimately leads to the inhibition of protein synthesis. Protein synthesis can be inhibited due to a lack of template (mRNA) and due to the breakdown of the synthesis machinery which is composed of rRNA containing ribosomes (Decker and Keppler, 1974). It has been proposed that inhibition of RNA and protein synthesis may be responsible for the inefficient translation of a putative short-lived apoptosis inhibitory protein (Kerr *et al.*, 1991). This mechanism however would not apply to all incidences of apoptosis as certain apoptotic inducers require RNA and protein synthesis (Orrenius, 1995).

A loss in CTP may also decrease the availability of CDP, a substrate of ribonucleotide reductase and may consequently deplete dCTP pools (Heinemann *et al.*, 1995). A dCTP shortage can lead to erroneous DNA strand formation and DNA strand breaks by misincorporation in mammalian cells (Meuth, 1989). It is likely that a depletion in any one of the four NTPs all of which are essential for nucleic acid synthesis would have a major impact on cell survival. In fact the specific depletion of UTP has been associated to RNA and DNA synthesis impairment and cell death (Decker and Keppler, 1974).

A decrease in viability in batch and glucose-limited cultures was concomitant with a reduction in the intracellular UTP pool. As was the case with CTP, UTP reduction may be caused by the transfer of the high energy phosphate to ADP by nucleoside diphosphokinase. Studies have shown that in cells subjected to energy drains due to mitochondrial inhibitors, CTP and UTP are the first NTPs to be depleted (Snyder *et al.*, 1994). This observation was correlated to the relative abundance of the NTPs in the cell which was determined to be ATP, GTP > UTP > CTP. This order of importance of NTPs however is not shared in CC9C10 hybridomas where the relative abundance of nucleotides is distributed as follows: ATP > UTP > GTP > CTP. The significant decrease in UTP may also be due to the action of CTP synthetase (Heinemann *et al.*, 1995). CTP synthetase is an enzyme of the *de novo* synthesis pathway of CTP and catalyzes an irreversible reaction requiring ATP (equation 8.2). A decrease in CTP levels would cause a concomitant decrease in UTP.

$$\text{UTP} + \text{glutamine} + \text{ATP} \xrightarrow[\text{CTP synthetase}]{} \text{CTP} + \text{glutamate} + \text{ADP} + \text{Pi} \qquad \text{(equation 8.2)}$$

No significant decrease in ATP and GTP pools were observed during the onset of death in CC9C10 hybridoma batch cultures. This indicates that cell death by apoptosis can ensue in the absence of ATP or GTP depletion. Smith *et al.* (1992) have also found that cells die with little effect on ATP levels. This is however contrary to the view that cells stay alive as long as certain ATP levels are maintained (Richter *et al*, 1996). Variable results with respect to ATP levels and apoptosis may be due to the method of apoptotic induction.

In glucose limited cultures, all four NTPs were significantly reduced prior to decreases in culture viability. The reduction of ATP and the related energy charge is a reflection of the cause of cell death (i.e. glucose starvation). CC9C10 hybridomas synthesize as much as 59 % of their ATP through glycolysis (Petch and Butler, 1994). An impairment of glycolysis through glucose starvation was therefore responsible for a reduction in the intracellular ATP concentration. A decrease in ATP concentration also contributed to the concomitant decrease in other NTPs as ATP is required for GTP, UTP and CTP synthesis through phosphate transfers and by the *de novo* synthesis pathway (Swain *et al.*, 1982). Although the intracellular ATP levels was reduced in glucose-limited cultures it was not totally depleted. This finding is consistent with studies showing that apoptosis is an energy dependent process (Richter *et al.*, 1996). Apoptosis has a high energy demand for the activity of hydrolytic enzymes and chromatin condensation.

The profile of cell death in hybridoma cultures indicates that the observed decrease in nucleotide concentration in itself is not sufficient to induce apoptosis, otherwise cell death would be induced in all cells at the same rate. One explanation for this is that nucleotide measurements are an average of the whole population of cells. One fraction of the cell culture could have normal nucleotide levels and not be susceptible to apoptosis. Another fraction of the culture could have severely depleted nucleotide levels which would lead to apoptosis. The problem with this theory is that all cells are exposed to the same environment and they would probably respond metabolically in the same manner. A more plausible explanation is that the susceptibility of a cell is dependent on the cell cycle.

Hybridoma cell populations are normally heterogeneous and distributed in various phases of the cell cycle. This distribution would account for only a fraction of the culture dying at any given time. Other studies have shown that cells in all stages of the cell cycle can become apoptotic, but some phases are more resistant than others. Al-Rubeai *et al.* (1995) found that S and G_2 phase hybridoma cells are more sensitive to apoptosis in agitated cultures while there is evidence of preferential survival of G_1 cells. Cell cycle analysis of apoptosis induced in hybridoma cell lines by a topoisomerase I inhibitor however shows selective sensibility of G_1 cells (Cotter *et al*, 1992). One recent study has shown that the specific depletion of UTP or CTP by ribonucleotide inhibitors causes a p53 dependent G_0/G_1 arrest in human fibroblasts (Linke *et al.*,1996). It has been proposed by this group that p53, a gene product linked to apoptosis induction, can serve as a metabolite sensor activated by the depletion of ribonucleotides or processes dependent on ribonucleotides. It is clear that the susceptibility of cells to apoptosis in the different cell cycles may be dependent on the mode of apoptotic induction.

To investigate whether apoptosis induction is reversible, hybridomas were grown in glucose-free medium and fed glucose at different time intervals. Energy charge values were used as a parameter to evaluate the global state of nucleotide levels in the cell culture. After 1 hour of incubation in the absence of glucose the energy charge rapidly declined to 0.5. Despite this low energy charge, cells remained viable for at least 5 hours. Similar findings were observed with Ehrlich ascites tumor cells and human embryonal fibroblasts which could remain at an energy charge level of 0.35 or less for several hours without any change in viability (Live and Kaminskas, 1975; Kristensen., 1989). Calderwood *et al.* (1985) however noticed an immediate decline in survivability when energy charge fell below 0.8 in CHO cells. Differences and similarities between these cell lines with respect to survivability and energy charge may be linked to the mode of cell death. CHO cells have been shown to die mainly by necrosis while Ehrlich ascites tumors and hybridomas die mainly by apoptosis (Singh *et al.*, 1994; Gabai *et al.*, 1995).

Apoptosis induction due to glucose starvation can be completely inhibited in hybridomas by feeding with glucose within 5 hours. This treatment restores energy charge values to > 0.86. Feeding glucose at 10 hours when no apparent change in viability had

occurred did not prevent a significant decline in cell number 5 hours later even though energy charge levels were restored. After 15 hours, decreases in viability ceased and cell growth was reinitiated indicating that the induction of apoptosis can be eventually prevented by replenishing nucleotide levels. Reasons for the initial decline in cell number may be explained by the method of determining viability. Detection of viability by the trypan blue exclusion method relies on membrane integrity. With this method a decline in viability is observed only after 15 hours of incubation in glucose-free medium. Previous studies using acridine orange and ethidium bromide however indicate that a significant increase in apoptotic cells with intact membranes occurs at the 10 hour time point. It can be concluded that a fraction of the cells that were viable as determined by trypan blue exclusion were actually in the early stages of apoptosis.

Low energy charge in itself is not sufficient to cause cell death as cultures can be partially rescued after 15 to 22 hours of exposure to these levels. As discussed previously, only a fraction of the cell population dies in response to glucose deprivation and low energy charge. This indicates that cells may require additional internal signals, perhaps related to the cell cycle, to complete the induction of apoptosis. Another reason for differences in survivability in the cell population may be related to the possible presence of heat shock proteins in certain cells. Other studies have shown ATP depletion stimulates the synthesis of hsp 68/70 in Ehrlich T-cells which allows tolerance to energy deprivation and apoptosis for a short period of time (Gabai *et al.*, 1995). It is not unreasonable to speculate that heat-shock protein synthesis may be more active during specific phases of the cell cycle thus conferring preferential survival to a fraction of the cell population in times of stress (i.e. low energy charge).

8.5 Conclusion

Hybridoma cells die mainly by apoptosis in batch and glucose-limited cultures. Cell death is preceded by the decrease in the intracellular concentration of CTP and UTP in batch cultures. In glucose-limited cultures the four NTPs (CTP, UTP, GTP, ATP) and energy charge decrease prior to the onset of cell culture death. Nucleotide levels may therefore act as mediators of apoptosis since their decline seems to be causal to the induction process. Intracellular CTP and UTP levels may be used as predictors of imminent cell culture death.

The decrease in nucleotide levels alone however is not sufficient to induce apoptosis. Only a fraction of the cell population dies at one time thus making it possible to rescue a culture that shows signs of decreases in viability. Apoptosis induction is a complex mechanism that relies on many cellular signals. This complexity causes cultures to gradually die instead of being totally annihilated in times of stress and allows for a possible recovery of the cell population.

CHAPTER 9

9.0 The relationship between nutrient levels and intracellular nucleotides

9.1 Introduction

The maintenance of intracellular nucleotide pools is dependent on the ability of cells to derive energy from available nutrients. Two major nutrients, glucose and glutamine are particularly important in hybridoma metabolism (Butler and Jenkins, 1989; Miller *et al.*, 1989a , 1989b). Both substrates provide energy and building blocks for biomass synthesis. Glucose which is normally present in culture medium at a concentration of 5 - 25 mM provides a majority of its energy through aerobic glycolysis (Fitzpatrick *et al.*, 1993; Petch and Butler, 1994). This energy yielding pathway, a characteristic of transformed cell lines, converts glucose to lactate even though oxygen is present (Medina and Nunez de Castro, 1990). Glucose also supplies energy via the tricarboxylic acid (TCA) cycle and the pentose phosphate pathway, the latter being an important supplier of nucleic acid precursors (Zielke *et al.*, 1976; Reitzer *et al.*, 1980).

Glutamine is also required as a precursor for nucleic acid synthesis and is normally supplied in culture medium at a concentration of 1 - 6 mM (Engstrom and Zetterberg, 1984). Glutamine provides energy via the TCA cycle by complete oxidation to CO_2 or partial oxidation to 3 or 4 carbon metabolites which include aspartate, lactate or alanine. This partial breakdown of glutamine has been termed glutaminolysis and is common to transformed cell lines (McKeehan, 1982; Lanks and Li, 1988).

Energy production measurements from glucose and glutamine are often limited to estimates of ATP synthesis based on end product analysis of substrates and oxygen consumption rates (Miller *et al.*, 1988; Fitzpatrick *et al.*, 1993; Petch and Butler, 1994; Meijer and van Dijken, 1995). These studies however do not take into account actual intracellular levels of ATP or other nucleotides in the cell which are subject to a balance between energy requiring processes, energy providing processes and *de novo* nucleotide synthesis. Understanding energy production and nucleotide pool maintenance in

hybridomas can form the basis for the development of control strategies such as nutrient feeding which would ensure sufficient energy is available for maintaining culture viability and high antibody production.

The purpose of the work reported here was to determine the intracellular nucleotide profiles of CC9C10 hybridomas during exposure to varying glucose and glutamine extracellular concentration. Nucleotide profile analysis provided information regarding the contribution of the two main substrates to actual energy levels. Specific oxygen uptake rates of hybridomas is also reported in relation to glucose, glutamine and nucleotide concentration. The level of cellular respiration serves as an indicator of the metabolic flux of substrates through oxidative pathways (Miller *et al.*, 1988b).

9.2 Results

9.2.1 Determination of the stability of intracellular nucleotide levels at different extracellular glucose and glutamine concentrations

In order to assess the effect of glucose and glutamine on nucleotide pools it was necessary to determine the optimal sampling time after exposure to the respective nutrients. The intracellular ATP concentration was used as a model for the stability of nucleotide levels because both glucose and glutamine are directly involved in its synthesis. Hybridoma cells from three day old cultures were collected by centrifugation at 190 g x 5 minutes, the supernatant was decanted and cells were washed once. Washing consisted of resuspending cells in the same type of medium to be used in the experiment followed by centrifugation and removal of the supernatant. Hybridomas were then resuspended at 5 x 10^5 cells/ml in 10 ml NB-SFM containing 0, 1, 5, 10 or 25 mM glucose and a constant glutamine concentration of 6 mM. Experiments were done in duplicate in 25 cm^2 T-flasks. Cultures were inoculated from the same cell stock.

As shown in the time course profile of CC9C10 hybridomas (Fig.9.1), the initial intracellular ATP concentration was 3.83 nmol/10^6 cells. After only 1 hour of incubation,

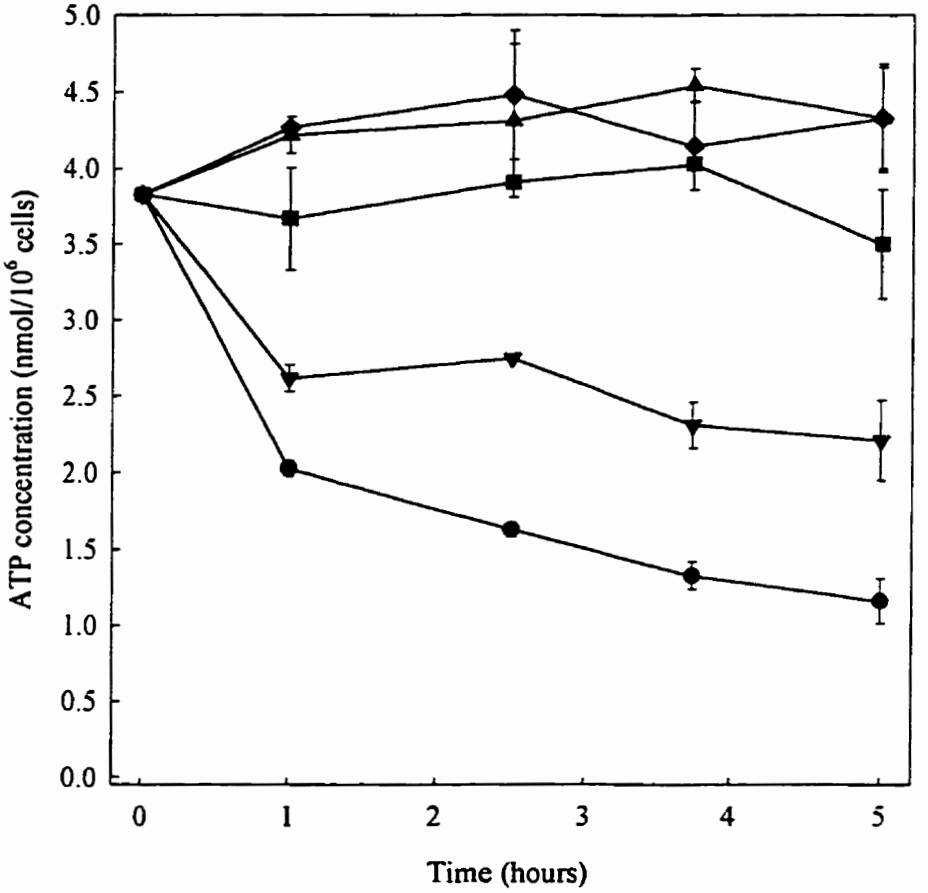

Figure 9.1 Time course profile of the effect of glucose concentration on the CC9C10 intracellular ATP pool. Hybridomas were inoculated into T-flasks (25 cm^2) containing 10 ml NB-SFM with varying glucose concentrations: 0 mM, (●); 1 mM, (▼); 5 mM, (■); 10 mM, (◆); 25 mM, control culture, (▲). All cultures contained 6 mM glutamine. ATP concentration values are the mean ± S.E.M. from two identical flasks inoculated from same cell stock.

the ATP concentration increased in cultures exposed to 10 and 25 mM glucose, remained the same at 5 mM glucose, and decreased significantly at 1 and 0 mM glucose. The intracellular ATP concentration was therefore proportional to the glucose in the medium. Incubating cells for up to 5 hours in 1 - 25 mM glucose did not significantly change the ATP level compared to initial fluctuation at the 1 hour time point. The ATP level in cultures exposed to 0 mM glucose however decreased for 4 hours until apparently stabilizing at 1.16 nmol/10^6 cells. The ATP concentration of the control culture (25 mM glucose, 6mM glutamine) was 4.33 nmol/10^6 cells after 5 hours.

In a separate experiment, cells were resuspended in 10 ml NB-SFM containing 0.5, 1, 3 or 6 mM glutamine and a constant glucose concentration of 25 mM. The time course profile of CC9C10 hybridomas in varying glutamine concentrations is shown in Fig.9.2. The initial intracellular ATP concentration of the stock culture was 5.10 nmol/10^6 cells. This is significantly higher (33 %) then the initial ATP value obtained in the previous experiment and may be due to the differences in the state of the cells at the time of inoculation (i.e. cell culture age and density). The intracellular ATP concentration increased in all cultures after 2.5 hours of incubation and remained relatively constant up to 5 hours. The ATP concentration did not vary more than 10 % in cultures exposed to 0.5 - 6 mM glutamine. The control culture ATP concentration after 5 hours of incubation was 6.24 nmol/10^6 cells which represented a 44% increase compared to the previously reported control culture.

9.2.2 The effect of glucose and glutamine extracellular concentration on intracellular nucleotide pools

It was shown in the last section that intracellular nucleotide levels are dependent on the cell culture history. In order to circumvent this problem, stock cultures were treated to a strict regimen prior to use in subsequent experiments. Stock cultures of CC9C10 hybridomas were inoculated at 1.0 x 10^5 cells/ml in T-flasks (150 cm^2) containing a total of 50 ml NB-SFM. After 46 hours of incubation at 37°C, 10 ml of the culture was removed and replaced with an equivalent volume of NB-SFM. Cultures were incubated

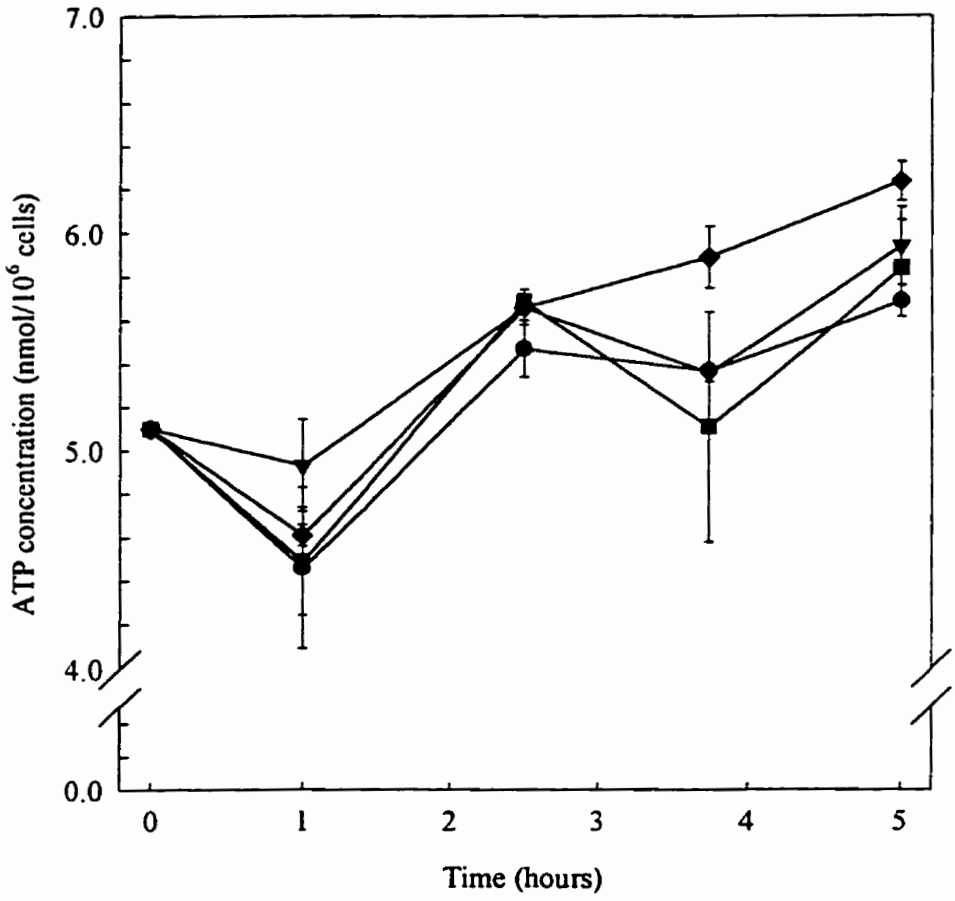

Figure 9.2 Time course profile of the effect of glutamine concentration on the CC9C10 intracellular ATP pool. Hybridomas were inoculated into T-flasks (25 cm^2) containing 10 ml NB-SFM with varying glutamine concentrations: 0.5 mM, (●); 1 mM, (▼); 3 mM, (■); 6 mM, control culture (◆). All cultures contained 25 mM glucose. ATP concentration values are the mean ± S.E.M. from two identical flasks inoculated from same cell stock.

for another 21 - 25 hours until cell density reached 0.8 - 1.0 x 10^6 cells/ml. Glucose and glutamine concentration in these cultures were 11.1 ● 0.6 mM and 3.3 ± 0.4 mM respectively. The mid-exponential phase cells were collected by centrifugation, washed and resuspended in NB-SFM as described in section 9.2.1.

The glucose and glutamine concentrations in the NB-SFM were varied from 0 - 25 mM and 0 - 9 mM respectively. Nucleotides were extracted after 5 hours of incubation. This incubation period had been shown previously to be sufficient to allow cells to stabilize intracellular nucleotide pools. Statistical analysis was done by analysis of variance (Appendix A1).

As seen in Table 9.1, increasing the media glucose concentration from 0 mM to 25 mM resulted in a concomitant increase in the intracellular ATP pool regardless of the glutamine concentration. The probability that glucose had an effect on the ATP pool was $P< 0.005$ in the presence of glutamine and $P< 0.05$ in the absence of glutamine. In contrast, increasing the media glutamine concentration from 0.5 - 9 mM did not significantly alter the intracellular ATP pool based on ANOVA. Averaging of ATP values from hybridomas grown in 0.5 - 9 mM glutamine at constant glucose levels resulted in a variation of less than 10 %. CC9C10 cultures exposed to glutamine (0.5 - 9 mM) were able to maintain ATP levels at 0.98, 1.76, 2.62, 3.71, 5.12, and 6.25 nmol/10^6 cells in media containing 0, 1, 3, 5, 10 and 25 mM glucose respectively. Assuming that glucose and glutamine provide 100 % of the energy produced in hybridoma cultures and that their metabolic pathways do not interfere with each other, the intracellular ATP concentration of cells exposed to 0 mM glucose would allow us to calculate the basal level contribution of glutamine to the ATP pool (0.98 nmol/10^6 cells). Glutamine therefore may have contributed 100, 56, 37, 26, 19 and 15 % of the energy for the intracellular ATP pool maintenance in the presence of 0, 1, 3, 5, 10, 25 mM glucose respectively.

The basal level contribution of glucose to the ATP pool can be estimated in the absence of glutamine. CC9C10 cultures maintained ATP levels of 3.20, 4.23, 4.49 nmol/10^6 cells when exposed to 0 mM glutamine and 5, 10 or 25 mM glucose respectively. When cells were exposed to 5 mM glucose, the addition of glutamine caused no statistically important change in the ATP level. When cells were

Table 9.1 The effect of glucose and glutamine concentration on the intracellular ATP pool (nmol/10^6 cells). Hybridomas were inoculated into T-flasks (25 cm^2) containing 11 ml NB-SFM at varying glucose and glutamine concentrations. Intracellular nucleotides were extracted after 5 hours of incubation at 37°C. The initial ATP value of stock cultures was 3.98 ± 0.59 nmol/10^6 cells/ml (n =3). Experimental values are the mean ± S.E.M. from two independent flasks inoculated from different stock cultures unless otherwise specified.

		Glucose (mM)					
		0	1	3	5	10	25
Glutamine (mM)	0	ND	ND	ND	3.20 ± 0.21[a]	4.23 ± 0.30[a]	4.49 ± 0.16[a]
	0.5	1.04 ± 0.07	1.99 ± 0.12	3.03 ± 0.32	3.84 ± 0.59	5.16 ± 0.61	6.20 ± 0.96
	3	0.94 ± 0.14	1.31 ± 0.18	2.21 ± 0.15	3.56 ± 0.08	4.81 ± 0.01	5.60 ± 0.10
	6	1.04 ± 0.19[a]	1.91 ± 0.20[a]	2.54 ± 0.20[a]	3.47 ± 0.20	5.24 ± 0.44[a]	6.75 ± 0.45[a]
	9	0.91 ± 0.06	1.95 ± 0.03	2.70 ± 0.19	3.99 ± 0.70	5.27 ± 0.45	6.48 ± 0.36
	0.5 - 9 mM (average)	0.98 ± 0.03	1.76 ± 0.16	2.62 ± 0.17	3.71 ± 0.12	5.12 ± 0.11	6.25 ± 0.24

[a]Values are the mean ± S.E.M. from three independent flasks inoculated from different stock cultures.
ND - not determined

exposed to 10 and 25 mM glucose, the addition of glutamine caused a 21 % and 39 % increase in the intracellular ATP concentration ($P< 0.05$).

The probability that energy charge was affected by glucose concentration in the presence of glutamine was $P< 0.0005$. As seen in Table 9.2, energy charge values increased with a concomitant increase in glucose concentration in the range of 0 - 25 mM. Glutamine levels in the range of 0.5 - 9 mM however did not significantly affect the adenylate nucleotide ratio. Averaging energy charge values from hybridomas grown in 0.5 - 9 mM glutamine resulted in less than a 10 % variation. Hybridoma cultures exposed to 0, 1, 3, 5, 10 and 25 mM glucose and glutamine (> 0.5 mM) had energy charge values of 0.38, 0.36, 0.49, 0.63, 0.81 and 0.96 respectively. High energy charge values of 0.85 - 0.94 present in hybridomas cultures exposed to 0 mM glutamine and 5 - 25 mM glucose were not statistically different. It was observed however that supplementation of NB-SFM (containing 5 - 10 mM glucose) with glutamine caused a significant decrease (0.1 - 0.2 units) in the adenylate energy charge ($P< 0.005$).

A representative graph of adenylate nucleotides and energy charge as a function of glucose concentration is shown in Fig.9.3. Values are from CC9C10 hybridomas exposed to a constant glutamine concentration of 0.5 mM. Similar graphs were obtained with constant glutamine concentrations of 3 - 9 mM. (data not shown). As shown previously, the intracellular ATP concentration and energy charge increased concomitantly with increases in glucose concentration. Analysis of the ADP pool however indicates a bell-shaped curve in response to variations in glucose level. A maximum intracellular ADP concentration of 1.0 nmol/10^6 cells was present in cells exposed to 3 - 5 mM glucose. A higher or lower media glucose concentration (0, 1, 10 or 25 mM) resulted in a reduction in the intracellular ADP pool to 0.4 - 0.8 nmol/10^6 cells.

The AMP pool in contrast is at its maximum value when cells are exposed to 1 mM glucose (3.17 nmol/10^6 cells). Further increases in the media glucose level resulted in a proportional decrease in the AMP pool down to < 0.1 nmol/10^6 cells. The intracellular AMP concentration also decreased significantly (37 %) in the absence of extracellular glucose (2.00 ± 0.31 nmol/10^6 cells). Further analysis has shown that the total adenylate pool (SA - sum of adenylates) was constant between 1 - 25 mM glucose (6.40 ± 0.48

Table 9.2 The effect of glucose and glutamine concentration on the intracellular adenylate energy charge. The adenylate energy charge is (ATP + ½ ADP) / (ATP + ADP + AMP). Hybridomas were inoculated into T-flasks (25 cm^2) containing 11 ml NB-SFM at varying glucose and glutamine concentrations. Intracellular nucleotides were extracted after 5 hours of incubation at 37°C. The initial EC value of stock cultures was 0.91 ± 0.01 nmol/10^6 cells/ml (n =3). Experimental values are the mean ± S.E.M. from two independent flasks inoculated from different stock cultures unless otherwise specified.

		Glucose (mM)					
		0	1	3	5	10	25
Glutamine (mM)	0	ND	ND	ND	0.85 ± 0.05[a]	0.94 ± 0.01[a]	0.92 ± 0.01[a]
	0.5	0.36 ± 0.02	0.40 ± 0.01	0.56 ± 0.03	0.67 ± 0.03	0.83 ± 0.00	0.95 ± 0.00
	3	0.47 ± 0.03	0.37 ± 0.03	0.50 ± 0.02	0.71 ± 0.04	0.87 ± 0.01	0.96 ± 0.02
	6	0.36 ± 0.03[a]	0.35 ± 0.05[a]	0.46 ± 0.03[a]	0.58 ± 0.04	0.80 ± 0.03[a]	0.96 ± 0.02[a]
	9	0.35 ± 0.06	0.34 ± 0.02	0.46 ± 0.02	0.58 ± 0.05	0.79 ± 0.00	0.95 ± 0.00
	0.5 - 9 mM (average)	0.38 ± 0.03	0.36 ± 0.01	0.49 ± 0.02	0.63 ± 0.03	0.81 ± 0.02	0.96 ± 0.01

[a]Values are from three independent flasks inoculated from different stock cultures.
ND - not determined

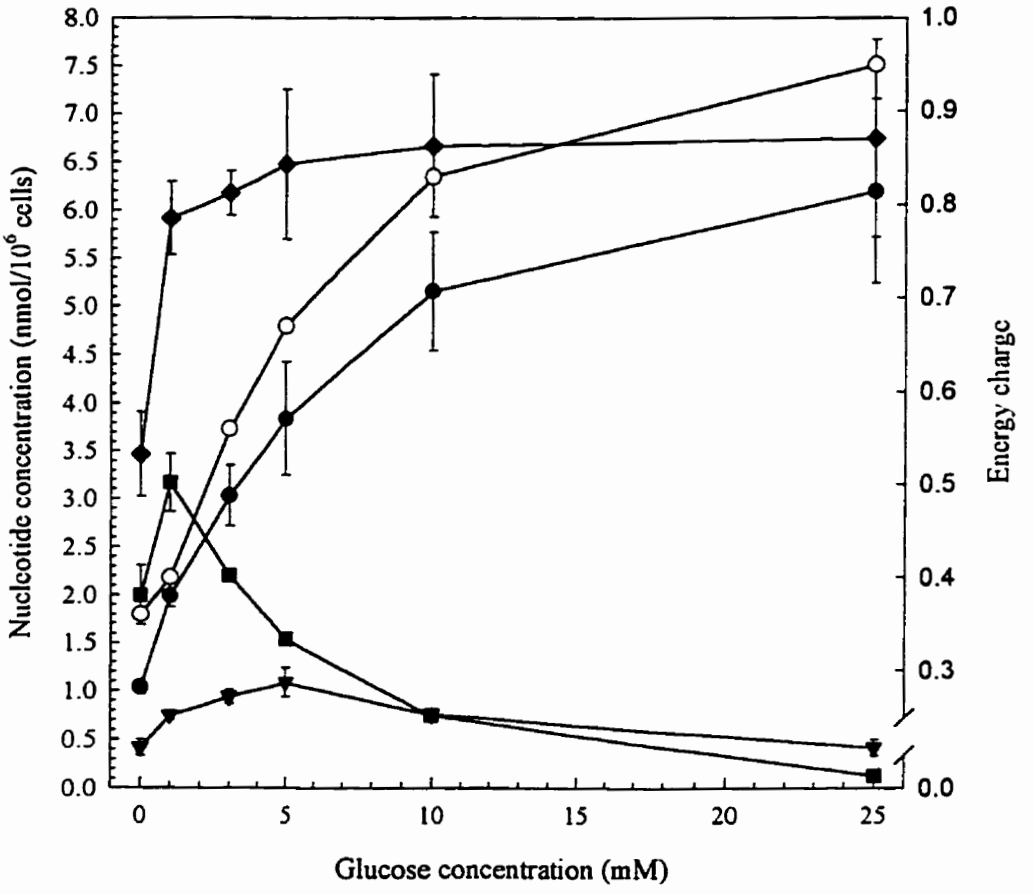

Figure 9.3 Typical adenylate nucleotide levels of CC9C10 hybridomas grown in varying concentrations of glucose. Hybridomas were inoculated into T-flasks (25 cm^2) containing 11 ml NB-SFM with varying glucose concentrations. All cultures contained 0.5 mM glutamine. Intracellular nucleotides were extracted after 5 hours of incubation at 37°C: ATP (●); ADP (▼); AMP (■); SA (◆) and energy charge (O). Values are the mean ±●S.E.M. from two independent flasks inoculated from different stock cultures. Energy charge errors were less than 6 % and not shown on the graph. This graph is also representative of CC9C10 hybridomas grown in constant glutamine concentrations of 3, 6 and 9 mM.

nmol/10^6 cells). Reducing the glucose concentration to 0 mM however resulted in a 46 % decrease in total adenylates (3.47 ● 0.44 nmol/10^6 cells).

The effect of glucose and glutamine on other nucleotide pools has also been investigated (Fig.9.4, Table 9.3). As was the case with adenylate nucleotides, the UTP, GTP, UDP-GNac and NAD intracellular concentrations did not significantly differ in the range of 0.5 - 9 mM glutamine as determined by ANOVA (data not shown). An increase in extracellular glucose concentration however resulted in the concomitant increase in UTP and GTP (Fig.9.4). In the absence of glucose, levels of UTP and GTP were 0.67 and 0.23 nmol/10^6 cells respectively. Maximum values of UTP and GTP were attained in the presence of 25 mM glucose: 2.90 and 1.30 nmol/10^6 cells respectively. The intracellular UDP-GNac and NAD levels in contrast were constant regardless of the glucose concentration (Fig.9.4). The UDP-GNac concentration for cells exposed to 0 - 25 mM glucose was 1.48 ± 0.06 nmol/10^6 cells while the NAD concentration was 0.65 ± 0.04 nmol/10^6 cells The intracellular CTP concentration was also dependent on glucose levels (Table 9.3). A concentration of glucose of 5 mM or less resulted in an undetectable CTP level (< 0.4 nmol/10^6 cells). Increasing the glucose concentration in the media to 10 or 25 mM resulted in the concomitant increase in the intracellular CTP level.

A summary of the effect of glutamine on the intracellular nucleotide pool is shown in Table 9.4. Exposing CC9C10 hybridomas to 0 mM glutamine and 25 mM glucose for 5 hours did not change significantly the nucleotide levels in comparison to initial values at the time of inoculation. Supplementation with glutamine (0.5 - 9 mM) however caused a 65 % increase in the total intracellular nucleotide pool. The greatest increase was for UTP at 128 %. The GTP, ATP, UDP-GNac and NAD pools increased by 65, 57, 47 and 45 % respectively. The total adenylate pool was also increased by 44 % in the presence of glutamine. In contrast, no significant changes were observed in the CTP, ADP and AMP pools. Similar results were obtained with respect to the effect of glutamine when cells were cultured in 5 to 10 mM glucose (data not shown). There was no significant difference in the intracellular nucleotide concentrations within the glutamine concentration range 0.5 - 9 mM.

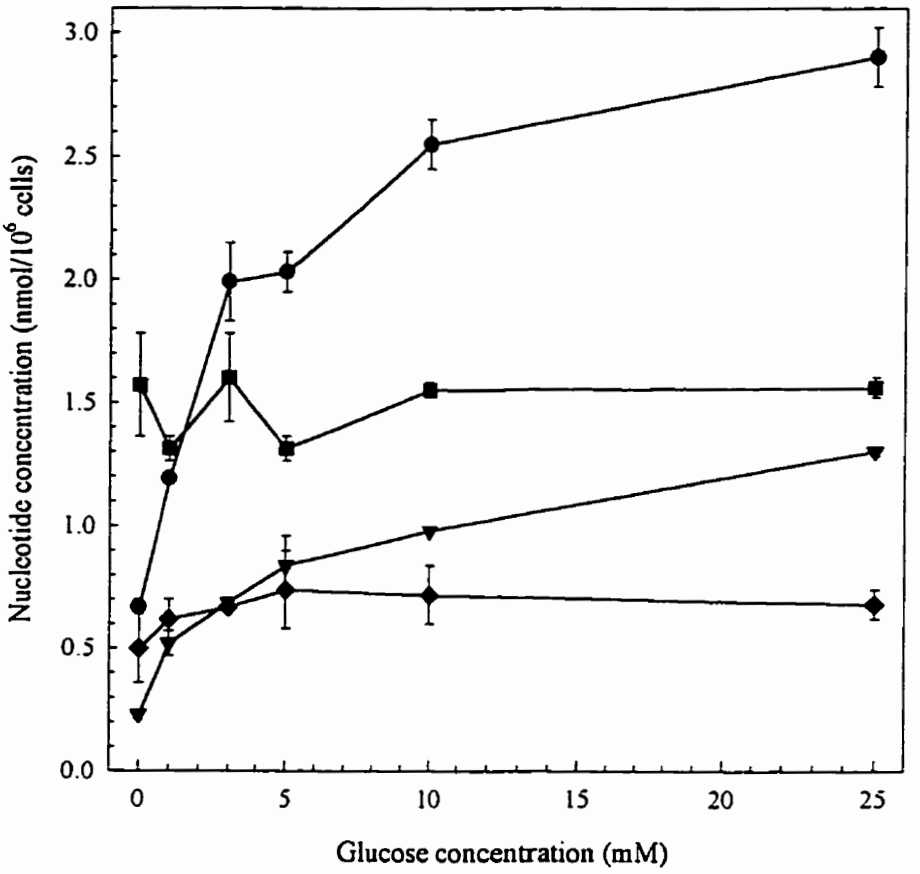

Figure 9.4 Typical UTP, GTP, UDP-GNac and NAD levels of CC9C10 hybridomas grown in varying concentrations of glucose. Hybridomas were inoculated into T-flasks (25 cm^2) containing 11 ml NB-SFM with varying glucose concentrations. All cultures contained 0.5 mM glutamine. Intracellular nucleotides were extracted after 5 hours of incubation at 37°C: UTP (●); GTP (▼); UDP-GNac (■); NAD (◆). Values are the mean ±S.E.M. from two independent flasks inoculated from different stock cultures. This graph is also representative of CC9C10 hybridomas grown in constant glutamine concentrations of 3, 6 and 9 mM.

Table 9.3 The effect of glucose and glutamine concentration on the intracellular CTP pool (nmol/10^6 cells). Hybridomas were inoculated into T-flasks (25 cm^2) containing 11 ml NB-SFM at varying glucose and glutamine concentrations. Intracellular nucleotides were extracted after 5 hours of incubation at 37°C. CTP concentrations lower than 0.4 nmol/10^6 cells were not quantified due to limitations of the detection system. The initial CTP value of stock cultures was < 0.4 nmol/10^6 cells (n =3). Experimental values are the mean ± S.E.M. from two independent flasks inoculated from different stock cultures unless otherwise specified.

		Glucose (mM)					
		0	1	3	5	10	25
Glutamine (mM)	0	ND	ND	ND	< 0.4	< 0.4	0.45 ± 0.22[a]
	0.5	< 0.4	< 0.4	< 0.4	< 0.4	0.56 ± 0.23	0.92 ± 0.09
	3	< 0.4	< 0.4	< 0.4	< 0.4	0.73 ± 0.08	0.74 ± 0.43
	6	< 0.4	< 0.4	< 0.4	< 0.4	0.75 ± 0.26[a]	0.59 ± 0.29[a]
	9	< 0.4	< 0.4	< 0.4	< 0.4	1.12 ± 0.03	0.90 ± 0.12
	0.5 - 9 mM (average)	< 0.4	< 0.4	< 0.4	< 0.4	0.79 ± 0.11	0.79 ± 0.08

[a]Values are from three independent flasks inoculated from different stock cultures.
ND - not determined

Table 9.4 The effect of glutamine on intracellular nucleotide pools (nmol/10^6 cells). Hybridomas were inoculated into T-flasks (25 cm^2) containing 11 ml NB-SFM supplemented with 25 mM glucose and varying concentrations of glutamine: 0, 0.5, 3, 6, 9 mM. Intracellular nucleotides were extracted after 5 hours of incubation at 37°C. " TOTAL" refers to the sum of all detectable nucleotides. Glucose and glutamine concentrations of stock cultures at the time of cell harvest were 11.1 ± 0.6 and 3.3 ± 0.4 mM respectively.

	ATP	UTP	GTP	CTP	UDP-GNac	NAD	ADP	AMP	SA	TOTAL
Initial values	3.98 ± 0.59	1.26 ± 0.18	0.73 ± 0.15	0.40 ± 0.10	1.03 ± 0.11	0.47 ± 0.07	0.57 ± 0.11	0.14 ± 0.08	4.68 ± 0.78	8.72 ± 1.32
0 mM glutamine[a]	4.49 ± 0.16	1.56 ± 0.44	0.81 ± 0.28	0.45 ± 0.22	0.72 ± 0.30	0.44 ± 0.12	0.50 ± 0.10	0.15 ± 0.02	4.65 ± 0.72	9.46 ± 1.36
0.5 - 9 mM glutamine[b]	6.25 ± 0.24	2.88 ± 0.12	1.21 ± 0.03	0.79 ± 0.08	1.52 ± 0.09	0.68 ± 0.04	0.41 ± 0.05	0.07 ± 0.02	6.75 ± 0.29	14.43 ± 0.63

[a]Values are the mean ± S.E.M. from 3 independent flasks inoculated from different stock cultures (n = 3).
[b]Values are the mean ± S.E.M. from cultures inoculated in 0.5, 3, 6 and 9 mM glutamine (n = 4).

9.2.3 The effect of glucose and glutamine extracellular concentration on the oxygen uptake rate

The purpose of determining the oxygen uptake rate (OUR) at different nutrient levels was to evaluate the extent of substrate oxidation. In addition, oxygen uptake rates will be compared to the observed levels of intracellular nucleotides. This comparison will provide insights into the contribution of substrate oxidation to energy levels.

CC9C10 hybridomas were prepared as in section 9.2.2 and oxygen uptake rates were determined after 3 - 5 hours of incubation in specific media at 37°C (section 2.13). The effect of glucose and glutamine extracellular concentration on the CC9C10 hybridoma oxygen uptake rate is shown in Table 9.5. CC9C10 cultures exposed to 0 mM glutamine and 5, 10 or 25 mM glucose had oxygen uptake rates of 0.12 - 0.15 μmol/hour per 10^6 cells. Media containing the same level of glucose but with 0.5 mM glutamine resulted in the doubling of the oxygen uptake rate ($P< 0.005$). The addition of glutamine alone therefore caused an oxygen uptake rate of 0.13 - 0.15 μmol/hour per10^6 cells. A further increase in the glutamine concentration (> 0.5 mM) did not result in a further increase in OUR.

Cultures exposed to 0 mM glucose had similar oxygen uptake rates as cultures exposed to 5 - 25 mM glucose. The oxygen uptake rates of cultures exposed to 1 mM glucose however was 0.41 μmol/hour per 10^6 cells and was not dependent on glutamine concentration in the range of 0.5 - 10 mM. The oxygen uptake rate was 41 - 105 % higher in cultures exposed to 1 mM glucose than cultures exposed to 0, 5, 10 or 25 mM glucose ($P< 0.005$). Further investigations on the effect of glucose on oxygen uptake rates show that a range of 0.1 - 1 mM glucose is the optimal concentration for cell respiration (Fig.9.5).

Table 9.5 The effect of glucose and glutamine concentration on the CC9C10 hybridoma oxygen uptake rate (μmol/hour per 10^6 cells). Experimental values are the mean ± S.E.M. from independent flasks (n=2) inoculated from different stock cultures unless otherwise specified.
*P< 0.005 compared to 0 mM glucose cultures.
**P< 0.007 compared to 0.5 - 6 mm glutamine cultures. Statistical analysis was done by ANOVA.

		Glucose (mM)				
		0	1	5	10	25
Glutamine (mM)	0	ND	ND	0.15 ± 0.02**	0.14 ± 0.02**	0.12 ± 0.01**
	0.5	0.29 ± 0.01	0.42 ± 0.04*	0.29 ± 0.03	0.29 ± 0.02	0.25 ± 0.02[a]
	3	0.28 ± 0.00[b]	0.43 ± 0.04*	ND	ND	0.28 ± 0.03
	6	0.27 ± 0.02[a]	0.38 ± 0.04[a]*	0.31 ± 0.01	0.31 ± 0.03	0.30 ± 0.02[c]
	8	0.24 ± 0.03	0.42 ± 0.04*	ND	ND	ND
	10	0.20 ± 0.05	0.41 ± 0.02*	ND	ND	ND

[a](n = 4).
[b](n = 3).
[c](n = 12).
ND- not determined

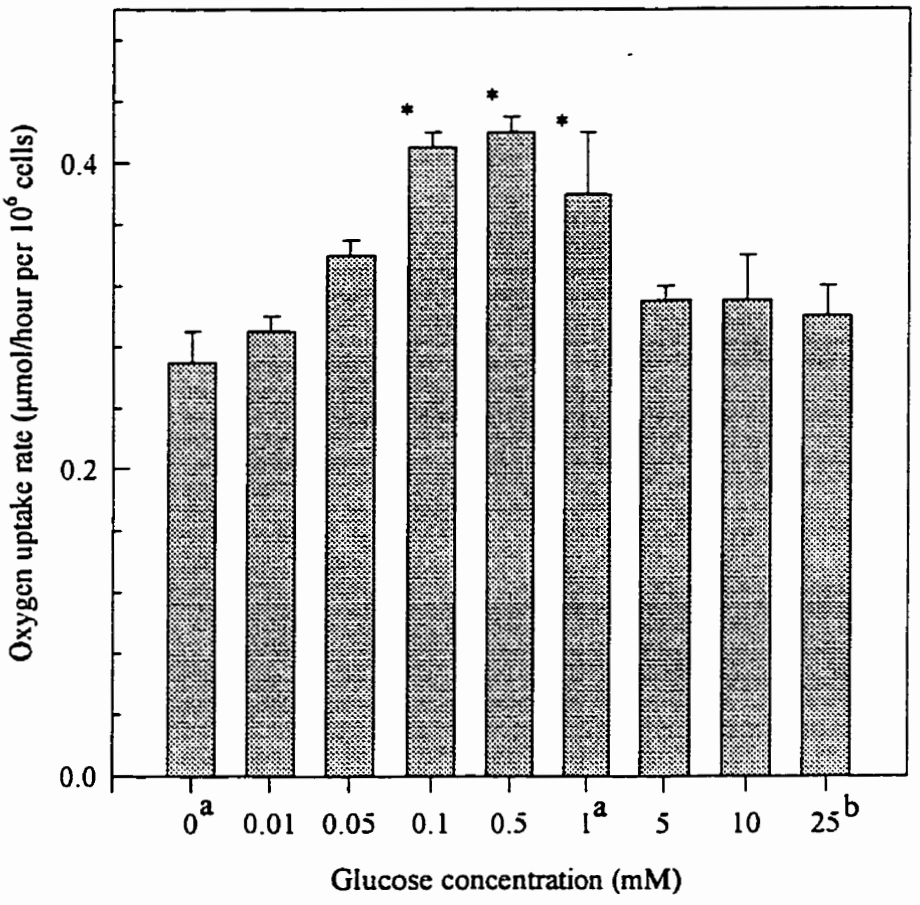

Figure 9.5 Determination of the effect of glucose concentration on cell respiration. Hybridomas were inoculated into T-flasks (25 cm^2) containing 11 ml NB-SFM with varying glucose concentrations. All cultures contained 6 mM glutamine. Experimental values are the mean ± S.E.M. from two independent flasks inoculated from different stock cultures unless otherwise specified.

[a]n = 4

[b]n-12

*P < 0.05 compared to base line values at 0 mM glucose.

9.3 Discussion

Glucose and glutamine are the two major nutrients in hybridoma metabolism. Both substrates are directly involved in intracellular nucleotide pool synthesis. In addition to supplying precursors for the *de novo* synthesis of nucleotides, glucose and glutamine provide energy by coupling catabolic or oxidative reactions to nucleotide phosphorylation (Henderson and Paterson, 1973). The purpose of this study was to determine the relative contribution of extracellular glucose and glutamine to the maintenance of intracellular nucleotide pool levels. The intracellular concentration of nucleotides is an important determinant of cell viability (chapter 8). Fluctuations in these levels may also lead to changes in other cell behavior such as growth and differentiation (De Korte *et al.*, 1987; Ryll and Wagner, 1992).

A protocol was developed in which nucleotides were extracted after 5 hours of incubation in serum-free medium. This incubation period was sufficient to allow cells to react to the external environment and to stabilize nucleotide levels in response to different substrate concentrations. A strict regimen of cultivation was also employed prior to inoculation of experimental cultures in order to obtain reproducible results.

Analysis of nucleotide profiles shows that an increase in media glucose concentration from 0 - 25 mM was concomitant with an increase in the intracellular ATP pool. This relationship was similar to that reported for cultured human myocytes (Frenes *et al.*, 1992). This observation suggests that the rate of glucose metabolism (i.e. ATP production) is dependent on the extracellular glucose level. In fact, studies have shown that the glucose metabolism rate is dependent on its concentration in the media in the range of 0.01 - 5 mM, but is unchanged by further increases in glucose levels (Miller *et al.*, 1989a). Results presented here with CC9C10 hybridomas suggest that glucose metabolism may be dependent on its concentration up to 25 mM. This is supported by evidence that at a high glucose concentration (5 - 25 mM) there is a concomitant increase in the intracellular ATP pool without any change in the oxygen uptake rate. The energy for increased ATP synthesis was therefore probably provided by an anaerobic process such as glycolysis rather than oxidative pathways such as the TCA and pentose phosphate cycles.

Glycolysis is the major pathway of glucose metabolism in transformed cell lines (Fitzpatrick *et al.*, 1993; Petch and Butler, 1994).

An increase in glucose concentration was also related to a concomitant increase in the GTP, UTP and CTP pools similar to the increase observed in the ATP pool. The increase in these three nucleotide pools is probably due to the acquisition of the terminal phosphate group from ATP in reactions catalyzed by nucleoside diphosphokinases (Henderson and Paterson, 1973). The glucose concentration in the media did not however affect the UDP-GNac and NAD pools. The unchanged UDP-GNac pool is contrary to the expected findings since glucose is a precursor to the sugar-nucleotide pool (Ryll *et al.*, 1994). It is probable that UDP-GNac synthesis is more dependent on another presursor such as the ammonium ion. Ammonium ions are provided to the media by the spontaneous degradation of glutamine and by glutaminolysis (Tritsch and Moore, 1962; McKeehan, 1982). It was observed that the addition of glutamine to the medium did result in an increase in the UDP-GNac pool. NAD probably does not exhibit in a net change intracellular levels with an increase in glucose concentration due to a balance between NAD reduction and regeneration reactions in the glycolysis pathway. For every mole of glucose that passes through the glycolysis pathway, 2 moles of NAD are reduced and 2 moles are subsequently regenerated by the formation of lactate (Lehninger, 1982).

Intracellular AMP levels decreased concomitantly with an increase in media glucose concentration from 1 to 25 mM. A reduction of the media glucose level to 0 mM however caused a decrease in the AMP pool. This decrease is probably due to the deamination of AMP via adenylate deaminase, an enzyme that converts AMP to the non-adenylate nucleotide IMP. (Atkinson, 1977).

$$AMP + H_2O \leftrightarrow IMP + NH_3 \qquad \text{(equation 9.1)}$$

Removal of AMP from the cell would tend to cause a reduction in total adenylates and prevent a decrease in the adenylate energy charge. This is consistent with our findings with the CC9C10 hybridoma. Studies have shown that the production of IMP (i.e AMP

degradation) in ascites tumor cells is concomitant with a decrease in the adenylate pool and energy charge (McComb and Yushak, 1964; Lomax and Henderson, 1973).

Intracellular ADP levels were also dependent on glucose concentration. Minimum ADP levels were obtained when cells were exposed to extremes of media glucose levels (i.e. 0 and 25 mM). Maximum ADP levels however were obtained when cells were exposed to 3 and 5 mM glucose. The glucose dependency of ADP resulted in a bell-shaped curve of ADP concentration as a function of glucose concentration. This curve shape is similar to the one described by Atkinson (1977) who plotted the relative concentration of ADP as a function of energy charge assuming an adenylate kinase reaction equilibrium. Adenylate kinase transfers activated phosphate groups reversibly between adenylate nucleotides (equation 9.2).

$$AMP + ATP \leftrightarrow 2\ ADP \quad \text{(equation 9.2)}$$

The dependency of all three adenylate nucleotides on the extracellular glucose concentration resulted in the fluctuation of the adenylate energy charge. It was observed that the energy charge increased concomitantly with an increase in media glucose concentration from 1 to 25 mM. Cells exposed to 0 mM glucose had similar energy charge levels (0.37 ● 0.01) as cells exposed to 1 mM glucose. This was probably due to the action of adenylate deaminase as previously discussed. The total adenylate nucleotide pool of cells exposed to 1 - 25 mM glucose was constant while in cells exposed to 0 mM glucose it decreased. This suggests that glucose by itself does not stimulate the *de novo* synthesis of nucleotides.

CC9C10 hybridomas responded differently to a variation in the concentration of extracellular glutamine. The addition of 0.5 mM glutamine to the medium caused a 45 - 128 % increase in NTP, NAD and UDP-GNac levels compared to cultures exposed to 0 mM glutamine. A net increase in the total adenylate nucleotide pool (SA) was also observed suggesting that glutamine may stimulate the *de novo* synthesis of intracellular nucleotides. The addition of glutamine to medium has been shown to stimulate growth which requires an elevated level of nucleotides in order to duplicate DNA (Glacken,

1988). Glutamine is required as a precursor for nucleotide synthesis (Engstrom and Zetterberg, 1984). The presence of glutamine also caused a 0.1 - 0.2 unit decrease in the energy charge level in cultures exposed to 5 - 10 mM glucose but did not affect cultures at 25 mM glucose. Energy charge values are also decreased in the presence of glutamine in isolated mesenteric lymphocytes (Ardawi and Newsholme, 1983). This result suggests that glucose only is sufficient to maintain the bioenergic status of the cell. Glutamine may reduce the energy charge by increasing the *de novo* synthesis of the total adenylate pool especially ADP and AMP.

Increases in glutamine concentration from 0.5 - 9 mM did not significantly alter nucleotide pools, the energy charge nor the oxygen uptake rate. This indicates that a limitation in glutamine utilization may exist. It has been proposed that at a glutamine concentration higher than 2 mM, the transport of this amino acid is the limiting factor in its utilization (Fitzpatrick *et al.*, 1993). Another possible rate limiting step in glutamine metabolism may be the reduced activity of enzymes of the glutaminolysis pathway. (Glacken, 1988; Sri-Pathmanathan *et al.*, 1990). Enzymes function as regulators of glutaminolysis and may be slow in responding to changes in the glutamine concentration (Neerman and Wagner, 1996).

ATP is the most abundant nucleotide in the CC9C10 hybridoma. Its importance as a metabolic link between energy-producing and energy-utilizing pathways makes ATP a good candidate for determining the relative contribution of glucose and glutamine to energy production. In order to estimate the relative contribution of each nutrient to the intracellular nucleotide pool two assumptions were made. First it was assumed that 100 % of the energy produced was derived from glucose and glutamine metabolism. Glucose and glutamine are the major nutrients in hybridoma metabolism and are present in at least at 10 - 20 fold the concentration of other carbon sources. In the absence of glucose, most of HeLa cell energy is derived from glutamine oxidation (Reitzer *et al.*, 1980). The second assumption was that the minimum ATP level contributed by glutamine could be calculated in the absence of glucose and vice versa.

It was found that the relative contribution of both substrates to the intracellular ATP pool was dependent on the glucose concentration only. An increase in the media

glucose level (0 - 25 mM) resulted in the increase in the proportion of ATP derived from glucose and a decrease in the proportion of ATP derived from glutamine. In contrast, an increase in media glutamine level (0.5 - 9 mM) did not have any significant effect on the relative contribution of glutamine to the intracellular ATP pool. This suggests that when both glucose and glutamine are available, glucose is the preferred substrate. In fact, CC9C10 hybridomas metabolize more moles of glucose than glutamine when both are present in the medium (data not shown). Glucose is the preferred substrate in many tumor cell lines (Medina and Nunez de Castro, 1990).

It was estimated that when cells were exposed to 10 - 25 mM glucose and 0.5 - 9 mM glutamine, glutamine provided the energy for the maintenance of 15 - 28 % of the intracellular ATP pool while glucose supplied the rest of the energy. Reports by Petch and Butler (1994) estimated that when CC9C10 hybridomas were exposed to 20 mM glucose and 2 mM glutamine, glutamine contributed close to 41 % of the total ATP production. Comparison of these results suggest that although glutamine may supply a significant portion of total ATP production only a small percentage is utilized for the maintenance of intracellular levels. This result may be due to the preferential use of glucose-derived ATP for intracellular nucleotide pool maintenance. Cells could possibly discriminate between glucose and glutamine-derived ATP by compartmentalization of the nucleotides. This is plausible since glycolysis occurs in the cytoplasm while the energy yielding reactions of glutaminolysis occurs mainly in the mitochondria (Lehninger, 1982; McKeehan, 1982). Compartmentalization of the ATP pool may also cause differences in the kind of reactions that utilize ATP and consequently cause differences in the rate of ATP utilization. It has been suggested that ATP-derived from glycolysis may provide energy to specific areas such as ion pumps and other maintenance functions (Glacken, 1988).

The oxygen uptake rate of CC9C10 hybridomas in the presence of 5 - 25 mM glucose and 0.5 - 6 mM glutamine was approximately 0.29 μmol/hour per 10^6 cells. This value is similar to the one reported by Jan *et al.* (1997) for the same cell line. Removal of glutamine from the media cut the oxygen uptake rate in half to approximately 0.14 μmol/hour per 10^6 cells. Whether a significant proportion of this rate is attributable to the presence of glucose is not known. Reports show that the flux of glucose through oxidative

pathways is less than 5 % in CC9C10 hybridomas and other cell lines (Fitzpatrick *et al.*, 1993; Petch and Butler, 1994). It is possible that the observed oxygen uptake rate in the absence of glutamine is due to the oxidation of other substrates such as other amino acids and lipids. Guppy *et al.* (1997) suggest that the contribution of glucose and glutamine to total ATP production is overestimated due to the omission of the oxidation of other substrates in energy calculations. Alternatively, it has been hypothesized that in mammalian cells that a substantial proportion of cellular respiration is not linked to oxidative reactions which lead to ATP synthesis (Berry *et al.*, 1993).

Maximum oxygen uptake rates were observed when cells were exposed to 0.1 - 1 mM glucose in the presence of glutamine. Increasing the extracellular glucose concentration from 1 mM to 5 - 25 mM resulted in a 30 % decrease in the respiration rate. A significant reduction in respiration rate with glucose levels above 3 mM has been shown in swine testicular cells and fibroblasts (Glacken, 1988; Wohlpart *et al.*, 1990). This phenomenon is commonly referred to as the Crabtree effect (Dell'Antone, 1994). High glucose concentrations have also been associated to a decrease in the utilization of glutamine in mammalian cells (Zielke *et al.*, 1978; Reitzer *et al.*, 1979). Removal of glucose from the media also caused a decrease in the respiration rate. and this may be reflective of a reduced glutaminolysis rate. Glucose plays an important role in glutaminolysis by providing pyruvate, an acceptor of the amine group in the transamination reaction involving glutamate (Meijer and Dijken, 1995).

9.4 Conclusion

Intracellular ATP, GTP, UTP, CTP and energy charge levels are dependent on the medium glucose concentration in the range 0 - 25 mM. An increase in extracellular glucose resulted in a concomitant increase in these nucleotide pools and ratios. The ADP and AMP levels also fluctuated in response to the glucose concentration in the range of 1 - 25 mM but this did not affect the total adenylate nucleotide concentration indicating that glucose levels do not stimulate the *de novo* synthesis of nucleotides.

A concentration of 0.5 mM glutamine caused a significant increase in the ATP, GTP, UTP, UDP-GNac and NAD pools. All nucleotide pools were however constant within the range of 0.5 - 9 mM glutamine indicating that there exists a rate limiting step in glutamine utilization. Glutamine also caused an increase in the total adenylate pool indicating that the amino acid may stimulate the *de novo* synthesis of nucleotides. It was concluded that the relative contribution of glucose and glutamine to the intracellular ATP pool was dependent on the glucose concentration only.

The oxygen uptake rate (OUR) was dependent on the glucose concentration. Maximal OURs were obtained in the presence of 0.1 - 1 mM glucose. Glucose concentrations < 0.1 mM or > 1 mM resulted in OUR values similar to cultures grown in the absence of glucose. A concentration of 0.5 mM glutamine caused a doubling of the OUR compared to glutamine-free cultures wheras no significant effect on OUR was observed within the glutamine range of 0.5 - 9 mM.

It was estimated that in the presence of high concentrations of glucose, glutamine provides the energy for the maintenance of 15 - 28 % of the intracellular ATP pool. Glucose is therefore the major nutrient involved in maintaining the energy status of the cell.

CHAPTER 10

10.0 Conclusions, comments and future work.

The aims of this thesis were to:

i. Test the hypothesis that specific Mab productivity is dependent upon the metabolic state of the hybridoma cell. (The metabolic state was determined from intracellular nucleotide pool levels).

ii. Test the hypothesis that cell culture viability is dependent upon the metabolic state of the cell.

iii. Test the hypothesis that intracellular nucleotide levels are dependent upon the extracellular nutrient concentration.

iv. Develop a serum-free medium for the culture of the CC9C10 hybridoma cell line.

1) To determine whether Mab productivity was dependent upon the metabolic state of the cell, the qMab was altered in cell cultures and intracellular nucleotides were monitored for fluctuations. The qMab was successfully enhanced by increasing the cultivation temperature, supplementing the medium with thymidine or supplementing the medium with sodium butyrate. The three methods resulted in several common metabolic characteristics. First, the maximum growth rate was either reduced or growth was partially arrested in cultures with enhanced qMab. Second, the relative UDP-GNac pool was significantly higher in qMab enhanced cultures. Third, the relative ATP pool was significantly lower in these same cultures. The supplementation of cultures with sodium butyrate was the only method which resulted in higher Mab yields compared to control cultures. In the other treated cultures the enhanced qMab was off-set by a lower cell yield. Future studies exploiting the effects of sodium butyrate may be useful in developing culture conditions for optimal Mab productivity, an important consideration in large-scale processes.

Comparisons between the Mab-secreting hybridoma (CC9C10) and the non-Mab secreting myeloma (SP2/0) also indicated that the UDP-GNac pool was significantly

higher in the Mab-secreting cell line. Based on the data, further experimentation was done to determine if Mab productivity was dependent on the UDP-GNac pool. Hybridomas were grown in conditions favorable for the sugar-nucleotide accumulation: 1) hybridomas were grown in the presence of tunicamycin which inhibits UDP-GNac incorporation into glycoproteins; 2) hybridomas were grown in the presence of NH_4Cl which enhances UDP-GNac synthesis. Both methods were shown to significantly enhance the intracellular UDP-GNac pool (up to 5-fold). Several conclusions were drawn from these UDP-GNac studies. First, the resulting high sugar-nucleotide levels did not affect significantly the qMab showing that the availability of UDP-GNac is a not a limitation to higher productivity. Second, the glycosylation process does not appear to limit productivity in CC9C10 hybridomas as non-glycosylated and glycosylated forms of the Mab are secreted at the same rate. Third, the data suggests that a reduction in growth rate rather than UDP-GNac accumulation was the cause of increased qMab.

Specific Mab productivity is therefore not dependent upon the intracellular UDP-GNac concentration. The level of UDP-GNac however may be used to monitor periods of reduced growth which was concomitant with a higher qMab. A further examination of the relationship between growth rate and UDP-GNac levels would prove to be worthwhile. It is to be noted that, the reduction in the growth rate does not always cause an increase in the qMab. This was seen in CC9C10 batch cultures where there was a constant productivity during the exponential, stationary and death phases. Cell cycle analysis of CC9C10 cultures during periods of high and low qMab could provide useful information on the distribution of cell population during the Mab production

Conditions that caused an increase in qMab, an increase in UDP-GNac pool and decrease in growth rate in the CC9C10 hybridoma (i.e. increase in cultivation temperature, supplementation with thymidine or sodium butyrate) have also been shown to be inducers of apoptosis in several cell lines (Hague *et al.*, 1993; Singh *et al.*, 1994; Gabai *et al.*, 1995). Recent studies have also shown that inhibition of N-linked glycosylation using tunicamycin triggers apoptosis in cancer cell lines (Dricu *et al.*, 1997). The relationship between apoptosis, reduced cell growth and qMab needs further investigation.

In addition to revealing a difference in the intracellular UDP-GNac pool, the comparison between CC9C10 hybridoma and SP2/0 myeloma led to other useful observations. The two cell lines could be distinguished by characteristic nucleotide ratio profiles (NTP, U-, NTP/U ratios) during batch culture. The difference in nucleotide ratio profiles between hybridomas and myelomas may be related to Mab synthesis. The NTP and NTP/U ratios increased in CC9C10 cells as the cultures progressed through the exponential phase and remained at high levels during the stationary and death phases whereas the U-ratio typically decreased during the exponential phase. The opposite behavior was observed in SP2/0 myelomas. Differential nucleotide profiles may however also be attributed to other genetic differences between the cell lines. Future experimentation might include comparing a hybridoma cell line to a mutant hybridoma lacking a functional Mab gene. This may prove to be a better model for comparing metabolic and nucleotide profiles of Mab^+ versus Mab^- cells.

2) To determine whether cell culture viability was dependent upon the metabolic state of the cell, hybridomas were subjected to two conditions that caused different rates of cell culture death. The first involved the inoculation of cells at different cell densities. The second approach involved the inoculation of cells in different concentrations of glucose. In both cases it was shown that cell death was preceded by a significant decrease in the intracellular CTP and UTP pools. In glucose limited cultures ATP, GTP and energy charge were also reduced prior to cell death. We concluded that CTP and UTP levels can be used as predictors of imminent cell culture death and that viability is dependent on the maintenance of these nucleotides at high levels. Analysis of hybridomas also indicated that apoptosis was the preferred mode of cell death in batch, glucose-limited and glutamine-limited cultures. This suggested that this gene regulated process may be triggered by nucleotide depletions.

A low nucleotide level in itself, however, is not sufficient to induce apoptosis as shown by glucose rescue studies. The death of the cell population was staggered over several hours thus allowing for the rescue of cultures by reenergization of nucleotide

pools. Analysis of the distribution of the culture in the cell cycle phases may give a further insight into which cells are more susceptible to apoptosis.

It was also found during the course of the study that the use of ethidium bromide/acridine orange for the detection of apoptosis was more accurate in determining the viability of a cell culture than the trypan blue exclusion method. This is due to the detection of early apoptotic cells which have not yet lost membrane integrity. The EB/AO method is however not recommended for routine use in animal cell cultures. The time span between early apoptosis and loss of membrane integrity is relatively short (approx. 6 hours). This earlier detection of a loss in viability does not give a significant advantage in most applications. Furthermore, ethidium bromide and acridine orange are highly cancerigenic and thus require special handling and disposal.

3) It was shown that intracellular nucleotide levels and oxygen uptake in CC9C10 cells are dependent on glucose and glutamine extracellular concentration. The presence of both nutrients in the medium caused a significant increase in the intracellular NTP levels. The effect of glucose on NTP levels was proportional to the extracellular glucose concentration in the range of 0 - 25 mM. The addition of 0.5 mM glutamine caused a 45 - 128 % increase in NTP levels compared to cultures exposed to 0 mM glutamine. However, increases in the extracellular glutamine concentration from 0.5 - 9 mM did not further enhance the NTP levels. Oxygen uptake analysis complements analysis of intracellular NTP levels in that no significant change in OUR was observed in cultures exposed to 0.5 - 9 mM glutamine. These results suggest that there exists a rate limiting step in glutamine utilization.

Glucose is the preferred substrate and may supply as much as 70 % of the intracellular ATP concentration in the presence of glutamine. Oxygen uptake analysis shows that most of the ATP derived from glucose was from anaerobic metabolism. It was also found that glutamine not glucose stimulates the *de novo* synthesis of nucleotides.

Future experimentation might include adapting the CC9C10 hybridoma to a glucose-free medium by supplementation of a pentose source. This would be done to

determine if cells can increase glutamine utilization and intracellular nucleotide levels in the absence of glucose.

4) A serum-free medium (NB-SFM) was developed for the CC9C10 hybridoma cell line. NB-SFM consisted of 1:1 mixture of DMEM: Ham's F12 basal medium supplemented with insulin, transferrin, NaSe, ethanolamine, phosphoethanolamine and Pluronic F-68. CC9C10 hybridoma secreted a monoclonal antibody directed against bovine insulin, one of the media supplements. Concerns over the interaction of insulin and anti-insulin and its effects on cell growth and metabolism suggest an alternative growth factor should be used in future studies. In fact, M. Norm Huzel in our laboratory has shown that insulin can be replaced by a recombinant analogue of insulin-like growth factor, Long R^3 IGF, with no change in growth yields (Butler *et al.*, 1997). Long R^3 IGF does not bind the CC9C10 anti-insulin. Removal of insulin from the serum-free formulation may also be an option as the growth factor is not absolutely essential for CC9C10 growth (Butler *et al.*, 1997). Future improvement on the serum-free formulation may also include the elimination of transferrin as this would reduce the cost and reduce the contaminating protein content. Transferrin can be replaced by ferric citrate (Schneider and Lavoix, 1990; Eto *et al.*, 1991).

5) In conclusion, the role of nucleotides in the productivity of the CC9C10 cell line may be limited to regulating culture viability and growth rather than regulating synthesis and secretion of the Mab. Optimization of Mab production in hybridoma cultures may be done by reducing cell growth and at the same time preventing cell death, two events that are apparently under the same metabolic control.

Glucose metabolism was shown to be important for the maintenance of high energy nucleotide levels (NTPs) which are needed for cell survival. The major role of glutamine however seems to be the expansion of the nucleotide pool population which is needed for cell growth. The relationships between intracellular nucleotides levels (ratios)

and growth, cell death and extracellular nutrient concentration are potentially useful for monitoring cell cultures in bioreactors (i.e. large scale production processes). Studies have shown that adjusting the bioreactor perfusion rate according to NTP and U ratios can keep Baby Hamster Kidney (BHK) cells in an exponential growth phase (Valley *et al.*, 1994). These researchers argue that they can predict growth rates by these ratios and they recommend a course of action with respect to medium replacement. Manipulating nucleotide levels through medium formulation may also prove to be an important tool for the control of hybridoma cell growth and the prevention cell culture death in large scale systems.

BIBLIOGRAPHY

Adams, R. L. P. (1980) Cell culture for biochemists. In: *Laboratory techniques in biochemistry and molecular biology*. T. S. Work and R. H. Burdon (eds.), Elsevier Science Pub. New York, p.176 - 177.

Al-Awadi, F. M. and Al-Bader, A. A. (1987) Energy status in HeLa cells after treatment with an arresting anticancer drug. *Oncology* 44: 60 - 63.

Al-Rubeai, M., Singh, R. P., Goldman, M. H., and Emery, A. N. (1995) Death mechanisms of animal cells in conditions of intensive agitation. *Biotechnol. Bioeng.* 45: 463 - 472.

Altshuler, G. L., Dziewalski, D. M., Sowek, J. A., and Belfort, G. (1986) Continuous hybridoma and monoclonal antibody production in hollow fiber reactors-separators. *Biotechnol. Bioeng.* 28: 646 - 658.

Anderson, D. C., and Goochee, C. F. (1995) The effect of ammonia on the O-linked glycosylation of granulocyte colony-stimulating factor produced by Chinese hamster ovary cells. *Biotechnol. Bioeng.* 47: 96 - 105.

Ardawi, M. S. M., and Newsholme, E. A. (1983) Glutamine metabolism in lymphocytes of the rat. *Biochem. J.* 212: 835 - 842.

Ashbrook, J. D., Spector, A. A., Santos, E. C., and Fletcher, J. E. (1975) Long chain fatty acid binding to human plasma albumin. *J. Biol. Chem.* 250: 2333 - 2338.

Atkinson, D. E. (1968) The energy charge of the adenylate pool as a regulatory parameter, interaction with feedback modifiers. *Biochemistry* 7: 4030 - 4034.

Atkinson, D. E. (1977) *Cellular energy metabolism and its regulation.* Academic Press. New York, pp. 85 - 107 and pp. 200 - 224.

Barnabé, N., and Butler, M. (1994) Effect of temperature on nucleotide pools and monoclonal antibody production in a mouse hybridoma. *Biotechnol. Bioeng.* 44: 1235 - 1245.

Barnes, D., and Sato, G. (1980) Methods for growth of cultured cells in serum-free medium. *Anal. Biochem.* 102: 255 - 270.

Bayer, E. A., Ben-Hur, H., and Wilchek, M. (1990) Analysis of proteins and glycoproteins on blots. *Met. Enz.* 184: 415 - 427.

Benkovic, S. J. (1992) Catalytic antibodies. *Ann. Rev. Biochem.* 61: 29 - 54.

Berry, M. N., Grivell, A. R., and Phillips, J. W. (1993) Hypothesis: the electrochemical regulation of metabolism. *Pure Appl. Chem.* 65: 1957 - 1962.

Bibila, T. and Flickinger, M. C. (1991) A structural model for monoclonal antibody synthesis in exponentially growing and stationary phase hybridoma cells. *Biotechnol. Bioeng.* 37: 210 - 226.

Bibila, T. A., Ranucci, C. S., Glazomitsky, K., Buckland, B. C. and Aunins, J. G. (1994) *Biotechnol. Prog.* 10:1: 87 - 96.

Birch, J. R., Thompson, P. W., Lambert, K., and Boraston, R. (1985) The large-scale production of monoclonal antibodies in airlift fermenters. In: *Large-scale mammalian cell culture.* J. Feder and W. R. Tolbert (eds.) Academic Press, New York, pp.1-18.

Bjare, U. (1992) Serum-free culture. *Pharmac. Ther.* 53: 355 - 374.

Bjursell, G and Reichard, P. (1973) Effects of thymidine on deoxyribonucleoside triphosphate pools and deoxyribonucleic acid synthesis in Chinese hamster ovary cells. *J. Biol. Chem.* 248: 11: 3904 - 3909.

Bloemkolk, J-W., Merchant, F., and Mosmann, T.R. (1992) Effect of temperature on hybridoma cycle and MAb production. *Biotechnol. Bioeng.* 40: 427 - 431.

Bogard, W. C., Dean, R. T., Deo, Y., Fuchs, R., Matlis, S. A., Mclean, A. A., and Berger, H. J. (1989) Practical considerations in the production, purification and formulation of monoclonal antibodies for immunoscintigraphy and immunotherapy. *Sem. Nucl. Med.* 19(3): 202 - 220.

Borth, N., Heider, R., Assadian, A., and Katinger, H. (1992) Growth and production kinetics of human x mouse and mouse hybridoma cells at reduced temperature and serum content. *J. Biotechnol.* 25: 319 - 331.

Borys, M. C., Linzer, D. I. H., and Papoutsakis, E. T. (1994) Ammonia affects the glycosylation patterns of recombinant mouse placental lactogen-I by Chinese hamster ovary cells in a pH - dependent manner. *Biotechnol. Bioeng.* 43: 505 - 514.

Bossuyt, X., and Blanckaert, N. (1993) Effect of GTP on the dolichol pathway for protein glycosylation in rat liver microsomes. *Biochem. J.* 296: 633 - 637.

Braun, J. (1992) The second century of the antibody: molecular perspectives in regulation, pathophysiology and therapeutic applications. *West. J. Med.* 157(2): 158 - 168.

Bretscher, M. S. (1985) The molecules of the cell membrane *Sci. Am.* 253: 100 - 109.

Broome, J., and Jeng, M. (1973) Promotion of replication in lymphoid cells by specific thiols and disulphides in vitro. *J. Exp. Med.* 138: 574 - 592.

Brown, G. C. (1992) Control of respiration and ATP synthesis in mammalian mitochondria and cells. *Biochem. J.* 284: 1 - 13.

Bruce, J. H., Ramirez, A., Lin, L and Agarwal, R. P. (1992) Effects of cyclic AMP and butyrate on cell cycle, DNA, RNA, and purine synthesis of cultured astrocytes. *Neurochem. Res.* 17: 4: 315 - 320.

Butler, M. (1988) Processes with animal cell and tissue culture. In: *Biotechnology* V.6b H. J. Rehm and G. Reed (eds.) VCH Verlagsgesellchaft, Weinheim pp.250 - 316.

Butler, M., and Jenkins, H. A. (1989) Nutritional aspects of the growth of animal cells in culture. *J. Biotechnol.* 12: 97 - 110.

Butler, M. (1991) Parameters associated with the selection of high productivity hybridomas. SERC grant report GR/F/15984, personal communication.

Butler, M. (1992) Serum-free media for neuronal cell culture. In: *Neuronal cell lines: a practical approach.* J. N. Wood (ed.), IRL Press, Oxford., pp. 55 - 75.

Butler, M., Huzel, N. and Barnabé, N. (1997) Unsaturated fatty acids enhance cell yields and perturb the energy metabolism of an antibody-secreting hybridoma. *Biochem. J.* 222: 615 - 623.

Calderwood, S. K., Bump, E. A., Stevenson, M. A., Kersen, I. V., and Hahn, G. M. (1985) Investigation of adenylate energy charge, phosphorylation potential, and ATP concentration in cells stressed with starvation and heat. *J. Cell. Physiol.* 124: 261 - 268.

Castiglione, S., Paggi, M. G., Delpino, A., Zeuli, M., and Floridi, A. (1990) Inhibition of protein synthesis in neoplastic cells by rhein. *Bioch. Pharm.* 40(5): 967 - 973.

Chapman, A. G., Fall, L., and Atkinson, D. E. (1971) Adenylate energy charge in *Escherichia coli* during growth and starvation. *J.Bact.* 108: 1072 -1086.

Chapman, A. G. and Atkinson, D. E. (1973) Stabilization of adenylate energy charge by the adenylate deaminase reaction. *J. Biol. Chem.* 248: 8309 - 8312.

Chapman, A. G., Miller, A. L., and Atkinson, D. E. (1976) Role of adenylate deaminase reaction in regulation of adenine nucleotide metabolism in Ehrlich ascites tumor cells. *Cancer Res.* 36: 1144 - 1150.

Chattopadhyay, D., Rathman, J. F., and Chalmers, J. J. (1995) The protective effect of specific medium additives with respect to bubble rupture. *Biotechnol. Bioeng.* 45: 473 - 480.

Cohen, G. M., Sun, X. M., Snowden, R. T., Dinsdale, D., and Skilleter, D. N. (1992) Key morphological features of apoptosis may occur in the absence of internucleosomal DNA fragmentation. *Biochem. J.* 286: 331 - 334.

Cole, C.R., Smith, C.A., and Butler, M. (1993) Specific activities of glycosyltransferase enzymes vary with monoclonal antibody productivity in murine hybridomas. *Biotech. Lett.* 15(6): 553 - 558.

Collins, R. J., Harman, B. V., Gobé, G. C., and Kerr, J. F. R. (1992) Internucleosomal DNA cleavage should not be used as the sole criterion for identifying apoptosis. *Int. J. Radiat. Biol.* 61: 451 - 453.

Costello, M. E. (1990) *Growth and productivity of hybridoma cell lines in vitro.* PhD thesis, Manchester Polytechnic, Manchester, UK.

Cotter, T. G., Glynn, J. M., Echeverri, F., and Green, D. R. (1992) The induction of apoptosis by chemotherapeutic agents occurs in all phases of the cell cycle. *Anticancer Res.* 12: 773 - 780.

Curling, E. M. A., Hayter, P. M., Baines, A. J., Bull, A. T., Gull, K., Strange, P. G., and Jenkins, N. (1990) Recombinant human interferon-gamma - differences in glycosylation and proteolytic processing lead to heterogeneity in batch culture. *Biochem. J.* 272: 333 - 337.

Dalili, M. and Ollis, D. F. (1988) The influence of cyclic nucleotides on hybridoma growth and monoclonal antibody production. *Biotechnology Lett.* 10: 11: 781 - 786.

Dalili, M., Sayles, G. D. and Ollis, D. F. (1990) Glutamine-limited batch hybridoma growth and antibody production: experiment and model. *Biotechnol. Bioeng.* 36: 74 - 82.

Dawes, E. A. (1986) *Microbial energetics.* Chapter Two. E. A. Dawes (ed.) Blackie and Sons Ltd., Glasgow pp. 9 - 20.

Decker, K., and Keppler, D. (1974) Galactosamine hepatitis: key role of the nucleotide deficiency period in the pathogenesis of cell injury and cell death. *Rev. Physiol. Biochem. Pharmacol.* 71: 77 - 106.

De Korte, D., Haverkort, W.A., deBoer, M., van Gennip, A.H., and Roos, D. (1987) Imbalance in the nucleotide pools of myeloid leukemia cells and HL-60 cells: correlation with cell cycle phase, proliferation, differentiation and transformation. *Cancer Res.* 47: 1841 - 1847.

Dell'Antone, P. (1994) Metabolic pathways in Ehrlich ascites tumor cells recovering from a low bioenergetic status. *FEBS Lett.* 350: 183 - 186.

De Matteis, M. A., Di Tullio, G., Buccione, R. and Luini, A. (1991) Characterization of calcium-triggered secretion in permeabilized rat basophilic leukemia cells. *J. Biol. Chem.* 266: 10452 - 10460.

Doyle, C., and Butler, M. (1990) The effect of pH on the toxicity of ammonia to a murine hybridoma. *J. Biotechnol.* 9: 346 - 352.

Dricu, A., Carlberg, M., Wang, M. and Larsson, O. (1997) Inhibition of N-linked glycosylation using tunicamycin causes cell death in malignant cells: role of down-regulation of insulin-like growth factor 1 receptor in induction of apoptosis. *Cancer Res.* 57: 543 - 548.

Duval, D., Demangel, C., Miossec, S. and Geahel, I. (1992) Role of metabolic waste products in the control of cell proliferation and antibody production by mouse hybridoma cells. *Hybridoma* 11: 3: 311 - 322.

Eagle, H. (1955) Nutrition needs of mammalian cells in tissue culture. *Science.* 122: 501 - 504.

Emery, A. N., Lavery, M., Williams, B., and Handa, A. (1987) Large scale hybridoma culture. In: *Plant and animal cells: process possibilities.* C. Webb and F. Mavituna (eds.) Ellis Horwood Ltd., Chicester pp.137 - 148.

Engstrom, W., and Zetterberg, A. (1984) The relationship between purines, pyrimidines, nucleotides, and glutamine for fibroblast cell proliferation. *J. Biol. Chem.* 256: 7812 - 7819.

Epstein, N., Warner-Efrati, E., and Catane, R. (1989) Monoclonal antibodies in cancer diagnosis and therapy. In: *Advances in biotechnological proceses* v.11 A. Mizrahi (ed.) Alan R. Liss Inc., New York, pp.306 - 320.

Eto, N., Yamada, K., Shito, T., Shirahata, S. and Murakami, H. (1991) Development of a protein-free medium with ferric citrate substituting transferrin for the cultivation of mouse-mouse hybridomas. *Agric. Biol. Chem.* 55:3: 863 - 865.

Fazekas de St.Groth, S. (1983) Automated production of monoclonal antibodies in a cytostat. *J. Immunol. Methods* 57: 121 - 136.

Fitzpatrick, L., Jenkins, H. A., Butler, M. (1993) Glucose and glutamine metabolism of a murine B-lymphocyte hybridoma grown in batch culture. *Appl. Biochem. Biotechnol.* 43: 93 - 116.

Frenes, S. E., Furukawa, R. D., Li, R. K., Tumiati, L. C., Wersel, R., D., wersel, R. D., Mickle, D. A. (1992) In vitro assessment of the effects of glucose added to the University of Wisconsin solution on myocyte preservation. *Circulation* 86 (5 Suppl.): II289 - II294.

Freudenberg, H., and Mager, J. (1971) Studies on the mechanism of the inhibition of protein synthesis induced by the intracellular ATP depletion. *Biochim. Biophys .Acta.* 232: 537 - 555.

Gabai, V. L., Zamulaeva, I. V., Mosin, A. F., Makarova, Y. M., Mosina, V. A., Budagova, K. R., Malutina, Y. V., and Kabakov, A. E. (1995) Resistance of Ehrlich tumor cells to apoptosis can be due to accumulation of heat shock proteins. *FEBS Lett.* 375: 21 - 26.

Glacken, M. W. (1988) Catabolic control of mammalian cell culture. *Bio/Technology* 6: 1041 - 1050.

Glassy, M. C., Tharakan, J. P., and Chau, P. C. (1988) Serum-free media in hybridoma culture and monoclonal antibody production. *Biotechnol. Bioeng.* 32: 1015 - 1028.

Guppy, M., Abas, L., Neylon, C., Whisson, M. E., Whitham, S., Pethwick, D. W., and Niu, X. (1997) Fuel choices by human platelets in human plasma. *Eur. J. Biochem.* 244: 161 - 167.

Hagedorn, J. and Kargi, F. (1990) Coiled tube membrane bioreactor for the cultivation of hybridoma cells producing monoclonal antibodies. *Enz. Microb. Tech.* 12: 824 - 829.

Hague, A., Manning, A. M., Hanlon, K. A., Huschtscha, L. I., Hart, D. and Paraskeva, C. (1993) Sodium butyrate induces apoptosis in human colonic tumour cell lines in a p53-independent pathway: implications for the possible role of dietary fibre in the prevention of large-bowel cancer. *Int. J. Cancer* 55: 498 - 505.

Hale, A. J., Smith, C. A., Sutherlanf, L. C., Stoneman, V. E. A., Longthorne, V. L., Culhane, A. C., and Williams, G. T. (1996) Apoptosis: molecular regulation of cell death. *Eur. J. Biochem.* 236: 1 - 26.

Hamako, J., Matsui, T., Ozeki, Y., Mizuochi, T., and Titani, K. (1993) Comparative studies of asparagine - linked sugar chains of immunoglobulin G from eleven mammalian species. *Comp. Biochem. Physiol.* 106B: 949 - 954.

Harold, F. M. (1986) *The vital force: A study of bioenergetics.* W.H. Freeman and Co., New York, pp.28 - 56.

Hayter, P. M., Kirkby, N. F., and Spier, R. E. (1992) Relationship between hybridoma growth and monoclonal antibody production. *Enzyme Microb. Technol.* 14: 454 - 461.

Heinemann, V., Schulz, L., Issels, R. D., and Plunkett, W. (1995) Gemcitabine: a modulator of intracellular nucleotide and deoxynucleotide metabolism. *Sem. Oncol.* 22 (4) Suppl 11: 11 - 18.

Henderson, J. F., and Paterson, A. R. P. (1973) *Nucleotide metabolism: an introduction*. Academic Press, New York, pp. 28 - 56.

Hickman, S., Kulczycki, A., Lynch, R. G., and Kornfeld, S. (1977) Studies of the mechanism of tunicamycin inhibition of IgA and IgE secretion by plasma cells. *J. Biol. Chem.* 252: 4402 - 4408.

Ito, T., Takatsuki, A., Kawamura, K., Sato, K., and Tamura, G. (1980) Isolation and structures of components of tunicamycin. *Agric. Biol. Chem.* 44: 695 - 698.

Jackson, R. C., Lui, M. S., Boritzki, T. J., Morris, H. P., and Weber, G. (1980) Purine and pyrimidine nucleotide patterns of normal, differentiating, and regenerating liver and of hepatomas in rats. *Cancer Res.* 40: 1286 - 1291.

James, K. (1990) Therapeutic monoclonal antibodies - their production and applications. In: *Animal cell biotechnology* V.4 , R. E. Spier and J. B. Griffiths (eds) Academic Press Ltd. London pp. 206 - 255.

Jan, D. C. H., Petch, D. A., Huzel, N., and Butler, M. (1997) The effect of dissolved oxygen on the metabolic profile of a murine hybridoma grown in serum-free medium in continuous culture. *Biotechnol. Bioeng.* 54: 2: 153 - 164.

Jenkins N, Parekh R.B., and James D.C. (1996) Getting the glycosylation right: Implications for the biotechnology industry. *Nature Biotechnology* 14: 975 - 981.

Kawamoto, T., Sato, J. D., Le, A., McClure, D. B., and Sato, G. H. (1983) Development of a serum-free medium for the growth of NS-1 mouse myeloma cells and its application to the isolation of NS-1 hybridomas. *Anal. Biochem.* 130: 445 - 453.

Kerr, J. F. R., Winterford, C. M., and Harmon, B. V. (1991) Apoptosis: its significance in cancer and cancer therapy. In: Apoptosis: the molecular basis of cell death. L. D. Tomei and F. O. Cope (eds.) *Curr. Commun. Cell. Mol. Biol.* Vol. 3 pp. 2013 - 2026.

Kimata, H., Yoshida, A., Ishioka, C., and Mikawa, H. (1991) Erythropoietin enhances immunoglobulin production and proliferation by human plasma cells in serum-free medium. *Clin. Immunol. Immunopath.* 59: 495 - 501.

Kohler, G. and Milstein, C. (1975) Continuous cultures of fused cells secreting antibody of predefined specificity. *Nature* 256: 495 - 497.

Kornfield, S., Kornfield, R., Neufeld, E. F., and O' Brien, P. J. (1964) The feedback control of sugar nucleotide biosynthesis in liver. *Proc. Natl. Acad. Sci. USA*. 52: 371 - 379.

Kristensen, S. R. (1989) A critical appraisal of the association between energy charge and cell damage. *Biochim. Biophys. Acta* 1012: 272 - 278.

Krug, E., Zweibaum, A., Schulz-Holstege, C., and Keppler, D. (1984) D-glucosamine-induced changes in nucleotide metabolism and growth of colon - carcinoma cells in culture. *Biochem. J.* 217: 701 - 708.

Laemmli, U. K. (1970) Cleavage of structural proteins during assembly of the head of bacteriophage T4. *Nature* 227: 680 - 685.

Lambert, K. J., Birch, J. R. (1985) Cell growth media. In: *Animal cell biotechnology* Vol.1, R. E. Spier and J. B. Griffiths (eds.), Academic Press, Inc., London, pp. 85 - 121

Lanks, K. W., and Li, P. W. (1988) End products of glucose and glutamine metabolism by cultured cell lines. *J. Cell. Physiol.* 135: 151 - 155.

Leatherbarrow, R. J., and Dwek, R. A. (1983) The effect of aglycosylation on the binding of mouse IgG to staphylococcal protein A. *FEBS Lett.* 164: 227 - 230.

Leatherbarrow, R. J., Rademacher, T. W., Dwek, R. A., Woof, J. M., Clark, A., Burton, D. R., Richardson, N., and Feinstein, A. (1985) Effector functions of a monoclonal aglycosylated mouse IgG2a: binding and activation of complement component C1 and interaction with human monocyte Fc receptor. *Mol. Immunol.* 22:407 - 415.

Lee, Y. K., Yap, P. K., and Teoh, A. P. (1995) Correlation between steady-state cell concentration and cell death of hybridoma cultures in chemostat. *Biotechnol. Bioeng.* 45: 18 - 26.

Lehninger, A. L. (1982) *Principles of biochemistry*. Worth Publishers, Inc. New York 1011p.

Leno, M., Merten, O. W., and Hache, J. (1992) Kinetic studies of cellular metabolic activity, specific IgG production rate, IgG mRNA stability and accumulation during hybridoma batch culture. *Enz. Microb.Tech.* 14: 135 - 140.

Linke, S. P., Clarkin, K. C., Di Leonardo, A., Tsou, A., and Wahl, G. M. (1996) A reversible, p53-dependent G_0/G_1 cell cycle arrest induced by ribonucleotide depletion in the absence of detectable DNA damage. *Genes Develop.* 10: 934 - 947.

Live, T. R., and Kaminskas, E. (1975) Changes in adenylate energy charge in Ehrlich ascites tumor cells deprived of serum, glucose, or amino acids. *J. Biol. Chem.* 250: 1786 - 1789.

Lomax, C. A., and Henderson, J. F. (1973) Adenosine formation and metabolism during adenosine triphosphate catabolism in Ehrlich ascites. *Cancer Res.* 33: 2825 - 2829.

Long, W. J., Palombo, A., Schofield, T. L., and Emini, E. A. (1988) Effects of culture media on murine hybridomas: definition of optimal conditions for hybridoma viability, cellular proliferation, and antibody production. *Hybridoma* 7(1): 69 - 77.

Lund, P. (1985) L-glutamine and L-glutamate. In: *Methods of enzymatic analysis.* H.U. Bergmeyer (eds) 3rd edition VCH Verlagsgesellschaft, Weinheim p. 357 - 363.

Lundin, A., Hasenson, M., Persson, J., and Pousette, A., (1986) Estimation of biomass in growing cell lines by adenosine triphosphate assay. *Met. Enz.* 133: 27 - 42.

Marinovich, M., Viviani, B., and Galli, C. L. (1990) Reversibility of tributyltin-chloride induced protein synthesis inhibition after ATP recovery in HEL-30 cells. *Toxic. Lett.* 52: 311 - 317.

Martens, D. E., de Gooijer, C. D., van der Velden-de-Groot, C. A. M., Beuverg, E. C., and Tramper, J. (1993) Effect of dilution rate on growth, productivity, cell cycle and size, and shear sensitivity of a hybridoma cell in continuous culture. *Biotechnol. Bioeng.* 41: 429 - 439.

Martin, J. F. and Demain, A. L. (1980) Control of antibiotic biosynthesis. *Microbiol. Rev.* 44: 2: 230 - 251.

Martinelle, K. and Haggstrom, L. (1993) Mechanisms of ammonia and ammonium ion toxicity in animal cells: transport across cell membranes. *J. Biotechnol.* 30: 339 - 350.

Matsui, Y., Kitade, H., Kamiya, T., Kanemaki, T., Hiramatsu, Y., Okumura, T. and Kamiyama, Y. (1994) Adenylate energy charge of rat and human cultured hepatocytes. *In Vitro Cell. Dev. Biol.* 30A: 609 - 614.

Matsumoto, S. S., Raivo, K. O., and Seegmillar, J. E. (1979) Adenine nucleotide degradation during energy depletion in human lyphoblasts. *J. Biol. Chem.* 254: 8956 - 8962.

McComb, R. B., and Yushok, W. D. (1964) Metabolism of ascites tumor cells IV. Enzymatic reactions involved in adenosine triphosphate degradation induced by 2-deoxyglucose. *Cancer Res.* 24: 198 - 203.

McKeehan, W. L. (1982) Glycolysis, glutaminolysis and cell proliferation. *Cell Biol. Int. Rep.* 6: 7: 635 - 650.

McQueen, A., and Bailey, J. E. (1991) Growth inhibition of hybridoma cells by ammonium ion: correlation with effects on intracellular pH. *Bioproc. Eng.* 6: 49 - 61.

Medina, M. A., and Nunez de Castro, I. (1990) Glutaminolysis and glycolysis interactions in proliferant cells. *Int. J. Biochem.* 22: 7: 681 - 683.

Meijer, J. J., and van Dijken, J. P. (1995) Effects of glucose supply on myeloma growth and metabolism in chemostat culture. *J. Cell. Physiol.* 162: 191 - 198.

Meikrantz, W., and Shlegel, R. (1995) Apoptosis and the cell cycle. *J. Cell. Biochem.* 58: 160 - 174.

Mercille, S., and Massie, B. (1994a) Induction of apoptosis in nutrient-deprived cultures of hybridoma and myeloma cells. *Biotechnol. Bioeng.* 44: 1140 - 1154.

Mercille, S., and Massie, B. (1994b) Induction of apoptosis in oxygen-deprived cultures of hybridoma cells. *Cytotechnology* 15: 117 - 128.

Meuth, M. (1989) The molecular basis of mutations induced by deoxyribonucleoside triphosphate pool imbalances in mammalian cells. *Exp. Cell. Res.* 181: 305 - 316.

Meyer, R., and Wagner, K.G. (1985) Nucleotide pools in suspension cultured cells of Daturia innoxia. *Planta* 166: 439 - 451.

Michaels, J. D., Petersen, J. F., McIntire, L. V., and Papoutsakis, E. T. (1991) Protection mechanisms of freely suspended animal cells (CRL 8018) from fluid-mechanical injury. Viscometric and bioreactor studies using serum, Pluronic F-68, polyethylene glycol. *Biotechnol. Bioeng.* 38: 169 - 180.

Miller, W. M., Blanch, H. W., and Wilke, C. R. (1988a) A kinetic analysis of hybridoma growth and metabolism in batch and continuous suspension culture: effect of nutrient concentration, dilution rate and pH. *Biotechnol. Bioeng.* 32: 947 - 965.

Miller, W. M., Wilke, C. R., and Blanch, H. W. (1988b) Transient responses of hybridoma metabolism to changes in the oxygen supply rate in continuous culture. *Bioprocess Engineering* 3: 103 - 111.

Miller, W. M., Wilke, C. R., and Blanch, H. W. (1989a) Transient responses of hybridoma cells to nutrient additions on continuous culture: I. Glucose pulse and step changes. *Biotechnol. Bioeng.* 33: 447 - 486.

Miller, W. M., Wilke, C. R., and Blanch, H. W. (1989b) The transient responses of hybridoma cells to nutrient additions on continuous culture: II. Glutamine pulse and step changes. *Biotechnol. Bioeng.* 33: 487 - 499.

Mizrahi, A. (1986) Production of biologicals from animal cells - an overview. *Process Biochemistry.* Aug.1986, 108 - 112.

Modha, K., Whiteside, J.P., and Spier, R.E. (1992) Dissociation of monoclonal antibody production from cell division using DNA biosynthesis inhibitors. In: *Animal Cell Technology*: Developments, Processes and Products. R. E. Spier, J. B. Griffiths and C. Macdonald (eds), Butterworth-Heinemann Ltd., Oxford, pp. 81 - 87.

Mohan, S.B., and Lydiatt, A. (1991) Passive release of monoclonal antibodies from hybridoma cells. *Cytotechnology* 5: 201 - 209.

Morin, M. J., Porter, C. W., McKernan, P., and Bernacki, R. J. (1983) The biochemical and ultrastructural effects of tunicamycin and D - glucosamine in L1212 leukemic cells. *J. Cell. Phys.* 114:162 - 172.

Morton, H. J. (1981) Known cellular requirements and the composition of currently available defined media. In: *The growth requirements of vertebrate cells in vitro*. C. Waymouth, R. G. Ham and P. J. Chapple (eds.) Cambridge Univ. Press, London, pp. 16 - 24.

Mosser, D. D., and Massie, B. (1994) Genetically engineered mammalian cell lines for the increased viability and productivity. *Biotechnol. Adv.* 12: 253 - 277.

Murakami, H (1989) Serum-free media used for the cultivation of hybridomas. In: *Monoclonal Antibodies: Production and Applications.* Alan R. Liss Inc. pp. 107 - 141.

Murphree, S., Moore, E. C., Peterson, D. (1974) Temporal variation of adenine ribonucleotides during the cell cycle of Chinese hamster fibroblasts in culture. *Exp. Cell. Res.* 83: 189 - 190.

Neermann, J., and Wagner, R. (1996) Comparative analysis of glucose and glutamine metabolism in transformed mammalian cell lines, insect and primary liver cells. *J. Cell. Physiol.* 166: 1: 152 - 169.

Nielsen, F. H. (1981) Consideration of trace element requirements for preparation of chemically defined media. In: *The growth requirements of vertebrate cells in vitro*. C. Waymouth, R. G. Ham and P. J. Chapple (eds.) Cambridge Univ. Press, London, pp. 68 - 77.

Nose, M. and Wigzell, H. (1983) Biological significance of carbohydrate chains on monoclonal antibodies. *Proc. Natl. Acad. Sci. USA.* 80: 6632 - 6636.

Oh, S. K. W., Vig P., Chua, F., Teo, W. K., and Yap, M. G. S. (1993) Substantial overproduction of antibodies by applying osmotic pressure and sodium butyrate. *Biotechnol. Bioeng.* 42: 601 - 610.

Orrenius, S. (1995) Apoptosis: molecular mechanisms and implications for human disease. *J. Int. Med.* 237: 529 - 536.

Oyaas, K., Berg, T. M., Bakke, O., Levine, D. W. (1989) Hybridoma growth and antibody production under conditions of hyperosmotic stress. In: Advances in animal cell biology and technology for bioprocesses. R. E. Spier, J. B. Griffiths, J. Stephenne and P. J. Crooy (eds), Butterworths, London p.212 - 220.

Ozturk, S. S. and Palsson, B. O. (1991a) Physiological changes during the adaptation of hybridoma cells to low serum and serum-free media. *Biotechnol. Bioeng.* 37: 35 - 46.

Ozturk, S. S., and Palsson, B. O. (1991b) Effect of medium osmolarity on hybridoma growth, metabolism and antibody production *Biotechnol. Bioeng.* 37: 989 - 993.

Pall, M. L., and Robertson, C. K. (1988) Growth regulation by GTP: Regulation of nucleotide pools in Neurospora by nitrogen and sulfur control systems. *J. Biol. Chem.* 263(23): 11168 - 11174.

Passini, C. A., and Goochee, C. F. (1989) Response of a mouse hybridoma cell line to heatshock, agitation, and sparging. *Biotechnol. Prog.* 5: 4: 175 - 188.

Passonneau, J. V. and Lowry, O. H. (1962) Phosphofructokinase and the Pasteur effect. *Biochem. Biophys. Res. Comm.* 7: 10 - 15.

Petch,, D. A. (1994) A metabolic analysis of glucose and glutamine utilization in hybridoma CC9C10. *Ph.D thesis*, University of Manitoba

Petch, D., and Butler, M. (1994) A profile of energy metabolism in a murine hybridoma: glucose and glutamine utilization. *J. Cell. Physiol.* 161: 71 - 76.

Petronini, P. G., Urbani, S., Alfieri, R., Borghetti, A. F., and Guidotti, G. G. (1996) Cell susceptibility to apoptosis by glutamine deprivation and rescue: survival and apoptotic death in cultured lymphoma-leukemia cell lines. *J. Cell. Phys.* 169: 175 - 185.

Ramirez, O. T. and Mutharasan, R. (1990) Cell cycle and growth phase dependent variations in size distribution, antibody productivity, and oxygen demand in hybridoma cultures. *Biotechnol. Bioeng.* 36: 836 - 848.

Rapaport, E., Garcia-Blanco, M. A., and Zamecrik, P. C. (1979) Regulation of DNA replication in S phase nuclei by ATP and ADP pools. *Proc. Natl. Acad. Sci. USA.* 76: 1643 - 1647.

Reitzer, L. J., Wice, B. M., and Kennell, D. (1979) Evidence that glutamine, not sugar, is the major energy source for cultured HeLa cells. *J. Biol. Chem.* 254: 2669 - 2676.

Reitzer, L. J., Wice, B. M., and Kennell, D. (1980) The pentose cycle: control and essential function in HeLa cell nucleic acid synthesis. *J. Biol. Chem.* 255: 12: 5616 - 5626.

Renard, J. M., Spagnoli, R., Mazier, C., Saller, M.F., and Mandino, E. (1988) Evidence that monoclonal antibody kinetics is related to the integral of the viable cells curve in batch systems. *Biotech. Lett.* 10(2): 91 - 96.

Reuveny, S., Velez, D., Macmillan, J. D., and Miller, L. (1986) Factors affecting cell growth and monoclonal antibody production in stirred reactors. *J. Immunol. Meth.* 86: 53 - 59.

Reuveny, S., Velez, D., Macmillan, J. D., and Miller, L. (1987) Factors affecting monoclonal antibody production in culture. *Dev. Biol. Stand.* 66: 169 - 175.

Richter, C., Scheizer, M., Cossarizza, A., and Franceschi, C. (1996) Control of qpoptosis by the cellular ATP level. *FEBS Lett.* 378: 107 - 110.

Roitt, I. M., Brostoff, J., and Male, D. K. (1989) *Immunologie fondamentale et appliquée*. 2e edition. Medsi-McGraw Hill, Paris 338p.

Rubin, H. N., Almendarez, E., and Halim, M., N. (1988) Do pyrimidine nucleotides regulate translatabilility of globin mRNA as purine nucleotides do? *Eur. J. Biochem.* 20: 10: 1051 - 1059.

Rudd, P. M., and Dwek, R. A. (1997) Glycosylation: heterogeneity and the 3D structure of proteins. *Crit. Rev. Biochem. Mol. Biol.* 32: 1-100.

Ryll, T., Jager, V., and Wagner, R. (1991) Variations in the ratios and concentrations of nucleotide triphosphates and UDP-sugars during a perfused batch cultivation of hybridoma cells. In: *Animal Cell Culture and Production of Biologicals.* R. Sasaki and K. Ikura (eds.) Kluwer Academic Pub., Norwell, Ma., pp.307 - 317.

Ryll, T., and Wagner, R. (1991) Improved ion-pair high-performance liquid chromatographic method for the quantification of a wide variety of nucleotides and sugar-nucleotides in animal cells. *J. Chromatography* 570: 77 - 88.

Ryll, T., and Wagner, R. (1992) Intracellular ribonucleotide pools as a tool for monitoring the physiological state of in vitro cultivated mammalian cells during production processes. *Biotechnol. Bioeng.* 40: 934 - 946.

Ryll, T., Valley, U., and Wagner, R. (1994) Biochemistry of growth inhibition by ammonium ions in mammalian cells. *Biotechnol. Bioeng.* 44: 184 - 193.

Schmid, G., Blanch, H.W., and Wilke, C.R. (1990) Hybridoma growth, metabolism, and product formation in HEPES-buffered medium: I. Effect of passage number. *Biotech. Lett.* 12: 627 - 632.

Schneider, Y. J. and Lavoix, A. (1990) Monoclonal antibody production in semi-continuous serum-free and protein-free culture: effect of glutamine concentration and culture conditions on cell growth and antibody secretion. *J. Immunol. Methods* 129: 251 - 268.

Schroer, J. A., Bender, T., Feldmann, R. J., and Jin Kim, K. (1983) Mapping epitopes on the insulin molecule using monoclonal antibodies. *Eur. J. Immunol.* 13: 693 - 700.

Schubert, D. (1979) Insulin-induced cell-substratum adhesion. *Exp. Cell. Res.* 124: 446 - 451.

Shacter, E. (1989) Serum-free media for bulk culture of hybridoma cells and the preparation of monoclonal antibodies. *TIBTECH* 7: 248 - 253.

Sharma, R.K., Pascale, R.M., Narasimham, S., and Rajalakshmi, S. (1993) Effect of orotic acid on B 1-4 galactosyltransferase during lives regeneration. *Carcinogenesis* 14(6): 1095 - 1099.

Shen, L. C., Atkinson, D. E. (1970) Regulation of adenosine diphosphate glucose synthase from *Escherichia coli. J. Biol. Chem.* 245: 3996 - 4000.

Sidman, C. (1981) Differing requirements for glycosylation in the secretion of related glycoproteins is determined neither by the producing cell nor by the relative number of oligosaccharide units. *J. Biol. Chem.* 256: 9374 - 9376.

Sikora, K., and Smedley, H. M. (1984) *Monoclonal antibodies.* Blackwell Scientific Pub. Oxford. 132p.

Singh, R. P., Al-Rubeai, M., Gregory, C. D., Emery, A. N. (1994) Cell death in bioreactors: a role for apoptosis. *Biotechnol. Bioeng.* 44: 720 - 726.

Singh, R. P., Emery, A. N., and Al-Rubeai, M. (1996) Enhancement of survivability of mammalian cells by overexpression of the apoptosis-suppressor gene bcl-2. *Biotechnol. Bioeng.* 52: 166 - 175.

Slingerland, R. J., Van Gennip, A. H., Bodlaender, J. M., Voûte, P. A., and Van Kuilenburg, A. B. P. (1995) Cyclopentenyl cytosine and neuroblastoma SK-N-BE(2)-C cell line cells. *Eur. J. Cancer* 31A: 627 - 631.

Smith, G. K., Duch, D. S., Dev, I. K., and Kaufmann, S. H. (1992) Metabolic effects and kill of human T-cell leukemia by 5-deazacyclotetrahydrofolate, a specific inhibitor of glycineamide ribonucleotide transformylase. *Cancer Res.* 52: 4895 - 4903.

Smith, J. B., Knowlton, R.P., and Agarwal, S. (1978) Human lymphocyte responses are enhanced by culture at 40°C. *J. Immunol.* 121(2): 691 - 693.

Smith, P. K., Krohn, R. I., Hermanson, G. T., Mallia, A. K., Gartner, F. H., Provenzano, M. D., Fujimoto, E. K., Goeke, N. M., Olson, B. J., and Klenk, D. C. (1985) Measurement of protein using bicinchoninic acid. *Anal. Biochem.* 150: 76 - 85.

Snyder, R. D., Beach, D. C., and Loudy, D. E. (1994) Anti-mitochondrial effects of bisethyl polyamines in mammalian cells. *Anticancer Res.* 14: 347 - 356.

Sokolova, I. A., Volgim, A. U., Makarova, N. V., Volgina, V. V., Shishkin, S. S., and Khodarev, N. N. (1992) Internucleosomal chromatin degradation in myeloma and B-hybridoma cell cultures. *FEBS Lett.* 313(3): 295 - 299.

Sri-Pathmanathan, R. M., Braddock, P., and Brindle, K. M. (1990) ^{31}P-NMR studies of glucose and glutamine metabolism in cultured mammalian cells. *Biochim. Biophys. Acta* 1051: 131 - 137.

Stevens, V. L. (1993) Regulation of glycosylphosphatidylinositol biosynthesis by GTP. *J. Biol. Chem.* 268: 9718 - 9724.

Stouthamer, A. H. (1979) The search for correlation between theoretical and experimental growth yields. In: *International Review of Biochemistry*. Univ. Park Press pp.1 - 47.

Subjeck, J. R., Sciandra, J. J., and Johnson, R. J. (1982) Heatshock proteins and thermotolerance; a comparison of induction kinetics. *Brit. J. Radiol.* 55: 579 -584.

Sureshkumar, G. K., and Mutharasan, R. (1990) The influence of temperature on a mouse-mouse hybridoma growth and monoclonal antibody production. *Biotechnol.. Bioeng.* 37: 292 - 295.

Swain, J. L., Sabina, R. L., McHale, P. A., Greenfield, J. C., and Holmes, E. W. (1982) Prolonged myocardial nucleotide depletion after brief ischemia in the open-chest dog. *Am. J. Physiol.* 242: H818 - H826.

Swedes, J. S., Sedo, R. J., and Atkinson, D. E. (1975) Relation of growth and protein synthesis to the adenylate energy charge in an adenine requiring mutant of *Escherichia coli*. *J. Biol. Chem.* 250: 6930 - 6938.

Tharakan, J. P., Lucas, A., and Chau, P. C. (1986) Hybridoma growth and antibody secretion in serum supplemented and low protein serum-free media. *J. Immunol. Meth.* 94: 225 - 235.

Thorens, B., and Vassalli, P. (1986) Chloroquine and ammonium chloride prevent terminal glycosylation of immunoglobulins in plasma cells without affecting secretion. *Nature* 321: 618 - 620.

Tkacz, J. S., and Lampen, J. O. (1975) Tunicamycin inhibition of polyisoprenyl-N-acetylglucosaminyl pyrophosphate formation in calf-liver microsomes. *Biochem. Biophys. Res. Commun.* 65: 248 - 257.

Towbin, H., Staehelin, T., and Gordon, J. (1979) Electrophoretic transfer of proteins from polyacrylamide gels to nitrocellulose sheets: procedures and some applications. *Proc. Natl. Acad. Sci. USA*. 76: 4350 - 4354.

Tritsch, G. L., and Moore, G. E. (1962) Spontaneous decomposition of glutamine in cell culture media. *Exp. Cell Res.* 28: 360 - 364.

Trowbridge, I. S., and Omary, M. B. (1981) Human cell surface glycoprotein related to cell proliferation is the receptor for transferrin. *Proc. Natl. Acad. Sci. USA*. 78: 3039.

Valley, U., Ryll, T., and Wagner, R. (1994) Growth control of production processes with BHK cells and regulation of the perfusion rate by montoring the intracellular nucleotide pools. In: *Animal cell technology: products of today, prospects for tomorrow*. ESACT 12th meeting, R. E. Spier, J. B. Griffiths and W. Berthold (eds) Butterworth-Heinemann. Oxford pp. 465 - 469.

Velez, D., Reuveny, S., Miller, L., and Macmillan, J. D. (1986) Kinetics of monoclonal antibody production in low serum growth medium. *J. Immunol. Meth.* 86: 45 - 52.

Viola, J. J., Agbaria, R., Walbridge, S., Oshiro, E. M., Johns, D. G., Kelley, J. A., Oldfield, E. H., and Ram, Z. (1995) *In situ* cyclopentenyl cytosine infusion for the treatment of experimental brain tumors. *Cancer Res.* 55: 1306 - 1309.

Vomastek, T., and Franek, F. (1993) Kinetics of development of spontaneous apoptosis in B cell hybridoma cultures. *Immunol. Lett.* 35: 19 - 24.

Walker, M. R., Lund, J., Thompson, K. M., and Jefferies, R. (1989) Aglycosylation of human IgG1 and IgG3 monoclonal antibodies can eliminate recognition by human cells expressing FcgRI and/or FcgRII. *Biochem J.* 259: 347 - 353.

Wang, L, Ben-Bassat, H., and Inbar, M. (1989) Use of monoclonal antibodies in immunodiagnostics systems. In: *Advances in biotechnological proceses* v.11 A. Mizrahi (ed.) Alan R. Liss Inc., New York, pp.216 - 266.

Weitzman, S., and Scharff, M. D. (1976) Mouse myeloma mutants blocked in the assembly, glycosylation and secretion of immunoglobulin. *J. Mol. Biol.* 102: 237 - 252.

Wice, B. M., Reitzer, L. R. and Kennell (1981) The continuous growth of vertebrate cells in the absence of sugar. *J. Biol. Chem.* 256: 7812 - 7819.

Wice, B. M., Trugnan, G., Pinto, M., Rousset, M., Chevalier, G., Dussaulx, E., Lacroix, B., and Zweilbaum, A. (1985) The intracellular accumulation if UDP-N-acetylhexosamines is concomitant with the ability of human colon cancer cells to differentiate. *J. Biol. Chem.* 260: 139 - 146.

Williams, S. P., Newton, R. P., and Brown, E. G. (1987) Analysis of the effects of ethanol, fructose and nicotinamide on the free nucleotides of rat liver using high performance liquid chromatography *Int. J. Biochem.* 19(9): 879 - 884.

Wohlpart, D., Kirman, D., and Gainer, J. (1990) Effects of cell density and glucose and glutamine levels on the respiration rates of hybridoma cells. *Biotechnol. Bioeng.* 36: 630 - 635.

Wooten, R. M., Clem, L. W., and Bly, J. E. (1993) The effects of temperature and oleic acid on murine memory and virgin T cell activation: interleukin-2 secretion and interleukin-2 receptor expression. *Cell Immunol.* 152: 35 - 48.

Wyllie, A. H. (1980) Glucocorticoid-induced thymocyte apoptosis is associated with endonuclease activation. *Nature* 284(10): 555 - 556.

Yelton, D. E. and Scharff, M. D. (1981) Monoclonal antibodies: a powerful tool in biology and medicine. *Ann. Rev. Biochem.* 50: 657 - 680.

Zielke, H. R., Ozand, P. T., Tildon, J. T., Sevdalian, D. A., and Cornblath, M. (1976) Growth of human diploid fibroblasts in the absence of glucose utilization. *Proc. Natl. Acad. Sci, USA* 73: 4110 - 4114.

Zielke, H. R., Ozand, P. T., Tildon, J. T., Sevdalian, D. A., and Cornblath, M. (1978) Reciprocal regulation of glucose and glutamine utilization by cultured human diploid fibroblasts. *J. Cell Physiol.* 95: 41 - 48.

Zielke, H. R., Zielke, C. L. and Ozand, P. T. (1984) Glutamine: a major energy source for cultured mammalian cells. *Federation Proc.* 43: 121 - 125.

APPENDIX

A1. Sample calculations of analysis of variance (ANOVA) - single factor.

ANOVA was used to test the hypothesis that means from two or more samples are equal. Data analysis was done with the Excel v.7.0 (Microsoft).

Example: Test the hypothesis that extracellular glucose has an effect on the intracellular ATP concentration in hybridomas.

Data : ATP levels (nmol/10^6 cells) in hybridomas grown in varying glucose concentrations (0 - 25 mM) and 0.5 mM glutamine.

	0 mM glucose	1 mM glucose	3 mM glucose	5 mM glucose	10 mM glucose	25 mM glucose	
	1.11	2.11	3.35	4.44	5.77	7.16	
	0.98	1.88	2.71	3.25	4.55	5.24	
n_i	2	2	2	2	2	2	N = 12
T_i	2.09	3.99	6.06	7.69	10.32	12.40	G = 42.55
x_i	1.045	1.955	3.03	3.845	5.16	6.20	
A_i	2.184	7.960	18.362	29.568	53.251	76.88	$\sum A_i$ = 188.205

where n_i = number of samples per group and $N = \sum_{i=1}^{k} n_i = (2) + (2) + (2) + (2) + (2) = 12$

k = number of different groups = 6

where $T_i = \sum_{j=1}^{n_i} x_{ij}$ (sum per group) and $\bar{x}_i = Ti/n$ (average per group)

$G = \sum T_i = (2.09) + (3.99) + ... + (12.40) = 42.55$

$\bar{x} = G/N = 42.55 / 12 = 3.55$

$A_i = (T_i)^2/n_i$

$$B = \sum_i \sum_j x_{ij}^2 = (1.11)^2 + (0.98)^2 + (2.11)^2 + \ldots + (5.77)^2 + (7.16)^2 + (5.24)^2 = 191.74$$

total degrees of freedom (total DF) = N - 1 = 12 - 1 = 11

groups degrees of freedom (group DF) = k - 1 = 6 - 1 = 5

error degrees of freedom (error DF) = N - k = 12 - 6 = 6

$C = G^2/N = (42.55)^2 / 12 = 150.87$

total sum of squares (total SS)= B - C = 191.74 - 150.87 = 40.87

groups sum of squares (group SS) = $\sum A_i$ - C = 37.33

error sum of squares (error SS) = total SS - group SS = 3.54

source of variation	SS	DF	MS (SS/DF)
total	40.87	11	
groups	37.33	5	7.466
error	3.54	6	0.59

$$F = \frac{\text{groups MS}}{\text{error MS}} = \frac{7.466}{0.59} = 12.65$$

F critical for 95 % confidence level ($P < 0.05$) = 4.39 Value determined from tables or from software package.

F > F critical therefore the groups are different (i.e.glucose has an effect on the ATP level). $P < 0.05$

A2. Sample calculations of one - tailed paired *t*-test (sample means)

The paired *t*-test is used to determine whether a sample's means are distinct. This test does not assume that the variances of both populations are equal. The paired *t*-test is use when there is a natural pairing of observations. Data analysis was done with the Excel v.7.0 (Microsoft).

Example: Test the hypothesis that temperature has an effect on the % of UDP-GlcNac in hybridomas.

Data : % of UDP-GlcNac in hybridomas grown at 37°C and 39°C over 6 days.

Days	37°C	39°C	d	d^2
1	9.21	8.31	0.9	0.81
2	9.67	12.41	- 2.71	7.51
3	12.06	17.09	- 5.03	25.30
4	15.84	22.04	- 6.20	38.44
5	19.37	25.35	- 5.98	35.76
6	22.16	26.31	- 4.15	17.22
sum			- 23.2 (S1)	125.04 (S2)

where d = difference between paired samples and n = number of paired groups = 6

S1 = sum of d S2 = sum of d^2 $\bar{d} = d/n = - 3.86$

$$(sd)^2 = \frac{(n)(S2) - (S1)^2}{(n)(n-1)} = \frac{(6)(125.04) - (-23.2)^2}{(6)(5)} = 7.07$$

$$t = \frac{\bar{d} - d0}{\sqrt{sd}/\sqrt{n}} = \frac{- 3.86 - 0}{\sqrt{7.07}/\sqrt{6}} = - 3.55$$

t critical for 95 % confidence level, one tailed ($P < 0.05$) = 2.02 Value determined from tables or from software package.

$t < t$ critical, therefore samples are different. Temperature has an effect on the % UDP-GlcNac in the cell.

A3. Sample calculations of standard of error of the mean (S.E.M.)

Data: 1.04 1.15 0.96

number of data points = n = 3

$$\text{mean} = \bar{y} = \frac{\sum y_i}{n} = \frac{1.04 + 1.15 + 0.96}{3} = 1.05$$

$$\text{variance} = s^2 = \frac{\sum (y_i - \bar{y})^2}{n - 1} = \frac{(1.04 - 1.05)^2 + (1.15 - 1.05)^2 + (0.96 - 1.05)^2}{3 - 1} = 0.0091$$

$$\text{standard deviation} = s = \sqrt{s^2} = \sqrt{0.0091} = 0.09539$$

$$\text{standard error of the mean (S.E.M.)} = \frac{s}{\sqrt{n}} = \frac{0.09539}{\sqrt{3}} = 0.06$$

IMAGE EVALUATION TEST TARGET (QA-3)

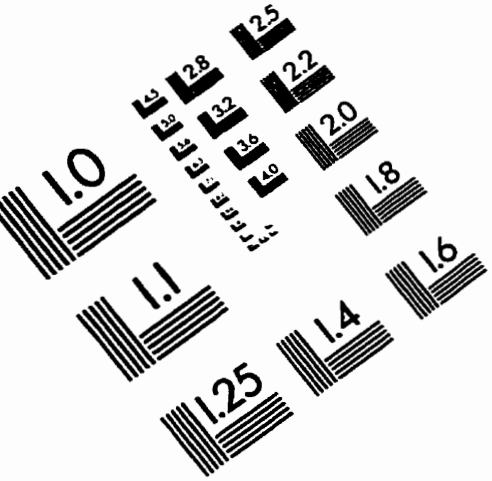

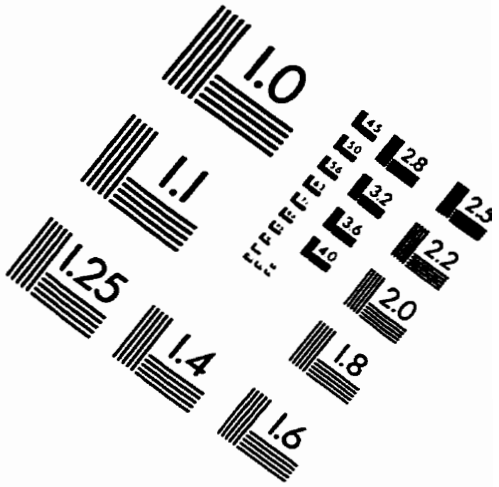

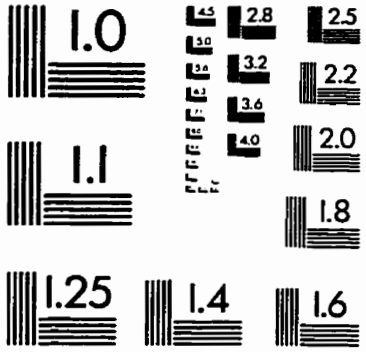

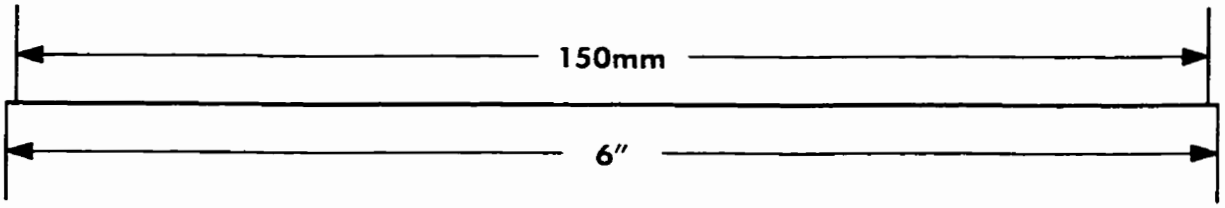

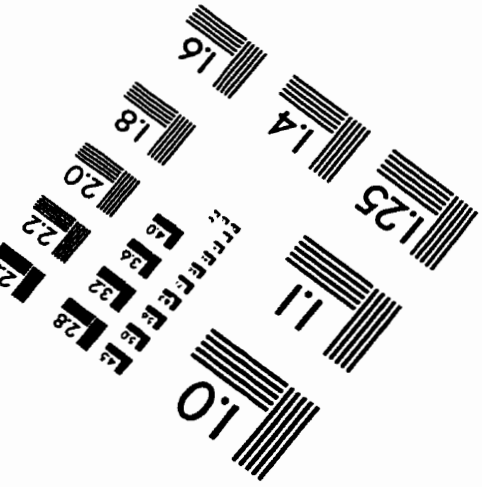

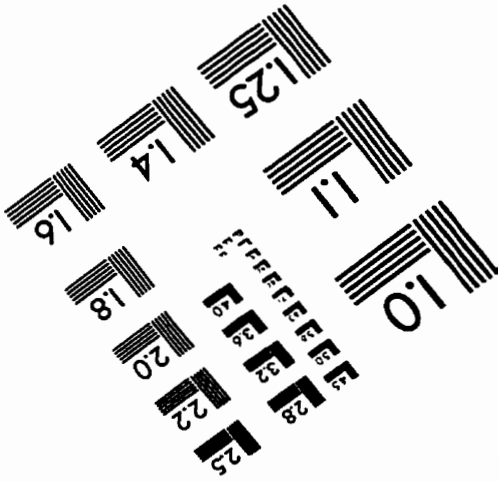

APPLIED IMAGE, Inc
1653 East Main Street
Rochester, NY 14609 USA
Phone: 716/482-0300
Fax: 716/288-5989